Characterisation of the microtubule-interacting protein, tau, in pancreatic beta cells

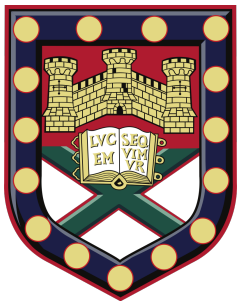

Submitted by Christiana Lekka,
to the University of Exeter as a thesis for the degree of Doctor of Philosophy in Medical Studies, February 2023

I certify that all material in this thesis which is not my own work has been identified and that any material that has previously been submitted and approved for the award of a degree by this or any other University has been acknowledged.

I would like to dedicate this thesis to my parents who have supported me throughout my journey and have been inspirational role models,
to Nick for making me laugh a little louder and smile a little bigger when I most needed it and to the Augusta team without whom this experience would not have been the same.

Declaration

I hereby declare that except where specific reference is made to the work of others, the contents of this dissertation are original and have not been submitted in whole or in part for consideration for any other degree or qualification in this, or any other university. This dissertation is my own work and contains nothing which is the outcome of work done in collaboration with others, except as specified in the text and Acknowledgements. This dissertation contains fewer than 65,000 words including appendices, bibliography, footnotes, tables and equations and has fewer than 150 figures.

Acknowledgements

I would like to thank the people who directly and indirectly contributed to this project.

I would first like to thank my supervisor, Prof. Sarah Richardson, whose guidance was invaluable in the formulating of the research topic and methodology in particular and has supported me throughout this roller-coaster journey and Prof. Noel Morgan for his input and support.

I would like to acknowledge the IBEx team, as they taught me about team work and dedication. Special thanks to Dr. Christine Flaxman, who has been an incredibly help in the lab, Dr. Pia Leete and Dr. Hopkinson, with whom we've developed new multiplex protocols and to Dr. Shalinee Dhayal, with whom we've worked closely on this project.

Last but not least, Dr. Marie Louise Zeissler and Dr. John Chilton, who conducted some of the preliminary work setting an incredible basis and, the collaborators, Dr. Irina Stefana and Prof. John Todd, who have supported this project and brought amazing ideas.

Abstract

Background: Alterations in the microtubule associated protein Tau are associated with neurodegenerative disorders, such as Alzheimer's Disease (AD). Neuronal Tau can be hyperphosphorylated (pTau) to yield aggregates of poorly-soluble paired helical filaments (PHFs) which have been associated with disease pathology. Tau expression has also been reported outside the brain, and alterations in Tau have been implicated in Type 2 diabetes. This study explores the expression of Tau in the pancreas, with a focus on β cells. **Aim**: The aim of this project was to characterise the expression and phosphorylation signature of Tau and explore the expression of relevant Tau modifiers in human islets. **Methods**: A panel of 35 anti-Tau antibodies were validated by Western blot (WB) and immunohistochemistry (IHC). Antibodies that met the validation criteria were used to stain human pancreas sections from the EADB and nPOD collections. Signal intensity quantification analysis and statistical analyses were performed. **Results**: This study presents the validation of antibodies against Tau, generating a toolbox of reagents for the careful evaluation of Tau protein expression in formalin-fixed paraffin-embedded tissue. It further demonstrates that Tau is present in the pancreatic β cells and that Tau is phosphorylated at several residues in human β cells, including some that are considered pathological in human brain. Interestingly, some pTau forms are present in the nuclei of β cells in young donors, but pTau forms increase in the cytoplasm with age. Preliminary work suggests that the expression of a selection of Tau modifiers found in β cells may be altered with age and disease states. **Conclusion**: Pancreatic Tau has a differential phosphorylation signature compared to neuronal Tau highlighting that its regulation is cell-dependent. Distinct Tau forms are localised in different subcellular compartments in β cells and this could be related to distinct physiological roles of Tau. Furthermore, the translocation of some pTau forms with age suggests that Tau may be dysregulated with age, potentially influencing insulin secretion. **Significance**: This study introduces a visualisation system that provides crucial information about the specificity and efficacy of widely used antibodies and is the first study to suggest the expression of at least two Tau forms in the human pancreas.

Table of contents

List of figures

List of tables

Nomenclature

Acronyms / Abbreviations

AD Alzheimer's disease

AF Autofluorescence

$AGEs$ Advanced glycation end products

ATP Adenosine triphosphate

BMI Body Mass Index

$CaMKII$ Ca2+/calModulin-dependent protein Kinase II

$CDK5$ Cyclin-dependent protein kinase-5

CNS Central nervous system

DAB 3,3-Diaminobenzidine

DD Deacetylase domain

DPX Dibutylphthalate Polystyrene Xylene

$DYRK1A$ Dual specificity tyrosine phosphorylation-regulated kinase 1A

$EADB$ Exeter Archival Diabetes Biobank

$Erk1/2$ Extracellular signal-regulated kinases 1 and 2

FA Formic acid

FDA Food and Drug Administration

$FFPE$ Formalin-Fixed Paraffin-Embedded

FTD Frontotemporal Degeneration

GGT Globular Glial Tauopathy

$GLUT4$ Glucose transporter type 4

$GSIS$ Glucose stimulated insulin secretion

GTP Guanosine-5'-triphosphate

$HDAC$ Histone deacetylase

$HDAC6$ Histone deacetylase 6

$HIER$ Heat-induced epitope retrieval

HMW High Molecular Weight

$HNRNP$ Heterogeneous nuclear ribonucleoproteins

HS Heat shock

$hTau$ humanised Tau

ICI Insulin-containing islet

IDI Insulin-deficient islet

IF Immunofluorescence

IHC Immunohistochemistry

IR Insulin receptor

JNK c-Jun N-terminal kinase

$KDAC$ Lysine Deacetylase

KO Knock out

Lys Lysine

MAP Microtubule associated protein

$MAPK$ Mitogen-activated protein kinases

$MARK$ Microtubule affinity-regulating kinase

MBD Microtubule binding domain

MFI Mean fluorescent intensity

MT Microtubule

MW Molecular weight

NBF Neutral buffered formalin

NCT Nucleocytoplasmic transport

NFT Neurofibrillary tangle

NGS Normal Goat Serum

$NMDAR$ N-methyl-D-aspartate receptor

NPC Nuclear pore complex

$nPOD$ network of Pancreatic Organ Donors

Nup Nucleoporins

OD Organ donor

$PART$ Primary Age Related Tauopathy

PD Parkinson's disease

$PDPK$ Proline-directed protein kinases

PET Positron-emission tomography

PHF Paired helical filament

PhK Phosphorylase kinase

PiD Pick's disease

PK Protein kinase

PLA Proximity ligation assay

PNS Peripheral nervous system

PPP Phosphoprotein phosphatase

PRD Proline rich domain

PSP Progressive Supreanuclear Palsy

$PTEN$ Phosphatase And Tensin Homolog Protein

PTM Post-translational modifications

PTP Protein tyrosine phosphatase

$RAGEs$ Receptor for advanced glycation endproducts

$RNAseq$ RNA sequencing

ROI Region of interest

Ser Serine

SFK Src family kinase

SP Senile plaque

$STWS$ Scott's Tap Water Substitute

$T1D$ Type 1 diabetes

$T1DE1$ Type 1 diabetes endotype 1

$T1DE2$ Type 1 diabetes endotype 2

$T2D$ Type 2 diabetes

$ThioS$ Thioflavin S

Thr Threonine

TLS Traffic Light System

TLS Traffic light system

TPK Tyrosine protein kinases

TSA Tyramide Signal Amplification

$TTBK1/2$ Tau-tubulin kinase 1/2

UPS Ubiquitin Proteasome System

VP Vectra Polaris

WB Western Blot

WT Wildtype

Chapter 1

Introduction

1.1 The discovery of Tau protein

1.1.1 Alzheimer's Disease and Tau protein

Alzheimer's disease (AD) was initially characterised as "a peculiar severe disease process of the cerebral cortex" by the clinical psychiatrist and neuroanatomist, Dr Alois Alzheimer, in 1906 [1, 2]. Using Bielschowsky's silver stain, a tool detecting nerve fibers, Alzheimer observed for the first time some unusual structures in the brain of the 51-year-old woman, Auguste Deter, the first individual to be diagnosed with AD [3, 2]. Today, these structures are known as neurofibrillary tangles (NFTs) and senile plaques (SPs). These observations were followed by the discovery of the microtubule associated protein Tau in 1975 [4] and further histological findings showed that hyperphosphorylated Tau is the major component of NFTs in 1985 [5–9]. Since then, Tau has been directly linked with AD pathology and is considered one of the key hallmarks of the disease.

Tau protein is a microtubule associated protein and is predominately expressed in the central nervous system (CNS). Tau is found in the neuronal axons where it acts as one of the key regulators of microtubule assembly (fig. 1.1a). Under basal

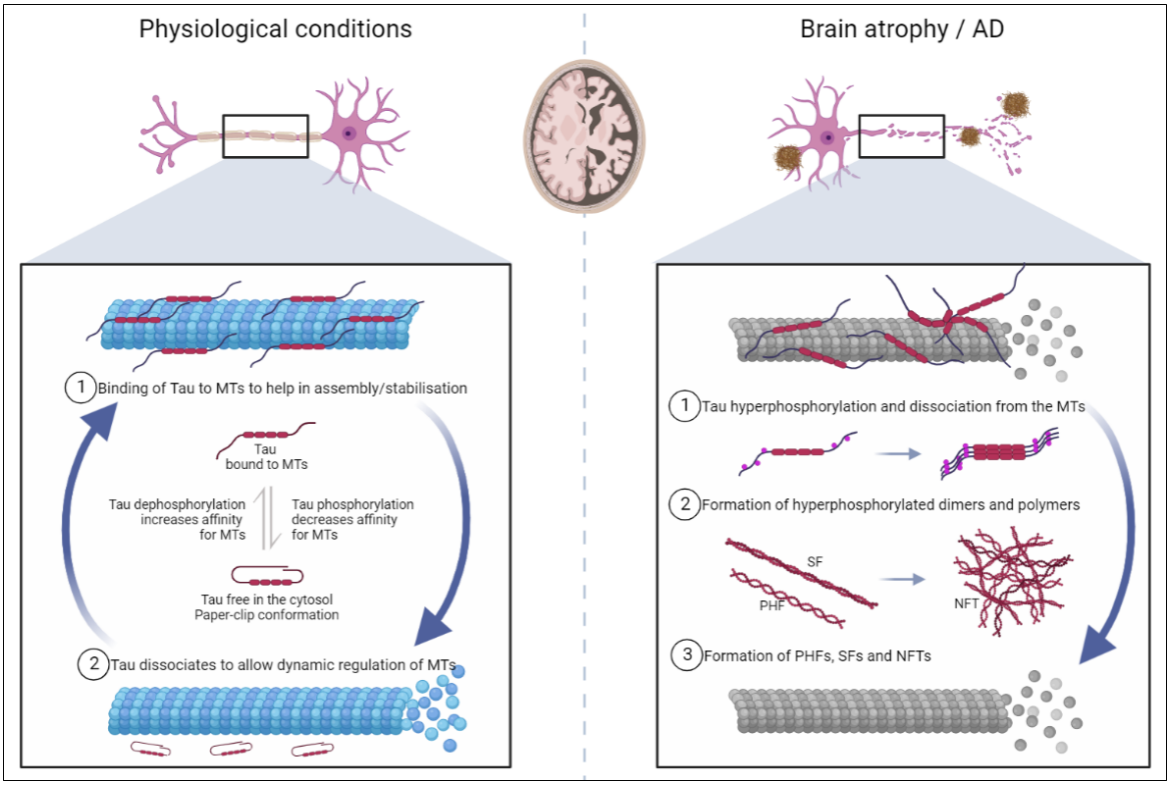

(a)

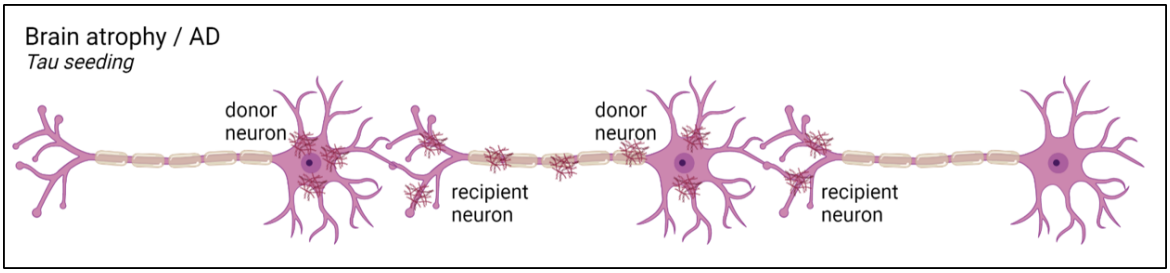

(b)

Fig. 1.1 **Tau binding to microtubules under physiological and brain atrophy conditions. 1.1a** | Under physiological conditions, Tau dynamically regulates the microtubule assembly creating a circular system that depends on the phosphorylation status of Tau [10, 11]. In brain atrophy conditions, disruption of this equilibrium leads to Tau hyperphosphorylation and the formation of pathogenic Tau forms, such as the paired helical filaments (PHFs) and the neurofibrillary tangles (NFTs), both important hallmarks of Alzheimer's disease. **1.1b** | Tau has prion-like properties meaning that it moves from the cell body of a donor neuron to the axon terminal of a recipient donor. Created in Biorender (https://biorender.com/).

conditions, Tau binds to the microtubules and promotes the microtubules assembly and stabilisation. Tau dissociation from the microtubules allows for the rearrangement of the microtubules. The association/dissociation cycle of Tau allows for the dynamic regulation of the microtubules and highly depends on the phosphorylation status of Tau protein. Phosphorylated Tau has low affinity for the microtubules and therefore detaches from the microtubules allowing them to reform. Dephosphorylated (or minimally phosphorylated) Tau has a higher affinity for the microtubules making the microtubules more stable. In AD, Tau becomes hyperphosphorylated and dissociates from the microtubules. It remains unclear whether the hyperphosphorylation of Tau takes place when Tau is bound to the microtubules or when it is dissociated with the most likely scenario being the latter. Therefore, the microtubules become unstable and begin to disintegrate causing axonal degradation and leading eventually to neuronal death. The hyperphosphorylated forms of Tau self aggregate and form PHFs and NFTs, both important hallmarks of AD. These pathological Tau forms alongside truncated Tau forms can act as prions, meaning that they can move from a donor neuron to a recipient neuron where they pair with physiological forms of Tau and further 'infect' the recipient neuron (fig. 1.1b). Through this mechanism Tau spreads across the human diseased brain and this abnormal distribution of Tau is well-linked with the progression of the relevant disorder. The specific residues that promote this mechanism have not been characterised but it is likely that the overall hyperphosphorylation of Tau contributes to this.

1.1.2 Primary and secondary tauopathies

Abnormal regulation and distribution of Tau protein have been associated with a variety of neurodegenerative diseases, such as AD, Parkinson disease (PD), Pick's disease (PiD), Progressive Supranuclear Palsy (PSP), Globular Glial Tauopathy (GGT), Primary Age

Related Tauopathy (PART) and others. Such neurodegenerative diseases are defined as Tauopathies [12–15]. Tauopathies are clinically, biochemically, and morphologically heterogeneous disorders and can be classified into primary or secondary tauopathies depending on whether abnormal Tau expression, regulation or distribution is the predominant feature.

Primary tauopathies are defined as the disorders in which Tau protein deposition is the predominant feature. Primary tauopathies can be further subdivided into three classes based on the expression of the relevant Tau isoforms (3R or 4R Tau isoforms, to be discussed in more depth in section 1.2.1); (i) 4R tauopathies which are characterised by abnormal regulation and/or distribution of the 4R-Tau isoform (e.g. PSP), (ii) 3R tauopathies characterised by abnormal regulation and/or distribution of the 3R-Tau isoform (e.g. PiD) and, (iii) mixed 3R+4R tauopathies in which both 3R- and 4R-Tau isoforms are abnormally regulated (e.g. PART). On the other hand, secondary tauopathies are defined as the disorders that present Tau pathologies but are considered to also have additional aetiologies. For example, AD is considered a secondary tauopathy as it is characterised not only by NFTs (tangles caused by Tau aggregation) but also by neuritic plaques (or β-amyloid protein deposits).

1.1.3 The NFT Braak Stages

The observation that tauopathies are characterised by the abnormal distribution of Tau protein within the diseased human brain lead to the characterisation of Braak stages. The NFT Braak staging system is a widely used method that helps to classify the degree of pathology in neurodegeneration diseases such as AD [16, 17] and PiD [18]. Interestingly, recent studies suggest that the Braak staging could also be utilised as a prognostic marker predicting patient-specific risk of clinical AD progression using positron-emission-tomography (PET)-Tau assessments [19]. The Braak staging refers

to the six stages of disease propagation that can be classified with respect to the differential spacio-temporal distribution of NFTs in the brain and the severity of clinical symptoms;

- The transentorhinal stages I-II are characterised by early NFT presence within the transentorhinal region. Clinically silent cases fall under this category.
- During the limbic stages III-IV, the pathology spreads to the limbic regions and the hippocampus (incipient AD).
- The neocortical stages V-VI involve broad cortical spread of NFT pathology. Individuals diagnosed with stages V-VI have fully developed AD [20, 21].

1.2 Tau isoforms, domains and structure

1.2.1 Alternative splicing and Tau isoforms

Tau protein is encoded by a single gene, the *MAPT* gene. The *MAPT* gene is 134kb long, maps on chromosome 17q21.31 and contains 16 exons that undergo complex alternative splicing [22]. Exons 1, 4, 5, 7, 9, 11, 12 and 13 are always translated whereas exon 8 has not been reported to be translated (fig. 1.2). Exons 2, 3, 4a, 6 and 10 are alternatively spliced to produce different isoforms. The alternative splicing of exons 2, 3 and 10 gives rise to six Tau isoforms expressed in the CNS (fig. 1.2). The CNS-Tau isoforms can be classified into two groups;

1. The N-repeat isoforms namely (i) 0N-Tau (exclusion of exons 2 and 3), (ii) 1N-Tau (inclusion of exon 2) and (ii) 2N-Tau (inclusion of exons 2 and 3) isoforms. Interestingly, the inclusion of exon 3 depends on the inclusion of exon 2, meaning that exon 3 can only be transcribed if exon 2 does so.

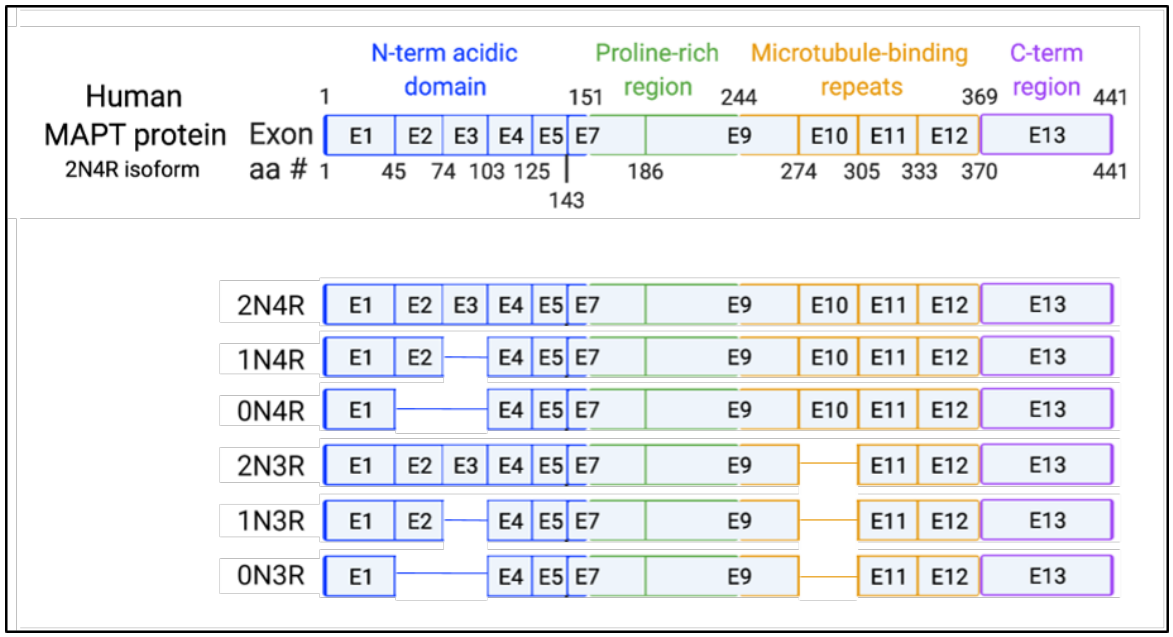

Fig. 1.2 **MAPT exons and isoforms in the central nervous system.** Tau protein consists of 11 exons and due to alternative splicing, Tau has 6 low molecular weight (LMW) Tau isoforms found in the central nervous system (CNS). Exons 2 and 3 give rise to the N-repeat Tau isoforms (0N, 1N, 2N) and exon 10 gives rise to R-repeat Tau isoforms (3R, 4R). Upon inclusion of exons 2,3 and 10, exons 4a and 6 can also be transcribed introducing the high molecular weight (HMW) or 'Big' Tau isoform which is found in the peripheral nervous system (PNS). The inclusion of exon 8 has not been described in human. Tau protein consists of four domains; (i) N-terminal acidic domains (blue), (ii) proline-rich domain (PRD; green), (iii) microtubule-binding domain (MBD; amber) and (iv) C-terminal domain (purple).

2. The R-repeat isoforms namely (i) 3R-Tau (exclusion of exon 10) and (ii) 4R-Tau (inclusion of exon 10) isoforms. Imbalance of the 3R and 4R-Tau isoforms in the adult human brain has been associated with disease.

Inclusion of exons 2,3 and 10 can also allow the inclusion of exons 4a and 6 giving rise to the 'High molecular weight' (HMW) Tau or 'Big' Tau isoform. HMW Tau is predominately found in the peripheral nervous system (PNS) but is also expressed in the CNS [23]. Little is known about the HMW Tau but it is becoming a more and more popular area of study [24].

Tau isoform expression in the human brain is age-dependent. In embryonic and early postnatal life in human brain, only the 3R-Tau isoform is expressed whereas, in the human adult brain, both the 3R- and 4R-Tau isoforms are expressed [25, 26]. The adult profile of Tau isoforms differs between humans and mice. The adult mouse brain only expresses the 3R-Tau isoform. Interestingly, such differences have only been described for the R-repeat isoforms, but not for the N-repeat isoforms. In tauopathies, the distribution and/or expression of Tau isoforms varies, depending on the disorder.

Tau mutations The Alzheimer Research Forum Web site (ALZFORUM, https://www.alzforum.org/) was queried to describe different Tau mutations. 112 mutations have been reported within the *MAPT* gene. Approximately 30% of these mutations have not been associated with any known disease, whereas the rest have been linked with AD, FTD, PSP, PD, GGT or other Tauopathies. However, the majority of these mutations have been classified as benign. The pathogenic MAPT mutations are mostly linked with Frontotemporal Degeneration (FTD).

1.2.2 Tau domains

The full length Tau protein (2N4R Tau isoform) consists of 11 exons and has 441 amino acids. The numbering of the amino acids of other Tau forms is based on the 2N4R Tau isoform. Each CNS-Tau isoform has four main domains (fig. 1.2).

1. The N-terminal (N-term) domain lies within the first 150aa of the Tau protein. However, the length of the N-term varies depending on the inclusion of exons 2 and 3. Functionally, the N-term domain acts as a projection domain allowing Tau to interact with its interaction partners. Interestingly, 1N3R and 1N4R are the most represented Tau isoforms in the adult human brain [27].

2. The proline-rich domain (PRD) lies within residues 151-243. The PRD consists of 22 prolines in a total of 143 residues. This region is prone to phosphorylation; it has 14 serine, 9 threonine and 1 tyrosine and notably, 20 out of 24 residues can be phosphorylated. As such, it is very important for Tau regulation and function.

3. The microtubule-binding domain (MBD) is found between residues 244-368 and its length varies depending on the inclusion of exon 10. The MBD allows Tau to bind the microtubules giving Tau its characteristic function. The 4R-Tau isoforms have a higher affinity for microtubules compared to the 3R-Tau isoforms [28, 29].

4. The C-terminal (C-term) domain lies within the terminal residues of the Tau protein (369-441aa). Truncation events within the C-term domain have been associated with pathogenic forms of Tau.

1.2.3 Tau structure

Tau is a complex, naturally unfolded and intrinsically disordered protein. Tau is a dipole with two domains of opposite charge and it can be heavily modulated by post-translational modifications (PTMs). The N-repeats (exons 2 and 3) add acidity to Tau, whereas the R-repeats (specifically exon 10) add positive charge. The N-term domain is negatively charged (pI[1] = 3.8), the PRD is positively charged (pI = 11.4) and the C-term domain is positively charged (pI = 10.8).

When Tau is free in the cytosol, it acquires a paper-clip conformation [30], in which the N-term and C-term domains come into close proximity (fig. 1.3). The C-terminus locates between the N-terminus and the MBD, potentially inhibiting their interaction. Truncation of the C-terminus would have a direct effect on the paper clip conformation

[1]The isoelectric point (pI) of a protein is defined as the pH at which the net charge of a protein molecule is zero.

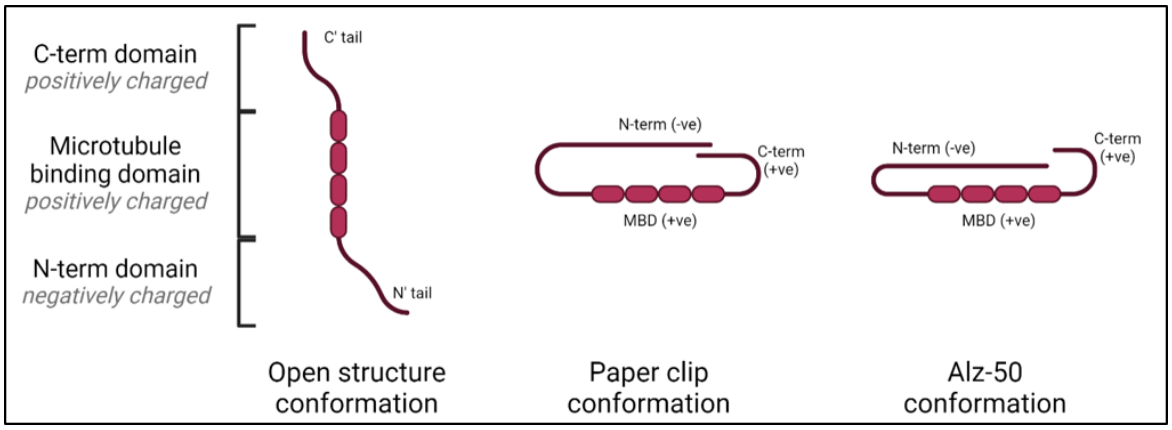

Fig. 1.3 **Tau structure in healthy neurons.** Tau consists of three functional domains. (i) The C-terminal domain, which is positively charged, (ii) the microtubules binding domain (MBD), which is positively charged and the (iii) N-terminal domain, which is negatively charged. Tau binds the microtubules via the MBD. When Tau is bound to the microtubules, it acquires an open structure conformation. When Tau is phosphorylated, it detaches from the microtubules and is free in the cytosol. When Tau is free in the cytosol, it acquires a paper clip conformation. Under pathological conditions, the C-terminal domain may be truncated and if that happens, Tau can acquire a presumed pathogenic "Alz-50" conformation. Created in Biorender (https://biorender.com/).

of Tau by allowing the N-terminus to interact with the MBD forming the Alz-50 conformation, a conformation observed in pre-tangle neurons [31, 32], entrapping the N-term projection domain and leading to Tau loss-of-function (fig. 1.3).

Under basal conditions, the N-term projection domain of Tau has at least two distinct functions. First, the projection domain of Tau competes with other proteins, such as dynein and kinesin, for microtubule binding, suggesting that Tau controls the intracellular trafficking of motor proteins [33, 34]. Second, the projection domain of Tau determines the localisation of Tau to the plasma membrane. The membrane-associated Tau is dephosphorylated, suggesting that phosphorylated Tau regulates its intracellular trafficking whereas dephosphorylated Tau may regulate the trafficking of motor proteins [35].

Tau may acquire an open structure conformation in order to bind to the microtubules (fig. 1.3). Tau binds the overall negatively charged microtubules using the positively

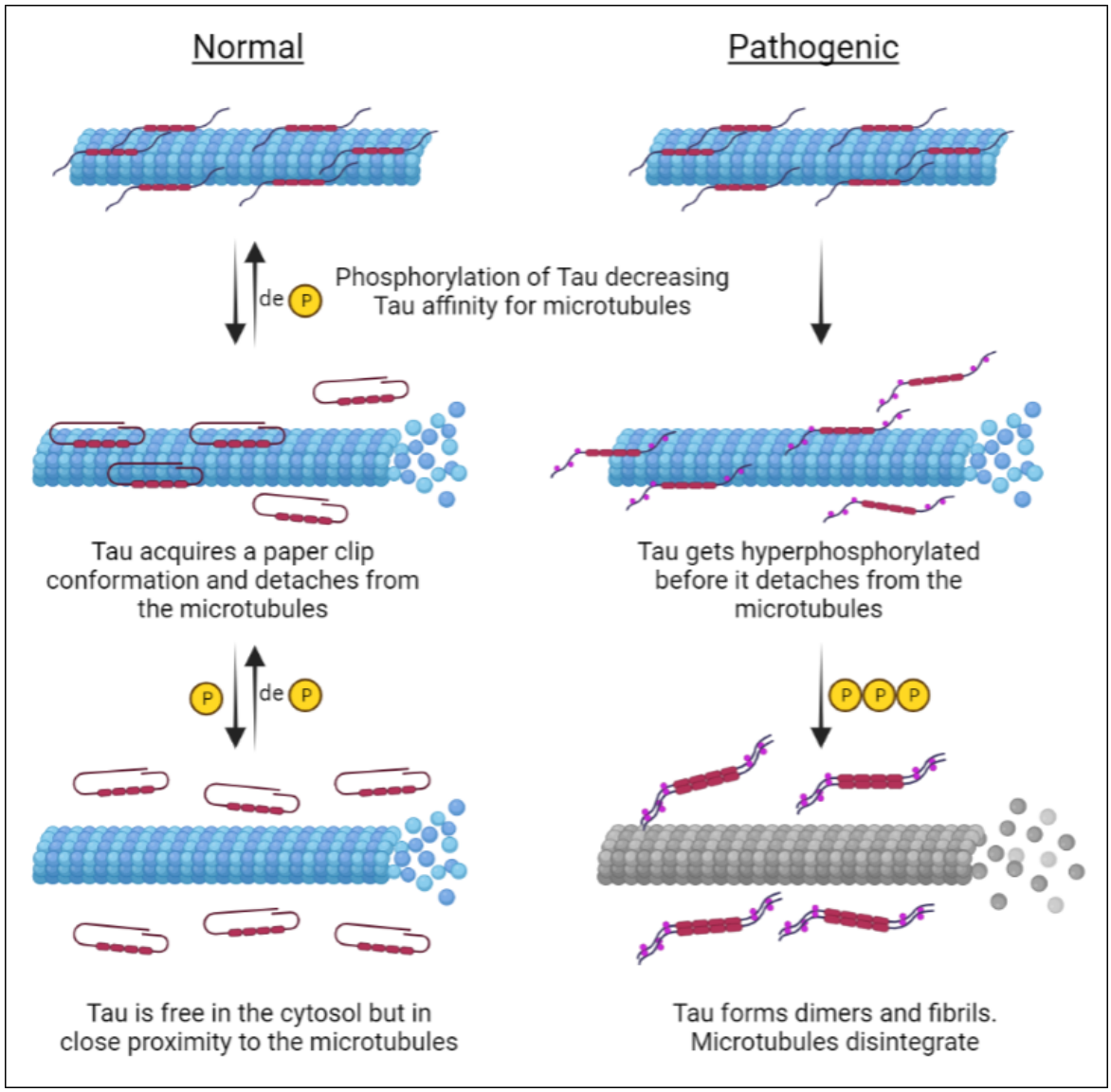

Fig. 1.4 **The structure and the phosphorylation status of Tau during microtubule assembly.** The binding of Tau to the microtubules is dynamically regulated by the phosphorylation status of Tau. When Tau is bound to the microtubules, it acquires an open structure conformation. Phosphorylation of Tau decreases Tau affinity for the microtubules. Under basal conditions, Tau acquires a paper clip conformation and it detaches from the microtubules. Tau is free in the cytosol but in close proximity to the microtubules. Then, Tau is dephosphorylated and its affinity for the microtubules increases. This loop allows for the dynamic assembly of the microtubules. Under pathogenic conditions, Tau get hyperphosphorylated and detaches from the microtubules. Hyperphosphorylated Tau is then prone to aggregation and it accumulates to the cytosol. As a result, the microtubules are unstable and begin to disintegrate. Created in Biorender (https://biorender.com/).

charged MBD and utilizes its projection domain to determine the spacing between microtubules in dendrites and axons [36]. Whether Tau acquires an open structure conformation because of this binding or because it gets modified in order to bind to the microtubules remains unexplored.

Under pathological conditions, Tau becomes hyperphosphorylated. Phosphorylation events make Tau more negatively charged decreasing its affinity for the microtubules. Additional PTMs may occur causing Tau not only to detach from the microtubules but also to self-aggregate. As such, abnormal interplay between Tau PTMs may affect the Tau structure, conforming Tau monomers into singlet fibrils, doublet fibrils, paired helical filaments or straight filaments [37]. These pathogenic forms of Tau can result in the formation of NFTs and/or their abnormal distribution across the brain.

1.3 Tau post-translational modifications (PTMs)

Tau is a natively unfolded and heavily post-translationally modified protein. The full-length 2N4R Tau isoform has 441aa and around 35% of it can potentially undergo PTMs, including phosphorylation, acetylation, methylation, SUMOylation, glycosylation and ubiquitination etc (fig. 1.5a) [38]. PTMs dynamically regulate the protein's function (microtubule binding, synaptic plasticity, DNA/RNA protection), degradation (proteasome, lysosomes/autophagy) and aggregation [38]. The disruption of the PTM equilibrium, especially that of phosphorylation, acetylation and ubiquitination, has been directly linked to pathological phenotypes and neurodegeneration emphasising the need to understand how Tau is regulated by PTMs in health and disease.

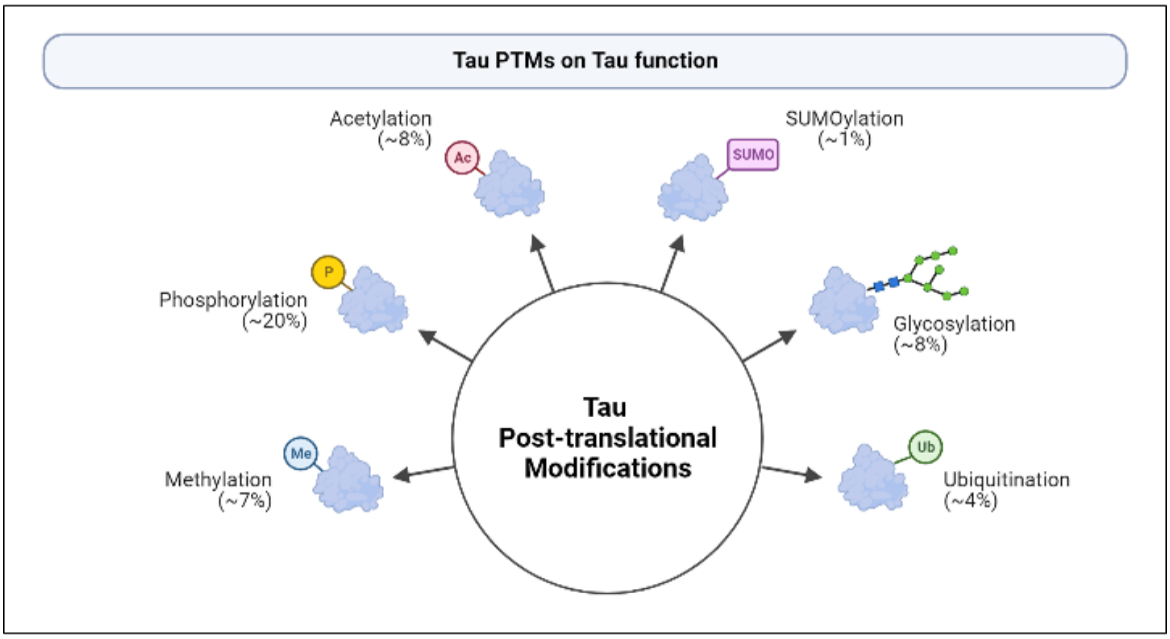

(a) Post-translational modifications of Tau

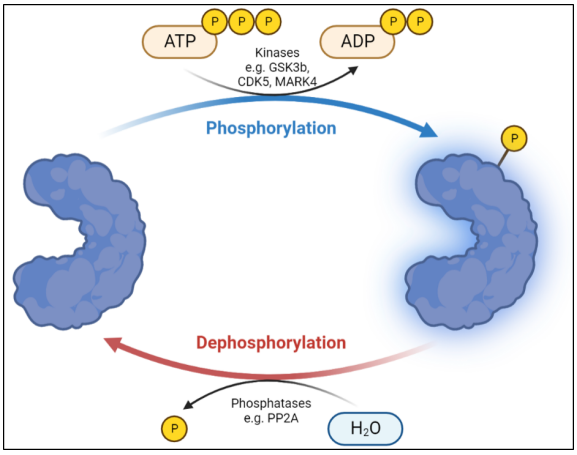

(b) Tau phosphorylation

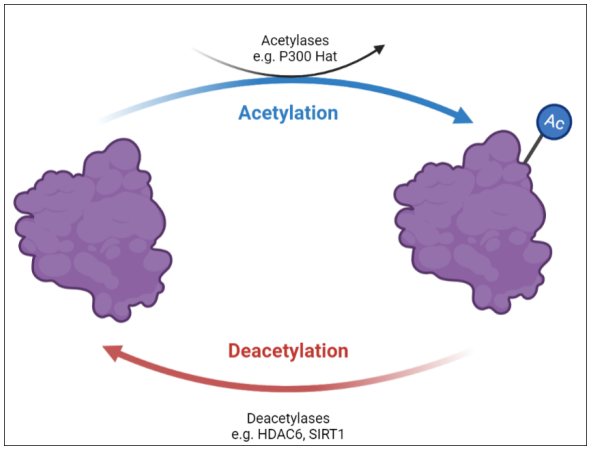

(c) Tau acetylation

Fig. 1.5 **Post-translational modifications of Tau. 1.5a** | Tau is a heavily post-translationally modified protein impacted by methylation, phosphorylation, acetylation, SUMOylation, glycosylation and ubiquitination. Percentage of Tau residues that have been reported to be modified are indicated here. **1.5b** | Phosphorylation is one of the most studied PTMs of Tau and has been linked with neurodegeneration. Major Tau kinases (GSK3-β, CDK5, MARK4) phosphorylate Tau and the major phosphatase (PP2A) dephosphorylates Tau. **1.5c** | Acetylation has also been linked to pathology phenotypes. Some of the major Tau acetylase (P300) and deacetylases (HDAC6, SIRT1) are noted. Created in Biorender (https://biorender.com/).

1.3.1 Tau Phosphorylation

Phosphorylation is a common reversible covalent modification which describes the transfer of phosphate groups from high-energy molecules, such as ATP or GTP, to specific substrates inducing a conformational change often associated with a change in activity (fig. 1.5b). The enzymes that catalyse these reactions are kinases (addition of phosphates) and phosphatases (removal of phosphates). The observation by Edmond H. Fischer and Edwin G. Krebs that phosphorylation is reversible was recognised by the award of Nobel Prize in Physiology or Medicine in 1992 [39]. Tau has 85 putative phosphorylation sites (45 serine, 35 threonine and 5 tyrosine residues) and 53 of these have been shown to be modified *in vivo* [40, 41]. Altered and/or defective Tau phosphorylation profiles have been directly linked with neurodegeneration diseases.

Under basal conditions Tau is phosphorylated at 2-3 phosphates per mol of protein, distributed over several sites [42, 43]. Dephosphorylation of Tau may determine the localisation of Tau to the plasma membrane regulating its intracellular trafficking and may increase its association with trafficking proteins [35]. Phosphorylation at Thr50 promotes association to the microtubules [44] whereas phosphorylation at Ser262 has been shown to decrease Tau affinity for microtubules but at the same time, it inhibits Tau aggregation [45, 46]. Thus, a phosphorylation/dephosphorylation equilibrium is essential for and dynamically regulates both trafficking of Tau and the interaction of Tau with other proteins and the microtubules.

Under pathological conditions Tau is phosphorylated at 6-8 phosphates per mol of protein [47]. Although some Tau residues can be phosphorylated both in the normal brain and/or in Alzheimer's disease [48, 49], disease-specific phosphorylation events have also been reported. Such events include phosphorylation at Ser208, Thr214, Thr238, Ser262, Ser409 and Ser422 and others [50, 51]. Phosphorylation at Thr231, Ser235, and Ser262 is required for maximal inhibition of Tau binding to microtubules

[52] and phosphorylation at Ser208 promotes aggregation [50]. These emphasise the severe impact of Tau hyperphosphorylation in Tau pathology and these phosphorylation events will be explored in Chapters 4, 5.

1.3.1.1 Kinases

The human kinome contains 518 protein kinases (PKs) comprising 1.7% of human genes [53]. PKs belong to a very extensive family of proteins that share a conserved catalytic core and can be classified based on a variety of criteria, such as the sequence similarity within the catalytic domain, the amino acid residues that are phosphorylated, their structure and their function. Tau can be phosphorylated by

- proline-directed protein kinases (PDPK), such as Glycogen synthase kinase-3 β (GSK3-β), cyclin-dependent protein kinase-5 (CDK5) and mitogen-activated protein kinases (MAPK) such as p38, extracellular signal-regulated kinases 1 and 2 (Erk1/2) and c-Jun N-terminal kinases (JNK),

- non-PDPK, such as Tau-tubulin kinase 1/2 (TTBK1/2), casein kinase 1α/1δ/1ϵ/2 (CK1α/1δ/1ϵ/2), Dual specificity tyrosine-phosphorylation-regulated kinase 1A/2 (DYRK1A/2), microtubule affinity-regulating kinases (MARK), phosphorylase kinase (PhK), protein kinase A and C (PKA, PKC), protein kinase N (PKN) and Ca2+/calModulin-dependent protein Kinase II (CaMKII),

- tyrosine protein kinases (TPK); Src family kinase (SFK) members such as Src, lymphocyte-specific protein tyrosine kinase (Lck), spleen tyrosine kinase (Syk) and Proto-oncogene tyrosine-protein kinase Fyn are TPK involved in Tau phosphorylation at tyrosine residues. Tyrosine residues of Tau protein can also be phosphorylated by c-Abl kinase or Abl-related gene (Arg) kinase.

The involvement of Tau kinases in Alzheimer's Disease has been extensively reviewed in [54]. The major Tau kinases in neuronal cells are GSK3-β and CDK5.

GSK3-β GSK3-β is involved in numerous signalling pathways, such as the insulin signalling pathway and the Wnt signalling pathway, and Tau is one of its downstream targets. GSK3-β phosphorylates Tau at (Ser/Thr)xx(x)p(Ser/Thr) consensus sequences. There are 25 such sequences within Tau and 12 sites have been reported to be phosphorylated by GSK3-β [55]. Notably, GSK3-β substrates require a 'priming phosphate' (which is a phosphorylated Ser/Thr residue) located four amino acids after the site of phosphorylation [56–58]. This means that GSK3-β could phosphorylate a protein at residues Ser400 if that protein is already phosphorylated at Ser403 or Ser404. Unlike other kinases, GSK3-β is constitutively active (unphosphorylated) and is inactivated when phosphorylated at Ser19 in response to cellular signals [57, 58].

GSK3-β may have a versatile effect on Tau as it can phosphorylate Tau at Thr231 and Ser262, to either promote or inhibit Tau aggregation, respectively. This may be regulated by the 'priming'. In AD brain, the active form of GSK3-β is increased [59] and it has been shown that GSK3-β co-localizes with Tau NFTs [60, 61], suggesting either that prior phosphorylation events on Tau enhanced GSK3-β targeting to Tau or that GSK3-β may phosphorylate pathogenic forms of Tau or both. Overexpression of GSK3-β in mouse and rat models and, in cell lines, has also been described and appears to result in hyperphosphorylation of Tau.

CDK5 CDK5 is a major PDPK kinase that phosphorylates Tau at Ser/Thr-Pro sequences and has been associated with abnormal phosphorylation, Tau aggregation and NFT formation in AD brains [62–66]. CDK5 activity is regulated by its activating partner, p35. The CDK5/p35 complex can phosphorylate Tau. CDK5 is inactivated when p35 detaches from the complex. If p35 undergoes proteolysis, it can form p25, a

p35 proteolytic fragment. Association of the CDK5/p25 complex leads to a deregulated kinase activity linked to Tau hyperphosphorylation and neurotoxicity [67, 68].

There are 16 Ser/Thr-Pro sequences in Tau and CDK5 has been reported to phosphorylate 9 to 13 residues, with different residues phosphorylated dependent on circumstances [69, 70]. Furthermore, CDK5 acts as the priming kinase for GSK3β in Tau phosphorylation at (Ser/Thr)-x-x-x-(pSer/pThr) sites in vitro and in cultured neurons [71]. It also increases MARK4 activity and augments pathological Tau accumulation and toxicity through Tau phosphorylation at Ser262 [71].

Under basal conditions, active CDK5 (CDK5/p35 complex) associate with the plasma membrane and phosphorylates substrates such as cytoskeletal proteins and those involved in neuronal survival, development and migration and, synaptic plasticity. Under neurotoxic or stress conditions, intracellular Ca^{2+} rises, activating calpain, a cytosolic cysteine protease, which in turn cleaves p35 to p25, leading to cell differentiation, proliferation and/or death [72]. The CDK5/p25 complex is more stable and hyperactive causing aberrant hyperphosphorylation of numerous cytoskeletal components such as Tau [63, 73, 74]. Notably, all Tau residues phosphorylated by CDK5 are phosphorylated in AD brain [54].

MARK4 MARKs are a family of serine/threonine kinases that phosphorylate the microtubule-associated proteins (MAPs). MARKs phosphorylate Tau and related MAPs on their tubulin binding repeats and consequently catalyze their detachment from microtubules *in vitro* and in cultured cells. MARK4 binds to the cellular microtubule network and to centrosomes [75] and is involved in the regulation of programmed cell death [76], in cell cycle progression and cytoskeletal dynamics [77].

MARK4 has been associated with early Tau phosphorylation in Alzheimer's disease [78]. Significant elevation of MARK4 expression and increased MARK4–Tau interactions in AD brains correlate with the Braak stages of the disease. These results suggest

the MARK4–Tau interactions are of functional importance in the progression of AD [79].

DYRK1A DYRK1A is involved in gene transcription, mRNA splicing, synapse function, and neurodegeneration with a range of different functions [80]. DYRK1A induces speckle disassembly [81], regulates caspase-9-mediated apoptosis during retina development [82] and attenuates Notch signalling [83]. DYRK1A has a nuclear localization signal [84, 81], but has also been detected in the soma and dendrites of neurons [85].

DYRK1A does not enhance *MAPT* gene transcription, but increases Tau mRNA stability suggesting that DYRK1A enhances Tau expression by stabilizing its mRNA [86]. DYRK1A can phosphorylate Tau on at least 11 residues and, it also primes Tau phosphorylation at Ser199, Ser202, Thr205 and Ser208 by GSK-3β [87, 88]. DYRK1A has been associated with hyperphosphorylation of Tau [89, 88] and, triple phosphorylation of Ser202, Thr205 and Ser208 has been shown to be sufficient to induce Tau aggregation [90]. Phosphorylation of Tau at Ser202 and Thr205 is associated with translocation of Tau from the neuronal axons to the neuronal soma, where further phosphorylation of Ser208 causes Tau to aggregate [50]. Moreover, overexpression of DYRK1A impacts on the alternative splicing of Tau [91], by increasing the 3R Tau isoform expression in a Down syndrome mouse model [92].

1.3.1.2 Phosphatases and phosphatases regulators

The human phosphatome contains 119 protein phosphatases [93]. Phosphatases or phosphomonoesterases are the hydrolytic enzymes that cleave the ester bond between the phosphate group and the organic residue of the organic phosphates (fig. 1.5b). Tau phosphatases have been extensively reviewed in [94] and, are generally classified into

groups according to their amino acids sequences, the structure of their catalytic site and their sensitivity to inhibitors. Tau can be dephosphorylated by

- phosphoprotein phosphatases (PPP) such as PP1, PP2A, PP2B and PP5 and,
- protein tyrosine phosphatases (PTP) such as the Phosphatase And Tensin Homolog Protein Coding (PTEN).

In AD brain, total phosphatase activity is reduced by half [95] with PP2A, PP1 and PP5 activities decreased by 50 %, 20 %, and 20 %, respectively [94, 96–98, 95, 99]. Therefore, PP2A is the major Tau phosphatase in neuronal cells.

PP2A Protein Phosphatase 2A (PP2A) is an important player in many cellular functions, such as cell metabolism, cell cycle, DNA replication, transcription and translation, signal transduction, cell proliferation, cytoskeleton dynamics and cell mobility and apoptosis and, has both cytosolic and nuclear substrates [100]. PP2A is a heterotrimeric holoenzyme that exists in multiple forms composed of a common core structure bound to different regulatory subunits [101]. The core enzyme is a complex between the catalytic (C) and structural (A) subunits. The third class of subunit, termed B, comprises several polypeptides that regulate PP2A activity and specificity. The principal PP2A isoform in the brain is the ABαC holoenzyme [102], which can bind to neuronal microtubules [103] and, has much higher Tau phosphatase activity than other forms of PP2A [104].

PP2A is the major Tau phosphatase dephosphorylating Tau at multiple sites in the human brain [95] and, is also the most efficient phosphatase acting on abnormally hyperphosphorylated Tau protein [96, 105–109, 94]. PP2A regulates Tau phosphorylation directly and also indirectly via inactivation of GSK-3β [110], while excess activation of PP2A under pathological conditions can result in cell damage or dysfunction [111–113]. Interestingly, insulin deprivation induces PP2A inhibition and Tau

hyperphosphorylation in hTau mice, a model of Alzheimer's disease-like Tau pathology [114].

SET SET protein, which is also known as SETα, I2^{PP2A}, TAF-1β, and PHAPII protein [115], acts as an inhibitor of PP2A. Overexpression of SET may lead to decreased PP2A activity and, subsequently, higher phosphorylation levels of Tau. SET interacts with the PP2A catalytic subunit rather than the PP2A regulatory subunits A and B [115], blocking the catalytic activity of PP2A.

1.3.2 Tau acetylation

Acetylation occurs with the transfer of acetyl groups from acetyl coenzyme A (acetyl CoA) to lysine residues by acetyltransferases leading to a neutralization of the Lysine's positive charge (fig. 1.5a). Acetylation is involved in gene transcription, DNA damage repair, cell division, signal transduction, subcellular localization and, crosstalk with other post-translational modifications by controlling interactions with DNA-binding proteins, non-nuclear proteins and proteins that shuttle from the nucleus to the cytoplasm [116]. Under basal conditions, acetylation of Tau at Lys259, Lys290, Lys321 and, Lys353 inhibits aggregation, prevents phosphorylation and, promotes degradation. Acetylation at Lys259 and Lys353 inhibits phosphorylation at Ser262 and Ser356, respectively, and Tau aggregation [117]. Under pathological conditions (i.e. AD), acetylation at Lys174, Lys280, Lys281 promotes aggregation [116, 118–120]. In addition, acetylation at Lys280 prevents clearance and, at Lys281 promotes Tau mislocalisation. Thus, the acetylation:deacetylation equilibrium is pivotal for Tau PTM and function.

1.3.2.1 Deacetylases

Histone deacetylases (HDACs), or lysine deacetylases (KDACs), are a family of eight proteins. The discovery of nuclear acetylases and deacetylases has enriched the cor-

relation between histone acetylation and increased transcription by verifying that histone acetylation regulates transcription [121–124]. However, histones are not the only proteins that can be acetylated and, non-histone protein acetylation has important impacts on protein function [116].

Tau is a lysine-rich protein, particularly in the region spanning the microtubule binding domain and, interestingly, Tau has intrinsic acetyltransferase activity [120].

HDAC6 HDAC6 is a microtubule-associated deacetylase [125] with two active catalytic deacetylase domains (DD1 and DD2). It plays a vital role in epigenetic regulation through histone lysine deacetylation and, in cytoskeletal assembly through acting on a large number of cytoplasmic proteins and, is involved in various signaling pathways. HDAC6 interacts and deacetylases Tau protein both *in vitro* and *in vivo* [126] and also deacetylates α-tubulin, a major component of the microtubules.

Under basal conditions, acetylation of α-tubulin at Lys40 protects microtubules from mechanical ageing by preventing microtubule breakage resulting in prolonged microtubule lifespan [127–129] and, it also reduces interprotofilament interactions increasing possibly the microtubule flexibility [130, 131]. Inhibition of HDAC6 has been linked with neurodegeneration.

1.4 Tau localisation and function

1.4.1 Tau in neuronal and non-neuronal cells

Tau was traditionally known as a neuronal specific protein that acts as a key regulator of cytoskeletal microtubule assembly [132]. Since then, it has been shown that Tau is expressed both in neuronal (eg. neurons, oligodendrocytes, astrocytes) and non-neuronal cells (eg. liver, pancreas) [133]. Although its expression and function in

non-neuronal cells remains unexplored, it has been proposed that Tau plays a key role in microtubule stability in non-neuronal cells as well [133].

1.4.2 Tau localisation and function

Tau was initially described as a microtubule associated protein and, therefore, its best-described characteristic function is to promote microtubule assembly and stability both in neuronal and non-neuronal cells. Interestingly, Tau is characterised by diverse cellular distribution (cytosol, nucleolus, synaptic cleft) illustrating that it may have a range of functions in synaptic plasticity and in neuronal DNA and RNA protection (fig. 1.6) [134].

1.4.2.1 Synaptic plasticity

Tau protein plays an important role in synaptic plasticity [135–137]. Synapses are the points of contact between neurons and allow information to pass from one neuron to another. During neuronal activity, Tau is released into the synaptic cleft where it acts as a link between microtubules and actin filaments. Tau also interacts with BAR domain-containing proteins and ensures the curvature and shaping of the neuronal membrane [138, 139, 137]. In addition, Tau may play a role in the removal of developmental N-methyl-D-aspartate receptor (NMDAR) and their replacement for mature NMDARs in dendrites which is important for the formation of new synaptic connections. Deletion of Tau leads to synaptic plasticity defects indicating that Tau is a major player of synaptic plasticity [137]. Tau can be released in the synaptic cleft but it remains yet unknown whether its presence there is pathological or indicates another potential physiological role of Tau. During pathological conditions, pathological forms of Tau promote synaptic dysfunction in multiple ways; post- and pre-synaptic dysfunction

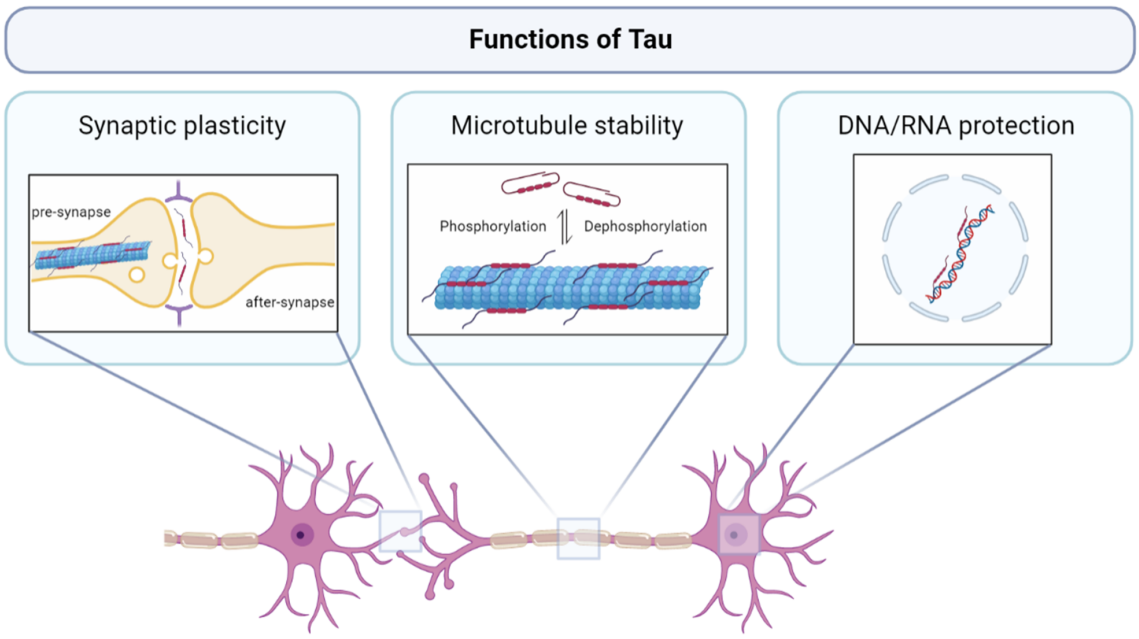

Fig. 1.6 **Tau functions in healthy neurons.** Tau is traditionally known as a neuronal protein that plays an important role in synaptic plasticity (section 1.4.2.1), microtubule assembly and stability (section 1.4.2.2), and DNA and RNA protection (section 1.4.2.3). Created in Biorender (https://biorender.com/).

due to reduced mobility results in decreased synaptic dendrites, impaired memory and disrupted calcium homeostasis [140–142].

1.4.2.2 Microtubule stability

Under basal conditions, cytosolic Tau contains, on average, two or three mols of phosphate per mol of the protein [6, 143–145]. Dephosphorylation of Tau increases its affinity for the microtubules and, as such, Tau acquires an open structure to bind to and stabilise the microtubules. Upon phosphorylation, Tau detaches and when free to the cytosol, it acquires a paper-clip conformation. The full-length 2N4R Tau isoform is the most effective at promoting microtubule assembly [146]. Interestingly, the neonate human brain only expresses the 3R-Tau isoforms whereas the adult human brain expresses both the 3R- and 4R-Tau isoforms [147, 148], suggesting that the microtubule assembly may be differentially regulated in the neonate and adult brain.

1.4.2.3 DNA/RNA protection

Nuclear expression of Tau has been described both in neuronal [149, 150] and non-neuronal cells [151, 152] but the transport of tau to the cell nucleus is not yet understood. Nuclear Tau was first reported in the human brain in 1995 [153] but the function and mechanism of nuclear Tau have not been extensively studied. Tau has been shown to localise with acrocentric chromosomes [149] and heterochromatin in human fibroblasts, lymphoblasts and HeLa cells, suggesting a role in nucleolar organization [154]. Moreover, it is suggested that nuclear Tau protects DNA and RNA from heat stress (HS)-induced damage in primary neuronal cultures [134, 155]. In addition, Tau can interact with RNA binding proteins such as the heterogeneous nuclear ribonucleoproteins (HNRNPs), a large family of RNA binding proteins playing an important role in alternative splicing and mRNA stabilization [156, 157]. It has been proposed that the Tau:HNRNP complex may drive Tau pathology and lead to neurodegenerative phenotypes [156].

1.4.3 Tau degradation and aggregation

Under basal conditions, aberrant Tau is cleared from the cell either by the proteasome or by autophagy. Under pathological conditions, Tau is ineffectively degraded and, as such, accumulates in the cell soma of the neuron. Aberrant expression of Tau and interplay between Tau PTMs have a direct effect on the filament structure of Tau, where Tau monomers can form into doublet fibrils, singlet fibrils, straight filaments, PHFs and NFTs (fig. 1.7) [37].

1.4.3.1 Proteasome

The Ubiquitin–proteasome system (UPS) is the major mechanism to eliminate misfolded and mutant proteins ensuring the protein quality in the nucleus and the cytosol [158]. Tau can be degraded by the proteasome via a ubiquitinated-dependent or

ubiquitinated-independent manner. Ubiquitin-tagged Tau is targeted by the 26S proteasome subunit. When Tau is not ubiquitin-tagged, it is targeted by the 20S proteasome subunit. Interestingly, UPS dysfunction has been associated with Tau degradation and aggregation in AD [159, 160].

1.4.3.2 Autophagy

Different Tau forms can be degraded by distinct autophagic pathways [161]. Unmodified wild-type Tau can be degraded by chaperon-mediated autophagy [162] and endosomal microautophagy [163, 164], whereas mutant Tau can only be degraded by endosomal microautophagy. Even though phosphorylated Tau and aggregates undergo macroautophagy [165–168], when Tau is phosphorylated at certain residues (pSer396/pSer404 and pSer262), it is degraded by the autophagy-independent endolysosomal pathway [169]. Defective clearance of Tau as well as lysosome leakage have been linked to neurodegeneration and are considered to contribute to the Tau build-up in the diseased brain [162, 170, 171].

1.4.3.3 Aggregation

Under pathological conditions, Tau undergoes insufficient degradation and, as such, it accumulates to the cytosol. Due to its structure and its PTM signature, Tau is prone to aggregation. Therefore, aberrant expression of Tau, deregulated PTM status and/or defective degradation of Tau results in the formation of presumed pathogenic forms (fig. 1.7). Pathogenic forms of Tau can act as prions and may spread across the brain. The abnormal distribution of Tau across the brain has been associated with neurodegeneration and is used to characterise the disease progression (Braak stages, section 1.1.3).

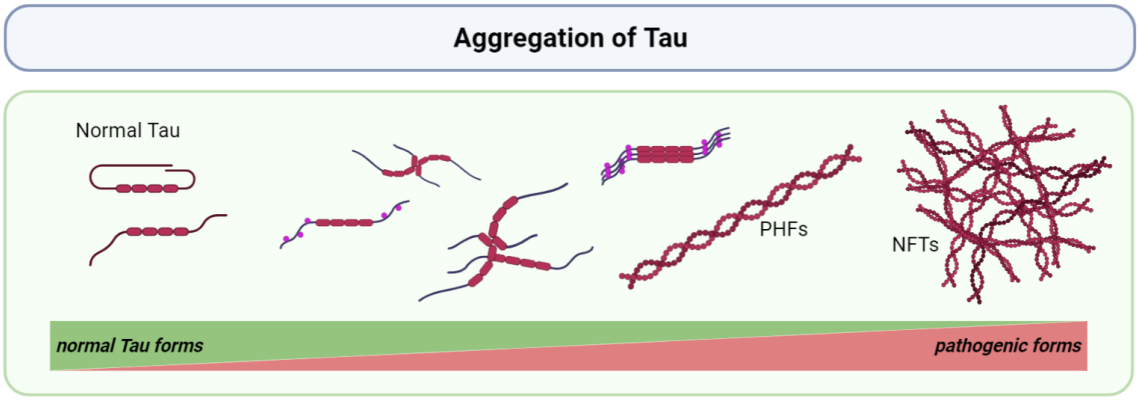

Fig. 1.7 **Tau aggregation and presumed pathogenic forms.** The complexity of Tau regulation and degradation can be illustrated by the different form of Tau that can be formed. Ineffective Tau degradation can lead to Tau accumulation and aggregation. Created in Biorender (https://biorender.com/).

1.5 Tau in the human pancreas

1.5.1 Evidence of Tau in the human pancreas

Although Tau expression in β cells has been described since 1998, it was not until recently that the role of Tau in β cells come into the spotlight. In 2012, a T1D protective SNP within the *MAPT* gene was identified. This was followed by a series of studies proposing that the *MAPT* promoter is active in human islet cells (http://pasqualilab.upf.edu/app/isletregulome,[172, 173]). In addition, the first evidence that Tau mRNA is expressed in human islets was published in 2016 [174, 175] and further studies proposed that Tau protein is present in the human islets [176, 177]. This has drawn attention to Tau and its relevance to the human pancreas. Interestingly, these studies propose that Tau is upregulated in insulinomas [176, 178] as well as in the rat insulinoma cell lines Rin-5F and Glucose-stimulated insulin secretion of insulinoma INS-1E cells [176]. In addition, elevated Tau expression and hyperphosphorylated Tau forms have been reported in the human pancreatic islets of those diagnosed with T2D

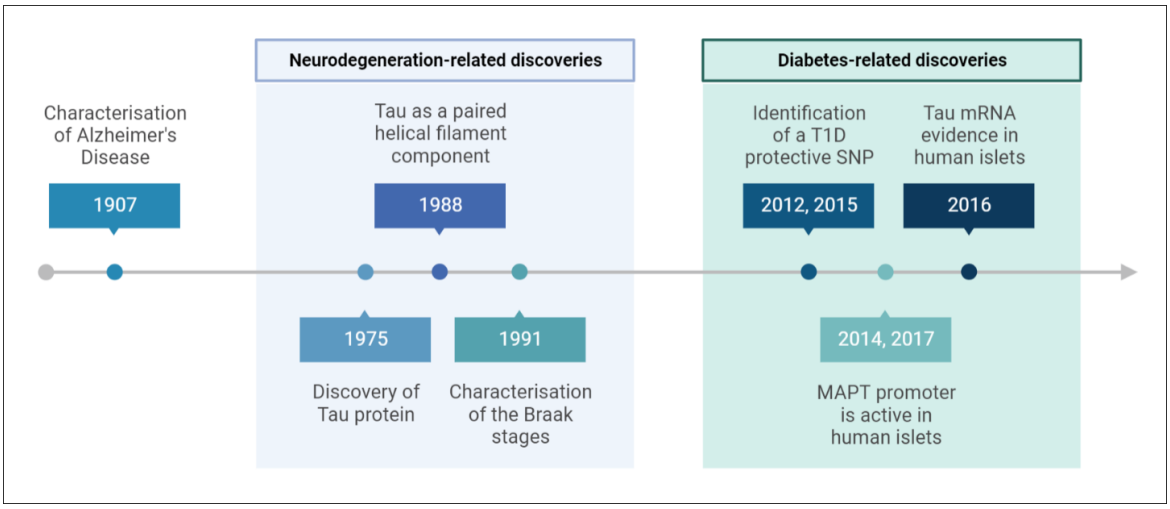

Fig. 1.8 **Neurodegeneration and diabetes related discoveries around Tau since its discovery.** Dr Alois Alzheimer first described Alzheimer's disease (AD) in 1906 and reported some unusual structures in the brain of the 51-year-old woman, Auguste Deter, the first individual to be diagnosed with AD. Tau was discovered in 1975 and was reported to be the main component of paired helical filaments (PHFs) and neurofibrillary tangles (NFTs) in 1988. The identification of a T1D protective SNP in 2012 was followed by a series of discoveries exploring the *MAPT* expression in the human islets.

[179, 177, 180]. Contrary to this, other studies argue that the expression of Tau is restricted to autonomic nerve fibers [181].

1.5.2 Putative role of Tau in β cells

Recent work has provided an interesting basis for studying the functional role of Tau in β cells. The research proposes that the microtubule stability in β cells is heterogenous and that the hyper-stabilization and depolymerization of the microtubules dynamically regulates β cell capacity for glucose stimulated insulin secretion [182], with highly stable microtubules suppressing the glucose stimulated insulin secretion. They further show that high levels of glucose induce rapid microtubule disassembly and induce Tau hyperphosphorylation via glucose-responsive kinases (GSK3, PKA, PKC, and CDK5). They speculate that glucose regulates microtubule disassembly via phosphorylation

of Tau and this then influences the level of insulin secretion [183]. Tau knockdown in mouse β cells not only uncouples microtubule destabilization from glucose stimulation but also increases basal insulin secretion depleting insulin vesicles from the cytoplasm, and impairing glucose stimulated insulin secretion (GSIS) [182]. As such, Tau may play an important role in regulating the microtubule-dependent trafficking of insulin and subsequently have an impact on the secretion of insulin. This work suggests that Tau suppresses microtubules to modulate insulin secretion in basal conditions and preserves the insulin pool that can be released following stimulation. Therefore, Tau may be a key regulator in insulin secretion.

1.6 Tau and Diabetes Mellitus

1.6.1 Diabetes mellitus

Diabetes mellitus describes a set of chronic metabolic disorders. More than 4.9 million people in the UK have diabetes. The predominant forms are type 1 (T1D) and type 2 (T2D) diabetes. T1D is an autoimmune disorder characterised by progression towards absolute insulin deficiency which is caused by pancreatic β cell destruction, whereas T2D is a progressive disease caused by either β cell dysfunction or insulin resistance. Insulin resistance is a condition of insufficient or defective insulin signalling [184, 185].

1.6.1.1 The link between Alzheimer's disease and type 2 diabetes mellitus

A wealth of evidence proposes a strong link between AD and T2D [179, 186–189]. Interestingly, epidemiological studies suggest that 80% of individuals diagnosed with AD, also have T2D or insulin resistance [179, 190]. As previously described, one of the major hallmarks of AD is the presence of intracellular aggregates of hyperphosphorylated Tau protein in NFTs [191] and recent studies have proposed that hyperphosphorylated

Tau forms are also present in the pancreas of individuals with T2D [177]. Therefore, it has been proposed that AD may be 'type 3 diabetes' or the 'diabetes of the brain' and, vice versa, it could be argued that the presence of hyperphosphorylated Tau forms in the human pancreas would further classify diabetes as a secondary tauopathy (section 1.1.2).

Insulin resistance Biochemical findings have demonstrated the presence of insulin, insulin receptors (IRs) and neuronal expression of insulin-sensitive glucose transporter 4 (GLUT4) in the brain, providing important evidence that the brain is a target organ for insulin [192–195]. Insulin has powerful effects on the nervous system, impacting cognition as well as neuronal growth and survival. Insulin resistance correlates strongly with neurodegenerative diseases such as AD [196–198] and in animal models of diabetes [199–201].

T2D is characterised by insulin resistance which can lead to chronic hyperglycemia [202]. Under such conditions, the advanced glycation endproducts (AGEs)-receptor for advanced glycation endproducts (RAGEs) pathways are activated resulting in (i) increased oxidative stress, (ii) increased inflammation and (iii) accumulation of Aβ deposits and of hyperphosphorylated Tau [203–208], both important hallmarks of AD. In AD, the accumulation of Aβ deposits and hyperphosphorylated Tau can lead to increased oxidative stress and increased inflammation leading to insulin resistance [209]. Insulin resistance can directly promote the accumulation of Aβ deposits and hyperphosphorylated Tau forms.

1.6.2 Type 1 diabetes

T1D is characterized by severe loss of insulin secretion and individuals living with T1D require insulin replacement therapy for life. Before the discovery of insulin in 1922 (fig. 1.9a), T1D was a life-ending disease. The first patient to ever receive insulin was

Leonard Thompson, a fourteen year old boy hospitalised at Toronto General Hospital (fig. 1.9b). Leonard's life was in danger; he was cachectic and near death. On 21 January 1922, Leonard was injected with pancreatic extracts and it was observed that his glucose levels dropped [210, 211]. On 23–25 January 1922, a higher potency pancreas extract was prepared. It was observed that following the injection, the glucose levels were normalized, glycosuria was significantly decreased, and ketonuria was cleared. Leonard Thompson lived for 13 years and passed away at the age of 27 years old. Nowadays, 400,000 people are diagnosed with T1D in the UK, including around 29,000 children, the mortality rate has drastically reduced and advances in technology (eg. insulin pen, continuous glucose monitoring, insulin pump) have significantly improved the lives of individuals living with T1D (fig. 1.9a). Pancreas or islet transplantation are options for a small subset of people with T1D.

1.6.2.1 Stages of T1D

In 1984, George Eisenbarth developed a conceptual model for the pathogenesis of T1D that is still used to date (fig. 1.9c) [212]. Although it does not address the increasingly apparent complexity of T1D pathogenesis, the model representatively plots β cell mass against age and characterises the four stages of the development of T1D. Individuals that will develop T1D have a genetic predisposition and islet-specific autoimmunity is triggered by a precipitating event. This is followed by β cell loss, dysglycaemia, clinical diabetes, and progression to complete β cell loss. In summary the four stages of T1D development are;

- Stage I; normal insulin release, normal blood glucose,
- Stage II; normal glucose, progressive loss of insulin release,
- Stage III; clinical diagnosis and,

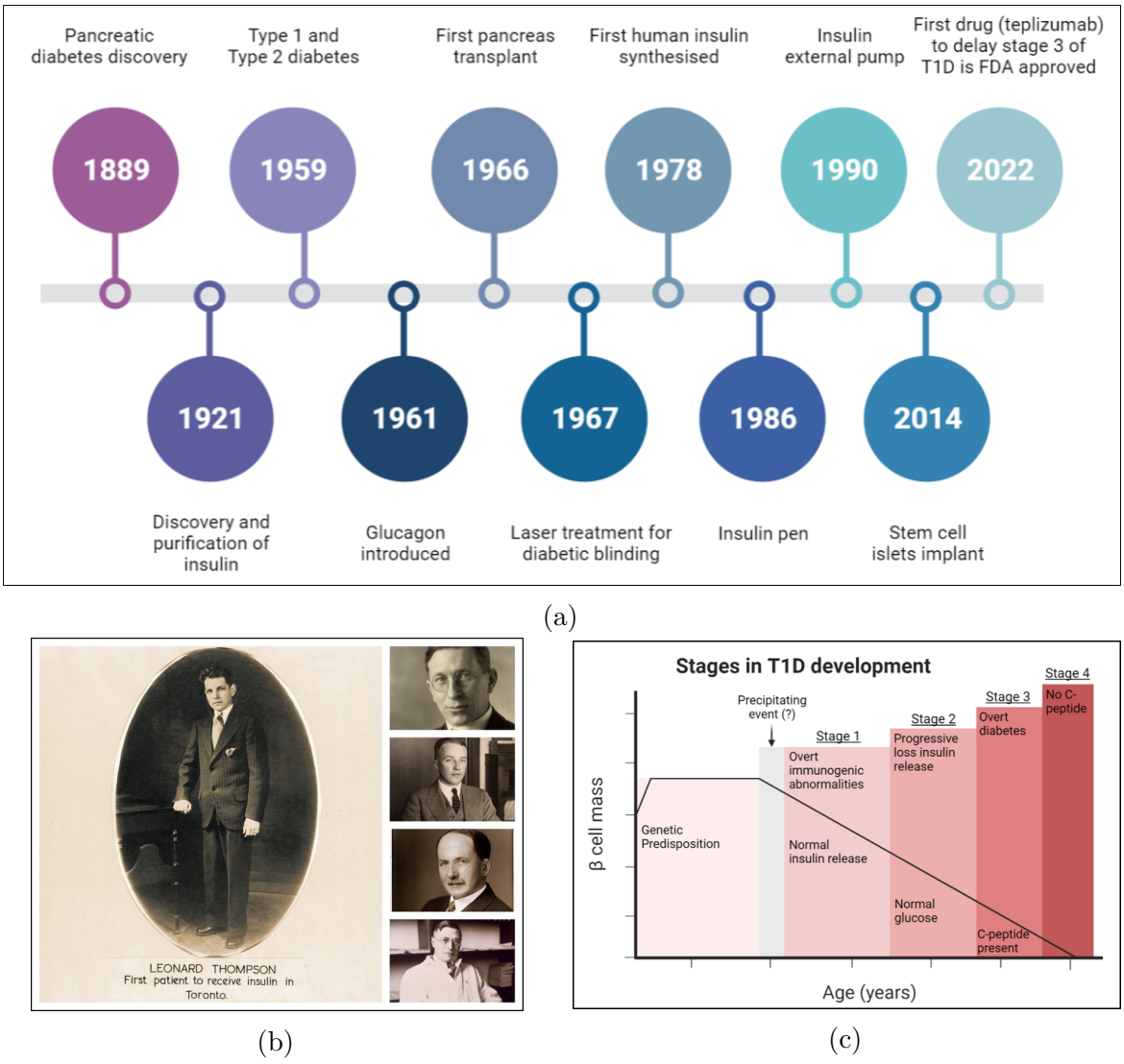

Fig. 1.9 **Type 1 diabetes timeline. 1.9a** | The timeline of type 1 diabetes and insulin-related discoveries. **1.9c** | George Eisenbarth developed a conceptual model that plots β cell mass (y axis) against age (years; x axis). The genetic predisposition is triggered by a precipitating event marks the beginning of type 1 diabetes development. The four stages of type 1 diabetes development are indicated. **1.9b** | Leonard Thompson was the first patient to receive insulin as a treatment for diabetes on January 1921. The team who discovered and purified insulin; Charles Best, Frederick Banting, James Collip, John MacLeod. Created in Biorender (https://biorender.com/).

- Stage IV; long-standing T1D, complete β cell loss.

Stages I-II are presymptomatic whereas Stages III-IV are symptomatic T1D.

1.6.3 Type 2 diabetes

T2D is a progressive disease caused by either β cell dysfunction or insulin resistance and is the most prevalent form of diabetes. In the UK, T2D makes up for 90% of all diabetes cases and T1D makes up for 10%. Strikingly, 850,000 people are estimated to live with T2D and not been diagnosed. Individuals with long term chronic T2D also need insulin replacement therapy. Multiple risk factors have been reported to contribute to T2D, from genetic variants to environmental factors, including sedentary lifestyle, physical inactivity, smoking and alcohol consumption [213–216]. Epidemiological studies demonstrate that obesity is one of the key risk factor for developing insulin resistance or T2D [217].

1.7 Pancreas, β cells and insulin

1.7.1 Pancreas histology

The pancreas is a leaf shaped organ of the digestive system located in the abdomen under the liver and close to the gallbladder, stomach and bowel (fig. 1.10a) and its role is to produce and secrete pancreatic enzymes. The pancreas is composed of two main compartments; the exocrine and the endocrine tissue.

1.7.1.1 Exocrine tissue

The exocrine tissue contains the acinar cells, the functional unit of the exocrine tissue and, their role is to synthesize and secrete digestive enzymes [218]. These enzymes are delivered to the duodenum where they are activated. The delivery of such enzymes is achieved via the pancreatic ducts [219]. The cells that line the ducts, ductal cells also secrete bicarbonate to neutralise stomach acid. The exocrine pancreatic secretion is modulated and controlled by the pancreatic nerves [220].

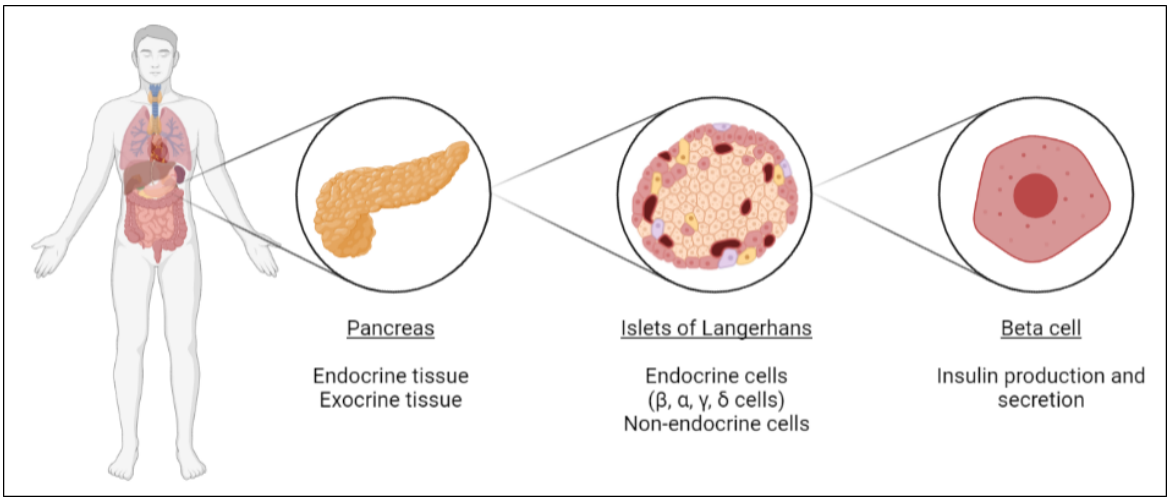

(a)

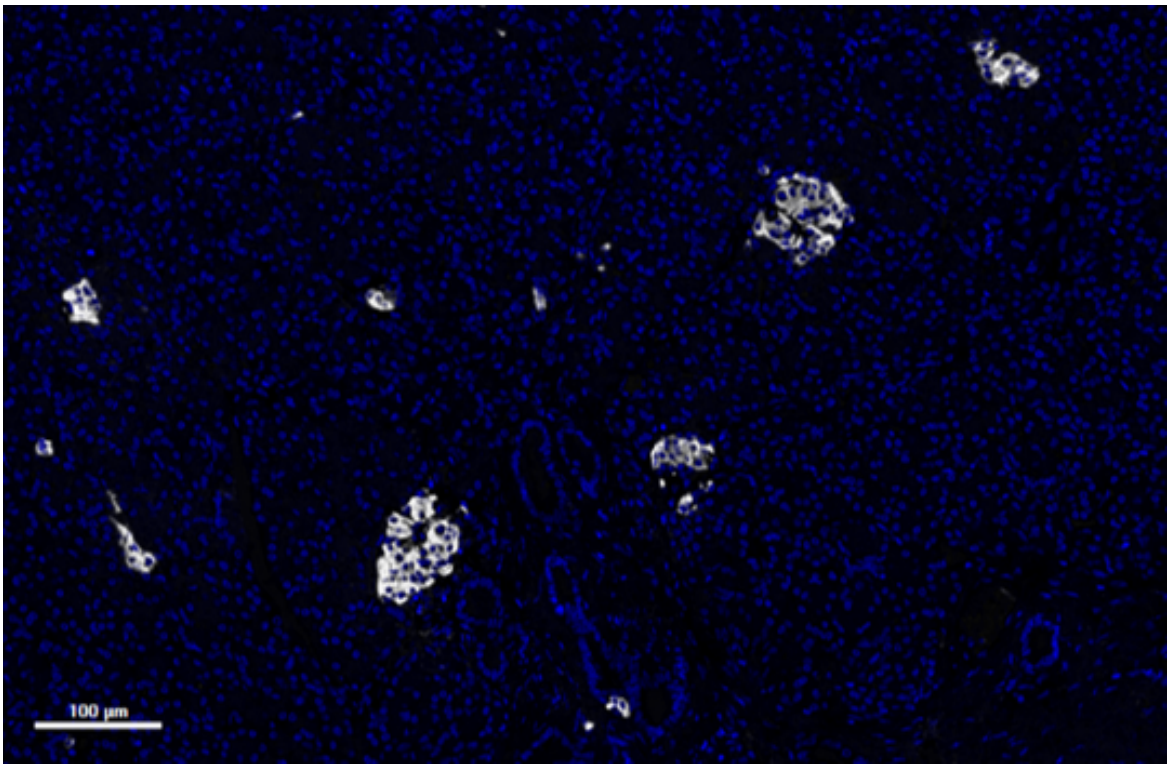

(b)

Fig. 1.10 **Pancreas and cells 1.10a** | The pancreas is located in the abdomen under the liver and close to the gallbladder, stomach and bowel. It consists of the exocrine tissue (98% of the pancreas) and the endocrine tissue (2% of the pancreas). The endocrine tissue, namely Islets of Langerhans, consists of the endocrine and the non endocrine cells. **1.10b** | The Islets of Langerhans visualised under the microscope as small 'islands' spread across the exocrine tissue. FFPE pancreas tissue was stained for DAPI, a marker of the nucleus, (blue) and insulin, a marker of pancreatic β cells, (white). Created in Biorender (https://biorender.com/).

1.7.1.2 Endocrine tissue

The endocrine parts of the pancreas are known as the Islets of Langerhans, referred to as islets from now on. The islets could be described and visualised under the microscope as small 'islands' distributed across the exocrine tissue composing around 1-2% of the pancreas (fig. 1.10b). The islets consist of the hormone-producing β, α, δ, γ and ϵ cells as well as some non-endocrine cells. β cells constitute approximately 60% of the islet cells and are responsible for the production and secretion of insulin, a peptide hormone that regulates blood glucose levels by stimulating the conversion of glucose to glycogen and reduces glucagon secretion by α cells. α cells (20% of the islet cells) are responsible for the production of glucagon, a hormone that helps raise blood glucose and counteracts the actions of insulin by stimulating glucose production in the liver. δ cells (<10% of islets cells) secrete somatostatin, a hormone that potently inhibits insulin and glucagon release from β and α cells, respectively. The communication of pancreatic islet cells is tightly regulated to ensure the appropriate regulation of blood glucose.

Histologically, we should be referring to β cells as insulin-containing β cells. This is because, even though insulin is a good marker of β cells, absence of insulin may not mean absence of β cells. Under disease conditions, such as T1D, there are both insulin-containing islets (ICIs; i.e. islets that contain insulin-containing β cells) and insulin-deficient islets (IDIs; i.e. islets that do not contain insulin-containing β cells). It remains poorly understood whether the T1D IDIs do not have any β cells or they have some 'form' of β cells (e.g. dedifferentiated, transdifferentiated) that no longer produce insulin. To keep it simple, insulin-containing β cells are referred to as β cells.

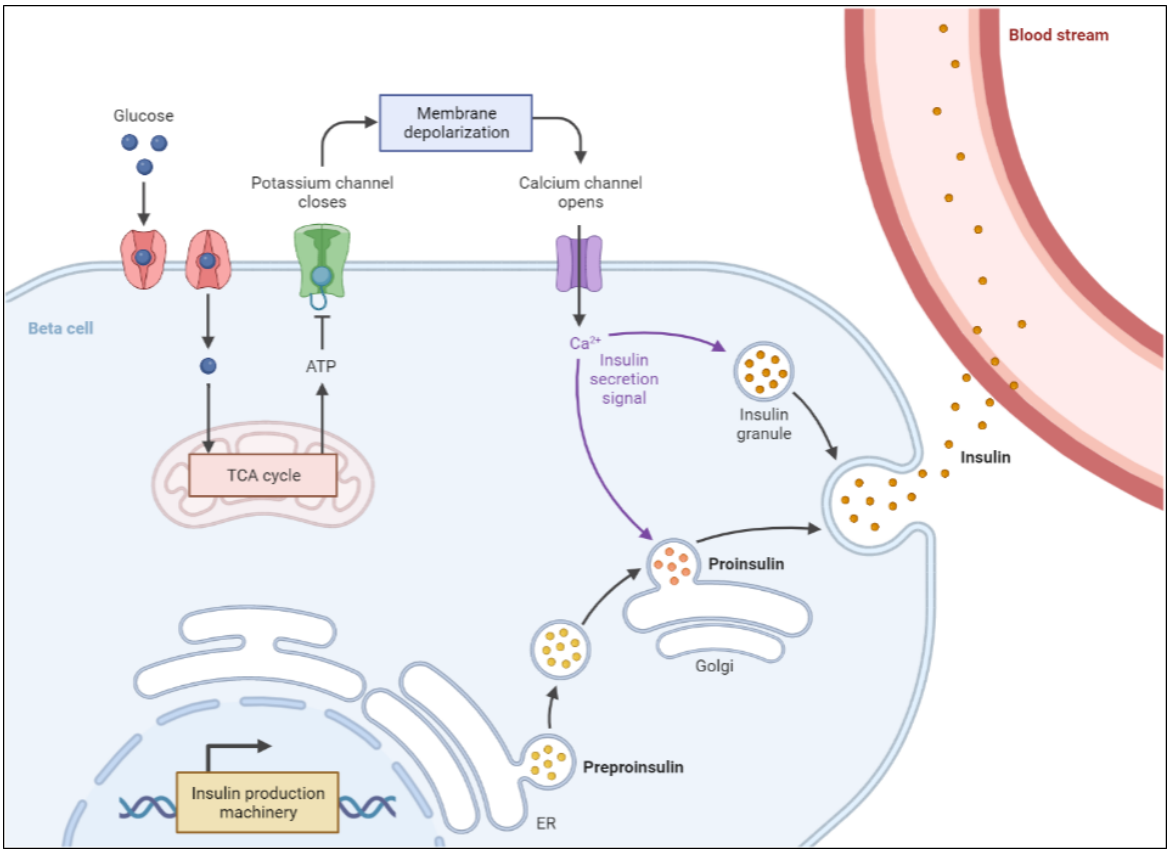

Fig. 1.11 **Glucose-stimulated insulin secretion.** Glucose-stimulated insulin secretion (GSIS). Glucose uptake increases ATP which then closes the potassium channels causing membrane depolarisation. The calcium channel opens and the increased Ca^{2+} promotes insulin secretion. Source; Biorender (https://biorender.com/).

1.7.1.3 Glucose stimulated insulin secretion

Glucose uptake into β cells promotes Ca^{2+} influx [221]. The elevated intracellular glucose results in the increase of ATP, which closes the ATP-sensitive K^+ channels [222, 223]. This leads to membrane depolarisation and the opening of the Ca^{2+} channels. Elevated levels of Ca^{2+} stimulate insulin secretion and the insulin granules undergo exocytosis [224].

1.7.1.4 Rare pancreas tissue resources

The pancreas is located deep in the abdominal cavity, it is highly vascularised and innervated and one of its key functions is to produce digestive enzymes. Due to its location and function, pancreas biopsies are highly invasive and and can be associated with severe post-operative complications. For that reason, access to pancreas donor tissue is limited worldwide and predominantly comes from donors who have sadly died. As such pancreas donor tissue collections are an extremely precious and finite resource, especially when derived from individuals with diabetes. [225, 226]. There are a number of accessible archival and contemporary pancreas biobanks available for researchers. The two used in these studies include the archival Exeter Archival Diabetes Biobank (EADB) formerly known as Foulis Biobank, which is curated in Exeter, and the network of Pancreatic Organs with Diabetes (nPOD) biobank. The EADB consists of predominantly archival, post-mortem pancreatic tissue from individuals both with and without T1D (more details available at (https://pancreatlas.org/). Importantly, this collection hosts the worlds largest of number of donors with T1D collected shortly after diagnosis of disease. The nPOD biobank includes organ donor cadaveric tissue from donors with and without diabetes. The tissue is carefully fixed and processed under standardised conditions, to provide high quality tissue for researchers.

1.7.1.5 T1D

T1D is characterised by a variety of abnormalities that involve both the endocrine and the exocrine pancreas [227]. The endocrine compartment suffers from variable loss of β cells and insulin secretion, as well as, variable distribution and severity of insulitis. β cell dysfunction exists more than 5 years before T1D diagnosis [228].

Recent studies of rare pancreatic donor material from individuals diagnosed soon after onset of T1D, have proposed that T1D is not a single disease and that distinct

endotypes (or different forms) exist [229]. These two endotypes were named "Type 1 diabetes endotype 1" (T1DE1) and "Type 1 diabetes endotype 2" (T1DE2) respectively. Individuals with T1DE1 tended to be diagnosed in individuals under the age of 13y and was associated with a more aggressive immune response and extensive loss of insulin-containing islets at onset. T1DE2, in contrast, was associated with a later diagnosis (>13 years) and was characterised by a less aggressive immune response and the significant retention of insulin-containing islets. These pancreatic endotypes mirror the clinically observed rapid loss of serum c-peptide (a measure of remaining functional β cells) in young individuals, and the retained c-peptide observed in individuals diagnosed later [230]. These observations (i) highlight the heterogeneity of the disease and (ii) propose that the different endotypes may require different treatment approaches.

1.8 Research questions and aims

To date, Tau has been described in the human pancreas of donors with T2D and in insulinomas [231, 178] and preliminary data have identified a SNP positioned on the *MAPT* region which seems to be protective for T1D. However, little is still known about the subcellular localisation of Tau, Tau isoforms and phosphorylated Tau (pTau) forms in the human pancreas. The complexity of Tau structure and PTM status (figs. 1.3, 1.5a) as well as the large number of forms that Tau can acquire (fig. 1.7) require for careful and appropriate planning and data interpretation. To identify and track Tau phosphorylation events, anti-Tau antibodies are widely used and have been previously validated in part in the brain [232–234]. Our unique access to biobanks of human pancreatic tissue allows us to characterise the expression of Tau in the human pancreas across different ages and disease states (T1D, T2D). This allow for future studies to investigate in depth the function of Tau in the pancreatic β cells and assess its role in insulin secretion.

Aims The key aims of this projects are summarised below;

1. Construct a well validated anti-Tau antibody panel and to develop a visualisation method to illustrate the suitability and specificity of each anti-Tau antibody for Western blot (WB) and immunohistochemical (IHC) approaches (Chapter 3). This panel will then allow the study of Tau protein in FFPE tissue.

2. Characterise the expression of Tau isoforms and phosphorylated Tau (pTau) forms in human pancreatic islets (Chapter 4).

3. Explore the expression and localisation of physiological Tau modifiers (cellular kinases and phosphatases) in pancreatic islets and investigate whether these are altered in the pancreas in disease (T1D/T2D) and aging (Chapter 5).

4. Investigate if Tau/pTau expression and localisation changes with disease status (T1D/T2D) or ageing (Development of methodology, Chapter 2, section 2.5).

Chapter 2

Material and Methods

2.1 Tissue samples and antibodies

2.1.1 Tissue samples

2.1.1.1 Human tissue sections

Human pancreas tissue sections were obtained from either the Exeter Archival Diabetes Biobank (EADB; https://pancreatlas.org/) or the network for Pancreatic Organ Donors with Diabetes (nPOD) programme. All EADB samples were used with ethical permission from the West of Scotland Research Ethics Committee (ref: 15/WS/0258). Full ethical approval was available for all nPOD tissue samples studied. Human brain tissue sections are supplied by Dr Irina Stefana (University of Oxford) with full ethical approval. Tissue sections were stained using standard immunohistochemistry (IHC), immunofluorence (IF) and multiplex staining.

2.1.1.2 Mouse tissue sections

rTG4510 mice used in the study were acquired from Eli Lily through collaboration with Dr Jonathan Brown (Exeter University, UK). rTG4510 mice express a repressible

form of human Tau containing the P301L mutation that has been linked with FTD. [235, 236]. Dissected brain was formalin-fixed and embedded in paraffin blocks and 4µM coronal sections were cut from the forebrain of 9-month-old rTg4510 male mice using a Leica RM2235 microtome (Leica Biosystems, Milton Keynes, UK).

Dissected brain and pancreas were formalin-fixed and embedded in paraffin blocks and 4µM saggital sections were cut from 9-month-old male from wildtype, MAPT knockout (MAPT-/-; [237]) and humanised Tau (hTau; [238]) mice, all of which were maintained on a C57Bl/6J background. Mouse brain and pancreas tissue sections were sent by Dr Irina Stefana (University of Oxford).

All housing and experimental procedures were carried out in compliance with the local ethical review panels of the Universities of Exeter and Oxford, respectively, under UK Home Office project licenses held in accordance with the Animals (Scientific Procedures) Act 1986 and the European Directive 2010/63/EU. Animals were housed under 12h light/dark cycle with ad libitum access to food and water.

2.1.2 Antibodies

An antibody (also known as an immunoglobulin) is a Y-shaped molecule produced by B-lymphocytes in response to the presence of an antigen and these antibody-secreting B-lymphocytes (i.e. plasma cells) are the major source of immunoglobulin production (fig. 2.1). Antibodies are the most diverse proteins known and are composed of two heavy chains and two light chains, which are held together by disulfide bonds. Antibodies may be produced by and react with proteins from different species and they have different isotypes (IgG, IgM, IgA, IgD, and IgE) and clonalities (monoclonal, polyclonal, recombinant). Based on how they bind to their immunogen, they can be used in different experimental systems i.e. IHC, WB etc (fig. 2.1).

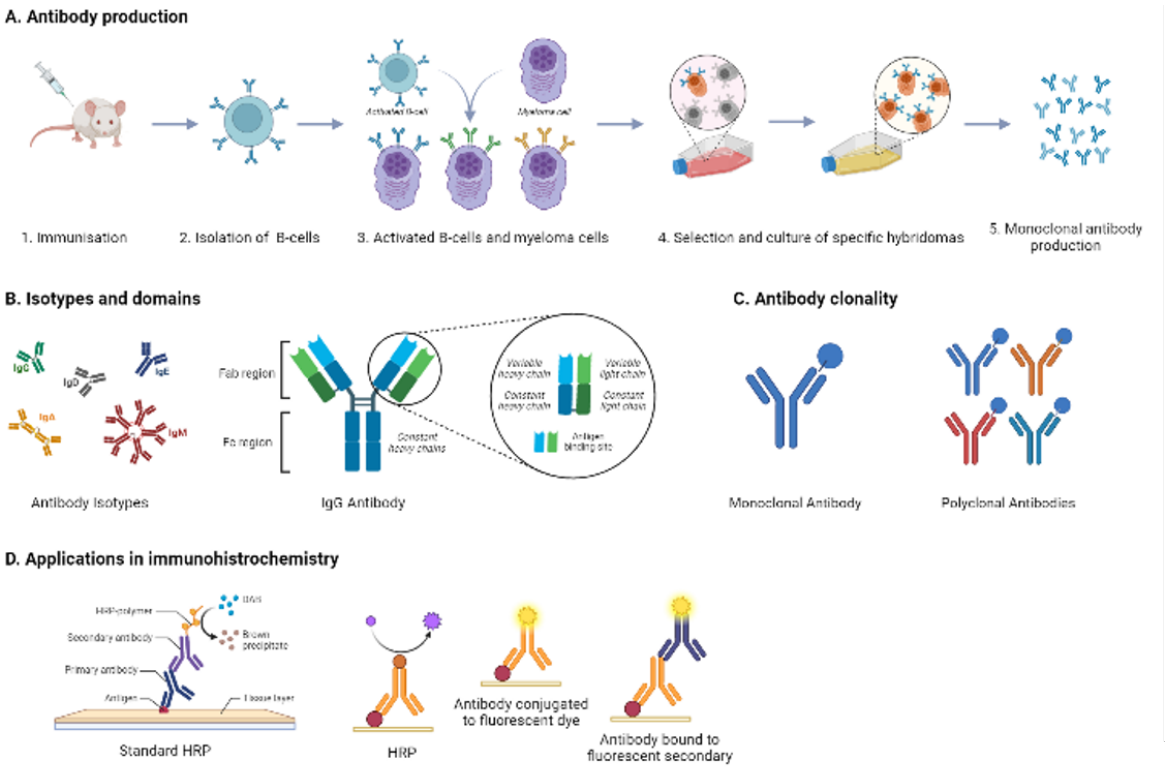

Fig. 2.1 **Antibodies: from production to application. A.** Immunisation of an animal (mouse, rat, rabbit etc) with protein antigen to stimulate an immune response. B-cells are activated, isolated and then co-cultured with myeloma cells to generate hydridomas. The specific hybridomas are selected and cultured to produce monoclonal antibodies. **B.** There are five types of antibodies classified into IgG, IgM, IgA, IgD, and IgE. Most anti-Tau antibodies are IgG1. **C.** Monoclonal antibodies bind to the same epitope on a target antigen and polyclonal antibodies bind to the same antigen, but multiple different epitopes. **D.** Standard Horseradish peroxidase (HRP) staining. Created in Biorender (https://biorender.com/).

To ensure the reproducibility of the experiments, strong emphasis was given to the choice of the antibodies and as such, a pipeline for deciding on an appropriate antibody for use in IHC was developed (fig. 2.2). Online resources such as CiteAb (https://www.citeab.com/), Antibody Registry (https://antibodyregistry.org/), Biocompare (https://www.biocompare.com/) and Alzforum (https://www.alzforum.org/) were utilised to compare antibodies from different suppliers. Parameters such as the clonality, species, reactivity, applications, knock-out (KO) validation were taken into account to

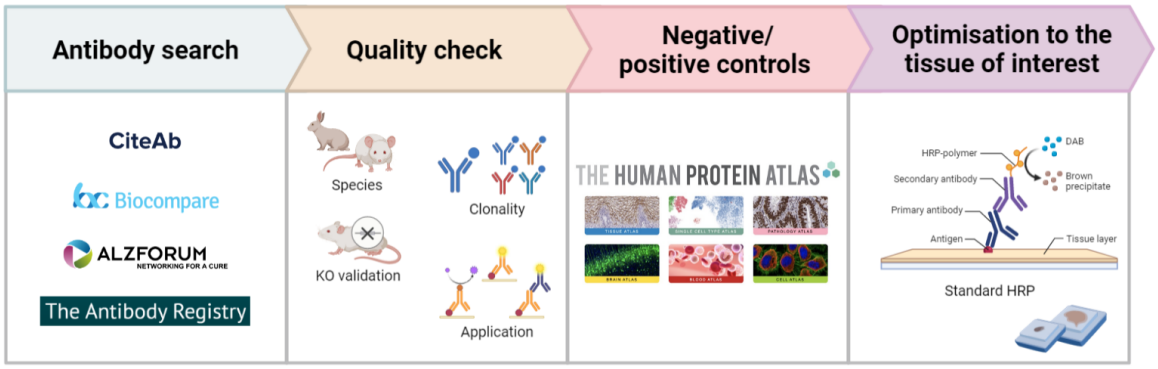

Fig. 2.2 **Pipeline for deciding on appropriate antibodies for use in immunohistochemistry.** This pipeline consists of the four initial steps for deciding on an appropriate antibody for use in immunohistochemistry (IHC). First, trustful companies are queried to generate information about commercially available antibodies allowing comparison between antibodies supplied by different manufacturers. The next step is the quality check of the antibody that ensures that the antibodies meet criteria, such as clonality, species, reactivity, applications. Importantly and if possible, knock-out validated antibodies should be preferred to ensure absence of non-specific signal. Third, the Human Protein Atlas, which is a large database of all the human proteins in cells, tissues and organs using integration of various omics technologies, should be consulted to identify positive and negative controls. Next, the antibody should be optimised in the tissue of interest and its staining pattern should be assessed. Created in Biorender (https://biorender.com/).

determine the optimum antibody for each experiment and/or technique. In addition, The Human Protein Atlas Swedish-based program (https://www.proteinatlas.org/) was consulted to (i) ensure that the antigen is expressed in the tissue of interest and (ii) to identify positive and negative control tissues for staining optimisation. Antibodies were then purchased and optimised in formalin-fixed paraffin-embedded (FFPE) tissue sections.

2.1.2.1 Anti-Tau antibodies

To characterise the expression of Tau protein in relevant mouse models and in the human pancreas, an anti-Tau antibody panel was constructed (Table 2.1). The panel consists of total, isoform-specific, phosphorylation-specific anti-Tau, PHF-raised, oligomeric and

Table 2.1 **Anti-Tau antibodies panel** This table has detailed information about antibodies directed against total Tau, Tau isoforms, phosphorylated and other Tau forms. The antibody name, clone, species, clonality, isotype, supplier and catalog number are indicated here, as well as, detailed conditions for use of these antibodies in immunostaining.

Antibody name [clone]	Species	Clonality	Isotype	Supplier	Catalog no.	Species reactivity	IHC conditions
Total Tau							
ab254256 [EPR22524-95]	Rabbit	monoclonal	IgG	Abcam	ab254256	Human, mouse	1:500 45min RT
N-term	Rabbit	polyclonal	IgG	Abcam	ab227760	Human	1:300 O/N 4°C
5A6	Mouse	monoclonal	IgG1	DSHB	5A6	Human	1:570 1hr RT
SP70	Rabbit	monoclonal	IgG	Abcam	ab93726	Human	1:200 1hr RT
43D	Mouse	monoclonal	IgG1	BioLegend	816601	Human	1:750 O/N 4°C
Tau-12	Mouse	monoclonal	IgG1	Merck Millipore	MAB2241	Human	1:500 1h RT
Tau-13	Mouse	monoclonal	IgG1	Santa Cruz	sc-21796	Human	1:500 1hr RT
HT7	Mouse	monoclonal	IgG1	Thermo Fisher	MN1000	Human	1:50 O/N 4°C
clone 2G9.F10 (aa 157-168)	Mouse	monoclonal	IgG1	BioLegend	824602	Human	1:100 1hr RT
clone 77E9 (aa 185-195)	Mouse	monoclonal	IgG1	BioLegend	814402	Human	1:1000 1hr RT
K9JA	Rabbit	polyclonal	IgG	Dako	A0024	Human, mouse	1:1000 1hr RT
"Ser622" [EP2456Y]	Rabbit	monoclonal	IgG	Abcam	ab76128	Human, mouse	1:350 O/N 4°C
Tau-5	Mouse	monoclonal	IgG1	BioLegend	806401	Human, mouse	1:100 1hr RT
Tau-5	Mouse	monoclonal	IgG1	Thermo Fisher	AHB0042	Human, mouse	1:200 O/N 4°C
Tau-5	Mouse	monoclonal	IgG1	Abcam	ab80579	Human, mouse	1:100 O/N 4°C
Tau-46	Mouse	monoclonal	IgG1	Santa Cruz	sc-32274	Human, mouse	1:65 2hr RT
Tau-2	Mouse	monoclonal	IgG1	Sigma	T5530	Human	1:300 1hr RT
Isoform-specific Tau							
0N Tau [3H6H7]	Mouse	monoclonal	IgG1	BioLegend	823801	Human	1:100 O/N 4°C
2N Tau [71C11]	Mouse	monoclonal	IgG2b	BioLegend	816803	Human	1:2000 O/N 4°C
1N and 2N [EPR2396(2)]	Rabbit	monoclonal	IgG	Abcam	ab109392	Human	1:250 1hr RT
RD3 (3R Tau) [8E6/C11]	Mouse	monoclonal	IgG	Merck Millipore	05-803	Human	1:250 O/N 4°C
4R Tau [7D12.1]	Mouse	monoclonal	IgG	Merck Millipore	MABN1185	Human	1:100 1hr RT
RD4 4R Tau [1E1/A6]	Mouse	monoclonal	IgG	Merck Millipore	05-804	Human, mouse	1:100 1hr RT
4R Tau [5F9]	Mouse	monoclonal	IgG1	BioLegend	823702	Human	1:1000 1hr RT
BigTau	Rabbit	polyclonal	IgG	Sigma	HPA069524	Human	1:5000 O/N 4°C
BigTau	Rabbit	polyclonal	IgG	Sigma	HPA048895	Human	1:400 O/N 4°C
Phospho-Tau							
pThr181 [D9F4G]	Rabbit	monoclonal	IgG	Cell Signalling	12885S	Human, mouse	1:200 O/N 4°C
pSer198 [EPR2400]	Rabbit	monoclonal	IgG	Abcam	ab79540	Human, mouse	1:200 O/N 4°C
pSer199 [EPR2401Y]	Rabbit	monoclonal	IgG	Abcam	ab81268	Human, mouse	1:500 O/N 4°C
pSer202+pThr205 [EPR20390]	Rabbit	monoclonal	IgG	Abcam	ab210703	Human	1:500 O/N 4°C
pSer214 [EPR1884(2)]	Rabbit	monoclonal	IgG	Abcam	ab170892	Human, mouse	1:100 O/N 4°C
pThr231 [EPR2488]	Rabbit	monoclonal	IgG	Abcam	ab151559	Human, mouse	1:500 O/N 4°C
pSer238 [12G10]	Mouse	monoclonal	IgG1	Abcam	ab128889	Human	1:200 O/N 4°C
pSer262	Rabbit	polyclonal	IgG	Thermo Fisher	OPA1-03142	Human	1:400 O/N 4°C
pSer396 [EPR2731]	Rabbit	monoclonal	IgG	Abcam	ab109390	Human, mouse	1:300 O/N 4°C
E178 (pSer396)	Rabbit	monoclonal	IgG	Abcam	ab32057	Human, mouse	1:750 O/N 4°C
pSer404 [EPR2605]	Rabbit	monoclonal	IgG	Abcam	ab92676	Human, mouse	1:250 O/N 4°C
pSer409	Rabbit	polyclonal	IgG	Thermo Fisher	44-760G	Human, mouse	1:100 O/N 4°C
pSer422 [EPR2866]	Rabbit	monoclonal	IgG	Abcam	ab79415	Human	1;58 O/N 4°C
PHF-raised Tau							
AT8	Mouse	monoclonal	IgG1	Thermo Fisher	MN1020	Human, mouse	1:500 O/N 4°C
AT100	Mouse	monoclonal	IgG1	Thermo Fisher	MN1060	Human	1:100 1hr RT
AT180	Mouse	monoclonal	IgG1	Thermo Fisher	MN1040	Human	1:50 O/N 4°C
PHF-13 (pSer396)	Mouse	monoclonal	IgG2b	BioLegend	829001	Human	1:250 O/N 4°C
Oligomeric Tau							
T22	Rabbit	polyclonal	IgG	Merck Millipore	ABN454	Human	1:1000 O/N 4°C
Other (PTM-specific) Tau							
Tau-1 [PC1C6]	Mouse	monoclonal	IgG2a	Merck Millipore	MAB3420	Human, mouse	1:200 O/N 4°C
D421 [Tau-C3]	Mouse	monoclonal	IgG1	Merck Millipore	MAB54030-C	Human, mouse	1:100 O/N 4°C
Blocking peptides							
pSer396 blocking peptide	Rabbit	monoclonal	IgG	Abcam	ab226770	Human, mouse	-

Table 2.2 **Antibodies against Tau modifiers, endocrine cells and other targets.** This table has detailed information about antibodies directed against Tau modifiers and markers of endocrine cells. The antibody named, clone, supplier, species, clonality and isotype are indicated here, as well as, detailed conditions for use of these antibodies in immunofluorescence staining.

Antibody name [Clone]	Species	Clonality	Isotype	Supplier	Catalong no.	IHC conditions
Kinases						
GSK3b [3D10]	mouse	monoclonal	IgG2a	Abcam	ab93926	1:200 O/N 4°C
pGSK3b [Y174]	rabbit	monoclonal	IgG	Abcam	ab183177	1:1000 1h RT
pGSK3b [EPR2286Y]	rabbit	monoclonal	IgG	Abcam	ab75814	1:1000 O/N 4°C
CDK5 [EP715Y]	rabbit	monoclonal	IgG1	Abcam	ab40773	1:100 1hr RT
CDK5	rabbit	polyclonal		CST 2506	2506	1:100 1hr RT
MARK4 [OTI9B7]	mouse	monoclonal	IgG1	Thermofisher	TA808507	1:150 1hr RT
DYRK1A	mouse	monoclonal	IgG	Novus Biologicals	H00001859-M01	1:380 1hr RT
Phosphatases						
PIN1 [G-8]	mouse	monoclonal	IgG2a	Santa Cruz	SC-46660	1:50 O/N 4°C
PIN1	mouse	monoclonal	IgG2b	R&D Systems	MAB2294-SP	1:87.2 O/N 4°C
PP2A [81G5]	rabbit	monoclonal	IgG	CST	2041	1:100 1hr RT
SET	rabbit	monoclonal	IgG	Abcam	ab181990	1:250 1hr RT
SET	rabbit	polyclonal	IgG	Protein Tech	55201-1-AP	1:100 1hr RT
SET/I2PP2A	mouse	monoclonal	IgG2a	Santa Cruz	SC-133138	1:200 1hr RT
Deacetylases						
HDAC6 [EPR1698(2)]	rabbit	monoclonal	IgG	Abcam	ab133493	1:50 1hr RT
Endocrine cells						
Insulin [ICBTACLS biotin]	mouse	monoclonal	IgG2aκ	Invitrogen	13-9769-80	1:200 1hr RT
Insulin [ICBTACLS]	mouse	monoclonal	IgG2aκ	Invitrogen	14-9769-82	1:400 1hr RT
Insulin	guinea pig	polyclonal		Dako	A0564	1:2 1hr RT
Glucagon	mouse	monoclonal	IgG1	Abcam	ab10988	1:2000 1hr RT
Glucagon [EP3070]	rabbit	monoclonal	IgG	Abcam	ab92517	1:4000 1hr RT

other anti-Tau antibodies. The anti-Tau antibodies included in this panel are widely used in research to study healthy and/or AD brain. The entire panel was validated for use in WB at the University of Oxford and/or IHC at the University of Exeter on relevant mouse models (Chapter 3). A selection of validated anti-Tau antibodies were then tested in the human pancreas (Chapter 4).

2.1.2.2 Identification of endocrine cells and Tau modifiers

Endocrine cells To characterise the subcellular localisation of Tau in the human pancreas and more specifically within the islets, antibodies against insulin, a marker of β cells and, glucagon, a marker of α cells were also utilised (Table 2.2). These antibodies have been optimised in the lab previously.

Tau modifiers To explore which Tau modifiers impact on the PTM signature of Tau in the human pancreas, a pipeline for identifying the key Tau modifiers in the brain and exploring their expression in the human pancreas in age and disease states (T1D/T2D) was developed (Chapter 5, pg. 165). The published literature was extensively searched and the TauPTM online tool for the visualization of Tau PTMs was also consulted to correlate modifiers and relevant Tau residues (https://abbvie1.outsystemsenterprise.com/tauptm/) [233]. β cell and pancreas RNAseq data were also explored to interrogate the expression of a selection of Tau modifiers. The relevant antibodies were purchased using the criteria described above (fig. 2.2). This allowed the construction of a panel of antibodies against Tau modifiers (Table 2.2) which where optimised in FFPE pancreas tissue (Chapter 5, pg. 165).

2.2 Sequence analysis of Tau

2.2.1 BLAST of Tau

To investigate whether Tau amino acid sequence presents similarities with other proteins, BLAST analysis of the Tau amino acid sequence was performed using the UNIPROT database of protein sequence and functional information (https://www.uniprot.org/).

2.3 Transcriptomics

To characterise the gene expression of Tau and a selection of Tau modifiers, we explored three RNA sequencing (RNAseq) databases;

- Next Generation RNAseq bulk β cell data from individuals diagnosed with (n=4) and without T1D (n=12) [239]. All bulk and single-cell RNA-Seq data

are available in the Gene Expression Omnibus repository (DataSet Identifier GSE121863).

- Next Generation RNAseq data from adult (n=7) and fetal (n=6) β cells and adult (n=6) and fetal (n=5) α cells [240]. RNA sequence data are deposited in the GEO database (http://www.ncbi.nlm.nih.gov/geo/).

- Next Generation RNAseq data from pancreatic islets of individuals diagnosed with (n=4) and without T2D (n=6) ([175]). Exploration of these data is allowed by the online database Sandberg (https://sandberglab.se/tool/pancreas/).

RNA sequencing data have been normalised in different ways and the gene expression levels between the datasets are not directly comparable but give an indication of relative levels of expression.

Statistical analysis Statistical analysis was performed using R, an open-source programming language that extensively supports built-in packages and external packages for statistical analysis. t-test was performed to explore whether there is any significant difference between two groups. The Bonferroni correction was used to adjust probability (p) values because of the increased risk of a type I error (false positive). Significant difference was assessed using the corrected p value (p.adj value). The p.adj value was used to determine if there is a significant difference between the groups of interest.

2.4 Antibody optimisation in tissue

2.4.1 Immunohistochemistry

To validate and optimise antibodies, a standard immunoperoxidase technique for paraffin sections was performed[1]. Human pancreas tissue sections were obtained from the EADB or nPOD collection. FFPE blocks were sectioned at 4μm. After the removal of wax with histoclear, the sections were rehydrated in degrading ethanols (100%, 90%, 70%) and permeabilized in 100% methanol. Heat-induced epitope retrieval (HIER), using a 10μM citrate buffer at a pH of 6 (recipe at Appendix A, Table A.1a), was performed to unmask the epitopes by placing the sections in a plastic pressure cooker in a microwave oven on full power for 20 min, unless specified otherwise. The sections were blocked with 5% normal goat serum (NGS) and incubated with the primary antibody (Tables 2.1, 2.2). The sections were then blocked with Dako REAL peroxidase blocking solution (S2023), probed with the secondary antibody Dako REAL^{TM} EnVision^{TM} /HRP, Rabbit/mouse (ENV) (Dako, Cat. #K5007) and stained with 3,3-Diaminobenzidine (DAB) substrate working solution according to the manufacturer's instructions. After haematoxylin (Sigma-Aldrich, Cat. #H3136), 2% copper sulphate (CuSO4) ((recipe at Appendix A, Table A.2b), Scott's Tap Water Substitute (STWS) ((recipe at Appendix A, Table A.2c) and counterstain, the sections were dehydrated and mounted using Dibutylphthalate Polystyrene Xylene (DPX) (Sigma-Aldrich, Cat. #06522) mounting medium. Microscopy was performed using the Nikon ECLIPSE 50i brightfield microscope.

[1] All general buffer recipes are included in the Appendix A.

2.4.2 Immunofluorescence

To determine which endocrine cells express the different proteins of interest and to examine their cellular localisation, immunofluorescence (IF) staining was performed. The sections were dewaxed, rehydrated, permeabilized in graded ethanols to 50% ethanol and HIER was performed as described above. The sections were blocked with 5% NGS and the Avidin Biotin Blocking Kit (Vector SP-2001) and were then incubated with the relevant primary antibody (Tables 2.1, 2.2). Primary antibodies of different species were probed with appropriate goat anti-mouse or anti-rabbit Alexa Fluor dyes (Table 2.3). To combine antibodies of the same species, the Tyramide Signal Amplification (TSA) technique was performed according to the manufacturers instructions (ThermoFisher #B40922). The TSA substrate binds irreversibly to the tissue at the location of the epitope. As such, the section is incubated with the first primary antibody which is then probed with the appropriate secondary in tyramide working solution and, the reaction is then stopped by adding equal amount of stop solution. This is followed by HIER to remove the primary antibody before staining with the next antibody from the same species and the appropriate secondary antibody. DAPI, 1μg/ml in Dako antibody diluent, was used to stain the nuclei. The sections were mounted using the Dako Fluorescence mounting medium (Dako, #53023). Microscopy was performed using the Leica DM4 B DFC7000T fluorescent microscope (Leica Microsystems, Milton Keynes, UK) and/or Leica DMi8 SP8 LIGHTNING modular (Leica Microsystems, Milton Keynes, UK) confocal microscope or tissue sections were imaged using the Akoya Vectra®Polaris™ slide scanner.

2.4.2.1 Blocking peptides

To validate the specificity of the antibodies, blocking peptide experiments were performed. The relevant primary antibody (pSer396 [EPR2731], pTau-E178) was incubated

Table 2.3 **Secondary antibodies.** This table has detailed information about secondary antibodies The antibody name, supplier, species and isotype are indicated here, as well as, detailed conditions for use of these antibodies in immunofluorescence staining.

Antibody	Supplier, Catalog No.	Species	Conditions (IF)
AlexaFluor 488	ThermoFisher, A11029	goat anti-mouse	1:400 1hr RT
AlexaFluor 488	ThermoFisher, A11006	goat anti-rabbit	1:400 1hr RT
AlexaFluor 555	Abcam, ab150114	goat anti-mouse	1:400 1hr RT
AlexaFluor 555	ThermoFisher, A21429	goat anti-rabbit	1:400 1hr RT
AlexaFluor 647	ThermoFisher, A21236	goat anti-mouse	1:400 1hr RT
AlexaFluor 647	ThermoFisher, A21245	goat anti-rabbit	1:400 1hr RT
Streptavidin 647	ThermoFisher, S21374	-	1:400, 1hr RT
AlexaFluor 488	ThermoFisher, B40922	goat anti-rabbit	1:400 1hr RT

with or without the relevant blocking peptide (pSer396 BP; which was x5 more concentrated than the primary antibody according to the supplier's instructions) overnight (Table 2.1). The buffers were labelled as blocked and control buffer, respectively. Serial tissue sections were dewaxed, rehydrated, permeabilized in graded ethanols to 50% ethanol and HIER was performed as described above. The sections were blocked with 5% NGS, incubated with either the blocked or the control buffer and probed with appropriate secondary antibody conjugated to Alexa Fluor dyes. DAPI was used to stain the nuclei. Microscopy was performed with using the Leica AF. Absence of signal on the section containing the peptide-bound antibody demonstrates that (i) the antibody binds to that specific peptide and, (ii) the antibody does not bind other non-specific antigen within the tissue. If immunostaining is observed, this raises concerns about the antibody specificity.

2.4.2.2 Phosphatase treatment

To test the specificity of phosphorylation-specific labelled antibodies, phosphatase treatment was performed. Human pancreas and/or mouse brain sections were dewaxed, rehydrated, permeabilized in graded ethanols to 50% ethanol and HIER was performed as described above (section 2.4.1). The sections were treated with lambda

(λ) phosphatase (10,000U/ml), 1mM MnCl2 (Biolabs #B17615) and 1x PMP buffer (Biolabs #B07615) overnight. The sections were then blocked with 5% NGS and incubated with primary antibody of interest, which was then probed with appropriate secondary antibody conjugated to Alexa Fluor dye. DAPI was used to stain the nuclei. Microscopy was performed with using the Leica AF. If the signal was abolished after the λPP treatment, the antibody was identified as a phosphorylation specific antibody. If the signal was unaltered, the antibody was identified as a non-phosphorylation specific (most likely to be a total Tau antibody). If the signal was increased, thus suggesting that the antibody may detect a dephosphorylated form preferentially.

2.4.2.3 Thioflavin S

To investigate whether an antibody has the ability to detect Tau aggregates, Thioflavin S (ThioS) was used. ThioS is a green fluorescent β-sheet dye that binds to protein fibrils but does not bind monomers. Human pancreas and/or mouse brain tissue sections were dewaxed, rehydrated, permeabilized in 50% ethanol and HIER was performed as described above. The sections were blocked with 5% NGS and incubated with primary antibody of interest, which was then probed with secondary antibody conjugated to Alexa Fluor dye. The sections were then stained with ThioS (Sigma #T1892). Microscopy was performed using the Leica AF. If there is co-localisation of the primary antibody and Thioflavin S detects the same structures, the antibody can bind aggregates. If not, it suggests it detects monomers.

2.4.2.4 Formic acid

Previous studies have used formic acid (FA) treatment to expose nuclear Tau epitopes in autopsy brain tissue [241]. To investigate whether FA treatment would have a similar effect on the binding of select anti-Tau antibodies, human pancreas tissue sections were

treated with FA (Merck Millipore, #64-18-6) and stained with specific Tau antibodies. The sections were dewaxed, rehydrated, permeabilized in graded ethanols to 50% ethanol and HIER was performed as described above (section 2.4.1). The sections were then treated with 10% FA diluted in distilled water (pH 1.6-2). Following incubation, sections were blocked with 5% NGS and incubated with the primary antibodies of interest, which were then detected using appropriate secondaryconjugated to Alexa Fluor dyes. Microscopy was performed using the Leica AF.

2.4.3 Image analysis

Quantification analysis of the immunofluorescent signal of a selection of markers was performed using the HALO®software, a gold standard image analysis platform for quantitative tissue analysis. Fluorescence images were inputted into HALO followed by a dynamic multistep process to phenotype the cells (fig. 2.3). For each image, the region of interest (ROI) was manually annotated (typically a specific brain region or islets). When the region of interest was a part of the human pancreas, extra caution was taken as the pancreas is a highly vascularised and innervated organ. To minimise false positive signal, blood vessels (which are highly autofluorescent structures) and nerves (which produce a very strong signal from Tau) were excluded from the ROIs.

The Highplex FL module (Indica Labs) allowed for simultaneous analysis of multiple fluorescent markers in different cellular compartments. This module was utilised to allow for the detection of immunostaining in the nucleus, cell membrane and cytoplasm. The first step was to identify the nuclei. Nuclear detection requires that several parameters be optimised. These include nuclear contrast and intensity, nuclear segmentation aggressiveness and nuclear roundness. The DAPI immunostain facilitated careful assessment of the efficiency of the nuclear detection. The next step is to identify cell membranes. Unfortunately, there are no good membrane markers available for the

detection of the β cell membrane. As such, the cytoplasm radius and cell size were set manually. Both were set in a way that was most representative to what was observed by the eye.

Next, the nucleus and cytoplasm positive signal threshold were set. This is an important step that allows the detection of the marker of interest and it will also be a key factor in cell phenotyping. For example, a tissue slide was stained for (i) Tau, (ii) insulin, (iii) glucagon and (iv) DAPI. β cells were defined as insulin-positive and glucagon-negative cells. α cells were defined as insulin-negative and glucagon-positive cells. Cells that were double positive for insulin and glucagon were defined as bihormonal cells. Cells that were double negative for insulin and glucagon were defined as non-insulin non-glucagon containing cells. Such cells could represent a broad category of cells; insulin-deficient β cells, γ, δ and/or ϵ cells. Therefore, even though in this example there are only two markers of two different endocrine cells, Highplex FL module and appropriate cell phenotyping allows the study of four distinct cell groups.

Signal quantification in the brain The Highplex FL module was used to quantify the signal intensity of anti-Tau antibodies in the rTg4510 mouse brain sections (cortex). The DAPI immunostain allowed careful assessment of the efficiency of the nuclear detection. The cytoplasm radius and cell size were set manually. Both were set in a way that was most representative to what was observed by the eye. Cell types (i.e. neurons) were phenotyped either as Tau positive or Tau negative.

Statistical analysis The object analysis data were outputted and saved as an Excel file. The outputted data provided information about the nuclear and cytoplasmic intensity of each marker. The intensity is described as the mean fluorescent intensity (MFI) per cell. Other information include measurements of the nucleus, cytoplasmic and cell area and the nucleus perimeter and roundness. Statistical analysis was performed

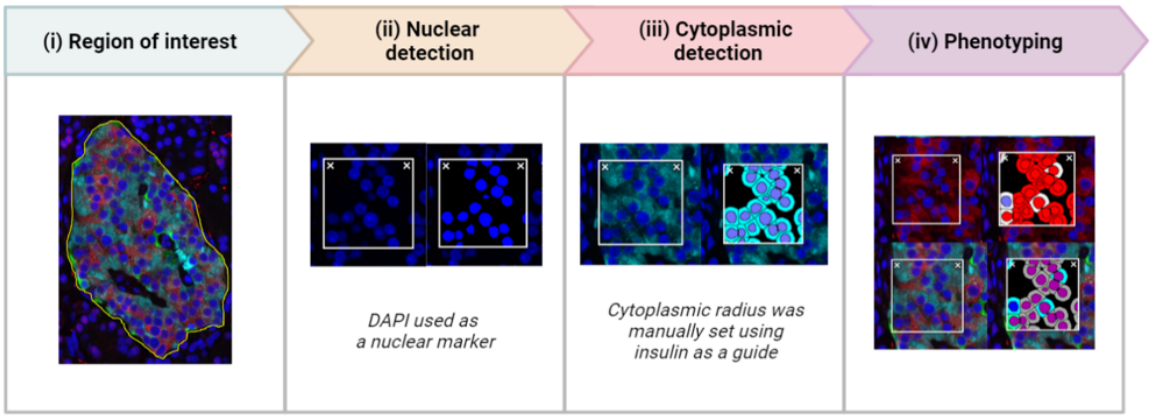

Fig. 2.3 **HALO image analysis pipeline.** The pipeline of image analysis using HALO software consists of four main steps. As an example, we have here considered a quantification analysis on the expression of certain markers expressed within an islet. (i) The annotation of the region of interest (ROI; islet) is highlighted with a yellow line. Within that ROI, the parameters were adjusted to allow for (ii) nuclear and (iii) cytoplasmic detection. To detect the nucleus, DAPI was used as a marker. Unfortunately, as there is no good marker for the β cells membrane, the cytoplasmic radius was manually set. (iv) The nucleus and cytoplasm positive threshold were set for each marker and that was then used to phenotype the cells. Tau (red), insulin (cyan), glucagon (green), DAPI (blue). Created in Biorender (https://biorender.com/).

on the signal quantification data using R, an open-source programming language. t-test was performed to explore whether there is any significant difference between two groups. The Bonferroni correction was used to adjust probability (p) values because of the increased risk of a type I error (false positive). Significant difference was assessed using the corrected p value (p.adj value). The p.adj value was used to determine if there is a significant difference between the groups of interest.

2.5 Development of multiplex staining protocol for Tau forms in human tissue

The findings presented in Chapter 4 demonstrate that multiple forms of Tau are present in human β cells. In order to establish how these different forms relate to one another

and to determine if these forms are altered with ageing and/or disease, the development of a multiplex panel followed.

2.5.1 Limitations

Appropriate anti-Tau antibody validation (Chapter 3) and careful characterisation of Tau forms within the human islets (Chapter 4) allow the construction of a multiplex anti-Tau antibody panel to thoroughly interrogate the expression of specific Tau forms in donors from a range of ages and disease states. The multiplex staining technique allows the combination of up to six unlabelled primary antibodies, including antibodies of the same species and DAPI - so seven coloured markers in total. The aim was to develop a panel of at least five anti-Tau antibodies, one anti-insulin antibody and DAPI to stain tissue slides from a number of donors (range of age and disease states). However, due to COVID limitations impacting on lab accessibility, the development of the Phenoptics assay was heavily impacted and as such, the antibody panel proposed here has not yet been used to stain the relevant pancreas tissue sections. However, valuable insight has been gained that allows the analysis to be completed in future studies.

2.5.2 Phenoptics assay philosophy

OPAL™ is a staining method for multiplex fluorescent IHC in FFPE tissue. It was initially developed for diagnostic purposes but it is becoming more and more popular in the research field. The technique described here allows the combination of up to seven markers in total. The probing of the primary antibodies is achieved by the use of OPAL™ reactive fluorophores. This technique ensures that after the labelling of the primary antibody, the antibody is removed in a way that does not interfere with its fluorescence signal and, as such, avoids antibody cross reactivity.

Vectra® Polaris™ (VP) is a slide scanner used to perform multispectral imaging. It is a multiplexed biomarker imaging system that allows the spectral unmixing of overlapping fluorophores (i.e. OPAL™ fluorophores, Alexa fluorophores) and tissue autofluorescence (AF). An important advantage of this technique is that it allows the acquisition of whole slide scans that can been normalised in a way that eliminates any fluorophore crosstalk and interference from tissue AF signal. As such, OPAL™ staining method allows the analysis of whole slide scans stained for up to seven markers ensuring that there is limited possibility of antibody cross reactivity, fluorophore crosstalk and interference from tissue AF signal within the tissue. In order to do this though, careful optimisation must be performed.

OPAL™ multiplex protocol The OPAL™ staining protocol is an intense five day protocol (fig. 2.4). The sections are baked at 60°C for 2 hours, dewaxed, fixed in 10% neutral buffered formalin (NBF) and then rehydrated in degrading ethanols (100%, 95%, 70%). HIER was performed to unmask the epitopes by placing the sections in a pressure cooker in a microwave oven on full power for 20 min. The sections were blocked with 5% NGS and incubated with the primary antibody (Table 2.4). The primary antibody was then probed with an appropriate OPAL™ secondary antibody conjugated to a fluorophore. This was followed by HIER to remove the primary antibody before staining with the next primary/secondary combination. The same steps (from blocking to antigen retrieval) were repeated six times (for each of the six primary/secondary combinations). The sections were counterstained with DAPI and mounted for fluorescence microscopy which was performed using the VP.

2.5.3 Manufacturer's workflow

According to the manufacturer's protocol, the Phenoptics assay is a four stage protocol that requires careful experimental design. The four stages are (i) primary antibody

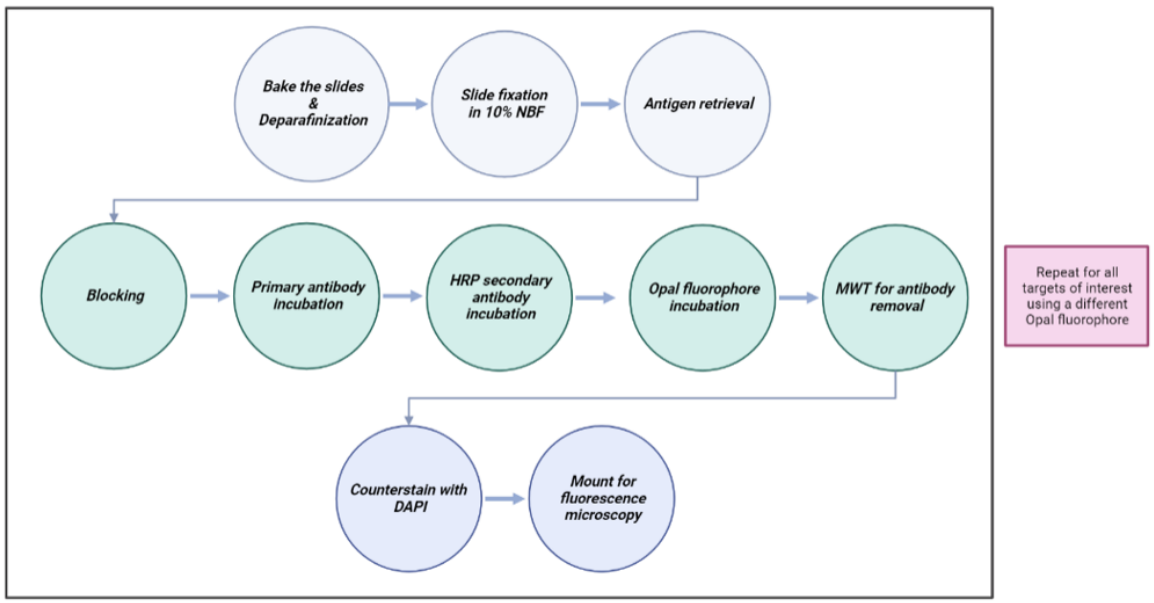

Fig. 2.4 **Development of multiplex staining protocol detecting a single marker in human pancreas tissue.** The Opal staining protocol is an intense and long protocol that consists of 10-steps. The tissue slides are (1) baked for 2hrs and dewaxed and (2) fixed in 10% neutral buffered formalin (NBF). (3) Antigen retrieval unmask the epitopes. (4-8) The tissue section is blocked, incubated with the primary antibody, the HRP secondary antibody and Opal fluorophore and then antigen removal is performed to remove the primary antibody. These steps (4-8) are repeated for all targets of interest using a different Opal fluorophore. (9) The tissue sections are then counterstained with DAPI and (10) mounted for fluorescence microscopy). Created in Biorender (https://biorender.com/).

titration, (ii) library development and assessment of OPAL monoplex results, (iii) OPAL multiplex assay development and (iv) image analysis (fig. 2.5).

2.5.3.1 Stage 1: Primary antibody titration

The relevant primary antibodies are selected and paired with appropriate OPAL™ secondary fluorophores. According to the manufacturer, markers that produce a weak signal should be paired with OPAL™ fluorophores that produce a strong signal and vice versa. It is also advised that markers directed against structures that are in close proximity should be paired with OPAL™ fluorophores that have distant spectrum to ensure optimal spectral unmixing. Each antibody is then optimised for appropriate

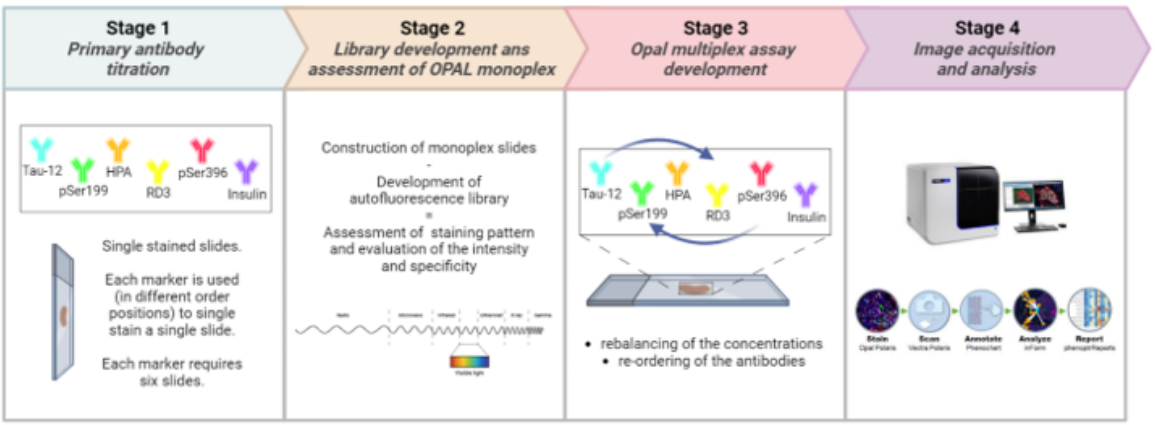

Fig. 2.5 **Development of the Phenoptics assay as suggested by the manufacturer.** The Phenoptics assay is a four stages workflow. (i) Stage 1: Primary antibody titration (section 2.5.3.1). Each marker is paired with a single OPAL fluorophore and is used to single stain a total of six slides in different order positions. The single stain signal is assessed to confirm appropriate staining pattern. (ii) Stage 2: Library development and assessment of OPAL monoplex (section 2.5.3.2, fig. 2.6). (iii) Stage 3: OPAL multiplex assay development (section 2.5.3.3). The order of the antibodies is selected. AF removal is performed to the multiplex slides and the signal intensity is assessed. Rebalancing of the concentrations and re-ordering of the antibodies may be required. (iv) Stage 4: Image analysis (section 2.5.3.4). Created in Biorender (https://biorender.com/).

autoexposure times (optimum 50-150ms). Each primary/secondary antibody is used to single stain six slides (fig. 2.5). This is because each repeated HIER step could influence epitopes in the tissue. Some epitopes can for example be impacted by repeated HIER and be lost, therefore these would need to be stained early in the process. As such, a standard optimisation of six antibodies requires at least thirty-six (36) tissue section slides. Each slide is single stained with that particular antibody in different stage positions (first to sixth).

This translates into two major disadvantages both relating to the resources required. The optimisation of the antibodies is time-consuming and requires numerous tissue sections. In cancer diagnostics, for example, this is not a major disadvantage because (i) there are limited markers of interest and the same panels are used to stain multiple tissue sections from different subjects and, (ii) there is a large number of tissue sections

available. However, this is not the case in the diabetes research where there is only limited collection of finite pancreas tissue available. Moreover, there is a larger number of markers that would be useful to study.

2.5.3.2 Stage 2: Library development and assessment of OPAL™ monoplex

One of the great benefits of the Phenoptics assay is that it eliminates any fluorophore crosstalk and interference from tissue AF signal. To ensure this, the development of an AF library is required followed by the assessment of the optimised OPAL™ single stain (monoplex) slides (fig. 2.6).

Development of AF library slides To develop the AF library slides, eight pancreas tissue section slides are used. Seven slides are stained with a single OPAL™ fluorophore (OPAL™ 480, 520, 570, 620, 670, 780) and the eighth slide is single stained with DAPI (fig. 2.6). These slides construct the AF library. It is important to note that this stage adds to the number of tissue sections required for the optimisation and development of the OPAL™ antibody panel, from 36 to a total of 44 tissue slides.

Development of OPAL™ monoplex slides In total, six pancreas tissue section slides are used. Each slide is stained for one marker with a single OPAL™ fluorophore and counterstained with DAPI (fig. 2.6). This stage adds to the number of tissue sections required, from 44 to a total of 50 tissue slides.

The monoplex slides are imaged using the Vectra Polaris. The sections are visualised using Akoya's Phenochart™ whole slide contextual viewer that allows for automated and default spectral unmixing of whole slide scans. Phenochart™ also allows to develop simulated IHC views to evaluate the intensity and specificity for each monoplex assay.

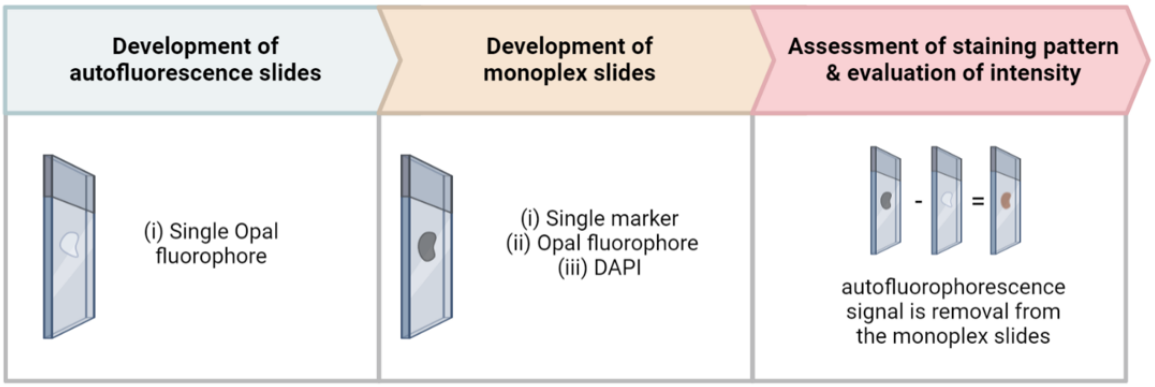

Fig. 2.6 **Development of the autofluorescence library.** The development of the autofluorescence and monoplex slides ensures the assessment of staining pattern and the evaluation of the intensity. Autofluorescence slides are stained with a single Opal fluorophore. Monoplex slides are stained for one marker with a single Opal fluorophore and counterstained with DAPI. Fluorescence microscopy which was performed using the Vectra® Polaris™ (VP) imaging system. The staining pattern and the intensity of the markers is then assessed. Created in Biorender (https://biorender.com/).

Assessment of staining pattern and evaluation of intensity The AF library slides are scanned using the VP. The AF library scans are visualised using Phenochart™ and the regions of interest annotated. The annotations are then imported into the InForm™, an automated image analysis software. InForm™ is used to create an AF library (fig. 2.6). The AF library is used to 'teach' the software the spectral signature of AF. It is important to note that the AF library created is specific to the OPAL™ fluorophores used and for the relevant tissue. Each tissue has a different AF signal intensity (for example brain is highly autofluorescent, whereas tonsils are not). As such, a different AF library is required for each tissue. Taking this a step further, different preservation methods may also impact on tissue AF and therefore, a different AF library for each preservation method would be beneficial.

Next, the OPAL™ monoplex slides are scanned using Vectra. The OPAL™ monoplex scans are visualised using Phenochart™ and the regions of interest are annotated. The annotations are then imported into InFORM™. The AF is removed from the annotations using the relevant AF library and the remaining signal can be evaluated

as a readout of the expression of the target of interest. The remaining signal is used to assess the staining pattern of each of the antibodies and evaluate the intensity and specificity for each monoplex assay in tissue sections.

2.5.3.3 Stage 3: OPAL™ multiplex assay development

Following the assessment of the monoplex results, the order of marker detection is selected and multiplex staining with DAPI is performed. Multispectral unmixing using Phenochart™ and AF removal using InFORM™ are performed to confirm that that there is no interference and crosstalk in the multiplex images. At this point, further assessment of the remaining signal from each marker is required. Rebalance of the antibody concentrations and/or re-order of the antibodies may be required. Therefore, more tissue sections may be required for multiplex staining optimisations - over 50 tissue slides so far. Once the optimal staining patterns and signal intensities are achieved, the antibody panel is ready to be used in the relevant tissue.

2.5.3.4 Stage 4: Image analysis

Once the optimised OPAL™ antibody panel is finalised, the relevant tissue sections are multiplex stained and the sections are then scanned. The whole slide scans acquired using the VP™ are viewed and annotated using Akoya's Phenochart™ whole slide contextual viewer. Following the assessment of the multiplex views using Phenochart™, the regions of interest are annotated and the annotated regions are imported into InFORM™ for visualization and quantification of biomarkers in tissue sections.

2.5.4 In house protocol

The Phenoptics assay was initially developed for diagnostic purposes but in recent years it has attracted the research community. As such, there are numerous barriers that we

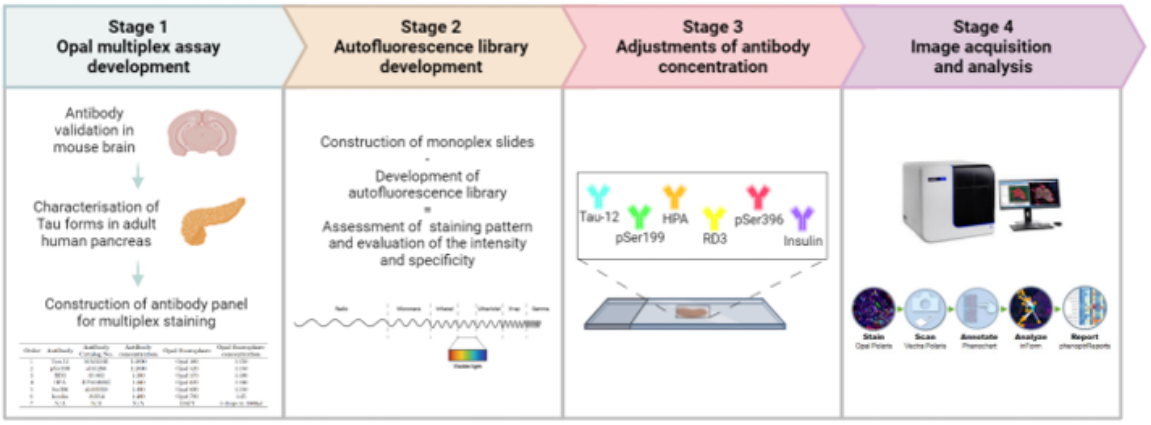

Fig. 2.7 **Development of multiplex staining protocol detecting a single marker in human pancreas tissue.** The phenoptics assay development flow chart consists of four steps; (i) Primary antibody titration (section 2.5.4.1), (ii) Autofluorescence library (section 2.5.4.2), (iii) OPAL multiplex assay development (section 2.5.4.3) and, (iv) the image acquisition and analysis (section 2.5.4.4). Created in Biorender (https://biorender.com/).

still need to overcome. First of all, the optimisation of the multiplex staining requires numerous resources; at least 50 tissue slides for optimisation of each antibody panel. In this case, there is only a limited collection of pancreas tissue available. Moreover, it is suggested by the manufacturer that the selected markers should target different structures and ideally different cells, which adds to the complexity as we aim to use five different markers against the same protein. For these reasons, it is important to carefully plan the OPAL™ staining in a way that ensures that (i) a minimum amount of human pancreas tissue sections is used and (ii) the antibody panel is carefully constructed to answer as many questions as possible. The manufacturer's protocol has therefore been adapted to these restrictions (fig. 2.7).

2.5.4.1 Stage 1: OPAL™ multiplex assay development

Following the optimisation of the anti-Tau antibodies for use in FFPE tissue (Chapter 3) and carefully assessing which Tau forms are present within human pancreas (Chapter 4), the next step was to establish a multiplex staining panel to allow for a more thorough

Table 2.4 **Antibody panel for Opal multiplex staining.** The construction of the antibody panel for multiplex staining using the Opal technique requires careful optimisation. This table has detailed information about the order of the antibodies, the antibodies selected and their concentrations and, the paired Opal fluorophores and Opal fluorophore concentrations. This panel may require further optimisation to achieve optimal intensities suitable for accurate multispectral unmixing and autofluorescence removal.

Order	Antibody	Antibody Catalog No.	Antibody concentration	Opal fluorophore	Opal fluorophore concentration
1	Tau-12	MAB2241	1:2000	Opal 480	1:150
2	pSer199	ab81268	1:2000	Opal 520	1:150
3	RD3	05-803	1:300	Opal 570	1:100
4	HPA	HPA048895	1:300	Opal 620	1:100
5	Ser396	ab109390	1:400	Opal 690	1:150
6	Insulin	A0564	1:400	Opal 780	1:25
7	N/A	N/A	N/A	DAPI	3 drops in 1000μl

interrogation of defined Tau forms in health, disease and aging. To characterise the expression of Tau isoforms and phosphorylated Tau forms in the human pancreas, we constructed an antibody panel for multiplex staining that consists of one total, two isoform-specific, two phosphorylation-specific anti-tau antibodies and, one anti-insulin antibody to allow detection of β cells (Table 2.4). This panel should allow the following;

1. Comparison of the fluorescent intensity of total tau in the β cells in age and in diabetes.

2. Investigation of whether there is an isoform imbalance associated with age, BMI and/or disease.

3. Confirmation of which residues are phosphorylated and examine whether there is a change in the cellular localisation of phosphorylation-specific antibodies.

The initial optimisation of the multiplex staining conditions (order of antibodies, concentration of antibodies and OPAL fluorophores) was mainly based on the antibody performance in standard IHC and IF staining techniques. First, the primary antibodies were paired with OPAL fluorophores (Table 2.4). Three slides were then stained using

the same six antibodies but in different order. Assessment of the staining pattern and intensity for each panel revealed that the order presented here is the optimal (Table 2.4). Next, to achieve the optimal exposure time of 50-150ms, ten slides were stained. The slides were stained with the antibodies listed at table 2.4 but with re-adjustments on the antibody and OPAL fluorophore concentrations.

2.5.4.2 Stage 2: Autofluorescence library development

Stage 2 of the Phenoptics assay is one of the most important stages as it is the one to ensure that there is no non-interference and crosstalk in the multiplex images (section 2.5.3.2). Moreover, optimal AF removal will also ensure that the remaining signal can be evaluated as a readout of the expression of the target of interest. As such, this stage has not be altered or adjusted. Eight slides were used to create the AF library and six slides were used to create the OPAL monoplex slides (fig. 2.6). It is important to note, that different tissue and fixatives may influence the tissue AF signal. Therefore, to ensure the most efficient AF removal, the development of the AF library slides as well as of the monoplex slides were performed using pancreas tissue sections from the nPOD collection. This is because (i) the nPOD slides are preserved under strictly controlled conditions and (ii) the final multiplex staining will be performed using pancreas tissue sections from nPOD.

2.5.4.3 Stage 3: Adjustments of antibody concentration

According to the manufacturer's protocol, this step would be the first multiplex staining attempt. However, as the protocol has been adjusted to meet the restrictions of this project, the primary antibodies have already been paired with the appropriate OPAL fluorophores and their stage position has been determined. Rebalancing of the concentrations of primary antibodies and OPAL™ fluorophores was been evaluated to

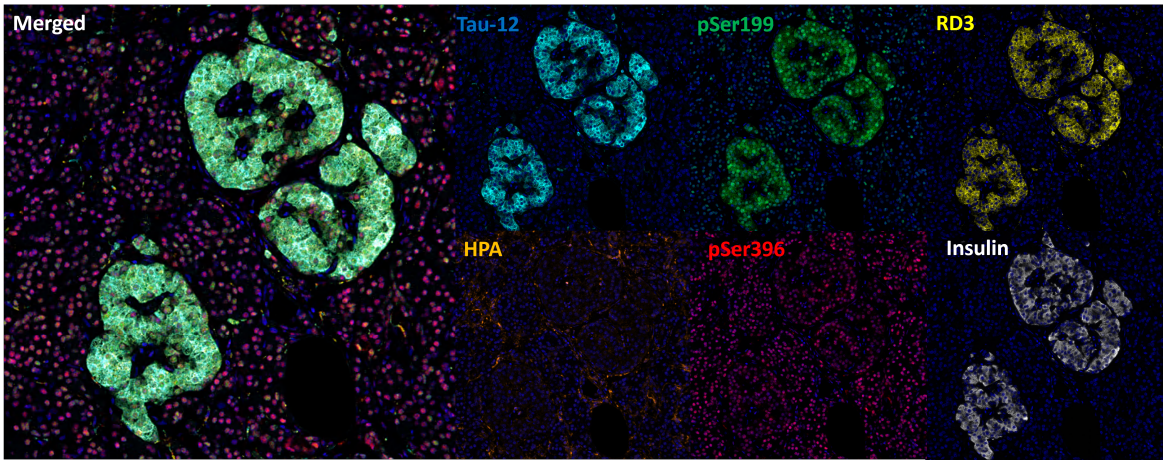

Fig. 2.8 **Representative immunofluorescence micrographs demonstrating the presence and localisation of different Tau forms in human islets.** An nPOD pancreas tissue section (donor ID; 6022) was stained with Tau-2; cyan, pSer199; green, RD3; yellow, HPA; orange, pSer396; red, insulin; white, using the Phenoptics assay. Whole slide scans were imaged at X20. Magnification x20.

ensure that the antibody staining pattern and the signal intensity match with previous data from IHC and IF staining. Taking these into account, an nPOD pancreas tissue section was stained (fig. 2.8). All antibodies (described at section 2.5.4.1, Table 2.4) immunostained as expected and the exposure times fell within the optimum range (50-150ms).

Future steps As a next step, three slides from different donors will be stained with the finalised antibody panel. The slides will be imaged using the VP. Slides will be viewed using Phenochart and the ROI will be imported into InFORM™. The AF library will then be used to remove the AF signal and the remaining signal will be assessed. Following this, the same antibody panel will be used to stain pancreas tissue section from 130 donors (range of age and disease states).

2.5.4.4 Stage 4: Image acquisition and analysis

Similarly to what is suggested by the manufacturer (section 2.5.3.4), multiplex-fluorescence scans were acquired using the VP imaging system, the scans were annotated using Phenochart™ whole slide contextual viewer and the AF removal was performed using the relevant AF library stored in InFORM™ image analysis software.

Chapter 3

Antibody validation

3.1 Introduction

The discovery of Tau protein in 1975 [4] and further histological findings showing that hyperphosphorylated Tau is the major component of NFTs in 1985 [5–9] lead to the development of anti-Tau antibodies raised against physiological, hyperphosphorylated and presumed pathological Tau forms [242–244]. The further observation that some Tau residues can be phosphorylated both in normal and AD brain biopsies [48, 49] highlighted the importance to develop highly specific antibodies, to allow distinguishing brain tissue from individuals with and without AD and led to an almost exponential increase in the production of anti-Tau antibodies.

Antibodies are widely used both in research and in clinical settings [245, 246] and yet, it is alarming that some of the most widely used antibodies can be unreliable [247]. Common issues with antibodies include cross-reactivity with nonspecific targets, variability between batches and, use of unsuitable experimental applications [248]. All these add to the reproducibility crisis and, although emphasis is now given on appropriate antibody validation, till today, there are no universally accepted guidelines for antibody validation.

The Food and Drug Administration (FDA) defines validation as "confirmation by examination and provision of objective evidence that the particular requirements for a specific intended use can be consistently fulfilled". The validation of an antibody ensures three key aspects; (i) the specificity of the antibody, (ii) the affinity of the antibody which is defined as the strength of the interaction between a receptor (epitope) and its respective ligand (antibody) and, (iii) the reproducibility of the experiment which secures that the experiment can be repeated both over time and by other researchers, giving the same results.

Tau protein is a complex, intrinsically disordered and heavily post-translationally modified protein which has six different isoforms expressed in the central nervous system (CNS) and one isoform expressed in the peripheral nervous system (PNS). Therefore, antibodies raised against Tau detect a variety of Tau forms such as isoform-specific, PTM-specific (i.e. phosphorylation-specific, acetylation-specific etc), truncated, oligomeric Tau forms and the list could go on. Notably, today, there are thousands of anti-Tau antibodies commercially available and, even though several papers validating Tau antibodies have been published in the last decade [232–234], there is still a long way to go.

In summary, the key objectives of this chapter were

- to construct a well validated anti-Tau antibody panel that will then be used to fully characterise the expression of Tau in the human pancreas (Chapter 4) and,
- to develop a visualisation method to illustrate the suitability and specificity of each Tau antibody for use in WB and IHC.

3.2 Validation strategies

To construct a toolbox of reliable validated anti-Tau antibodies for IHC and WB, a series of experiments was performed in collaboration with Prof John Todd and Dr Irina Stefana from the University of Oxford (fig. 3.1). The first step was to identify antibodies frequently used in research. These antibodies were divided into four categories;

- total anti-Tau antibodies detecting all forms of Tau regardless of isoform expression and PTMs, such as phosphorylation,
- isoform-specific anti-Tau antibodies detecting certain Tau isoforms,
- phosphorylation-specific (phospho-specific) anti-Tau antibodies detecting Tau forms phosphorylated at select residues and,
- PTM-specific (other than phosphorylation) anti-Tau antibodies detecting various forms of Tau such as truncated forms and dephosphorylated forms.

In total, 12 total anti-Tau antibodies, 6 isoform-specific anti-Tau antibodies, 17 phospho-specific anti-Tau antibodies and, 2 PTM-specific (other than phosphorylation) anti-Tau antibody were validated for use in IHC (Chapter 2, Table 2.1). To assess the specificity of anti-Tau antibodies on WB, anti-Tau antibodies were tested in various samples expressing either endogenous Tau (low levels) or overexpressing Tau (high levels) (fig. 3.1). WB analysis was performed at the University of Oxford by Dr. Irina Stefana and will not be discussed in depth here. However, key relevant WB data are included and discussed in this chapter. To assess the specificity of anti-Tau antibodies in IHC, a selection of anti-Tau antibodies guided by the WB data was used to stain (i) brain tissue sections from different mouse models and (ii) control and AD human brain (fig. 3.2).

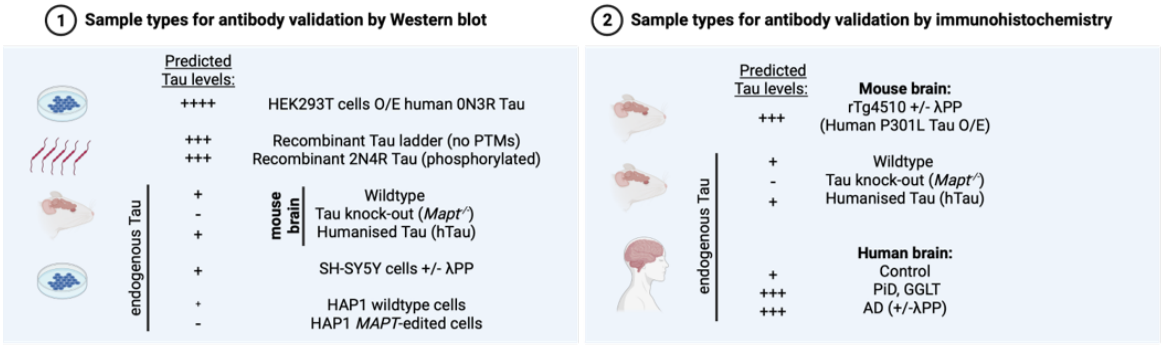

Fig. 3.1 **Antibody validation strategies.** A schematic illustrating the sample types for antibody validation by Western blot (WB; left hand side panel) and immunohistochemistry (IHC; right hand side panel). The list of the samples is presented alongside the predicted Tau levels. The levels of Tau expression are described; negative (-), positive (+), strong positive (+++).

From now on and to avoid future confusion, we refer to anti-Tau antibodies as Tau antibodies. To refer to a particular antibody, the name and the clone of the antibody will be utilised. If two or more antibodies were produced from the same clone, the supplier will be also noted in brackets.

3.2.1 rTg4510 mouse model

rTg4510 mice express a repressible form of human Tau containing the P301L mutation that has been linked with FTD. The rTg4510 is a popular mouse model of tauopathy. It overexpresses the 0N4R human Tau isoform and its expression has been enhanced in a way that is approximately 13 times the level of endogenous murine Tau [235]. Overexpression of Tau causes (i) Tau to aggregate and to form PHFs and NFTs and, (ii) Tau to translocate from the hippocampus to the cortex (fig. 3.2a) mimicking the alterations of human Tau in the neurodegenerative brain. Thus, the rTg4510 mouse model allows the study of a variety of physiological and alleged pathogenic Tau forms. rTg4510 mouse brain sections were treated with and without λPP to test the impact of phosphorylation on the binding of each Tau antibody. It is worth noting that the

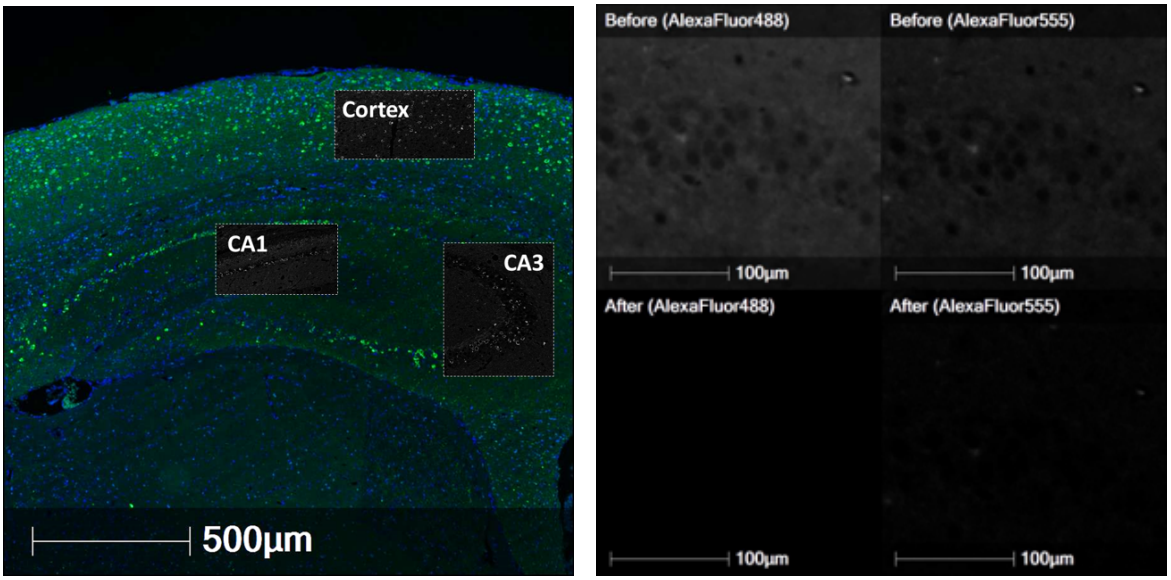

(a) Overview of rTg4510 brain (b) Autofluorescence removal

Fig. 3.2 **rTg4510 mouse brain. 3.2a** | Overview of the rTg4510 mouse brain. Section stained with total Tau 43D antibody (green) and DAPI (blue). The cortex and the hippocampal regions are indicated (gray-scaled boxes). Whole slide scans were imaged at X20. Scale bars 100μm. **3.2b** | Secondary only antibody controls; AlexaFluor 488 and 555, in the CA1 region of the rTg4510 mouse brain before (upper panel) and after (lower panel) autofluorescence removal.

rTg4510 mouse model comes with an important limitation. As this model expresses only the 0N4R Tau isoform, it does not allow the study of the rest of Tau isoforms but, nonetheless, it works as a negative control for those (Table 3.1).

3.2.2 WT, *Mapt*$^{-/-}$ and hTau mouse models

Next, Tau antibodies were used to stain tissue sections from three different mouse models (fig. 3.1, Table 3.1).

- Wildtype (WT) mouse brain is expected to express basal endogenous Tau levels. The WT mouse brain was used as the positive control for mouse-reactive anti-Tau antibodies.
- Tau knock out (KO; *Mapt*$^{-/-}$) mouse brain which should not express any form of Tau. The *Mapt*$^{-/-}$ mouse brain was used as the negative control for all anti-Tau

antibodies. The genetic background of the *Mapt*$^{-/-}$ mouse model was used to generate

- the humanised Tau (hTau) mouse model which is expected to express endogenous Tau levels of human Tau. The hTau mouse model was used as the positive control for human-reactive anti-Tau antibodies.

Table 3.1 **Tau isoforms expressed in four different mouse models.** Tau expression differs in human and murine models. The Tau isoform expression in four mouse models is described here and this table refers to 9-months rTg4510 male mice and 9-months WT, *Mapt*$^{-/-}$, hTau male mice. The mouse models and the genetic background of each model is mentioned in the first two columns followed by the isoforms that each mouse model expresses marked with a ✓for positive expression and with ×for negative expression. The overall levels of Tau expression are described; negative (-), positive (+), strong positive (+++).

Mouse model	Genetic background	0N3R	1N3R	2N3R	0N4R	1N4R	2N4R	Reactivity mouse	Reactivity human	Expression level of Tau
rTg4510	MAPT^{301L}	×	×	×	✓	×	×	×	✓	+++
WT	C57Bl/6J	?	?	?	?	×	✓	✓	×	+
Mapt$^{-/-}$	C57Bl/6J	×	×	×	×	×	×	×	×	-
hTau	C57Bl/6J	?	?	?	?	?	?	×	✓	+

These mouse models help to (i) explore the antibody performance in FFPE brain tissue that expresses endogenous levels of Tau (WT, hTau) or overexpresses Tau (rTg4510 mice), (ii) assess the reactivity of the antibodies for mouse and human Tau (WT, hTau, rTg4510 mice) and, (iii) ensure that the antibodies do not produce nonspecific signal (*Mapt*$^{-/-}$ mice). Both the WT and hTau mouse models express low endogenous levels of physiological Tau and previous studies have suggested that the detection of Tau in such models is challenging. To allow for clearer visualisation of low levels of Tau expression, AF removal was performed (fig. 3.2b). AF removal ensures that the tissue AF is removed and that the remaining signal can be evaluated as a readout of the expression of the target of interest.

3.2.3 Human brain and pancreas

To ensure that the immunostaining of the Tau antibodies in mouse model brains is representative of that in the human brain, a selection of Tau antibodies was also tested on control and AD brain tissue (fig. 3.1). Brain tissue sections from control and AD brain were provided by the University of Oxford Brain Biobank. PNS-specific Tau antibodies directed against the HMW Tau were also tested in human pancreas tissue sections provided by the EADB collection and the intrapancreatic nerves were used as positive controls.

3.2.4 Introduction of the Traffic Light System (TLS)

To assess the suitability and specificity of anti-Tau antibodies for use in WB and IHC, the traffic light system (TLS) is introduced in this chapter. Each Tau antibody is validated in the relevant samples described in fig 3.2. Next, each TLS-validated anti-Tau antibody is presented alongside two mini traffic lights - one for WB (black) and one for IHC (blue). The coloring scheme reveals the suitability and specificity of each antibody into a simple green (GO), amber (proceed with caution), red (STOP) labels. In more detail;

- Green signifies that the antibody detects Tau with high specificity,
- Amber signifies that the antibody detects Tau but either unexpected performance (e.g. “total” Tau antibody detects only subset of splice isoforms or is inhibited by phosphorylation, phospho-Tau antibody detecting unphosphorylated protein etc) and/or shows non-specific cross-reactivity with other proteins and,
- Red signifies that there are no evidence that it detects Tau (may or may not show non-specific cross-reactivity with other proteins).

3.3 Total anti-Tau antibodies

Total Tau antibodies are defined as the antibodies that are allegedly able to label all forms of Tau regardless of isoform expression and PTMs (eg. phosphorylation, acetylation, truncation etc). Overall, 12 total Tau antibodies directed against (i) the N-terminal domain (Tau N-term, 5A6, SP70, 43D, Tau-12, Tau-13), (ii) the PRD (Tau-5 Abcam, Tau-5 ThermoScientific, HT7, 77E9) and, (iii) the C-terminal domain (K9JA, Tau46) were validated in IHC (Chapter 2, Table 2.1). Antibodies against the MBD were not assessed here as; (i) they are not commonly used in research and (ii) MBD attaches to the microtubules and therefore, it is likely that the binding of antibodies against that epitope will be blocked.

Total Tau antibodies were used to immunostain the brain of rTg4510, WT, *Mapt*$^{-/-}$ and hTau mouse models and were expected to label all forms of Tau (e.g. physiological, phosphorylated, truncated, Tau aggregates). In more detail, it is expected that all total Tau antibodies will strongly stain the rTg4510 mouse cortex both in the control and λPP-treated tissue and that the signal intensity will not be affected by the λPP treatment. In addition, total Tau antibodies should detect Tau expressed at high levels (rTg4510 mice) and low levels (endogenous Tau; WT, hTau mice). Quantification analysis and statistical analysis (t-test to explore if there is a significant difference between the two groups; untreated and λPP-treated tissue) were also performed to assess the signal intensity of each total Tau antibody in the control and λPP-treated rTg4510 mouse brain.

3.3.1 N-terminal domain

Compared to other Tau domains, the N-terminal domain is the least prone to PTMs. This characteristic makes it an ideal immunogen for the generation of total Tau antibodies. In total, six Tau antibodies directed against the N-terminal region (Tau

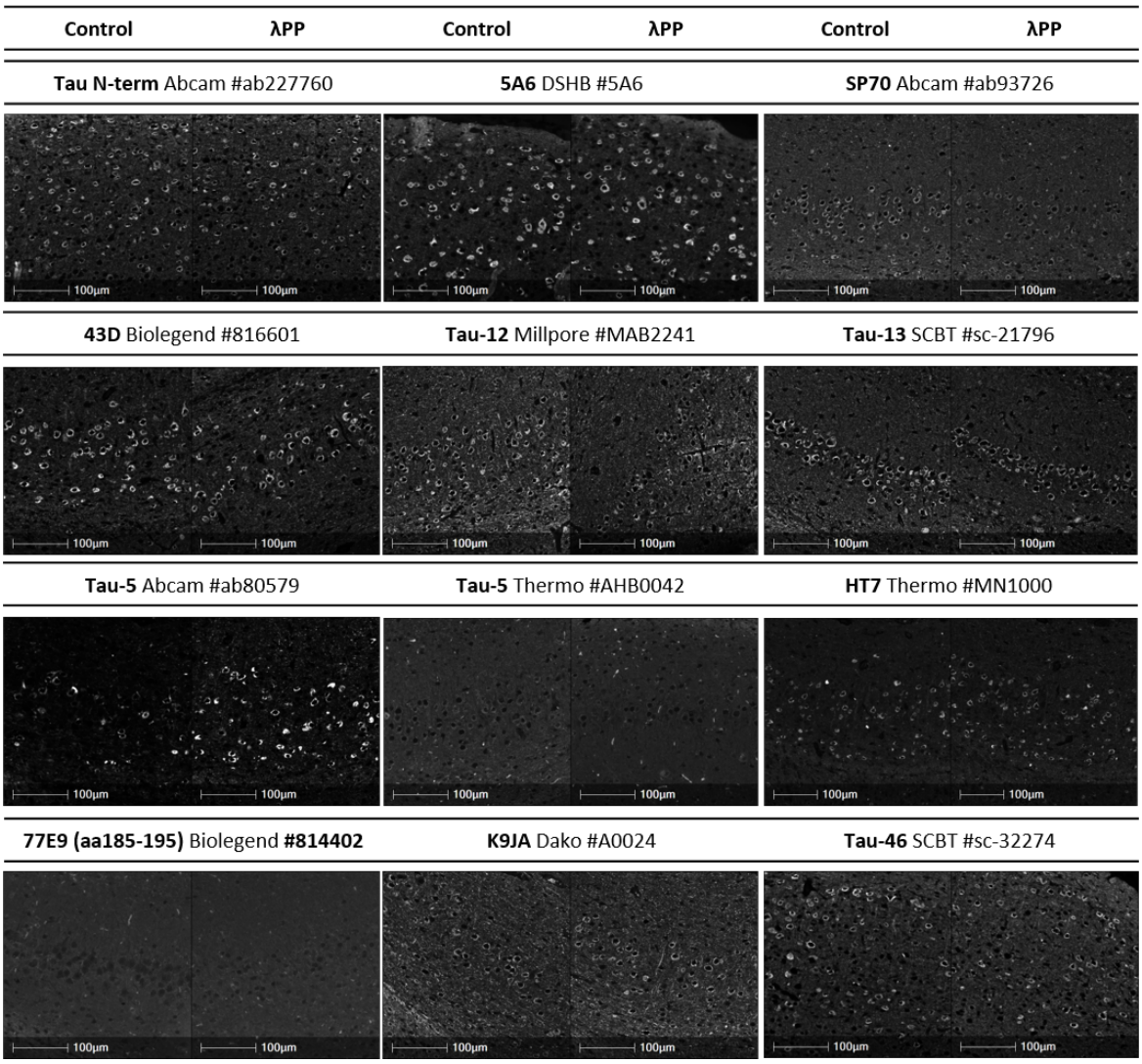

Fig. 3.3 **Total Tau antibody profiles in the rTg4510 mouse brain.** Representative immunofluorescence micrographs demonstrating the presence and localisation of twelve different total Tau forms (white immunostaining) in the cortex of 9-month old rTg4510 mice. Two serial FFPE brain sections per antibody were pre-incubated with or without lambda phosphatase (λPP), before incubation with each of the twelve different total Tau antibodies. Micrographs are presented in the order of the total Tau antibody immunogens moving from the N' terminus to the C' terminus of Tau. Whole slide scans were imaged at X20. Scale bars 100μm.

N-term, 5A6, SP70, 43D, Tau-12, Tau-13) were tested. As expected, all total Tau antibodies tested strongly immunostained the cortex of rTg4510 mice (fig. 3.3). Quantification analysis revealed that the signal intensity of 43D and Tau-13 antibodies

in the rTg4510 mouse cortex did not demonstrate any significant difference between the untreated and λPP-treated tissue (fig. 3.4a, full stats table A.3 in Appendix A), implying that these antibodies are not impacted by phosphorylation events. As such, these antibodies are classified as green. By contrast, the signal intensity of three antibodies (N-term, 5A6, Tau-12) was significantly increased in the λPP-treated rTg4510 mouse cortex compared to the control cortex (fig. 3.4a, full stats table A.3 in Appendix A). The 5A6 and Tau-12 antibodies showed a moderate increase (p.adj value = 0.00629 and 0.00442, respectively) whereas, the N-term antibody showed a dramatic increase (p.adj value = 6.75e-05). These data suggest that the binding specificity of these total Tau antibodies (N-term, 5A6, Tau-12) is improved upon treatment with λPP treatment. This implies that (i) these antibodies are inhibited by phosphatases groups and that (ii) they may fail to detect hyperphosphorylated forms of Tau. Therefore, N-term, 5A6 and Tau-12 antibodies were classified as amber because their binding to Tau is impacted by phosphorylation.

The immunoreactivity seen with SP70 was significantly reduced upon treatment with λPP treatment, with a p.adj value of 2.24e-11 (figs. 3.3, 3.4a). This signal reduction is unexpected and implies that this antibody may have preference for phosphorylated forms. WB data revealed that the SP70 antibody detected Tau with high specificity when used to probe mouse brain samples and it also detected two closely-spaced bands in λPP-treated SH-SY5Y lysates corresponding to the MW of (i) 3R and (ii) 4R Tau isoforms (fig. 3.5). WB data suggest that the SP70 antibody is a specific antibody and therefore is classified as green for use in WB. However, it was classified as amber in IHC because even though it stained the control tissue of rTg4510 mouse cortex as expected, its immunoreactivity was compromised upon λPP treatment.

Next, a selection of human Tau-reactive antibodies (Tau-12, Tau-13 and SP70), guided by WB data, were used to immunostain the WT, *Mapt*$^{-/-}$ and hTau mice. As

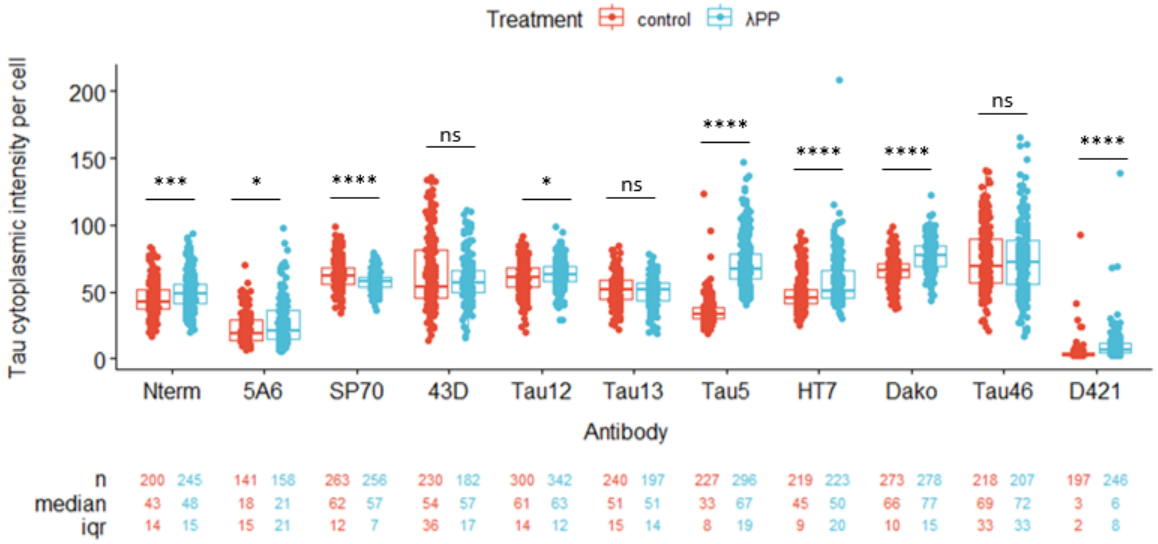

(a)

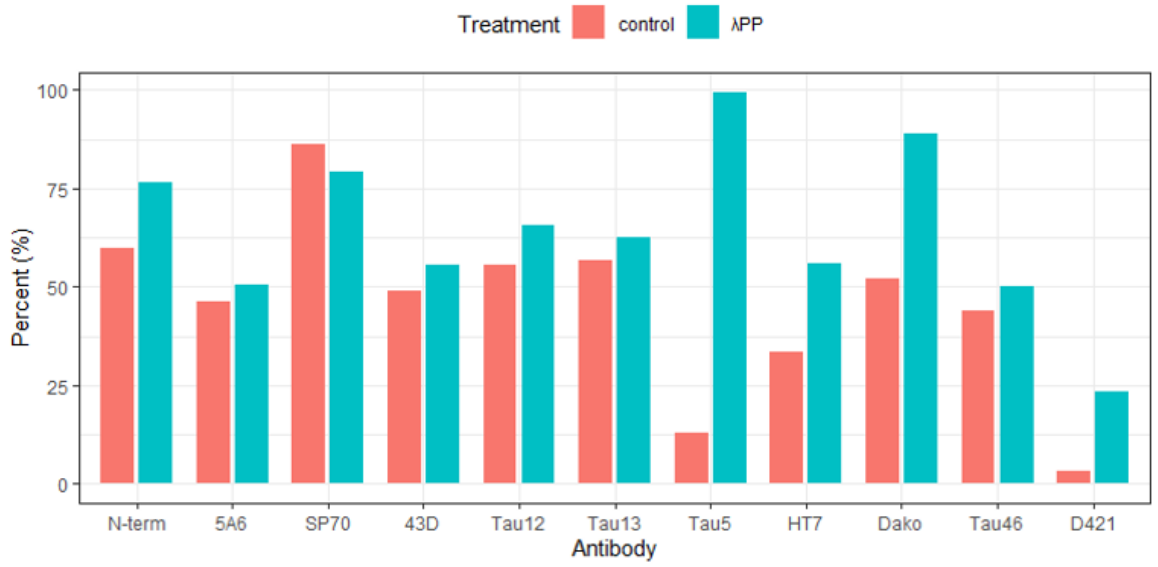

(b)

Fig. 3.4 **Quantification analysis of Tau signal in the rTg4510 mouse cortex before and after λPP treatments. 3.4a** | The signal of each total Tau antibody in control (red) and λPP-treated (blue) rTg4510 mouse cortex has been plotted as the Tau cytoplasmic intensity per cell in arbitrary units (y axis). x axis presents the antibodies presented in the order of the total Tau antibody immunogens moving from the N' terminus to the C' terminus of Tau. Statistical analysis was performed and the asterisks (*) reveal the significant difference (if any) in the control and the λPP-treated tissue. ns; not significant. Below each plot, there is a table with the n (number of cells), median and iqr (interquartile range). Full stats table available in Appendix A (Table 3.4a). **3.4b** | The plot presents the percentage of Tau positive cells in cortex before and after λPP (y axis). x axis presents the antibodies presented in the order of the total Tau antibody immunogens moving from the N' terminus to the C' terminus of Tau.

expected, Tau-12, Tau-13 and SP70 antibodies immunoreacted with Tau in the CA1 hippocampal region but did not immunostain the WT, suggesting a preference for human Tau. *Mapt*$^{-/-}$ mouse brain remained clear confirming that these antibodies do not produce non specific signal. Taken together these findings demonstrate that Tau-12, Tau-13 and SP70 are specific for human Tau (fig. 3.6).

3.3.2 Proline-rich domain

In total, four total Tau antibodies (Tau-5 Abcam, Tau-5 ThermoScientific, 77E9, HT7) directed against the PRD, a domain prone to phosphorylation, were tested. The Tau-5 (Abcam) and HT7 antibodies stained the rTg4510 mouse cortex as expected (fig. 3.3). The signal intensity of Tau-5 and HT7 antibodies and the percentage of Tau-positive cells were increased in the λPP-treated rTg4510 mouse cortex compared to the control cortex (fig. 3.4a), suggesting that the signal of these antibodies is improved upon λPP treatment and implying that their binding is partially inhibited by the presence of phosphorylated residues. This behaviour was replicated in WB using untreated and λPP-treated SH-SY5Y in that the signal intensity of both antibodies was drastically improved after λPP treatment (fig. 3.5). Based on this, the antibodies Tau-5 (Abcam) and HT7 were classified as amber. Tau-5 (ThermoScientific) weakly immunostained the rTg4510 mouse cortex (fig. 3.3) and was classified as amber.

The 77E9 antibody did not stain the control or the λPP-treated cortex of rTg4510 mice (fig. 3.3) and therefore was classified as red. WB data suggest that 77E9 detected Tau with high specificity when used to probe mouse brain samples and it only weakly immunoreacted with human Tau (fig. 3.5). Moreover, equal amounts of 2N4R recombinant Tau were phosphorylated with one of three different Tau kinases (GSK3-β, DYRK1A or CAMK2A). Quantification analysis revealed that the signal intensity detected for each lane revealed that many antibodies displayed differential

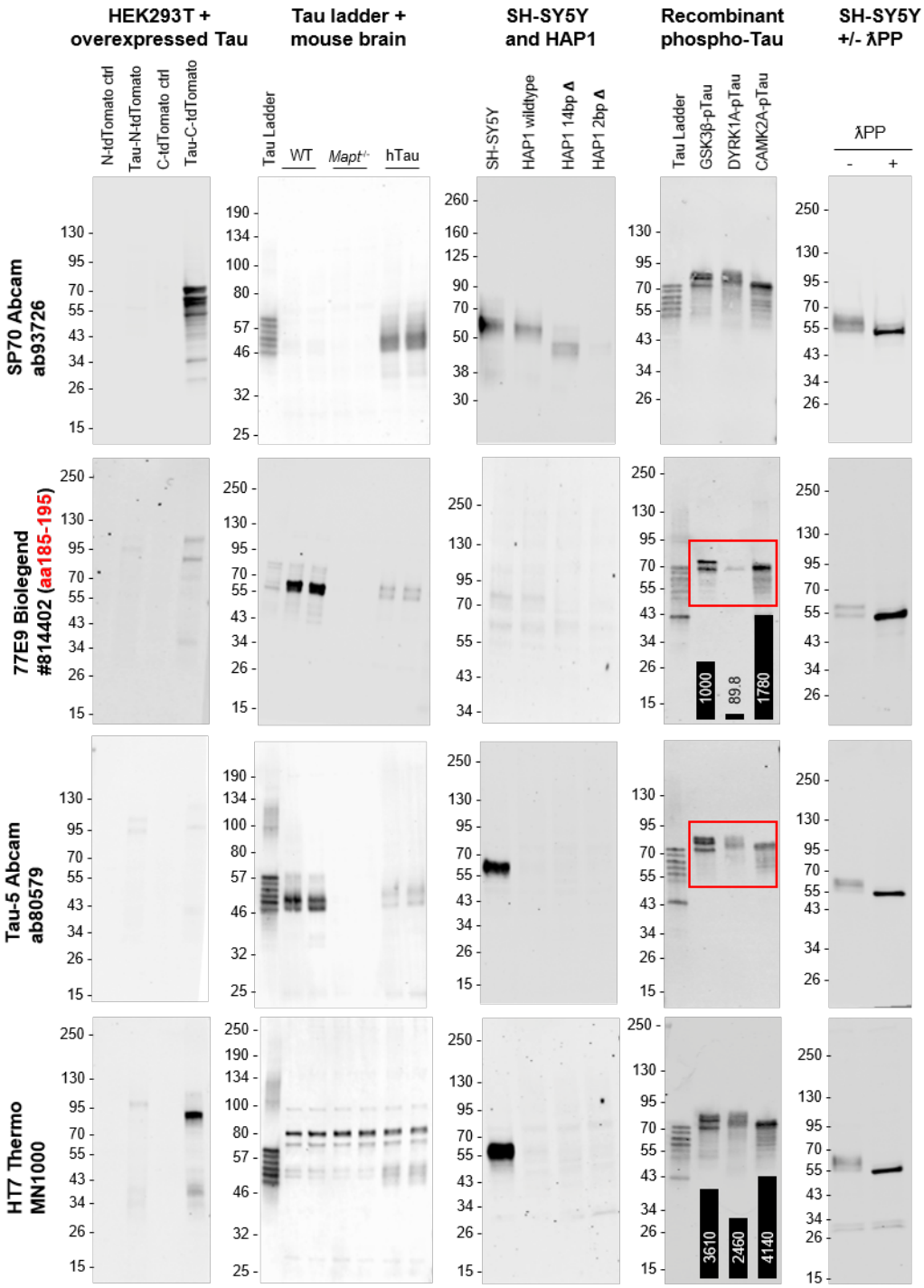

Fig. 3.5 **Immunoblotting using a range of lysates to confirm the specificity of total Tau antibodies.** Immunoblots demonstrating in the specificity of total Tau antibodies and their reactivity for human and mouse Tau. WBs of lysates from HEK293T cells overexpressing 0N3R human Tau and corresponding control cells (first column); recombinant human Tau ladder (5 ng/isoform/lane), plus adult mouse brain lysates from wildtype, Mapt-/- and hTau mice (second column); lysates from SH-SY5Y neuroblastoma cells, plus HAP1 cells, parental (wildtype) and two cell lines carrying either a 14 bp deletion (14 bp Δ) or a 2-bp deletion (2 bp Δ) in MAPT exon 4 (third column); recombinant human Tau ladder (50 ng/isoform/lane) plus recombinant 2N4R Tau that has been phosphorylated by one of three known Tau kinases: GSK3β, DYRK1A or CAMKIIA (fourth column); lysates from SH-SY5Y neuroblastoma cells that have been either untreated (-) or treated (+) with λPP (fifth column). Experiments performed by Dr Irina Stefana (University of Oxford).

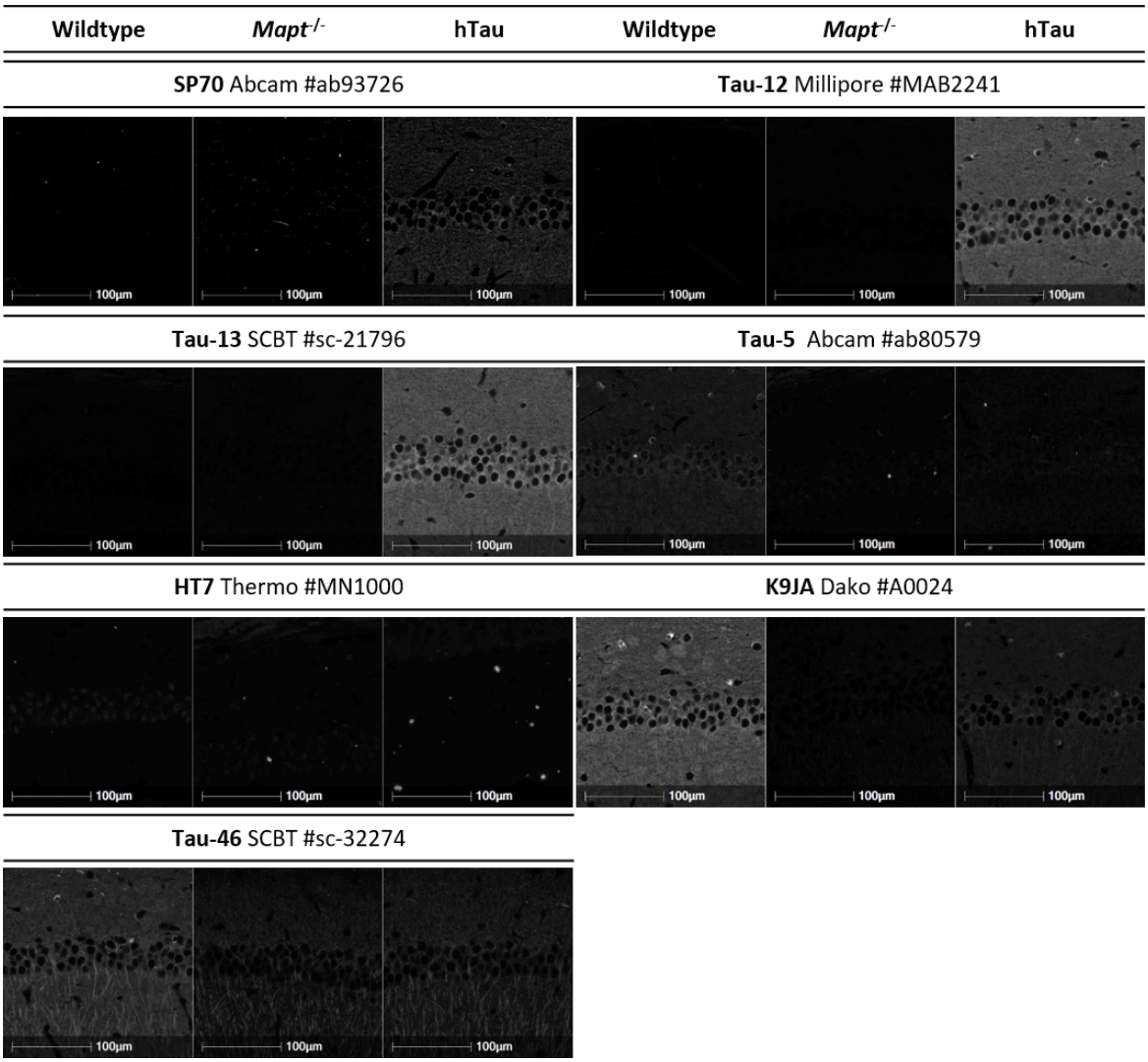

Fig. 3.6 **Total Tau antibody profiles in wildtype, *Mapt*$^{-/-}$ and humanised Tau transgenic (hTau) mice.** Representative immunofluorescence micrographs demonstrating the presence and localisation of different Tau forms (white immunostaining) in the hippocampus of wildtype, *Mapt*$^{-/-}$ and humanised Tau transgenic (hTau) mice. Seven different total Tau antibodies were assessed on FFPE brain sections from relevant mice. Whole slide scans were imaged at X20. Scale bars 100 μm.

reactivity with recombinant Tau that has been phosphorylated by different kinases. Some of the most affected Tau antibodies were 77E9 and Tau-5 Abcam (fig. 3.5). As such,77E9 and Tau-5 (Abcam) were classified as amber for use in WB. Taken together, our results demonstrate that binding of several total Tau antibodies, and in particular that of 77E9 and Tau-5 (Abcam), are partially inhibited by certain phosphorylation

events and that the events impact on the binding of select total Tau antibodies more than others.

Next, Tau-5 (Abcam) and HT7 antibodies were selected to immunostain the CA1 hippocampal region of the WT, *Mapt*$^{-/-}$ and hTau mice. Tau-5 immunodetected Tau in WT mouse brain sections, but failed to immunostain hTau mouse brain, suggesting a preference for mouse reactivity (fig. 3.6). The human-reactive HT7 antibody did not immunostain any of the WT, *Mapt*$^{-/-}$ and hTau mouse brain sections, suggesting that even though this antibody is specific (strongly stained the rTg4510 mouse brain and does not stain the *Mapt*$^{-/-}$ mice), it may not be suitable for detecting low levels of endogenous Tau.

3.3.3 C-terminal domain

Two antibodies against the C-terminal domain (K9JA, Tau-46) were tested. The human/mouse-reactive K9JA, which detects Tau between residues 243-441, strongly immunoreacted with Tau in the rTg4510 mouse cortex as expected (fig. 3.3). K9JA quantification analysis revealed that both the signal intensity and the percentage of Tau-positive cells were increased in the λPP-treated rTg4510 mouse cortex compared to the untreated tissue (fig. 3.4a) suggesting that its binding is partially inhibited by the presence of phosphorylated residues and therefore classifying K9JA as amber. K9JA immunoreacted with Tau in both WT and hTau (weakly) mouse cortex (fig. 3.6) but did not immunostain the *Mapt*$^{-/-}$ mice, demonstrating its specificity. As K9JA strongly detects human Tau in the rTg4510 mouse cortex (high levels) but only weakly detects human Tau in the hTau mice (endogenous; low levels), this could imply that the antibody struggles to detect Tau when expressed endogenously.

The Tau-46 antibody stained the rTg4510 mouse brain as expected (fig. 3.3) but the immunoreactivity seen in WT, *Mapt*$^{-/-}$ and hTau mouse models is different from what

was seen with other Tau antibodies (fig. 3.6). The Tau-46 antibody immunostained the dendrites of the hippocampal cells in the CA1 region of WT, *Mapt*$^{-/-}$ and hTau mice. According to the supplier, cross-reactivity of Tau-46 with the MAP-2 protein has been previously observed. As such, Tau-46 antibody may be specific for human Tau when that is expressed at high levels but it is likely that this antibody may cross react with MAP-2 in tissue where Tau is expressed at low levels. Tau-46 is classified as amber because even though it strongly stained the rTg4510 mouse brain and stained the CA1 hippocampal cell bodies of hTau mouse brain as expected and it may also cross reacts with MAP-2 producing non-specific signal.

3.4 Isoform-specific Tau isoforms

Tau protein consists of 13 exons and has six different isoforms found in the CNS that arise due to the alternative splicing of exons 2, 3 and 10 (Chapter 1, fig. 1.2). Inclusion of exons 2 and/or 3 gives rise to the 0N, 1N and 2N Tau isoforms whereas exclusion or inclusion of exon 10 to the 3R and 4R Tau isoforms, respectively. Upon inclusion of exons 2, 3 and 10, exons 4a and 6 may also be translated, introducing a larger isoform known as HMW Tau or 'Big' Tau, that is usually found in the PNS.

Eight isoform-specific Tau antibodies (Chapter 2, Table 2.1) were tested in FFPE brain tissue sections. A descriptive table of which Tau isoforms are expressed in which mouse model brain is presented at Table 3.1. In summary; (i) The rTg4510 mouse model overexpresses the 0N4R Tau isoform and thus only 4R Tau isoforms are expected to positively immunostain the TG4510 cortex. (ii) The adult WT mouse brain expresses 4R Tau isoforms but not 3R Tau isoforms [249]. As such, WT mouse brain is expected to express 0N4R, 1N4R and 2N4R Tau isoforms. (iii) The *Mapt*$^{-/-}$ should not express any Tau isoform. (iv) Conclusions about the isoform expression

of hTau cannot be made prior to experimental testing because it is possible that the transgenic mice may transcribe human genes in a different way to that of mouse genes.

3.4.1 0N, 1N and 2N Tau isoforms

As expected, the 0N antibody immunoreacted with Tau in rTg4510 mouse cortex whereas the 1N/2N antibody did not (fig. 3.7a). The immunoreactivity pattern and intensity of the staining for both antibodies appeared unaltered after treatment with λPP.

3.4.2 3R and 4R Tau isoforms

Antibodies defined as the RD3 and RD4 clones detect the 3R and 4R Tau isoforms, respectively. The human-reactive RD3 did not immunoreact with Tau in rTg4510 mouse cortex, as expected (fig. 3.7a). Interestingly, RD3 positively immunostained the hTau mouse CA1 region and no signal was detected in the *Mapt*$^{-/-}$ mouse CA1 region (fig. 3.7b). This suggests that the RD3 antibody is specific and further implies that the genetic background of the model may be affected explaining the 'switch' on the isoform expression. Therefore, RD3 antibody is classified as green in IHC.

The human/mouse-reactive RD4 immunoreacted with Tau in the rTg4510 mouse cortex but its immunoreactivity signal differs from what was seen with total and isoform-specific (0N) Tau antibodies. The RD4 antibody immunostained a few cell bodies and it mainly stained the neuronal dendrites. λPP treatment had no significant impact on its immunoreactivity (fig. 3.7a) suggesting that RD4 antibody is not impacted by phosphorylation events. In rTg4510 mouse brain, the expression of P301L hTau induces the formation of PHFs and NFTs. As such, aggregated Tau forms are expected to be found in the rTg4510. Taken together, these data imply that the binding of the RD4 to Tau in FFPE tissue is more likely to be impacted by the formation of PHFs/NFTs

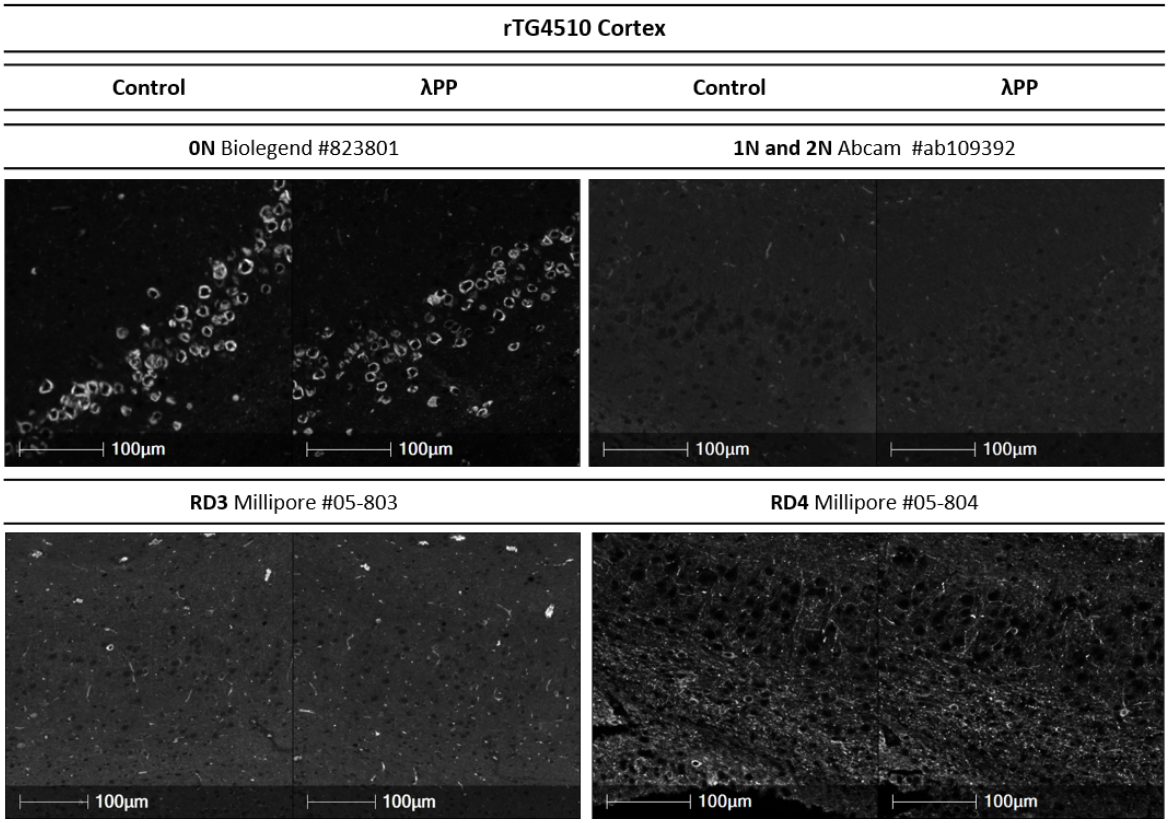

(a) TG4510 cortex

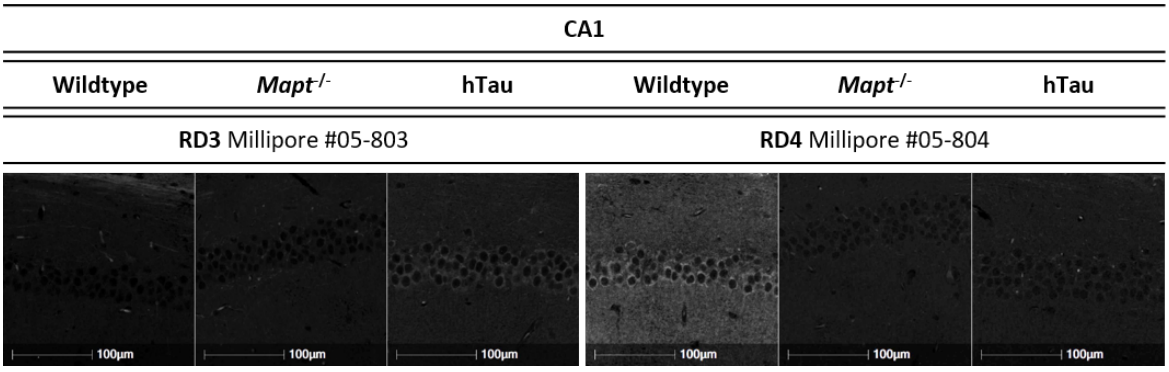

(b) CA1 hippocampal region

Fig. 3.7 **Isoform specific anti-Tau antibody profiles in the rTg4510 mouse cortex and in the hippocampus of wildtype, *Mapt*$^{-/-}$ and humanised Tau transgenic (hTau) mice. 3.7a** | Representative immunofluorescence micrographs demonstrating the presence and localisation of four different Tau antibodies against different Tau isoforms (white immunostaining) in the cortex of 9-month old rTg4510 mice. Two serial FFPE brain sections per antibody were pre-incubated with or without lambda phosphatase (λPP), before incubation with each of the four different antibodies that detect isoform-specific Tau forms. **3.7b** | Representative immunofluorescence micrographs demonstrating the presence and localisation of two different Tau isoforms (white immunostaining) in wildtype, *Mapt*$^{-/-}$ and hTau mice. Two antibodies that detect Tau isoforms were assessed on FFPE brain sections from relevant mice. Whole slide scans were imaged at X20. Scale bars 100μm.

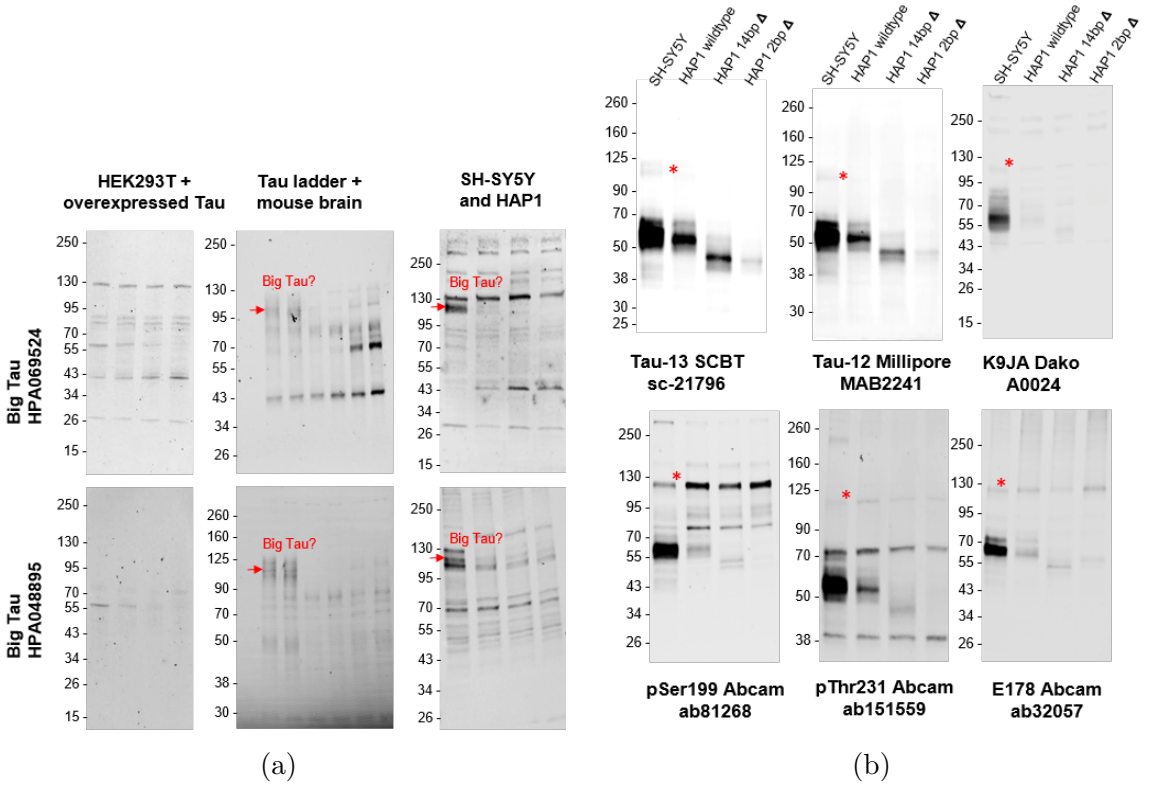

Fig. 3.8 **Immunoblotting using a range of lysates to confirm the specificity of isoform-specific Tau antibodies. 3.8a** | Immunoblots demonstrating in the specificity of isoform-specific Tau antibodies raised against the HMW Tau isoform and their reactivity for human and mouse Tau. WBs of lysates from HEK293T cells overexpressing 0N3R human Tau and corresponding control cells (first column); recombinant human Tau ladder (5 ng/isoform/lane), plus adult mouse brain lysates from wildtype, Mapt-/- and hTau mice (second column); lysates from SH-SY5Y neuroblastoma cells, plus HAP1 cells, parental (wildtype) and two cell lines carrying either a 14 bp deletion (14 bp Δ) or a 2-bp deletion (2 bp Δ) in MAPT exon 4 (third column). **3.8b** | Immunoblots demonstrating in the specificity of total and phospho-specific Tau antibodies in lysates from SH-SY5Y neuroblastoma cells, plus HAP1 cells, parental (wildtype) and two cell lines carrying either a 14 bp deletion (14 bp Δ) or a 2-bp deletion (2 bp Δ) in MAPT exon 4 (third column). Experiments performed by Dr Irina Stefana (University of Oxford).

and not by changes in the phosphorylation status of Tau (as λPP had no apparent impact on the immunoreactivity of the antibody). The RD4 antibody immunostained the WT mouse CA1 region but, not the hTau hippocampal cells (fig. 3.7b). No signal from the *Mapt*$^{-/-}$ mouse brain also suggests that this antibody is specific to Tau.

3.4.3 High Molecular Weight Tau or 'Big' Tau isoform

HMW Tau was initially discovered in the PNS and cell lines derived from neural crest [250, 251, 24]. HMW Tau resembles to the full-length 2N4R Tau isoform in that is contains exons 2, 3 and 10 and is characterised by the further inclusion of exons 4a and 6. Two antibodies directed against HMW Tau, #HPA048895 and #HPA069524, were tested in FFPE brain tissue. Both antibodies immunoreacted with Tau found in the cortex of all three mouse models (WT, *Mapt*$^{-/-}$ and hTau) but did not immunostain the CA1 region (fig. 3.9a). There are two possible scenarios; (i) immunoreactivity in mouse cortex is a result of non-specific signal (justified by the positive signal in the *Mapt*$^{-/-}$ cortex) or, (ii) 'HMW Tau' may not been knocked out and 'HMW Tau' antibodies immunoreact with Tau found in brain cells that project to the PNS. The fact that two HMW Tau antibodies directed against different epitopes of HMW Tau both label the rTg4510 mouse brain supports the second hypothesis but further work is required #HPA048895 immunoreacted with Tau in rTg4510 mouse brain regions (fig. 3.9b) and the immunoreactivity seen with the antibody was not affected by λPP treatment. In addition, the #HPA048895 was used to stain the human pancreas, where it positively stained the intrapancreatic nerves (fig. 3.9b, right panel) as it would be expected. Therefore, this antibody was classified as amber.

Interestingly, WB data demonstrate that a selection of total (Tau-13, Tau12 and K9JA) and phospho-specific (pSer199, pThr231, E178) Tau antibodies detect a high MW band in SH-SY5Y and HAP1 cell lines (fig. 3.8b). This band detected is around 120-130 kDa and corresponds to the MW of the HMW Tau isoform and this observation suggests that antibodies, other than HWM-specific ones, may also detect that isoform.

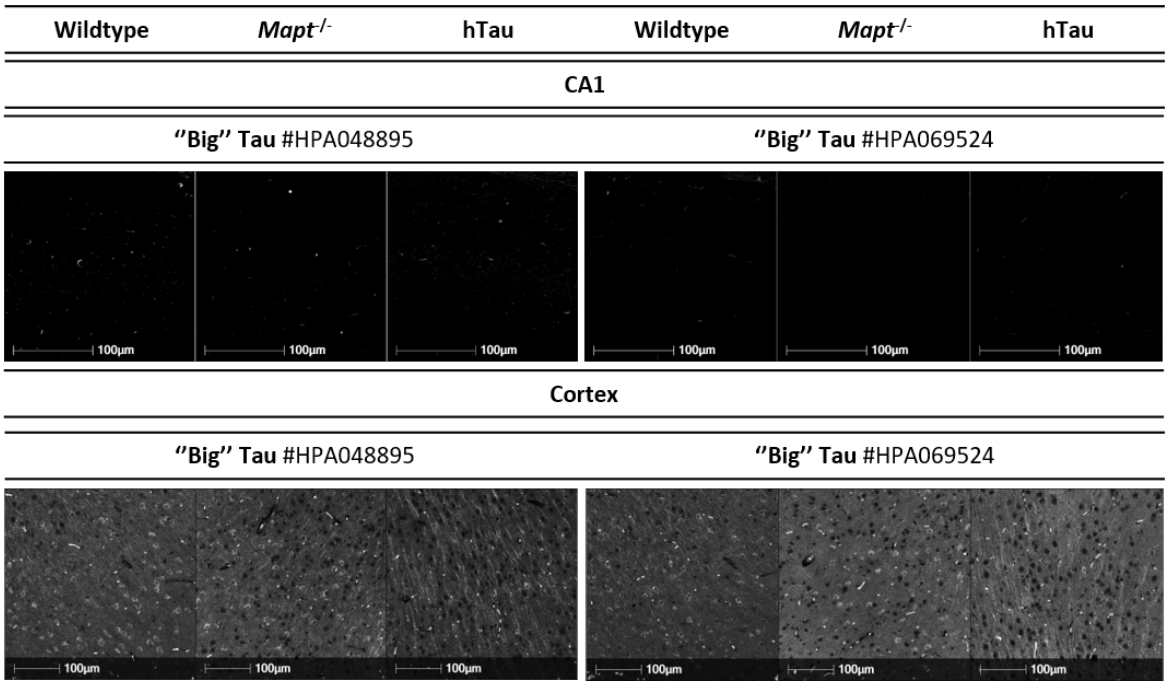

(a) CA1 hippocampal region

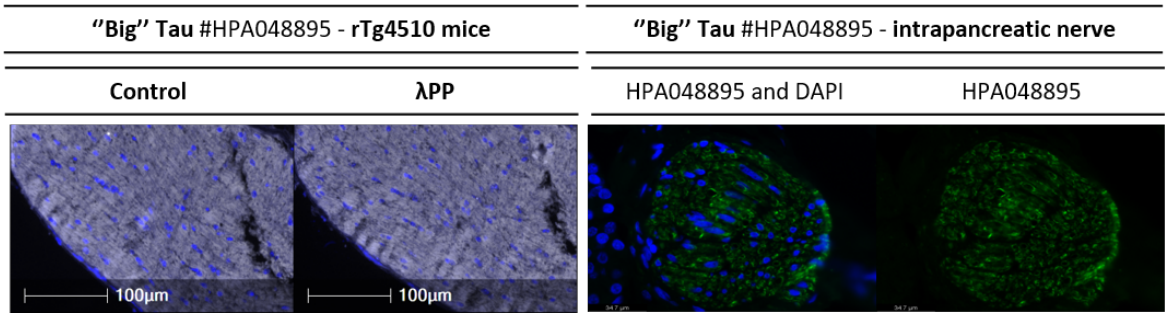

(b) TG4510 mouse cortex and human intrapancreatic nerve

Fig. 3.9 **Big Tau antibodies in the rTg4510 mouse cortex and in the hippocampus of wildtype, MAPT-/- and humanised Tau transgenic (hTau) mice. 3.9a** | Representative immunofluorescence micrographs demonstrating the presence and localisation of different antibodies. Two antibodies that detect Big Tau were assessed on FFPE brain sections from relevant mice. **3.9b**, left panel | Representative immunofluorescence micrographs demonstrating the presence and localisation of Big Tau in the cortex of 9-month old rTg4510 mice. Two serial FFPE brain sections/ antibody were pre-incubated with or without lambda phosphatase (λPP), before incubation with each of the two different antibodies that detect pTau forms. Whole slide scans were imaged at X20. Scale bars 100μm. **3.9b**, right panel | Representative immunofluorescence micrographs demonstrating the presence and localisation of Big Tau in the intrapancreatic nerve.

3.5 Other anti-Tau antibodies

3.5.1 Dephosphorylated-specific Tau forms

The Tau-1 antibody detects Tau forms dephosphorylated at residues Ser195, Ser198, Ser199 and, Ser202. Previous findings suggest that Ser198, Ser199 and, Ser202 are phosphorylated in the rTg4510 mouse cortex (fig. 3.11). As such, it is expected that Tau-1 may weakly stain the untreated rTg4510 mouse cortex and its signal intensity will be drastically increased in the λPP-treated tissue. As expected, immunoreactivity seen with the Tau-1 antibody in the control rTg4510 cortex is minimal and was significantly increased upon λPP treatment (fig. 3.10a). The human/mouse-reactive Tau-1 immunoreacted with Tau, in what was judged to be glial cells (fig. 3.10a, white arrows), in the WT mouse brain but not with Tau in the hTau mouse brain. Lack of positive signal in *Mapt*$^{-/-}$ (fig. 3.10b) demonstrates the specificity of the antibody. Tau-1 was classified as green in IHC.

3.5.2 Cleaved Tau forms

The proteolytic cleavage of Tau at D421 increases Tau aggregation and has been associated with AD [252, 253]. The D421 antibody detects Tau when cleaved at Asp421. The D421 antibody immunostained the rTg4510 mouse cortex (fig. 3.10a). Quantification analysis of the D421 reveals that both the signal intensity and the percentage of Tau-positive cells were drastically increased upon λPP treatment (figs. 3.4a, 3.4b) suggesting that the binding of this antibody is inhibited by the presence of phosphate groups and implying that a high proportion of Asp421 truncated Tau forms may be hyperphosphorylated. D421 antibody was classified as green in IHC.

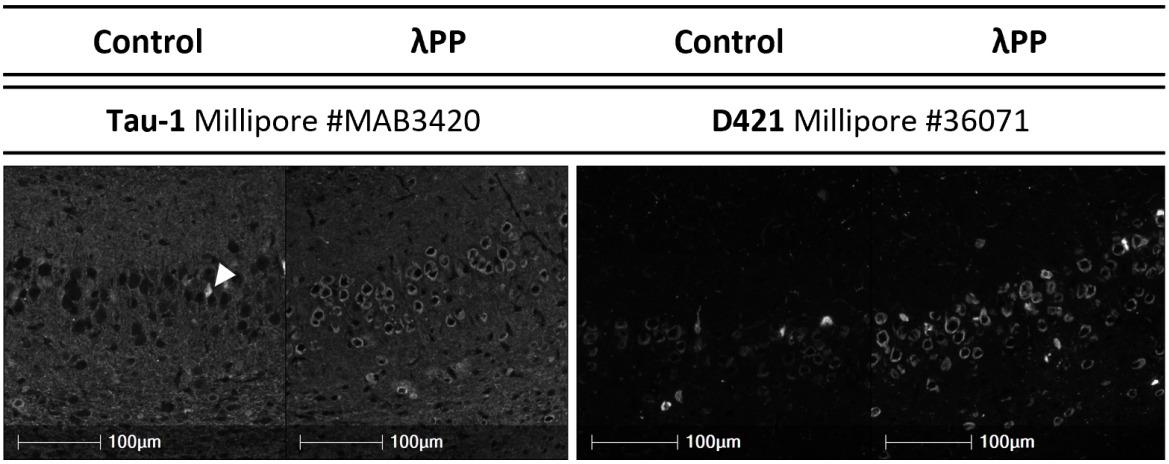

(a) TG4510 cortex

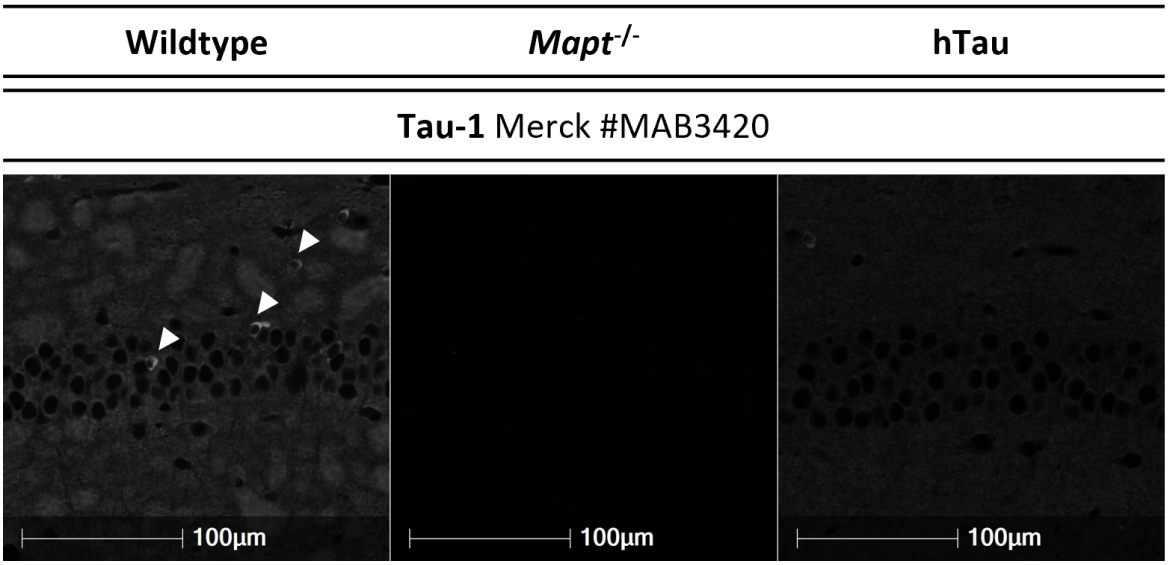

(b) CA1 hippocampal region

Fig. 3.10 **Other anti-Tau antibodies in the rTg4510 mouse cortex and in the hippocampus of wildtype, *Mapt*$^{-/-}$ and humanised Tau transgenic (hTau) mice 3.10a** | Representative immunofluorescence micrographs demonstrating the presence and localisation of 'other' anti-Tau antibodies (white immunostaining) in the cortex of 9-month old rTg4510 mice. Two serial FFPE brain sections per antibody were pre-incubated with or without lambda phosphatase (λPP), before incubation with each of the two different antibodies that detect Tau forms. White arrow; identified as glial cells. **3.10b** | Representative immunofluorescence micrographs demonstrating the presence and localisation of Tau-1 antibody (white immunostaining) which was assessed on FFPE brain sections from wildtype, *Mapt*$^{-/-}$ and hTau mice. Glial cells are indicated by white arrows. Whole slide scans were imaged at X20. Scale bars 100μm.

3.6 Phosphorylation-specific anti-Tau antibodies

Tau is a heavily post-translationally modified protein. One of the most common PTMs is phosphorylation and, notably, Tau has 85 putative phosphorylation sites (45 serine, 35 threonine and 5 tyrosine residues). 53 out of 85 sites have been shown to be modified experimentally [41]. There are more than 180 antibodies against specific phosphorylated Tau (pTau) forms and for the purpose of this project, 16 key phospho-specific Tau antibodies were validated in IHC (Chapter 2, Table 2.1). The selection of these Tau antibodies was guided by the published literature and, as such, the most commonly used phospho-antibodies used in health and disease were assessed here. The phosphorylation signature of Tau in mouse models may differ and it is expected that (i) all pTau antibodies will stain the rTg4510 mouse brain, which expresses a variety of Tau forms (physiological, pathogenic etc) but may present differential staining in the rest of the mouse models (WT, hTau). (ii) PHF-raised antibodies should detect Tau forms only in the rTg4510 but not the other mouse models which express physiological Tau. (iii) *Mapt*$^{-/-}$ should remain clear in all cases.

3.6.1 N-terminal domain

The N-terminal domain has 9 serine, 16 threonine and 2 tyrosine residues and in total, 11 out of 27 residues can be phosphorylated. One phospho-specific antibody (pThr181) was tested in IHC. pThr181 strongly immunostained the rTg4510 mouse cortex and, as expected, the signal was completely abolished after treatment with λPP (fig. 3.11). The human/mouse-reactive pThr181 was further tested in the WT, *Mapt*$^{-/-}$ and hTau mice CA1 region and no immunoreaction was noted (fig. 3.12). This implies that pThr181 is a specific antibody and it was classified as green. Lack of signal in the WT and hTau could signify that (i) Tau is not phosphorylated at this residue or (ii) the antibody does not detect endogenous levels of Tau.

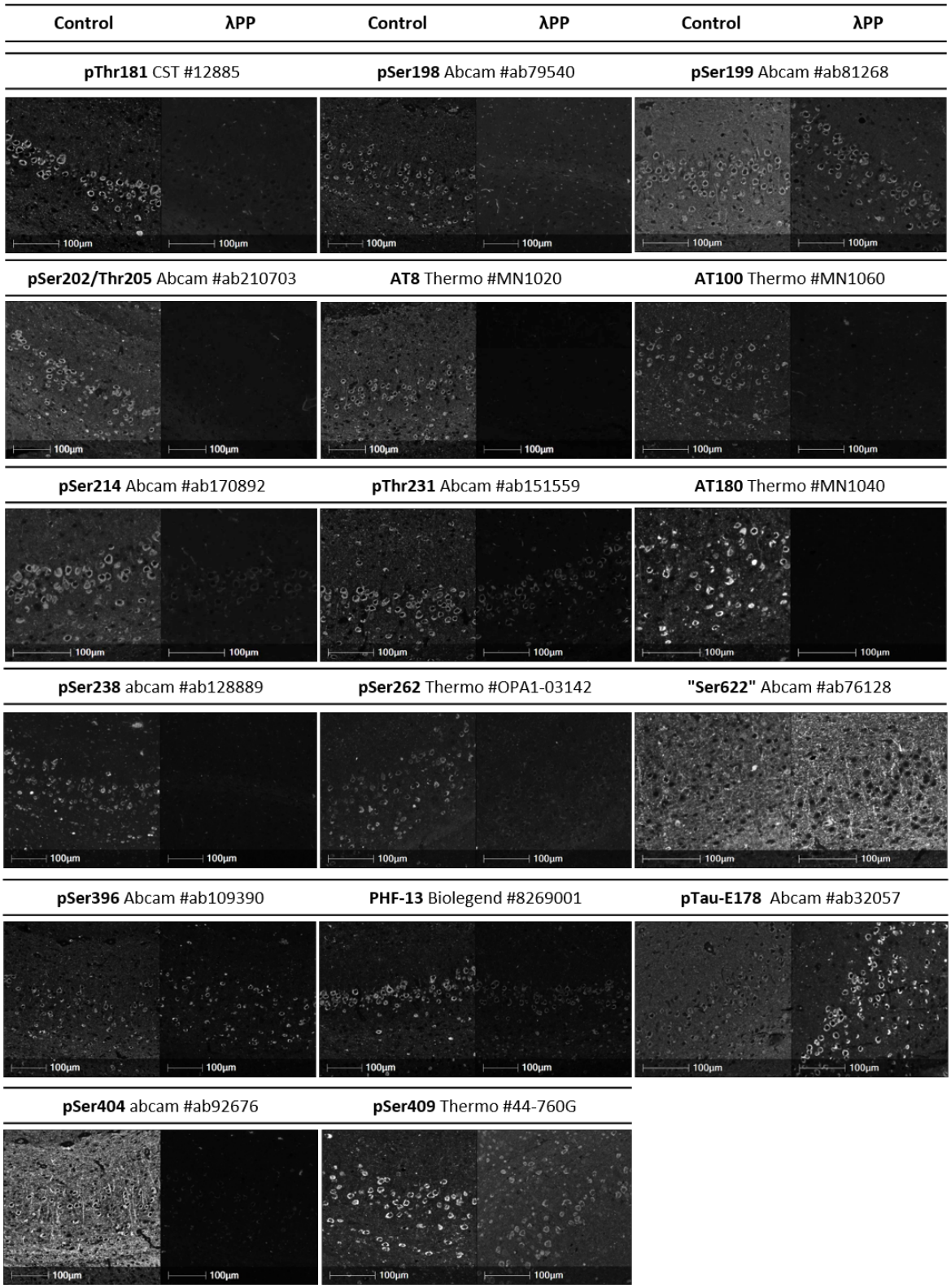

Fig. 3.11 **pTau antibody profiles in the rTg4510 mouse cortex.** Representative immunofluorescence micrographs demonstrating the presence and localisation of seventeen different pTau forms (white immunostaining) in the cortex of 9-month old rTg4510 mice. Two serial FFPE brain sections per antibody were pre-incubated with or without lambda phosphatase (λPP), before incubation with each of the seventeen different antibodies that detect pTau forms. Micrographs are presented in the order of the pTau antibody immunogens moving from the N' terminus to the C' terminus of Tau. Whole slide scans were imaged at X20. Scale bars 100μm.

3.6.2 Proline-rich domain

Compared to the other Tau domains, the PRD, consists of 22 prolines in a total of 143 residues and, is the most prone domain for phosphorylation. It has 14 serine, 9 threonine and 1 tyrosine and notably, 20 out of 24 residues can be phosphorylated. Six peptide-raised (pSer198, pSer199, pS202+pThr205, pSer214, pThr231 and pSer238) and three PHF-raised (AT8, AT100, AT180) Tau antibodies were tested in FFPE brain tissue and, all strongly immunoreacted with Tau in TG4510 mouse cortex as expected (fig. 3.11).

After treating the tissue with λPP, the signal produced with some antibodies was abolished (pSer198, pSer202+pThr205, AT8, AT100, AT180 and pSer238) whereas it was significantly reduced for others (pSer214 and pThr231). All these antibodies (pSer198, pSer202+pThr205, AT8, AT100, pSer214, pThr231, AT180 and pSer238) were classified as green. The pSer199 signal was reduced, although a significant reduction in the background signal was noted (fig. 3.11). This is in contrast to the WB data demonstrating that pSer199 immunoreactivity was abolished in λPP-treated SH-SY5Y lysates (fig. 3.13a). pSer199 was classified as amber for use in IHC and its improved signal will be discussed in depth in a later section (section 3.7).

Next, the pSer198, pSer199, AT8, AT100, pSer214 and AT180 antibodies were tested in the WT, *Mapt*$^{-/-}$ and hTau mice (fig. 3.12). As expected, none of the PHF-raised antibodies (AT8, AT100, AT180) immunoreacted with Tau in the hippocampus of WT, *Mapt*$^{-/-}$ or hTau mice, demonstrating their specificity for Tau and presumably the pathological forms of Tau. Firm conclusion on this however cannot be made as the lack of signal could be also justified by the low levels of Tau and incapability of the antibodies to detect Tau at low levels. Nonetheless, based on these findings, AT8, AT100, AT180 were classified as as green. The human/mouse-reactive pSer198 immunostained the cell bodies in the CA1 region of WT and hTau mouse brains but

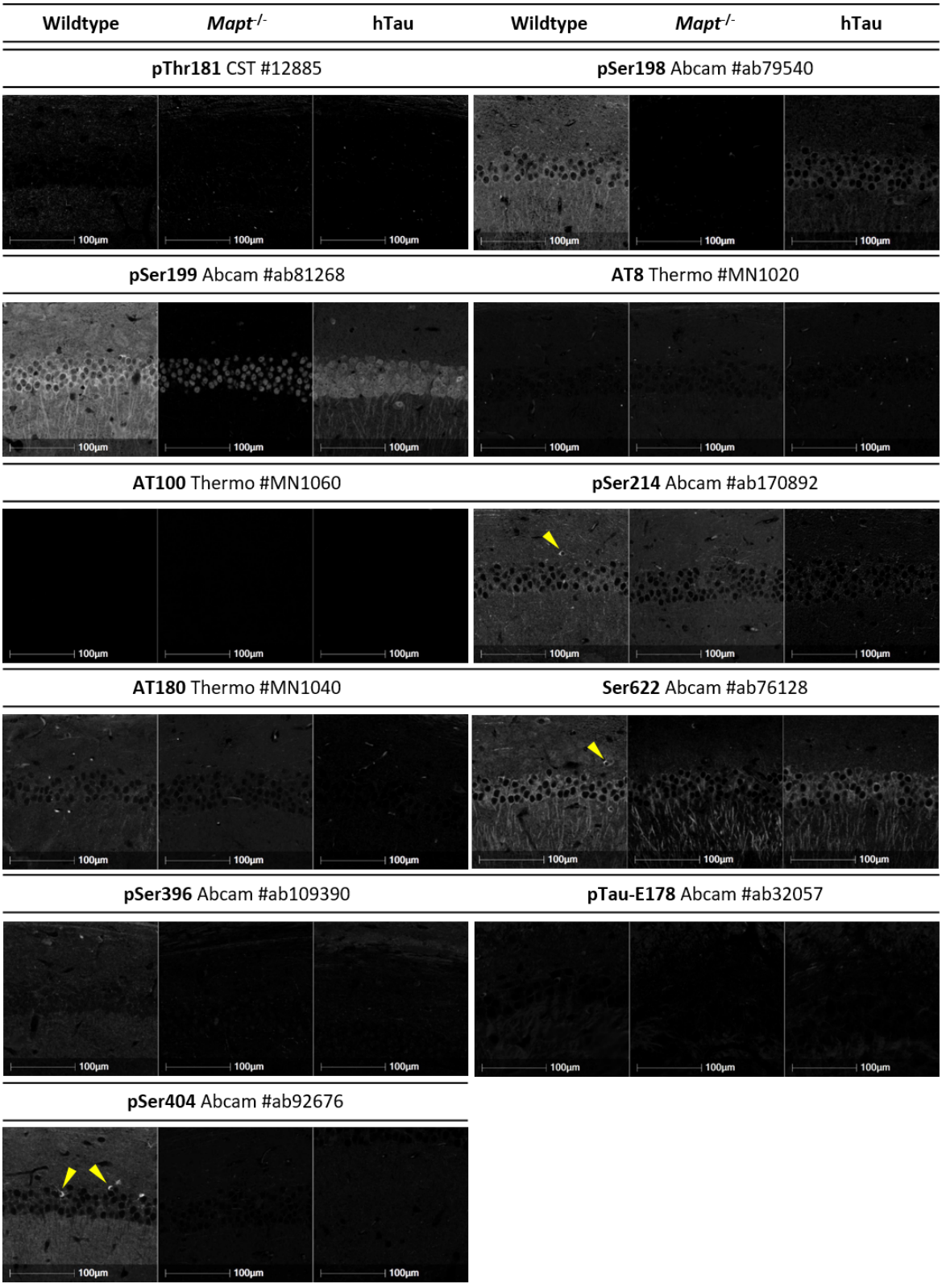

Fig. 3.12 **pTau antibody profiles in wildtype, *Mapt*$^{-/-}$ and humanised Tau transgenic (hTau) mice** Representative immunofluorescence micrographs demonstrating the presence and localisation of eleven different pTau forms (white immunostaining) in the hippocampus of wildtype, *Mapt*$^{-/-}$ and humanised Tau transgenic (hTau) mice. Eleven different antibodies that detect pTau forms were assessed on FFPE brain sections from relevant mice. Glial cells indicated by yellow arrows. Micrographs are presented in the order of the pTau antibody immunogens moving from the N' terminus to the C' terminus of Tau. Whole slide scans were imaged at X20. Scale bars 100μm.

not in *Mapt*$^{-/-}$ animals, demonstrating that it is a specific antibody (green). pSer198 also immunoreacted with Tau at the dendrites. The human/mouse-reactive pSer214 antibody detected Tau in the CA1 region of the WT mice, in what was judged to be glial cells of WT mouse brain (fig. 3.12, yellow arrows). No signal was detected with pSer214 in the hTau CA1 region whereas it produced background signal in the *Mapt*$^{-/-}$ mouse brain, classifying it amber.

The human/mouse-reactive pSer199 immunoreacted with Tau in the cell bodies of hippocampal cells in the WT and hTau mice (fig. 3.12). It also immunostained the projections of these cells in WT and hTau mice. Unexpectedly, it also stained the nuclei of the *Mapt*$^{-/-}$ and the hTau mice. Sequence analysis revealed that the region of Tau, spanning around Ser199, presents high homology similarity to the other microtubule-associated proteins (MAPs), such as the MAP-2 (Appendix A, fig. A.1). MAP isoforms are expressed in the nucleus of neurons [254, 255] and, as such, it is possible, that the pSer199 antibody immunoreacted with MAP-2 in the nucleus. This can be explained either by (i) increased levels of MAP-2 protein because of the lack of Tau protein or by (ii) the fact that the non-specific nuclear signal is visible because of the lack of real signal, or both. As this signal is non-specific and occurs only in the *Mapt*$^{-/-}$ and the hTau mice, but is not seen in the WT, the pSer199 antibody is considered a reasonable overall antibody and was classified as amber.

3.6.3 Microtubule-binding domain

The MBD has 12 serine, 4 threonine and 1 tyrosine residues and in total, 7 out of 17 residues can be phosphorylated. Two antibodies that detect phosphorylated residues within the MBD were tested, pSer262 and pSer622. pSer262 (Thermo) strongly immunoreacted with Tau in the rTg4510 mouse cortex and its signal was abolished after treatment with λPP (fig. 3.11). Therefore, it was classified as green.

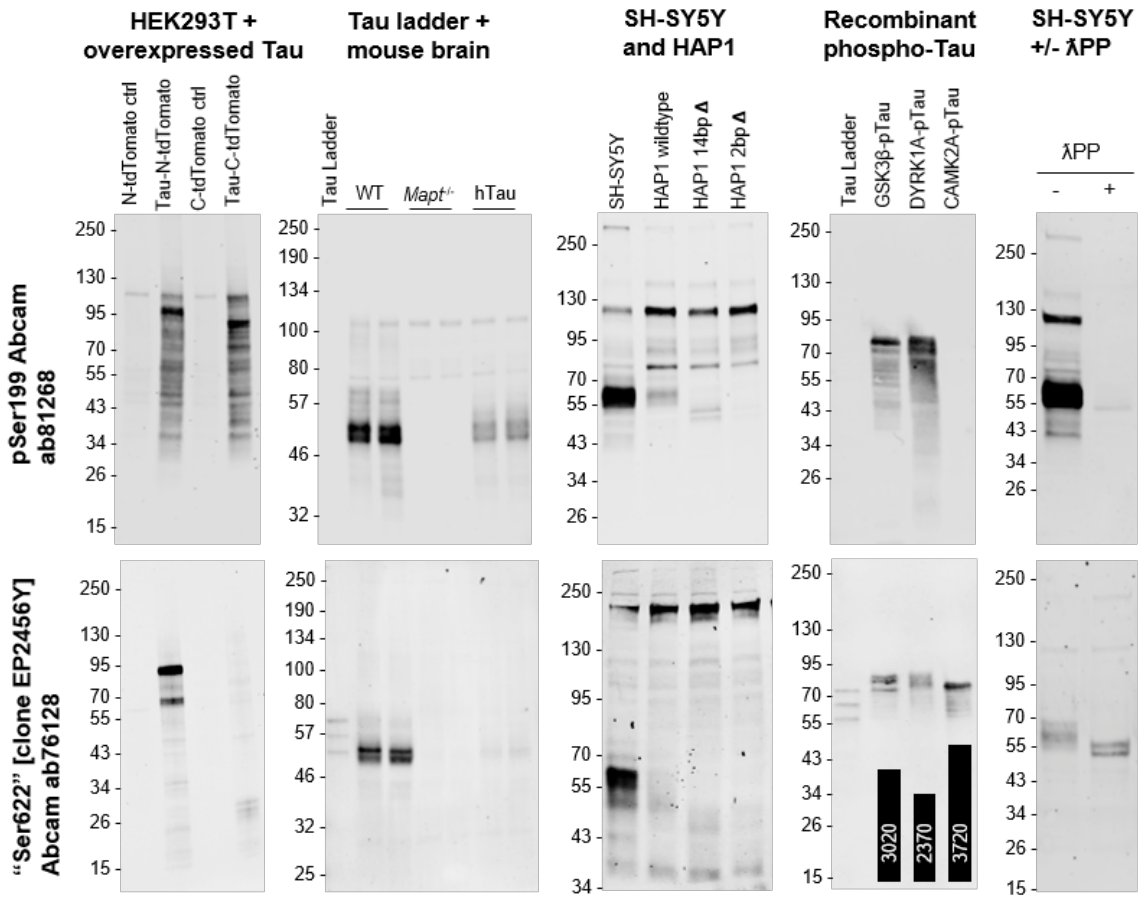

(a)

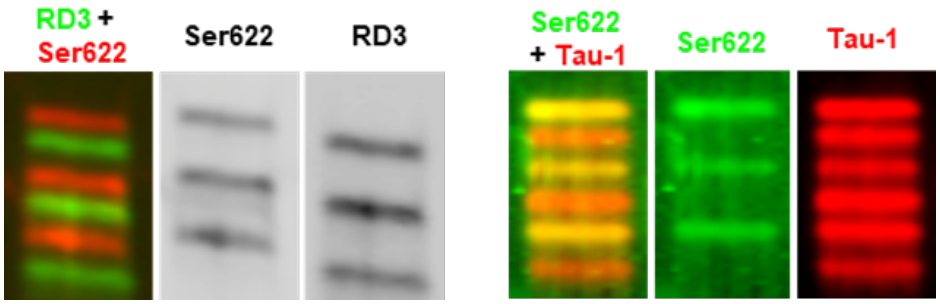

(b)

Fig. 3.13 **Immunoblotting using a range of lysates to confirm the specificity of phospho-specific Tau antibodies. 3.13a** | Immunoblots demonstrating in the specificity of isoform-specific Tau antibodies and their reactivity for human and mouse Tau. WBs of lysates from HEK293T cells overexpressing 0N3R human Tau and corresponding control cells (first column); recombinant human Tau ladder (5 ng/isoform/lane), plus adult mouse brain lysates from wildtype, Mapt-/- and hTau mice (second column); lysates from SH-SY5Y neuroblastoma cells, plus HAP1 cells, parental (wildtype) and two cell lines carrying either a 14 bp deletion (14 bp Δ) or a 2-bp deletion (2 bp Δ) in MAPT exon 4 (third column); recombinant human Tau ladder (50 ng/isoform/lane) plus recombinant 2N4R Tau that has been phosphorylated by one of three known Tau kinases: GSK3β, DYRK1A or CAMKIIA (fourth column); lysates from SH-SY5Y neuroblastoma cells that have been either untreated (-) or treated (+) with λPP (fifth column). **3.13b** | WB of recombinant human Tau ladder was co-probed with the Ser622 antibody and either the RD3 Tau antibody clone or the Tau-1 antibody. Experiments performed by Dr Irina Stefana (University of Oxford).

The Ser622 antibody was initially labelled as a phospho-specific Tau antibody picking up Tau phosphorylated at Ser622 (numbered based on PNS Tau; Ser305 on 2N4R Tau). The Ser622 antibody strongly immunostained the rTg4510 mouse cortex and its immunoreactivity was not affected by λPP treatment (fig. 3.11), suggesting that the antibody is not phospho-specific but rather it is a total or an isoform-specific antibody. The immunoreactive staining pattern of Ser622 in the rTg4510 cortex is similar to that of RD4, an antibody that detects the 4R Tau isoform (fig. 3.7a). This is also in alignment with sequence analysis revealing that the Ser622 antibody is raised against the Ser305 residue (2N4R Tau) which is the last residue of the exon 10 (inclusion of exon 10 gives rise to the 4R isoforms). Taken together these data suggest that Ser622 picks up 4R Tau isoforms. This observation is also in line with WB data suggesting that the Ser622 antibody detects a band of similar MW to the 4R Tau isoform in SH-SY5Y cell lysates (fig. 3.13a). However, it is important to note that WB data also demonstrated that that under specific circumstances, Ser622 may also detect the 3R isoform.

Next, Ser622 was used to stain the WT, *Mapt*$^{-/-}$ and hTau mice. Ser622 stained the cell bodies and the projections of CA1 region of the WT, *Mapt*$^{-/-}$ and hTau (fig. 3.12). Similarly to the Tau-46 antibody, sequence analysis for Ser622 antibody has revealed that the certain regions of Tau protein are very similar to the other microtubule-associated proteins (MAPs), such as the MAP-2 (Appendix A, fig. A.1). As such, it is possible that the Ser622 antibody labels 4R-Tau isoforms but produces non-specific signal when probed to detect low levels of Tau in FFPE tissue. However, it has similar staining pattern with RD4 isoform-specific antibody in the rTg4510 cortex (fig. 3.11) and with Tau-46 total antibody in WT, *Mapt*$^{-/-}$ and hTau mouse models (fig. 3.12). The λPP treatment experiment demonstrates that Ser622 is not a phospho-specific Tau antibody and BLAST search suggests that this antibody could cross-react with

MAP-2 and MAP-4. All the above render Ser622 is classified as red and is not suitable antibody for use in IHC.

3.6.4 C-terminal domain

The C-terminal domain has 10 serine, 6 threonine and 1 tyrosine residues and in total, 15 out of 17 residues can be phosphorylated. Four peptide-raised (pSer396, pTau-E178, pSer404, pSer409) and one PHF-raised (PHF-13) Tau antibodies were tested in FFPE brain tissue. All Tau antibodies tested (pTau-E178, pSer396, PHF-13, pSer404, pSer409) strongly immunoreacted with Tau in the rTg4510 cortex (fig. 3.11). Interestingly, the pSer404 antibody also immunoreacted with Tau within cell projections in the rTg4510 cortex. pSer404 signal was completely abolished in the λPP-treated tissue, whereas the signal was reduced for some antibodies (PHF-13, pSer409) and was unexpectedly enhanced for others (Ser396, pTau-E178). pSer409 was classified as amber because it strongly stained the rTg4510 cortex but, upon λPP treatment, it demonstrated nonspecific nuclear signal (fig. 3.11).

The pTau-E178, pSer396 and pSer404 antibodies were then selected to stain the WT, *Mapt*$^{-/-}$ and hTau mice. pTau-E178 and pSer396 did not detect Tau in any of the mouse models. pSer404 immunostained a few cells, possibly glial cells (fig. 3.12, yellow arrows). None of the antibodies stained the *Mapt*$^{-/-}$ mice demonstrating the specificity of these antibodies and classifying them as green in IHC.

3.7 Aggregated forms of Tau

Contrary to what was expected, a collection of phospho-specific Tau antibodies directed against the PRD (pSer199, pThr231) and the C-terminal Tau domains (E178 pSer396, pSer396, pSer409) demonstrated unchanged or an improved fluorescent signal in the

λPP-treated tissue compared to the control. Three possible scenarios would explain this; (i) λPP treatment was not successful which is unlikely as the λPP abolished staining with other phospho-specific Tau antibodies in the same experiment, (ii) these phospho-specific Tau antibodies have a high affinity for the relevant phosphorylated Tau residues, which is supported by their strong immunoreactivity with Tau before λPP treatment, but they may also detect dephosphorylated Tau forms and/or 'total' Tau forms hence explaining the signal after the λPP treatment or, (iii) λPP treatment removes the majority of phosphates groups but not all if Tau is in an aggregated form. The removal of nearby phosphatase sensitive residues then reveals epitopes for which these antibodies have higher affinity.

3.7.1 Tau aggregates in AD human brain

To investigate which scenario applies, two serial sections of AD brain tissue were treated with and without λPP treatment and were stained with (i) Thioflavin S (ThioS), a green β-sheet dye employed to detect Tau aggregates, (ii) pTau-E178, an antibody whose signal was improved after λPP treatment (fig. 3.11) and, (iii) AT8, an antibody that has previously shown to be completely abolished after λPP treatment (fig. 3.11). pTau-E178 and AT8 antibodies stained the same structures as ThioS in the untreated tissue demonstrating that both antibodies can detect Tau aggregates (fig. 3.14, top panel). After treating the tissue with λPP, AT8 signal was completely abolished and pTau-E178 signal was improved, which is in line with our previous results (fig. 3.11). Interestingly, pTau-E178 co-localised with ThioS in the λPP-treated tissue (fig. 3.14, bottom panel). These findings further confirm that the λPP treatment was successful (abolished AT8 signal) and are also replicable in human FFPE brain tissue.

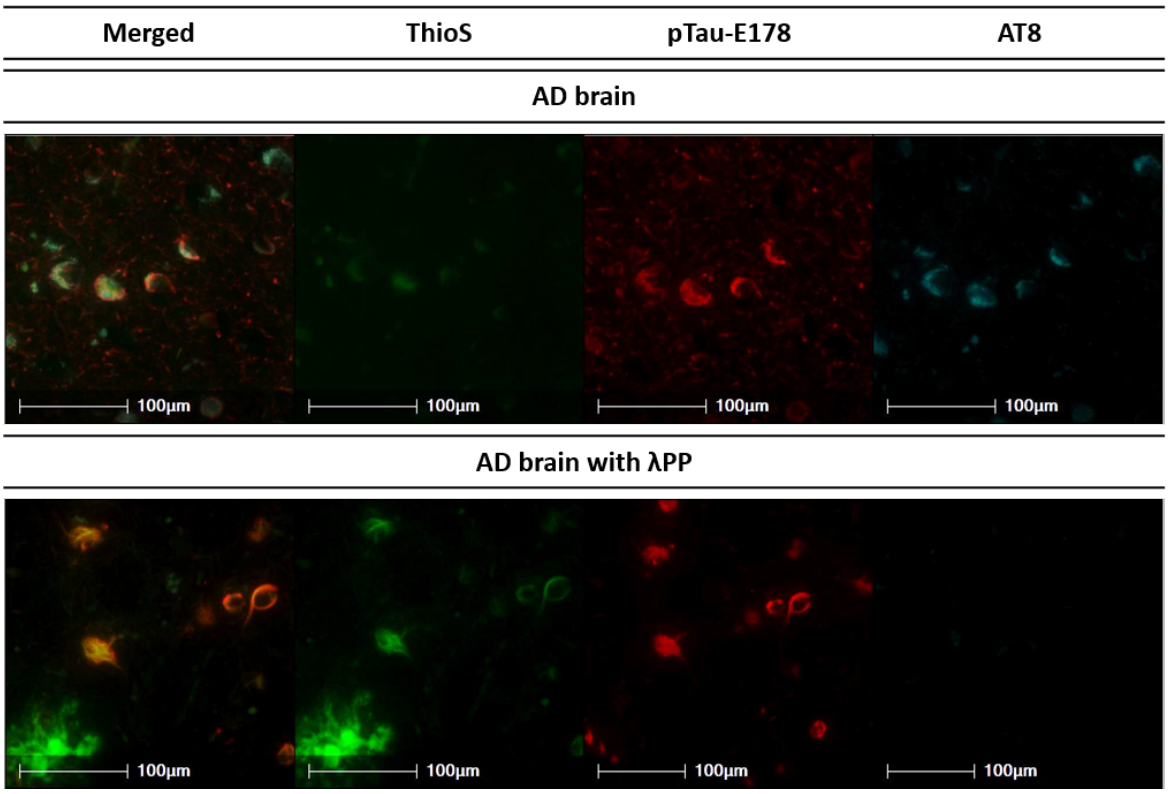

Fig. 3.14 **Thioflavin S and aggregated Tau forms in human Alzheimer's Disease (AD) brain.** Representative immunofluorescence micrographs demonstrating the presence and localisation of different peptide-raised and PHF-raised antibodies in relation to Thioflavin S (ThioS) in the human AD brain. Two serial FFPE AD brain sections were pre-incubated with or without lambda phosphatase (λPP), before incubation with pTau-E178 (red) and AT8 (cyan) phospho-specific antibodies and ThioS (green). ThioS is a green β-sheet fluorescent dye that labels aggregates. Scale bars 100μm.

3.7.2 Tau phosphorylation in intrapancreatic nerves

Next, to assess whether phospho-specific antibodies may also detect dephosphorylated Tau forms and/or 'total' Tau forms hence explaining the signal after the λPP treatment (second scenario), serial FFPE pancreas tissue sections were treated with and without λPP treatments and were then stained with (i) pThr231, a phospho-specific antibody whose signal was reduced but not abolished in the rTg4510 cortex after λPP treatment (fig. 3.11), (ii) Tau-1, a dephospho-specific antibody whose signal was improved in the rTg4510 cortex after λPP treatment (fig. 3.10a) and, DAPI. The intrapancreatic nerves

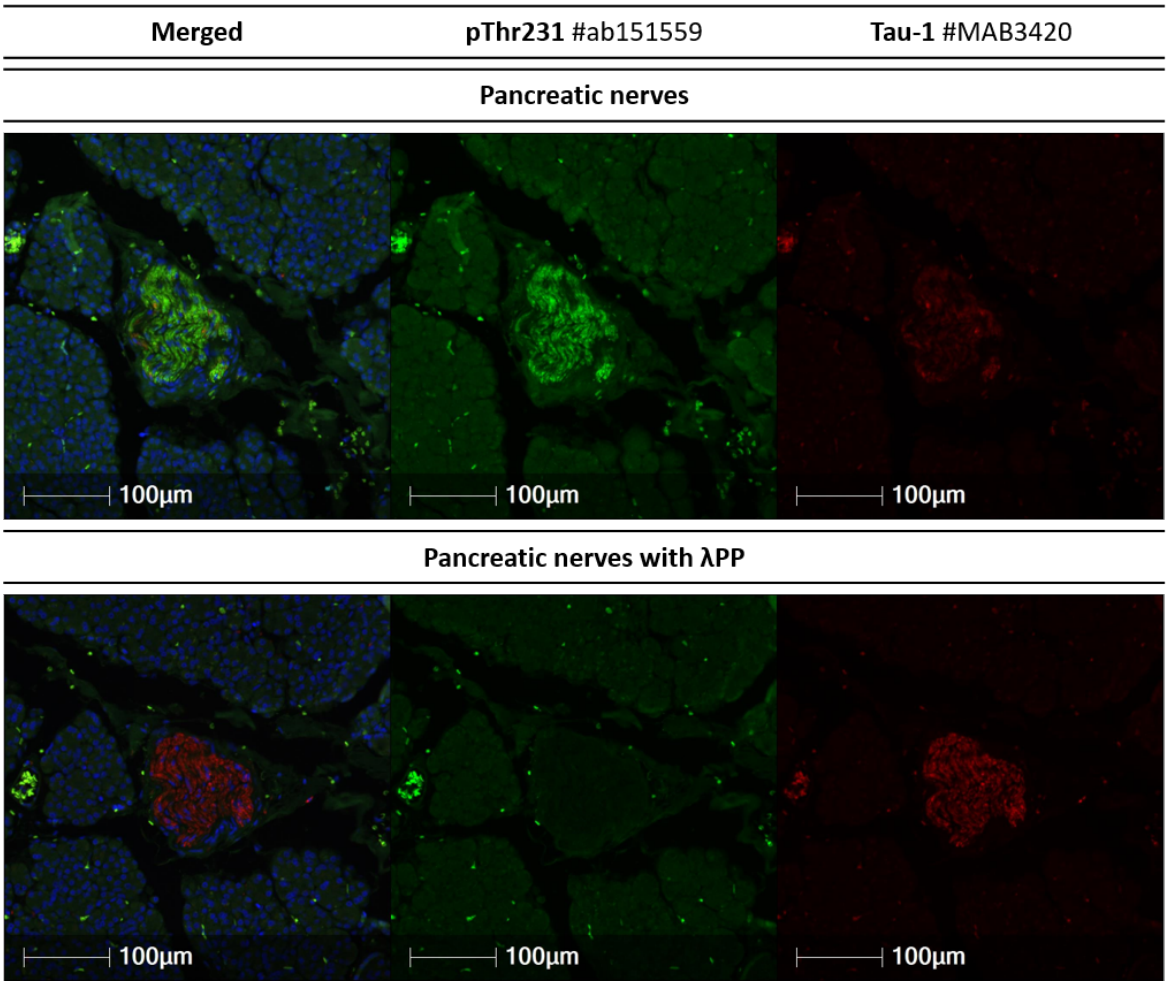

Fig. 3.15 **Tau antibody profiles in human pancreatic nerves.** Representative immunofluorescence micrographs demonstrating the presence and localisation of Tau antibodies in human pancreatic nerves. Two serial FFPE human pancreas sections were pre-incubated with or without lambda phosphatase (λPP), before incubation with pThr231 (green) and Tau-1 (red) antibodies and DAPI (blue). Microscopy was performed using a fluorescent microscope. Magnification x40. Scale bars 100μm.

were used as a positive control for Tau expression. As expected, both pThr231 an Tau-1 stained the pancreatic nerves (fig. 3.15). In alignment with previous observations in the rTg4510 mouse cortex, the Tau-1 signal was improved in the λPP-treated pancreas tissue compared to the control (fig. 3.15). Interestingly, pThr231 signal was abolished in the λPP-treated pancreas tissue compared to the control. These findings invalidate the second scenario and best support the third scenario, being that λPP treatment

removed the majority of phosphate groups and revealed previously masked epitopes of aggregated forms of Tau.

3.7.3 Tau aggregates in rTg4510 mouse brain

Next, five rTg4510 mouse brain sections were stained with (i) one of the following phospho-specific Tau antibodies (Ser202/Thr205, AT8, AT100, AT180, Ser396) and (ii) ThioS (fig. 3.16). It is expected that the peptide-raised phospho-specific antibodies (Ser202/Thr205, Ser396) would detect both ThioS positive and ThioS negative cells, whereas the PHF-raised antibodies (AT8, AT100, AT180) would detect only the ThioS positive cells. Interestingly, PHF-raised antibodies and ThioS showed differential immunostaining patterns; although they co-localised in most places (blue arrows), cells single positive for PHF-raised antibodies (blue arrows) and cells single positive for ThioS (white arrows) were detected. These data suggest that PHF-raised antibodies can detect both aggregated and physiological phosphorylated forms of Tau.

3.8 λPP effect on total Tau antibodies

Total and isoform-specific Tau antibodies can allegedly label all forms of Tau regardless of PTMs and, as such, it is expected that the λPP treatment would not affect their immunoreactivity. As expected, some antibodies (43D, Tau-13 and Tau-46) were not impacted. However, some total Tau antibodies were impacted by λPP treatment; with most (N-term, SP70, Tau-12, Tau-5, HT7, Dako) demonstrating more intense signal in the λPP-treated tissue and others (SP70) demonstrating less intense signal. Antibodies with epitopes directed against the PRD (Tau-5, HT7) were the most affected.

rTg4510 mouse brain sections were stained with (i) a total Tau and (ii) a phospho-specific Tau antibody and, it is expected that there will be cells that stain (i) double

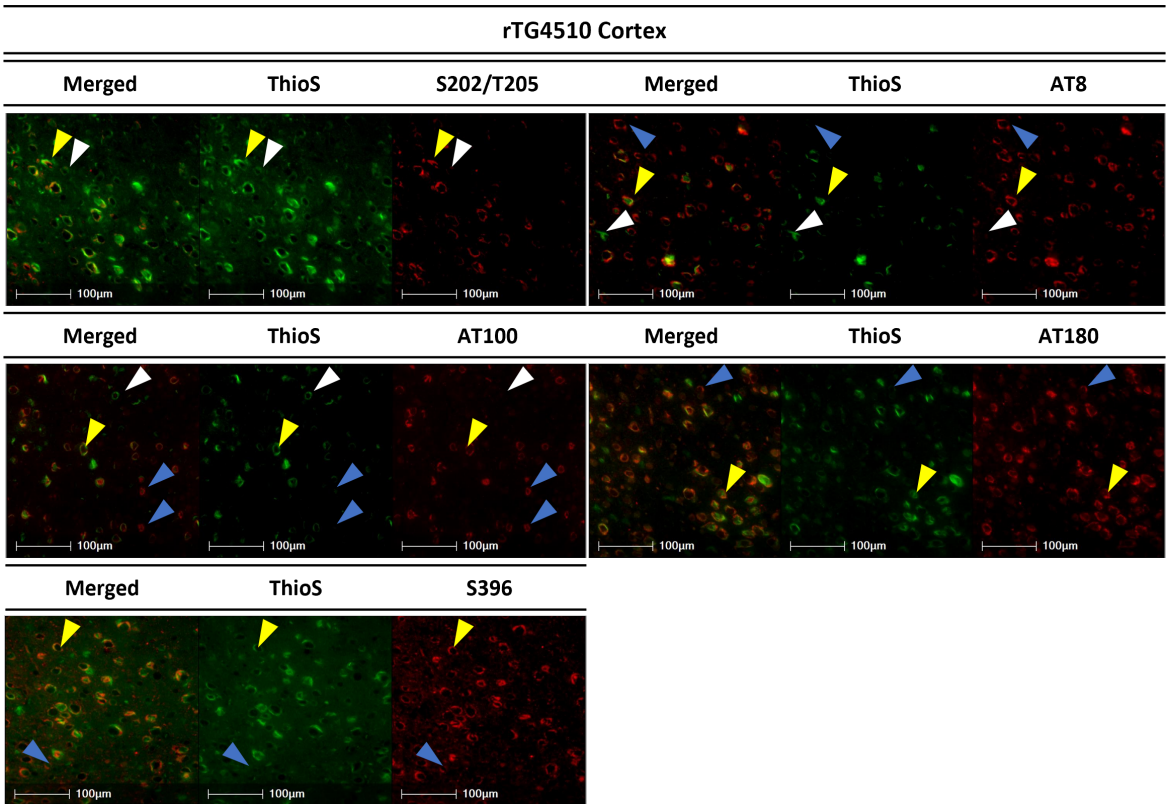

Fig. 3.16 **Thioflavin S and aggregated Tau forms in the rTg4510 mouse cortex.** Representative immunofluorescence micrographs demonstrating the presence and localisation of different peptide-raised or PHF-raised antibodies in relation to Thioflavin S (ThioS) in the cortex of 9-month old rTg4510 mice. Five different phospho-specific antibodies (red) were assessed in relation to ThioS (green) on FFPE brain sections from relevant mice. ThioS is a green β-sheet fluorescent dye that labels aggregates. Micrographs are presented in the order of the pTau antibody immunogens moving from the N' terminus to the C' terminus of Tau. White arrowheads; ThioS positive cells, blue arrowheads; Tau positive cells, yellow arrowheads; ThioS and Tau positive cells. Imaged at X40. Scale bars 100μm.

positive for total and phospho-specific antibodies or (ii) single positive for total Tau antibodies. It is not expected to observe cells that stain single positive for phospho-specific Tau antibodies. The same principle would apply for isoform-specific Tau antibodies. To carefully explore the impact of phosphorylation events on the binding ability of the total and isoform-specific Tau antibodies, careful assessment of the immunostaining pattern is required.

3.8.1 Total Tau antibodies directed against the N- and C-terminal domains of Tau

rTg4510 mouse brain sections were stained with one of the four following antibody combinations; (i) N-term and PHF-13, (ii) SP70 and AT8, (iii) Tau-12 and E178 and, (iv) K9JA and AT100. N-term, SP70, Tau-12 and K9JA antibodies co-localised with PHF-13, AT8, E178 and AT100, respectively, in the rTg4510 mouse hippocampus (fig. 3.17). In addition, the total Tau antibodies single stained cells in the rTg4510 mouse cortex. No single stained cells for phospho-specific antibodies were observed. These data demonstrate that SP70, K9JA, N-term total and Tau-12 Tau antibodies are able to detect all forms of Tau. In all cases, the cells within the cortex stained positive both for total and phospho-specific Tau antibodies whereas, cells single positive for total Tau antibodies can be detected only in the hippocampus.

3.8.2 Co-staining with isoform- and phospho-specific Tau antibodies

rTg4510 mouse brain sections were stained with RD4 and pSer202/pThr205. rTg4510 mouse brain overexpresses the 0N4R Tau isoform and therefore, it is expected that cells will stain (i) double positive for RD4 and pSer202/pThr205 or (ii) single positive for RD4 antibody. Unexpectedly, cells within the rTg4510 mouse cortex stained single positive for pSer202/pThr205 and no RD4 positive cells were observed (fig. 3.17e). Cells within the rTg4510 mouse hippocampus stained either (i) single positive for RD4 (white arrows) or, (ii) single positive for pSer202/pThr205 (orange arrows). These data demonstrate that RD4 and pSer202/pThr205 antibodies do not always co-localise in the cortex or the hippocampus of rTg4510 mouse, providing evidence that the binding

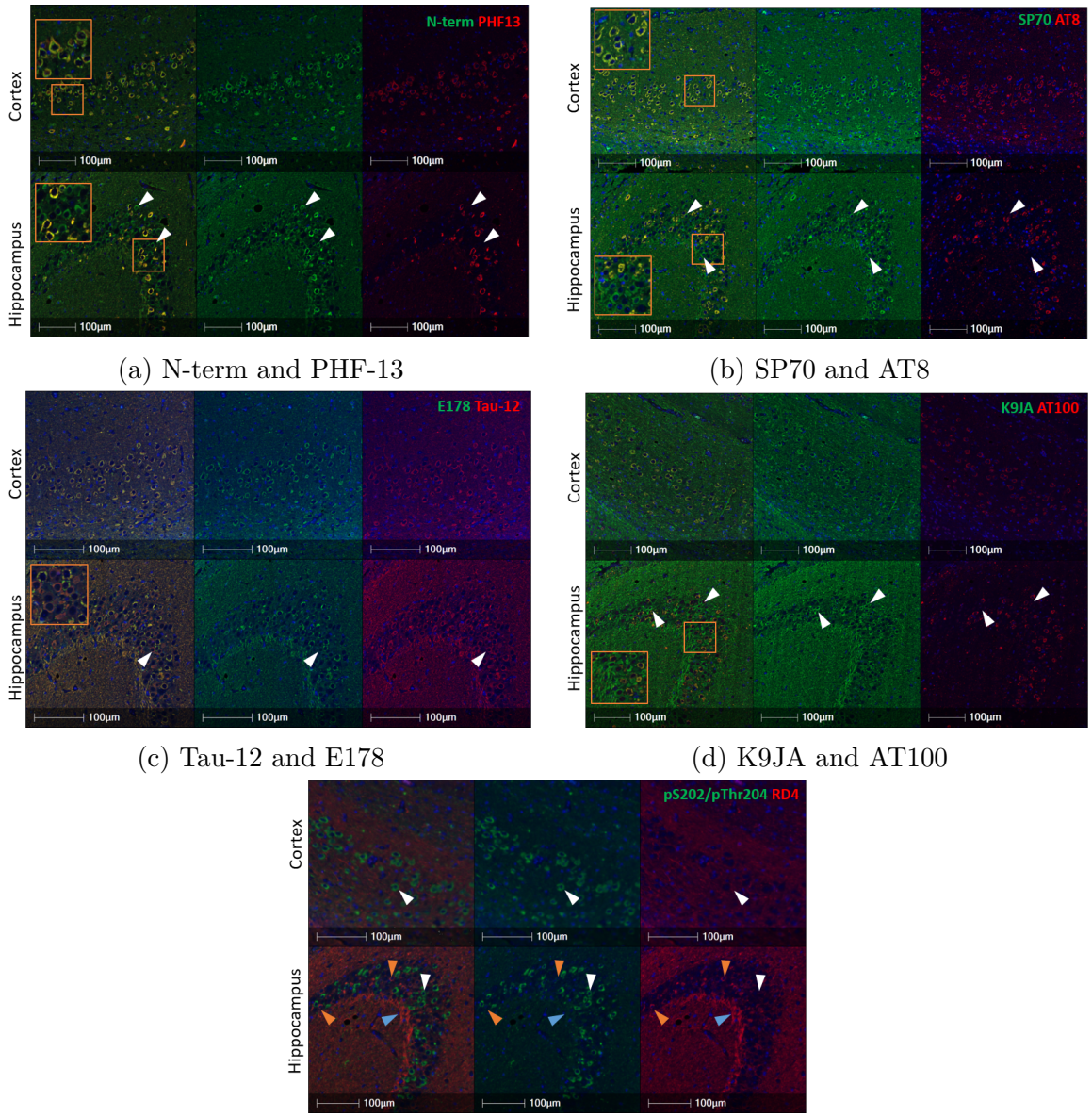

(a) N-term and PHF-13

(b) SP70 and AT8

(c) Tau-12 and E178

(d) K9JA and AT100

(e) RD4 and pSer202/pThr205

Fig. 3.17 **Differential immunoreactivity of total and phospho-Tau antisera within the rTG4510 brain.** FFPE rTg4510 brain tissue sections were stained for one of the following antibody combination; **3.17a** | N-term (green) and PHF-13 (red), white arrows; single positive for N-term antibody. **3.17b** | SP70 (green) and AT8 (red), white arrows; single positive for SP70 antibody. **3.17c** | Tau-12 (red) and E178 (green), white arrows; single positive for Tau-12 antibody. **3.17d** | K9JA (green) and AT100 (red), white arrows; single positive for K9JA antibody. **3.17e** | RD4 (red) and pSer202/pThr205 (green), white arrows; single positive for pSer202/pThr204 antibody, orange arrows; single positive for RD4 antibody and blue arrows; fimbria. DAPI (blue). Whole slide scans were imaged at X20. Scale bars 100μm.

of RD4 antibody to Tau in FFPE tissue is greatly impacted by excess phosphorylation events or conformational changes.

3.8.3 Total Tau antibodies directed against the PRD domain

rTg4510 mouse brain sections were pre-treated with and without λPP and were stained with either; (i) Tau-5 (Abcam) and pSer396 or, (ii) HT7 and pSer262. The Tau-5 (Abcam) and HT7 antibodies are directed against the PRD domain and previous work demonstrated that they were some of the most impacted total Tau antibodies upon treatment with λPP.

As expected, Tau-5 and HT7 co-localised with pSer396 and pSer262, respectively, in the control rTG4510 mouse cortex (fig. 3.18a, 3.18c). Immunostaining in the untreated rTg4510 cortex revealed that some cells stained single positive for Tau-5. Total Tau antibodies single stained cells in the rTg4510 mouse cortex. In both cases, single stained cells for phospho-specific antibodies were also observed. Immunostaining in the untreated rTg4510 hippocampus demonstrated that HT7 antibody detected Tau, whereas Tau-5 did not. These observations raises questions about the ability of HT7 and especially of Tau-5 antibodies to detect all forms of Tau.

Interestingly, in the λPP-treated tissue, pSer396 and Tau-5 co-localised both in the cortex and the hippocampus (fig. 3.18b). Previous quantification analysis demonstrated that the signal intensity and the percentage of Tau-5 positive cells are increased upon λPP treatment. Taking these findings together, it is concluded that the binding of Tau-5 antibody is inhibited by excess phosphorylation.

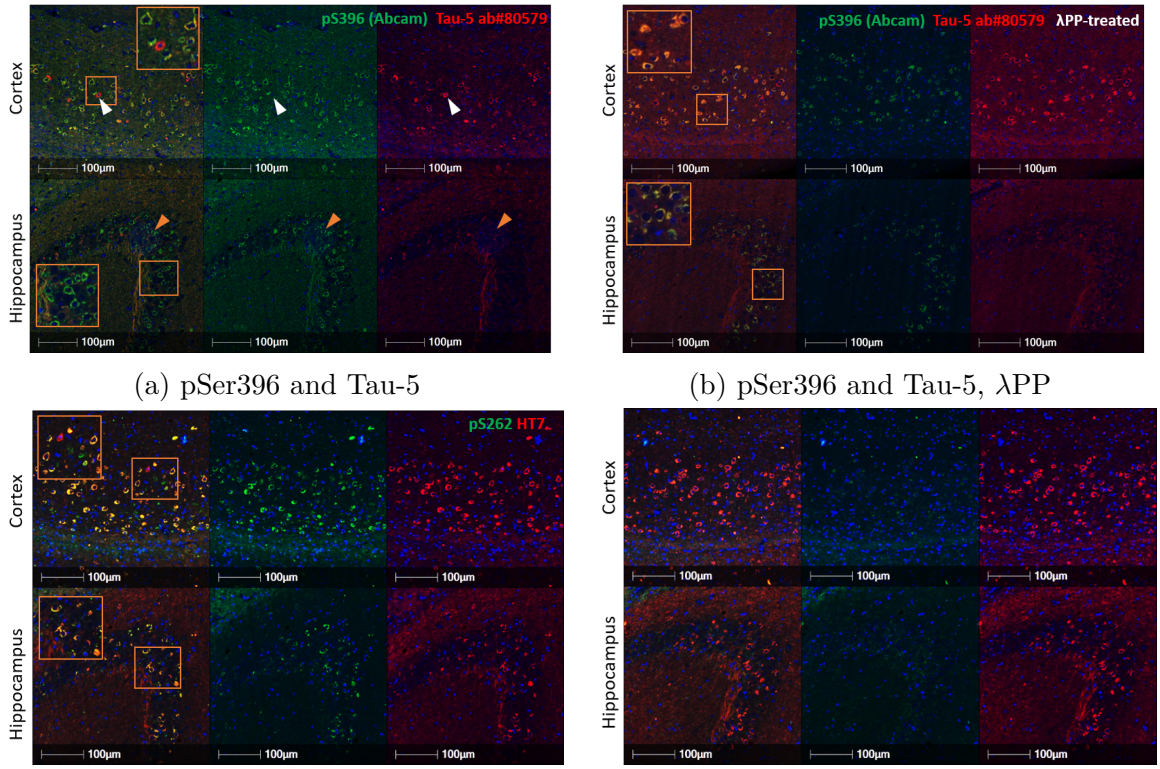

(a) pSer396 and Tau-5

(b) pSer396 and Tau-5, λPP

(c) pSer262 and HT7

(d) pSer262 and HT7, λPP

Fig. 3.18 **Differential immunoreactivity of total and phospho-Tau antisera within the rTG4510 brain cont.** FFPE rTg4510 brain tissue sections were stained for one of the following antibody combination; **3.18a** | pSer396 (green) and Tau-5 (red), white arrows; single stained for Tau-5 and orange arrows; single stained for pSer396. **3.18b** | pSer396 (green) and Tau-5 (red) with λPP. **3.18c** | pSer262 (green) and HT7 (red). **3.18d** | pSer262 (green) and HT7 (red) with λPP, plus DAPI (blue). Whole slide scans were imaged at X20. Scale bars 100μm.

3.9 Discussion

Tau is an exceptionally complex and heavily post-translationally modified protein, and therefore careful validation of Tau antibodies is required to ensure reproducibility and appropriate data interpretation. This chapter describes antibody validation strategies for use in IHC and assesses the suitability and specificity of each of the antibodies. Here, for the first time, the TLS is described. The TLS is a visualisation method to assess the suitability and specificity of an antibody for use in WB and IHC. In total 53 antibodies have been validated in WB (in Oxford) and guided by these data, 37

antibodies were then validated for use in IHC. Each TLS-antibody is represented by two mini traffic lights - one for WB (black) and one for IHC (blue). The coloring scheme demonstrates the suitability and specificity of each antibody; (i) green signifies that the antibody detects Tau with high specificity, (ii) amber signifies that the antibody detects Tau but either unexpected performance (e.g. "total" Tau antibody detects only subset of splice isoforms or is inhibited by phosphorylation, phospho-Tau antibody detecting unphosphorylated protein etc) and/or shows non-specific cross-reactivity with other proteins and, (iii) red signifies that there are no evidence that it detects Tau (may or may not show non-specific cross-reactivity with other proteins). The TLS visualisation method allows (i) to compare the specificity of each antibody in WB and IHC (figs. 3.19, 3.20, 3.21), (ii) assess the performance of each antibody in detecting Tau at low and high levels and, (iii) to evaluate the species reactivity of each antibody.

3.9.1 Total Tau antibodies do not detect all forms of Tau

In total, twelve antibodies were tested in FFPE mouse brain tissue; one antibody tested was marked as green (Tau-13), eleven as amber (N-term, 43D, 5A6, SP70, Tau-12, Tau-5; Abcam and Thermo, HT7, K9JA, Tau-46) and one as red (77E9) (fig. 3.19). 43D antibody was initially classified as green. However, it was not further tested for cross-reactivity and species reactivity and therefore was classified as amber, even though it is considered as an appropriate total Tau antibody. This work confirms that total antibodies can detect the same forms as peptide-raised and PHF-raised phospho-specific antibodies but imply that certain total Tau antibodies may fail to label certain hyperphosphorylated forms of Tau in FFPE brain tissue. Most total Tau antibodies (Tau N-term, 5A6, SP70, Tau-12, Tau-5, HT7, 77E9, K9JA with Tau-5 and HT7 being the most affected) are inhibited by excess phosphorylation events in FFPE brain tissue implying that these total Tau antibodies may not detect all forms of Tau.

This is alarming and urges careful re-evaluation of previously published data because numerous papers use the signal from total Tau antibodies to quantify the absolute amount of Tau in cells and to normalise changes in phosphorylated forms. Worryingly, according to the data presented here, this would lead to a dramatic underestimation of Tau protein levels within the system and over-inflate the change in phosphorylation status. The data suggest that antibodies with epitopes in the N-terminal domain (43D and Tau-13), which is the least prone to phosphorylation, and the end of the C-terminal (Tau-46, although this is prone to cross-reaction with MAPs when Tau is expressed at low levels), are likely more appropriate for studies examining total Tau expression and localisation compared to antibodies with epitopes in the PRD. However, it is important to note that some of the total Tau antibodies may not be as impacted in tissues other than rTg4510. This is because the Tau forms present in the rTg4510 are excessively phosphorylated and this may not be representative for human tissue or tissue that expresses Tau at basal levels. Therefore, careful and appropriate validation in relevant tissue is required prior to experimental design and data interpretation.

A selection of total Tau antibodies (SP70, Tau-12, Tau-13, HT7, K9JA, Tau-46) strongly immunoreacted with human Tau which was expressed at high levels in the rTg4510 mouse cortex, but antibodies immunoreacted with Tau in the hTau mouse brain only weakly (SP70, K9JA, Tau-46), whereas others did not immunoreact (Tau-5, HT7). Antibodies directed against epitopes that are expressed at low levels were found to be more prone to non-specific cross-reactivity [232]. Therefore, antibodies that strongly immunoreacted with Tau in rTg4510 mouse cortex but produced non-specific signal (Tau-46, Ser622) in the WT, *MAPT* and hTau have been classified as amber rather than red. These antibodies stained only as expected in FFPE mouse brain tissue and demonstrated high specificity for Tau, when expressed at high levels. Tau-12 and Tau-13 reacted more strongly to human Tau and K9JA to murine Tau at endogenous

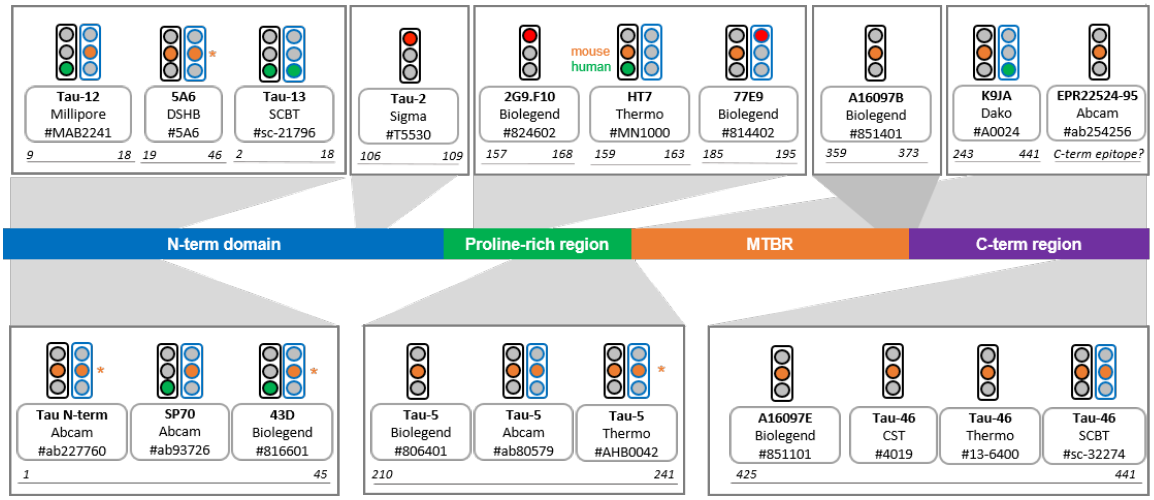

Fig. 3.19 **Traffic light system (TLS) for total anti-Tau antibodies.** The traffic light system allows visualisation of the specificity of immunostaining with each Tau antibody in Western blot (WB, black outline) and Immunohistochemistry (IHC, blue outline). The Tau protein consists of four distinct domains; the N-tail (blue), the proline-rich domain (green), the microtubule binding domain (orange) and the C-tail (purple). Each antibody has been classified as either green - correct sized bands on WB, stains as expected in IHC; amber - multiple bands, but correct MW - WB, unexpected tissue distribution – IHC; or red – incorrectly sized, or no bands - WB, no staining – IHC. The asterisk (*) indicates that the antibody has not been tested for detecting endogenous levels of human or murine Tau and has not been checked for cross reactivity with other proteins in FFPE *Mapt*$^{-/-}$ mouse brain tissue.

levels. This urges extra caution to be given when choosing a total antibody to study the expression of Tau two main criteria; (i) level of expression and (ii) species reactivity.

3.9.2 Phospho-specific Tau antibodies

Tau is a heavily post-translationally modified protein that has 85 putative phosphorylation sites. In total, seventeen antibodies were tested in FFPE mouse brain tissue; eight phospho-specific Tau antibodies tested were classified as green (pThr181, pSer198, AT8, AT100, pSer214, pThr231, AT180, pSer404) and nine as amber (pSer199, pSer202/pThr205, pSer238, pSer262, pTau-E178, pSer396, PHF-13, pSer409) (fig. 3.21). No phospho-specific Tau antibody was classified as red. Select antibodies (pSer202/pThr205, pSer238, pSer262, PHF-13, pSer409) were classified as amber be-

cause they were not further validated and as such, should be treated with caution. Select antibodies (AT8, AT100) were classified as yellow for use in WB applications because none of the samples tested in this study were expected to contain the Tau species that the respective antibody detects.

It was expected that λPP treatment would abolish the signal of phospho-specific Tau antibodies. As expected, for some antibodies the signal was abolished (pThr181, pSer198, pSer202/pThr205, AT8, AT100, AT180, pSer238, pSer404), for some signal was reduced (pSer214, pThr231, pSer262, PHF-13, pSer409) whereas, it was improved for others (pSe199, pSer396, E178). This is explained by (i) the fact that phosphorylation at the relevant epitopes is resistant to λPP in aggregated/PHF-Tau, combined with (ii) the fact that removal of potential inhibitory phosphorylation events from nearby residues might improve epitope accessibility.

3.9.3 Isoform-specific Tau antibodies and the putative detection of HMW Tau

Several total (e.g. Tau-12, Tau-13, K9JA) and phospho-Tau antibodies (e.g. pSer199, pThr231, pSer396, E178) detected high MW Tau-immunoreactive bands of approximately 120-130 kDa in SH-SY5Y and HAP1 cell lysates in WB. The data support the possibility that the bands at 120-130 kDa correspond to the MW of HMW Tau isoform, but further work is required to confirm this.

3.9.4 Limitations

Rodents are widely used in research to study disease [256] but they do come with a range of limitations. Firstly, the rTg4510 mouse brain only expresses the 0N4R Tau isoform, not allowing full validation of antibodies recognising 1N, 1N/2N and 3R Tau isoforms. For such Tau antibodies, rTg4510 mouse brain behaves as a negative

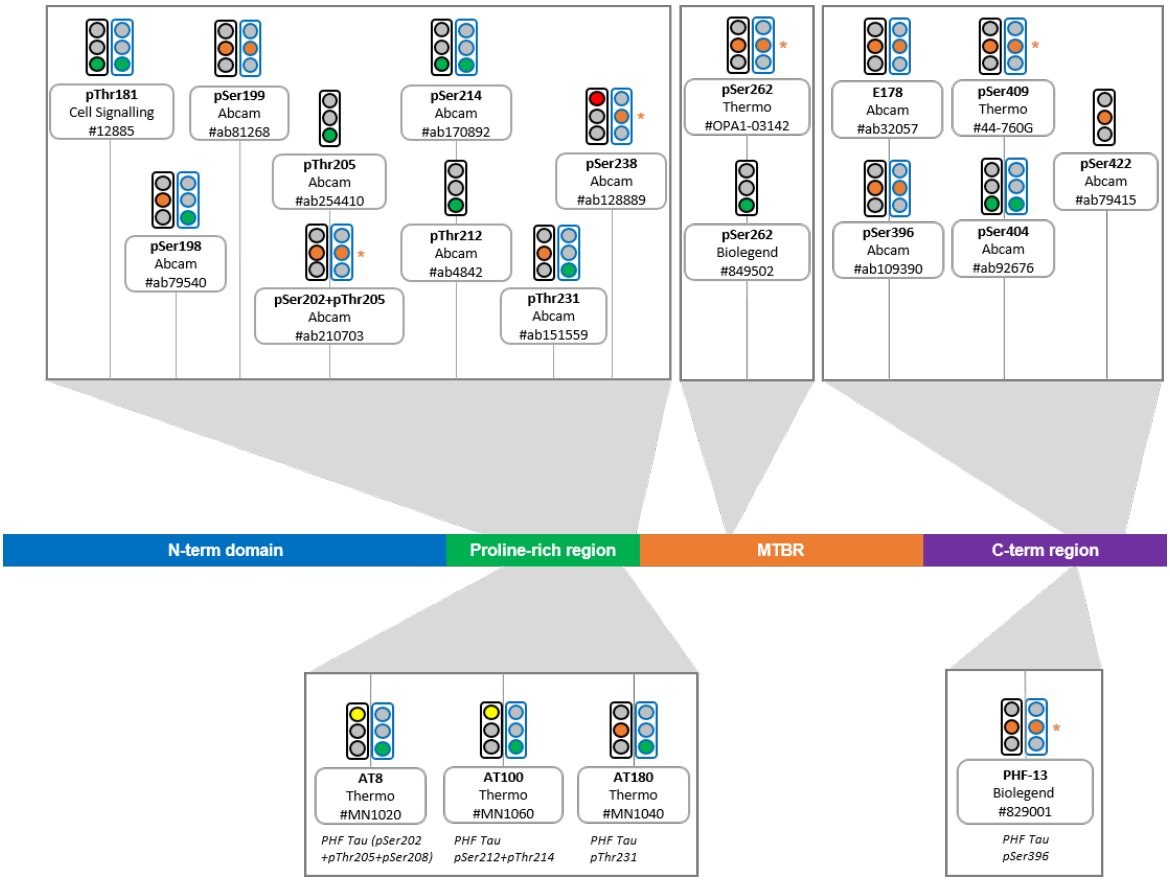

Fig. 3.20 **Traffic light system (TLS) for phosphorylation-specific anti-Tau antibodies.** The traffic light system allows visualisation of the specificity of immunostaining with each Tau antibody in Western blot (WB, black outline) and Immunohistochemistry (IHC, blue outline). The Tau protein consists of four distinct domains; the N-tail (blue), the proline-rich domain (green), the microtubule binding domain (orange) and the C-tail (purple). Traffic lights illustrate the specificity for WB, black outline, and IHC, blue outline. Each antibody has been classified as either green - correct sized bands on WB, stains as expected in IHC; amber - multiple bands, but correct MW - WB, unexpected tissue distribution – IHC; or red – incorrectly sized, or no bands - WB, no staining – IHC. Yellow - none of the samples tested in this study were expected to contain the Tau species that the respective antibody detects. The asterisk (*) indicates that the antibody has not been tested for detecting endogenous levels of human or murine Tau and has not been checked for cross reactivity with other proteins in FFPE *Mapt*$^{-/-}$ mouse brain tissue.

instead of a positive control. Second, endogenous Tau mouse models express only 4R Tau isoforms and not 3R Tau isoforms and thus, the RD4 antibody, but not RD3 antibody, was expected to immunoreact with Tau in rTg4510 and hTau mouse brain.

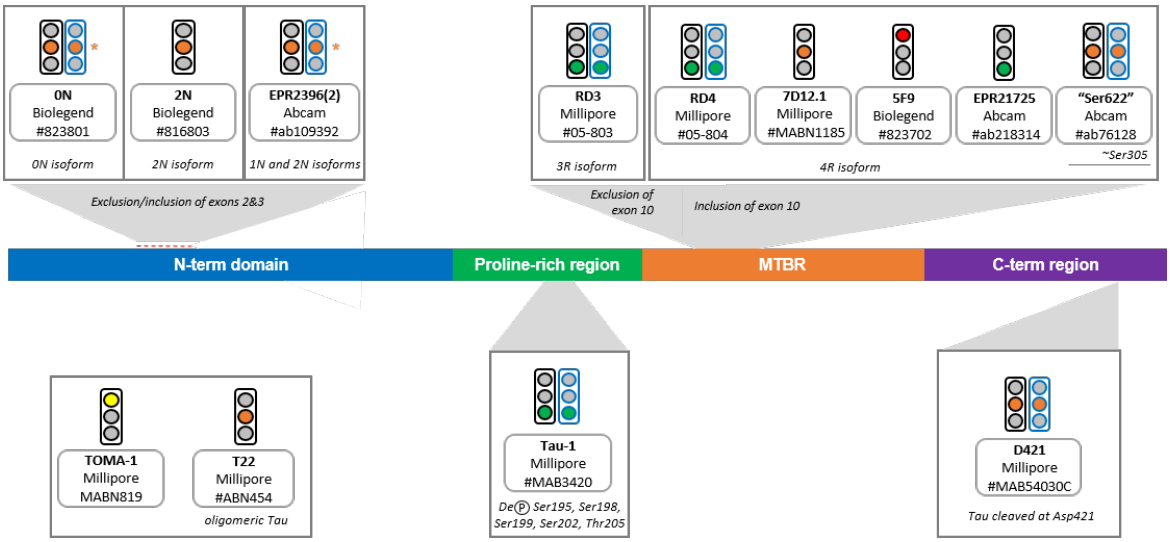

Fig. 3.21 **Traffic light system (TLS) for isoform-specific and other anti-Tau antibodies.** The traffic light system allows visualisation of the specificity of immunostaining with each Tau antibody in Western blot (WB, black outline) and Immunohistochemistry (IHC, blue outline). The Tau protein consists of four distinct domains; the N-tail (blue), the proline-rich domain (green), the microtubule binding domain (orange) and the C-tail (purple). Each antibody has been classified as either green - correct sized bands on WB, stains as expected in IHC; amber - multiple bands, but correct MW - WB, unexpected tissue distribution – IHC; or red – incorrectly sized, or no bands - WB, no staining – IHC. Yellow - none of the samples tested in this study were expected to contain the Tau species that the respective antibody detects. The asterisk (*) indicates that the antibody has not been tested for detecting endogenous levels of human or murine Tau and has not been checked for cross reactivity with other proteins in FFPE *Mapt*$^{-/-}$ mouse brain tissue.

Third, the PTM signature may also significantly differ between mouse models and between primates and rodents. That would mean that while the *Mapt*$^{-/-}$ mouse brain remains a good negative control, a positive control is also required. So, if an antibody does not label Tau in *Mapt*$^{-/-}$ mouse brain but immunoreacts with Tau in WT and/or hTau (always taking into account its reactivity), it was concluded that the antibody is performing as expected. For a limited number of antibodies, reactivity was further confirmed in appropriate human brain tissue adding further support to this conclusion. Moreover, the limited number of mouse tissue sections has restricted the signal intensity quantification of each antibody to one tissue section per untreated and one per treated.

3.9.5 Conclusions and further work

Antibody validation should always be the first step to all antibody-based techniques. There are no universally accepted guidelines to antibody validation and it is almost impossible to build an antibody validation protocol that applies to all antibodies. The antibody validation strategies and the traffic light system described and developed here have greatly enriched the existing Tau antibody validation data and have unravelled several key additional areas to be considered when exploring Tau pathologies.

Submitted manuscript The work presented in this Chapter has been prepared alongside the full WB dataset for publication in Molecular Neurodegeneration journal and has been published in Biorxiv https://www.bio.rxiv.org/content/10.1101/2023.04.13.536711v1.

Chapter 4

Characterisation of Tau forms in the human pancreas

4.1 Introduction

Tau is a complex protein discovered in 1975 [4] and it has been shown that hyper-phosphorylated Tau is the major component of NFTs in AD [5–9]. The expression of Tau isoforms in the CNS is age- and disease-dependent. The neonatal human brain expresses the 3R Tau isoform whereas the adult human brain expresses both the 3R and 4R Tau isoforms [25, 26]. However, it remains unknown why there is a change in the isoform expression with age. In the human brain, Tau localises at the neuronal axons. Tau phosphorylation at specific residues (i.e. Ser202/Thr205/Ser208) promotes Tau translocalisation to the cell body (soma) and the formation of NFTs. A well supported notion proposes that aggregated Tau may have prion-like properties meaning that it can move from the cell body of a donor neuron to the axon of a recipient neuron and as such, it could spread across the brain. According to the Braak stages detailed in Chapter 1, section 1.1.3, in the brain of older individuals, NFTs may be present within the transentorhinal region, a phenotype that could be classified as Stage I-II (clinically

silent cases) whereas, individuals diagnosed with clinical AD, have phenotypes of Stages III-IV (incipient AD) and V-VI (fully developed AD), characterised by broad cortical spread of NFT pathology.

Twenty years after its initial characterisation in the human brain, Tau was reported to be expressed in pancreatic cancer cells [257] and a few years later, in normal and tumoral pancreatic acinar cells [258]. Since then, it has been demonstrated that the *MAPT* promoter is active in human islets (http://pasqualilab.upf.edu/app/isletregulome) [172, 173] and both Tau RNA and Tau protein are expressed in islet cells including β cells [174, 175, 258, 259, 177]. Furthermore, epidemiological studies have strengthened the link between AD and T2D and, in 2010, it was further proposed that hyperphosphorylated Tau aggregates are present in the T2D pancreas [177]. Contrary to these, a recent study argues that the expression of Tau is restricted to autonomic nerve fibres [181]. All these findings highlight that the Tau has become an attractive protein for β cell studies potentially playing an important role in β cells by contributing to the regulation of insulin secretion.

To date, the expression of Tau in the human pancreas has not been characterised in detail and, it remains unknown whether Tau expression in the pancreas mirrors the complexity of that in the human brain. As such, this chapter aims to characterise the expression of Tau isoforms and pTau forms in the human pancreas and also asked whether the Tau isoform expression and phosphorylation signature differ in the pancreas of those diagnosed with T1D or T2D using the TLS-validated antibodies (Chapter 3, pg. 67). Understanding the distribution of Tau isoforms and pTau forms in the pancreas in health and disease could allow to explore the role of Tau in insulin secretion and investigate whether Tau hyperphosphorylation could cause β cell dysfunction by disrupting insulin secretion.

In summary, the key objectives of this chapter were;

- to explore the gene expression of Tau in β cells of individuals with and without T1D and T2D and in adult and foetal β cells,
- to explore the Tau isoform and Tau phosphorylation signature expression in adult human pancreas and,
- to determine whether the cellular expression of Tau alters with age, obesity and T1D/T2D.

Aims and objectives

Tau protein expression has previously been described in the human pancreas and, more specifically, in the β cells. However, to date, the expression of Tau isoforms, the Tau PTM signature has not been fully characterised in the human pancreas. Therefore, this is the first attempt to fully characterise Tau protein expression in the human pancreas (fig. 4.1).

We searched the published literature to identify all Tau isoforms and pTau forms that play an important role in the human brain. Then, we identified antibodies against relevant Tau isoforms and pTau forms that are widely used in research (Chapter 2, Table 2.1) and in collaboration with Dr. Irina Stefana (University of Oxford), we validated these antibodies using IHC and WB approaches (Chapter 3). The TLS validation of these antibodies allowed us to build a powerful tool box to start exploring the expression of Tau in the human pancreas.

To explore the *MAPT* gene expression in the human pancreas three RNAseq databases were utilised; (i) Next Generation RNA-Sequencing bulk β cell data from individuals diagnosed with (n=4) and without T1D (n=12) [239], (ii) Next Generation RNA-Sequencing data from adult (n=7) and foetal (n=6) β cells and adult (n=6) and foetal (n=5) α cells [240] and, (iii) Next Generation RNA-Sequencing data from pancreatic islets of individuals diagnosed with (n=4) and without T2D (n=6) (https:

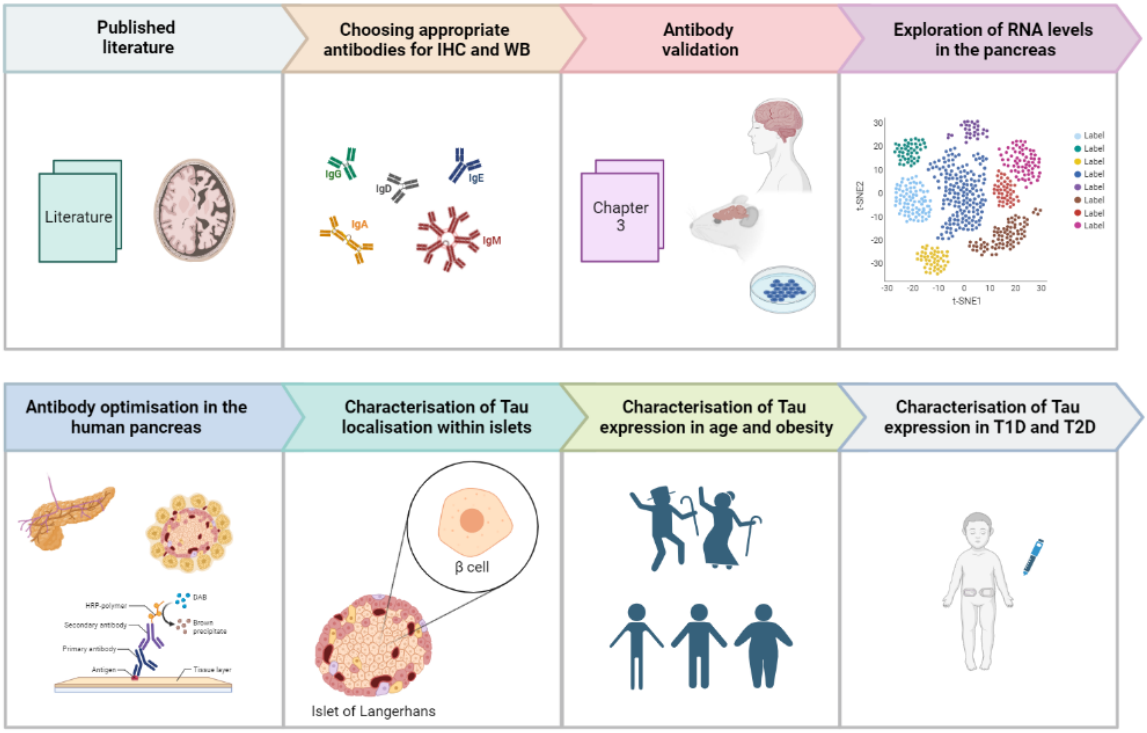

Fig. 4.1 **Pipeline schematic to illustrate the process of characterising the expression of Tau forms in the human pancreas.** This 8-step workflow summarises the methodology developed to fully characterise the expression of Tau, Tau isoforms and the phosphorylation signature of Tau in the human pancreas in conditions such as health, ageing, obesity, type I diabetes and type II diabetes. Created in Biorender (https://biorender.com/).

//sandberglab.se/tool/pancreas/, [175]). These data provided an initial guide for the characterisation of the RNA expression level of Tau in health and disease (T1D/T2D), as well as, in foetal and adult β and α cells. In addition, these data provided information about where Tau protein is expected to be expressed within the pancreas.

Standard HRP staining was then performed (Chapter 2, section 2.4.1) to optimise the TLS-validated antibody staining conditions in FFPE human pancreas tissue sections from the EADB collection and to determine the cellular localisation within the different pancreas compartments (i.e. islet, acinar, ductal cells and the nerves). Following the HRP optimisation of the Tau antibodies in human pancreas sections, IF staining was performed (Chapter 2, section 2.4.2) to determine the cellular localisation within

the islets. As such, each Tau antibody was combined with (i) insulin, a marker of β cells, (ii) glucagon, a marker of α cells and, (iii) DAPI, a marker of the nucleus. Subsequent quantification analysis of specific pTau forms, using the Halo software, was then performed to characterise their expression in human β cells in age, obesity, and disease (T1D, T2D).

4.2 RNA expression

The *MAPT* promoter is active in β cells and recent studies confirmed that Tau RNA is present in β cells [172–175]. To explore the RNA expression of Tau in the human pancreas, three RNAseq dataset were employed. One immediate limitation was that the RNAseq data used [240, 175, 239] have been normalised in different ways and, thus, the gene expression levels between the datasets are not directly comparable but give an indication of relative levels of expression. Also, it is important to note that each dataset comprises data from a limited number of donors or cells and, as such, does not allow for firm conclusions.

***MAPT* gene in β and α cells** Exploration of the *MAPT* expression in β and α cells [240] demonstrated that there is a moderate but significant increase in the *MAPT* expression level in adult β cells when compared to foetal β cells while, no difference between foetal and adult α cells was reported (fig. 4.2a). A t-test was performed to investigate whether there is a significant difference between the groups and p value was corrected based for multiple comparisons between different groups. The full statistical table can be found at the Appendix A (Table A.4). It is observed that the *MAPT* expression in α cells is generally low, whereas it is much higher in β cells. These data indicate that Tau could play an important role in β cells but may be less critical in α cells.

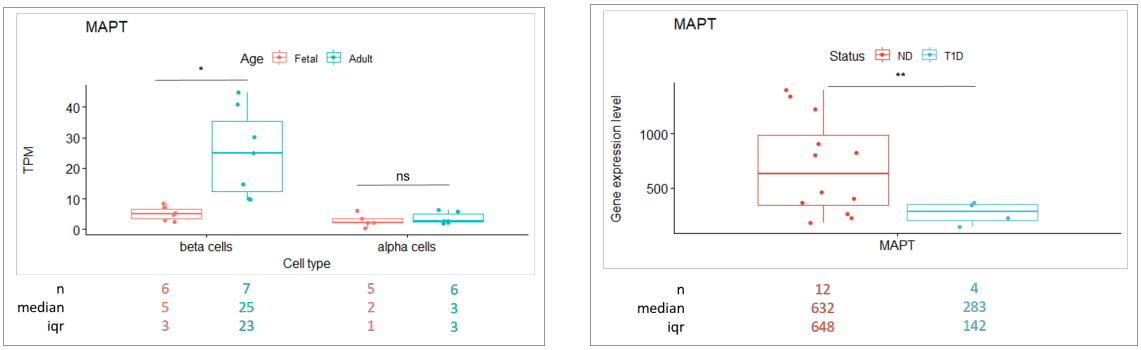

(a) (b)

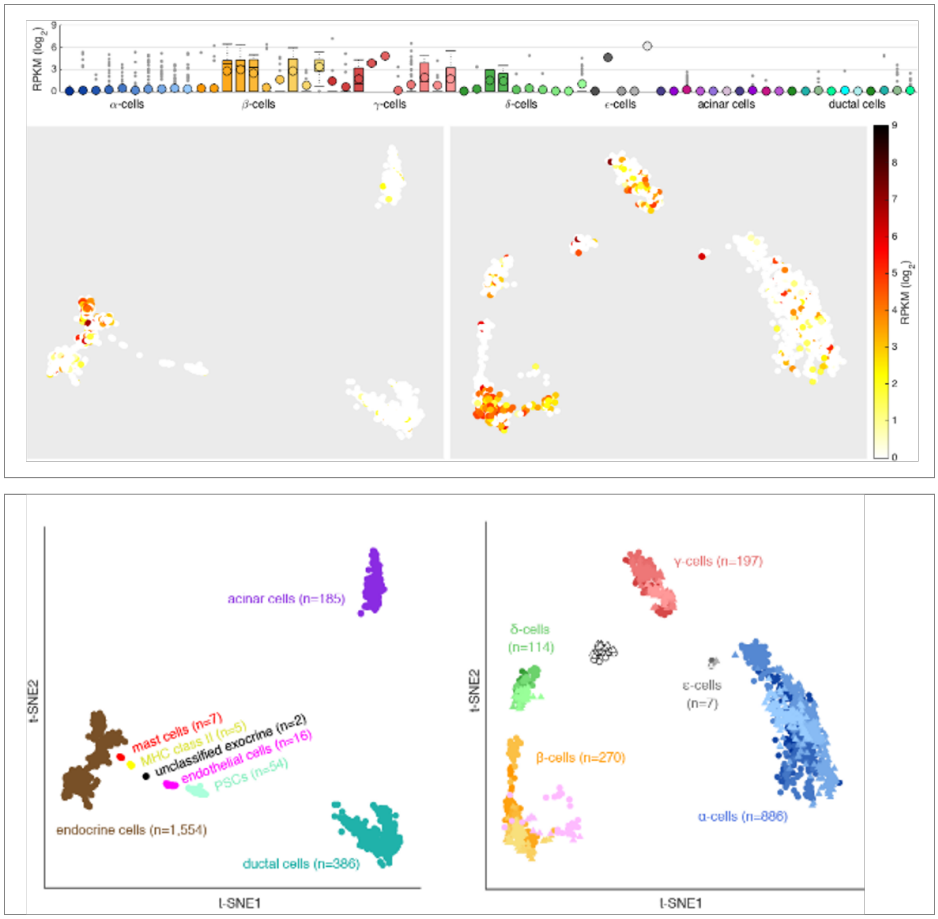

(c)

Fig. 4.2 **Gene expression level of the MAPT gene, encoding Tau protein, in the human pancreas. 4.2a** | Boxplots showing the *MAPT* expression in adult (n=7) and foetal (n=6) β cells and adult (n=6) and foetal (n=5) α cells [240] with x axis showing the cell type and the y axis the gene expression level. **4.2b** | Boxplots showing the *MAPT* expression in 12 ND and 4 T1D donors [239] with x axis containing the gene name of the kinases and the y axis the transcript per million (TPMs). TPMs for every 1,000,000 RNA molecules in the RNAseq sample. **4.2c** | Boxplots summarising GCG expression levels across the 7 major cell types (shown in different colors) for every donor (shown in different shades of each color). The first 6 boxes correspond to healthy individuals (H1 to H6) and the last 4 to T2D individuals (T2D1 to T2D4). ϵ-cells were captured only in 5 donors (H2, H3, H6, T2D1, T2D4). (https://sandberglab.se/tool/pancreas/, [175]). t-SNE representations colored according to GCG expression levels of: (Left) all sequenced cells (n=2,209) or (Right) endocrine cells only (n=1,554). Data from RNAseq have been normalised in different ways, the gene expression levels between the two datasets are not directly comparable but give an indication of relative levels of expression.

***MAPT* gene in ND and T1D β cells** In keeping with these data, a separate RNAseq study [239] confirmed that the *MAPT* gene is expressed both in ND and T1D β cells. It was further reported that *MAPT* expression was reduced by approximately half in T1D β cells when compared to β cells from individuals without diabetes (fig. 4.2b). Statistical analysis (t-test) confirmed that the *MAPT* expression is significantly reduced in T1D β cells compared to ND β cells (full stats table A.5).

***MAPT* gene in ND and T2D islet cells** The RNAseq dataset (https://sandberglab.se/tool/pancreas/, [175]) allowed the exploration of the *MAPT* expression in ND and T2D islet cells. According to this RNA seq dataset, the *MAPT* gene is expressed in the β, γ and ϵ cells of those diagnosed with or without T2D. Interestingly MAPT RNA was only detected in the δ cells of those without T2D (fig. 4.2c). In addition, this dataset demonstrated that *MAPT* showed a remarkably low gene expression level score in the endocrine α cells as well as in the acinar and ductal cells (fig. 4.2c), suggesting that *MAPT* RNA may not be present in these cell types. This is in agreement with other RNAseq data [240] that demonstrated a similarly low expression level of *MAPT* gene in α cells (fig. 4.2a).

4.3 Optimisation of Tau antibodies in pancreas

Antibodies against Tau were previously TLS-validated in IHC and WB in collaboration with Dr Irina Stefana from the University of Oxford (Chapter 3). Antibodies against total (n=15), isoform-specific (n=6), phosphorylation-specific (n=15) and other forms of Tau (n=3) were then tested in the human pancreas using HRP (Chapter 2, Table 2.1). Staining of the intrapancreatic nerves served as an internal positive control.

Tissue optimisation Previous work by the IBEx team has revealed that Tau antibodies can yield non-specific signals in post mortem tissue. Pancreas is very susceptible to post mortem changes due to its high protease content. This, could potentially have an impact on the detection of Tau. Furthermore, we speculate that the fixative and fixation time may have an impact on the accessibility of the antibodies. For these reasons, autopsy tissue was excluded from this study and only well preserved organ donor tissue, that was fixed and preserved under strictly controlled conditions (FFPE), was utilised. Pancreas tissue utilised for this study was obtained from either the EADB collection or the nPOD biobank, always with regard to the above mentioned criteria.

4.3.1 Total Tau antibodies

In total, 15 total Tau antibodies were tested in FFPE pancreas tissue. All total Tau antibodies tested (with only exception being the SP70 antibody) labeled the cytoplasm of a subset of islet cells (fig. 4.3). This is in alignment with the RNAseq data reporting that the *MAPT* gene is expressed in islets (fig. 4.2) and previously published data supporting that Tau protein is present in the islets.

The majority of the total Tau antibodies (exceptions being SP70, 2G9.F10 and Tau-2 antibodies) stained the nerves, providing confirmation that the antibodies 'work' in FFPE pancreas tissue and are specific to Tau (fig. 4.3). Some total Tau antibodies (43D and HT7 antibodies) appear to stain the nucleus of acinar and/or the ductal cells. This does not align with the RNAseq data [175] proposing that Tau RNA is not being detected in the these cell types (fig. 4.2c). Interestingly, 43D and HT7 antibodies also stained the nucleus of β cells. 43D and HT7 have been previously been classified as TLS-amber, suggesting that caution should be taken when interpreting results. As

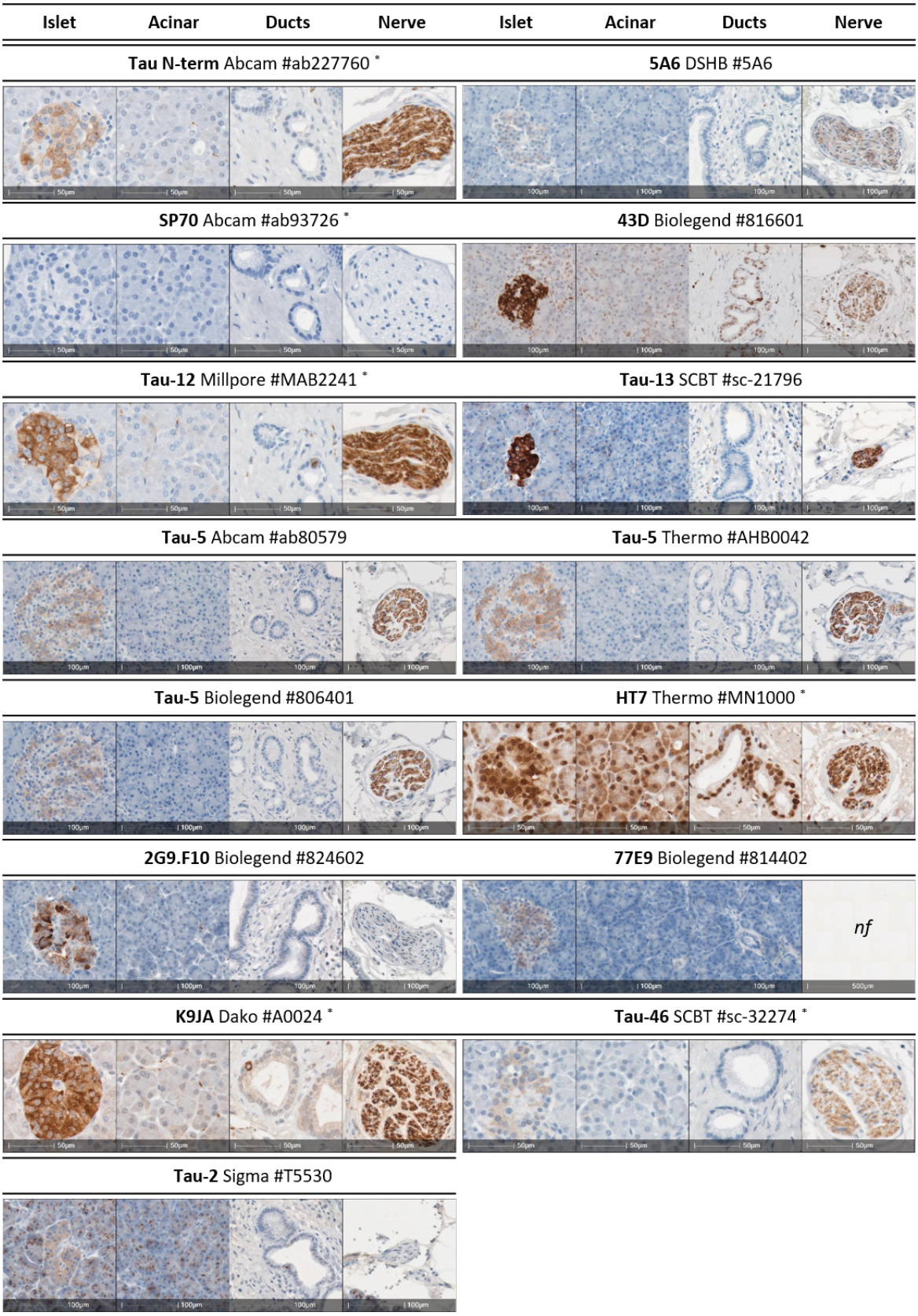

Fig. 4.3 **Total anti-Tau antibody profiles within the adult human pancreas (islet, acinar and duct cells and nerves).** Representative immunofluorescent micrographs demonstrating the presence and the subcellular localisation of 13 different total anti-Tau antibodies in the islet, acinar and ductal cells as well as in the intrapancreatic nerves in the pancreas of an organ donor. Anti-Tau antibodies marked with an asterisk (*) were stained by Dr. M.L. Zeissler. nf; not found. Whole slide scans were imaged at X40. Scale bars 50μm or 100μm.

such, the nuclear signal produced raises questions about whether the nuclear signal is (i) real Tau signal or (ii) non-specific signal.

Tau-2 was not validated in IHC but WB data showed weak reactivity in HEK293T cell line overexpressing Tau (fig. A.3). Tau-2 failed to stain the intrapancreatic nerves. Unexpectedly, it labeled structures within the cytoplasm of the acinar cells in a punctate manner (Appendix A, fig. 4.3). Unfortunately, the exact epitope of this antibody is not publically available and thus it is impossible to check for cross-reactivity with other proteins. As Tau-2 only weakly detects Tau in WB when overexpressed and does not stain the intrapancreatic nerves in FFPE pancreas tissue, there were no further analyses performed.

4.3.2 Isoform-specific Tau antibodies

Isoform-specific Tau antibodies were tested to further explore which isoforms are expressed in the adult human pancreas. Due to alternative splicing, Tau has 6 isoforms present in the CNS (0N3R, 1N3R, 2N3R, 0N4R, 1N4R, 2N4R) and 1 isoform present in the PNS (HMW or 'Big Tau'). CNS-Tau isoforms can be divided into (i) the N-repeat isoforms depending on the inclusion of exons 2 and 3 giving raise to the 0N, 1N and 2N Tau isoforms and into (ii) the R-repeat isoforms depending on the inclusion of exon 10 giving rise to the 3R and 4R Tau isoforms. There is a large number of isoform-specific Tau antibodies detecting different Tau isoforms and a summary is presented at Table 4.1. In total, eight antibodies against such Tau isoforms were tested in the human pancreas.

N repeat In total, two antibodies against the N-repeat region were tested using standard HRP staining; the '1N and 2N' and the 2N antibodies. The '1N and 2N' antibody is capable of detecting four Tau isoforms (1N3R, 2N3R, 1N4R, 2N4R) and stained the cytoplasm of a subset of islet cells and the nerves (fig. 4.4a, table 4.1). The

2N antibody detects only the 2N Tau isoforms (2N3R, 2N4R, table 4.1) and it only stained the nerves (fig. 4.4a). As such, these data suggest that the 1N Tau isoforms, but not the 2N isoforms, are expressed in the adult human islets. The data also suggest that both 1N and 2N isoforms are expressed in the intrapancreatic nerves.

R repeat In total, one antibody against 3R (RD3 #05-803) and two antibodies against 4R-Tau isoforms (RD4 #05-804, 4R #MABN1185) were tested in HRP. 'Ser622' which was previously characterised as a total antibody with a preference to 4R-Tau isoforms was also included in the isoform-specific Tau antibodies panel (Chapter 3).

The RD3 antibody, detecting 3R-Tau isoforms, stained the intrapancreatic nerves and the cytoplasm of a subset of islet cells (fig. 4.4a). Two antibodies were tested against the 4R-Tau isoforms; the 4R and the RD4 antibodies. The anti-4R antibody did not label the islet, acinar and ductal cells or the nerves (fig. 4.4a). By contrast, RD4 weakly stained the islet and acinar cells and the nerves. This staining pattern was unexpected because it does not resemble with that observed with the total Tau antibodies. As two antibodies against the same Tau isoform were tested and demonstrated differential

Table 4.1 **Isoform-specific anti-Tau antibodies and Tau isoforms** Isoform-specific anti-Tau antibodies are listed in the first column. A ✓is used to show that the antibody detects the isoform and a ×is used to show that the antibody does not detect the isoform. The Tau isoforms and the number (#) of the Tau isoforms detected by each antibodies are listed in the two last columns. The Big Tau isoform is similar to the 2N4R isoform but it contains two additional exons (exon 4a and exon 6). Antibodies marked with an asterisk (*) may also be able to label the Big Tau isoform.

Antibody	0N	1N	2N	3R	4R	Big Tau	Tau isoforms detected	# of isoforms detected
0N	✓	×	×	✓	✓	×	0N3R, 0N4R	2
1N	×	✓	×	✓	✓	×	1N3R, 1N4R	2
2N*	×	×	✓	✓	✓	✓*	2N3R, 2N4R	2*
1N and 2N*	×	✓	✓	✓	✓	✓*	1N3R, 2N3R, 1N4R, 2N4R	4*
RD3	✓	✓	✓	✓	×	×	0N3R, 1N3R, 2N3R	3
RD4*	✓	✓	✓	×	✓	✓*	0N4R, 1N4R, 2N4R	3*
HPA	×	×	×	×	×	✓	Big Tau	1

staining patterns, no firm conclusions can be made about the expression of the 4R-Tau isoform in the adult human pancreas.

The Ser622 antibody was initially labelled as a total Tau antibody and the TLS-validation showed that Ser622 antibody had a preference for 4R-Tau isoforms but, under specific circumstances, it was also able to detect 3R-Tau isoforms in WB (Chapter 3). The Ser622 antibody produced strong signal in the cytoplasm of a subset of islet and duct cells as well as in the nerves and it also weakly stained the cytoplasm of acinar cells (fig. 4.4a). BLAST analysis of the epitope detected by the Ser622 antibody previously revealed that Ser622 antibody could potentially also detect the MAP-2 protein (Appendix A, fig. A.1). Immunostaining data from the Human Protein Atlas (HPA) using a MAP-2 antibody (#HPA012828) in pancreas revealed a similar staining pattern to that of Ser622, especially within the islets and some duct cells. As such, it is possible that Ser622 antibody may be cross-reacting with MAP-2 protein in the human pancreas and therefore no firm conclusions can be made about the presence of the 4R-Tau isoform in the human pancreas using the Ser622 antibody.

These data suggest that the 3R isoform is expressed in the adult human islets, although further work is required to explore the expression of 4R-Tau isoform. So far, the immunostaining data suggest that the Tau isoform that is most likely to be present in the human pancreas is the 1N3R Tau isoform but final conclusions about the presence of 1N4R cannot be drawn.

HMW or 'Big Tau' Two antibodies against the HMW Tau isoform (#HPA048895 and #HPA069524) were tested in the human pancreas (fig. 4.4a). Both stained the nerves but only the 'Big Tau' #HPA048895 antibody stained the cytoplasm of a subset of islet cells. Interestingly, it also stained the nucleus of islet and acinar cells as well as the nucleus and the cytoplasm of duct cells.

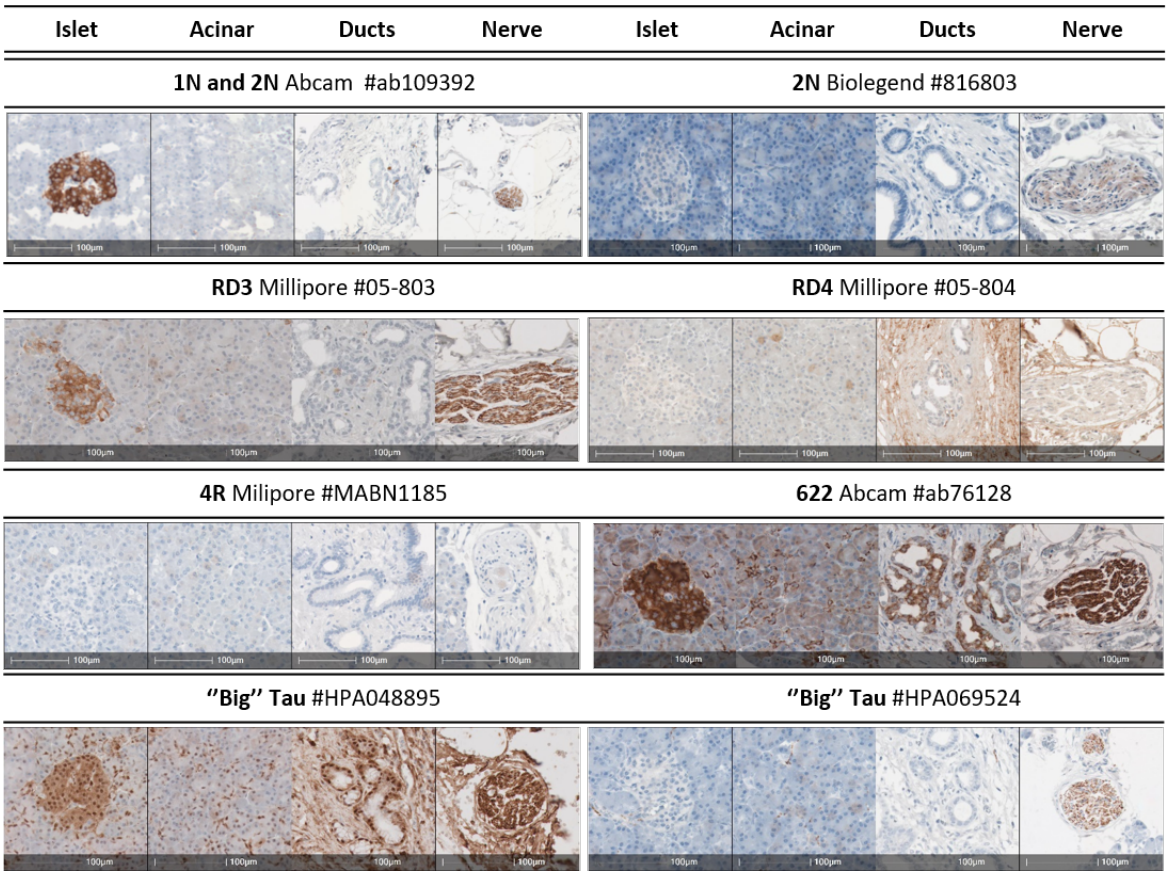

(a)

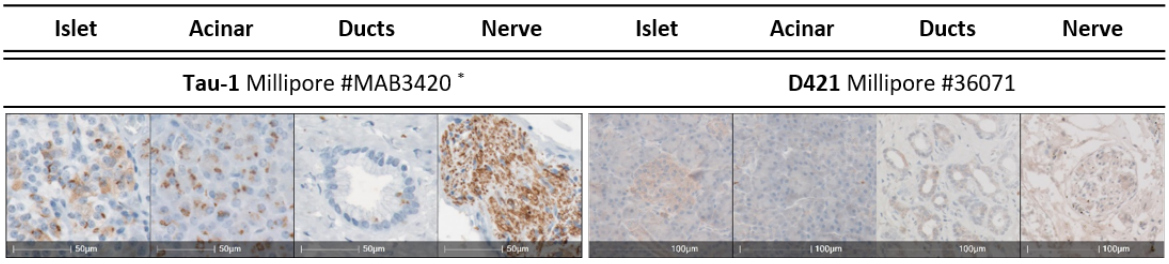

(b)

Fig. 4.4 **Isoform-specific and other anti-Tau antibody profiles within the adult human pancreas (islet, acinar and duct cells and nerves).** Representative immunofluorescent micrographs demonstrating the presence and the subcellular localisation of **4.4a** | Eight different isoform-specific anti-Tau antibodies and **4.4b** | two other (PTM-specific) anti-Tau antibodies in the islet, acinar and ductal cells as well as in the intrapancreatic nerves in the pancreas of an organ donor. Anti-Tau antibodies marked with an asterisk (*) were stained by Dr. M.L. Zeissler. Whole slide scans were imaged at X40. Scale bars 50μm or 100μm.

Interestingly, Big Tau #HPA048895 was unusual in producing nuclear signal since most Tau reagents labeled only the cytoplasm of a subset of islet cells and not the nucleus. According to the supplier, the HMW Tau detected by the Big Tau #HPA048895 antibody is raised against exon 4a of Tau which has almost no homology to other proteins [24] and, as such it is unlikely that this antibody cross-reacts with non-specific targets. Interestingly, 43D and HT7 antibodies, also labeled the nucleus of islet, acinar and ductal cells (fig. 4.3). Antibodies 43D and HT7 and the isoform-specific 'Big Tau' #HPA048895 demonstrated similar staining patterns in that they labelled the nucleus of a selection of islet, acinar and ductal cells. Taking into account that two total (43D and HT7) and one isoform-specific ('Big Tau' #HPA048895) Tau antibodies produce nuclear signal, more questions are raised about the specificity of the nuclear signal.

4.3.3 Other Tau antibodies

Due to time limitations, antibodies against other forms of Tau, such as acetylated, truncated, oligomeric etc, have not been extensively studied. However, antibodies against Tau dephosphorylated at specific residues (n=1) and truncated at Asp421 (n=1) forms were tested in the adult human pancreas.

According to the supplier, Tau-1 antibody detects Tau dephosphorylated at residues Ser195, Ser198, Ser199 and Ser202. Tau-1 antibody labeled Tau forms in the cytoplasm of a subset of islet cells and the nerves (fig. 4.4b). Interestingly, Tau-1, similarly to Tau-2 (total Tau antibody), labeled punctate structures within the cytoplasm of acinar cells. Tau-2 signal was previously judged as non-specific. Even though Tau-1 and Tau-2 presented similar staining pattern, Tau-2 antibody failed to stain the intrapancreatic nerves (fig. 4.3), whereas Tau-1 strongly stained the nerves (fig. 4.4b). It is likely that Tau-1 labels the intrapancreatic nerves where Tau is dephosphorylated at high levels.

Positive immunoreactivity with these punctate structures could be explained; (i) true Tau signal (which is unlikely because none of the total Tau antibodies demonstrated similar staining pattern), (ii) non-specific signal. Therefore, it can be assumed that dephosphorylated Tau at Ser195, Ser198, Ser199 and Ser202 is present in the nerves and the pancreas whereas the signal from the acinar cells could be judged as non-specific.

The D421 antibody detects forms of Tau that have been truncated at residue Asp421. The D421 antibody faintly stained the cytoplasm of a subset of islet cells as well as the nerves (fig. 4.4b), suggesting that truncated Tau forms may be present in the adult human pancreas. This antibody would benefit from further optimisation to boost its signal intensity.

4.3.4 Phosphorylation-specific Tau antibodies

So far, the IHC data suggest that Tau is present in the cytoplasm of a selection of islet cells and in the nerves. 3R-Tau isoform is expressed in islets and firm conclusions about the expression of 4R-Tau isoform cannot be made. Furthermore, a set of Tau antibodies (43D, HT7, #HPA048895) demonstrated unusual immunoreactivity in that they also stained the nucleus of a subset of islet, acinar and duct cells raising questions about the specificity of the nuclear signal. Next, the phosphorylation signature of Tau in the adult human pancreas was assessed. Phospho-specific Tau antibodies detect Tau when it is phosphorylated at a specific residue (or a set of residues) and, can be sub-divided into two categories; (i) peptide-raised antibodies detecting pTau forms both in the control and the AD brain and, (ii) PHF-raised antibodies detecting pathogenic pTau forms in the AD brain (Chapter 2, Table 2.1).

All peptide-raised phospho-specific antibodies tested in human pancreas (only exception being Ser238) stained the nerves (fig. 4.5). Some antibodies (pSer202, pSer422) labeled the pancreatic nerves but not the islet cells suggesting that these

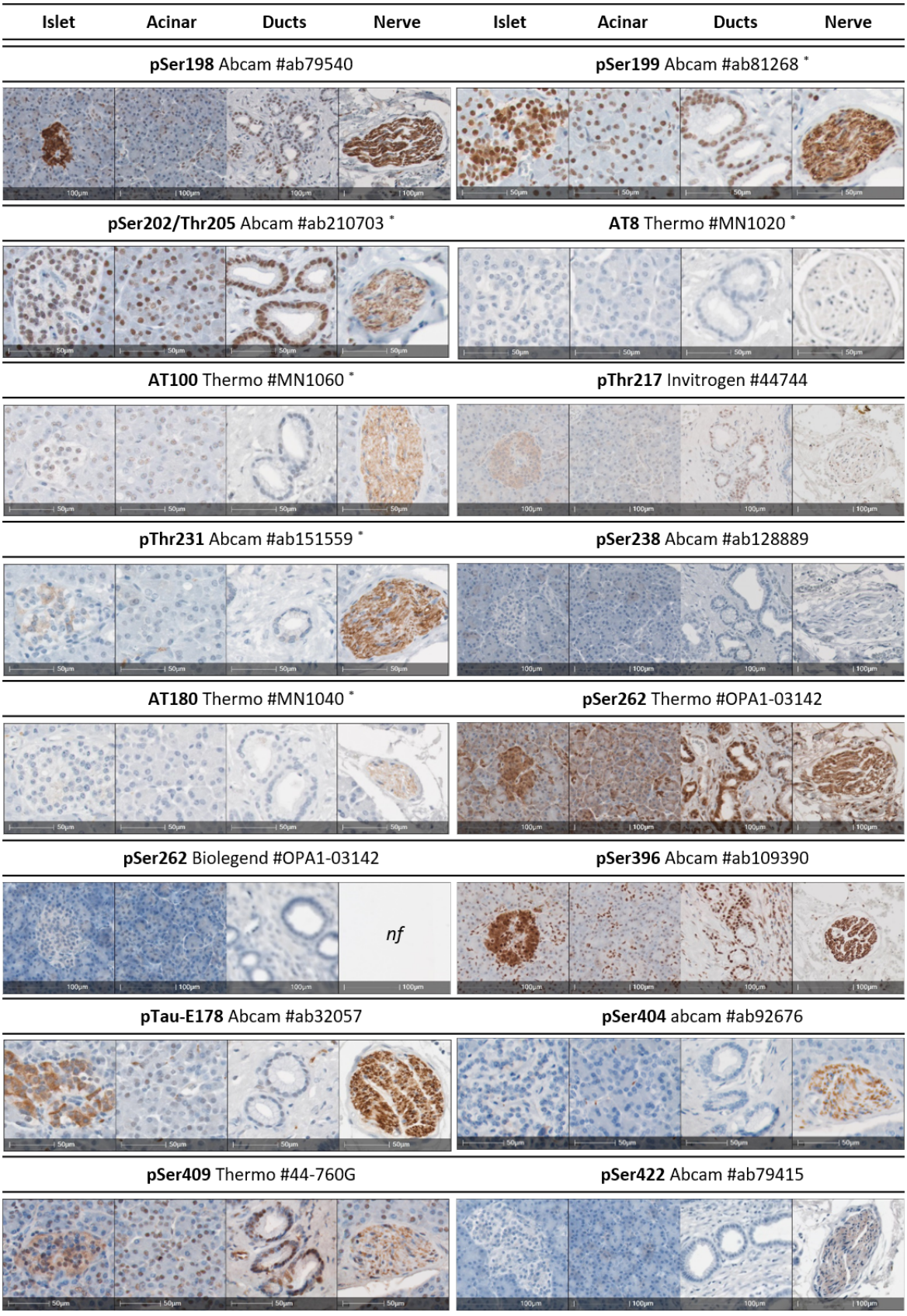

Fig. 4.5 **Phosphorylation-specific anti-Tau antibody profiles within the adult human pancreas (islet, acinar and duct cells and nerves).** Representative immunofluorescent micrographs demonstrating the presence and the subcellular localisation of 14 different phosphorylation-specific anti-Tau antibodies in the islet, acinar and ductal cells as well as in the intrapancreatic nerves in the pancreas of an organ donor. Anti-Tau antibodies marked with an asterisk (*) were stained by Dr. M.L. Zeissler. nf; not found. Whole slide scans were imaged at X40. Scale bars 50μm or 100μm.

residues may not be phosphorylated in the adult human islets. The majority of phospho-specific Tau antibodies (pSer198, pSer199, pThr231, pSer262, pSer396, pTau-E178, pSer409) stained the cytoplasm of a subset of islet cells. In total, 6 phospho-specific Tau antibodies raised against different Tau epitopes (pSer198, pSer199, pSer202/pThr205, pSer396, E178, pSer409) also detected Tau in the nucleus of islet cells, strongly supporting the nuclear signal as true Tau signal.

The majority of the PHF-raised antibodies (exception being the AT8 antibody), stained the pancreatic nerves (fig. 4.5). The AT8 (epitope; pSer202/pThr205/pSer208) antibody did not stain the nerves or the islets. The AT180 (epitope; pSer212/pSer214) antibody stained the nerves but not the islets whereas the AT100 (epitope; pThr231) antibody stained the nerves and the nucleus of islet and acinar cells. These data suggest that alleged pathogenic pTau forms that have been associated with neurodegeneration may not be strongly present in the adult human islet cells.

In contrast to the RNAseq data [175] showing that *MAPT* is not expressed in the ductal cells (fig. 4.2c) and immunostaining data using the total and isoform-specific Tau antibodies suggesting that Tau is not expressed in the duct cells, the immunostaining data using phospho-specific Tau antibodies suggest that pTau forms can be detected in the nucleus of ductal cells (fig. 4.5).

4.3.5 Nuclear pTau in islet, acinar and ductal cells

In order to understand subsequent data, an evaluation of the data so far is required. Based on the HRP immunostaining results using total and isoform specific Tau antibodies, it would be logical to assume that Tau is expressed in the cytoplasm of a subset of islet cells but not the nucleus. Intriguingly, most phospho-specific Tau antibodies (pSer198, pSer199, pSer202/pThr205, pSer396, E178, pSer409) also stained the nuclei not only of islet cells but also of acinar and duct cells. This is in agreement

with previous observations suggesting that two total (43D, epitope; 1-100aa and HT7, epitope; 159-163) and one isoform-specific ('Big Tau' #HPA048895, epitope; exon 4a) Tau antibodies produced nuclear signal. These observations raise questions about whether the nuclear signal is a true Tau signal. If it is true Tau signal, why do the total and isoform-specific antibodies not detect the nuclear Tau forms?

The majority of the antibodies used here have been TLS- and KO-validated; meaning that they have been tested both against KO mouse brain tissue (IHC) and, against Tau KO mouse brain lysates and HAP1 Tau KO cell lines (WB) (Chapter 3, fig. 3.2). The Tau antibodies (total, isoform-specific, phospho-specific) are well validated antibodies that do not produce non-specific signal (exceptions being Ser622 and Tau-46 when detecting Tau expressed at endogenous levels and pSer199 under certain circumstances; Chapter 3). Moreover, the TLS-validation suggests that many total Tau antibodies are impacted by excess phosphorylation events. As a large number of the phospho-specific Tau antibodies directed against different epitopes labelled the nucleus, it is hypothesised that nuclear Tau may be hyperphosphorylated and thus, may not be accessible for binding by the total Tau antibodies.

The localisation of Tau in the nucleus has been previously described both in neuronal and non-neuronal cells [149–152]. A tissue microarray (TMA) from normal and cancerous tissues confirms that the phospho-specific pTau-E178 antibody produces cytoplasmic signal in some tissues (fig. 4.6a), but nuclear in others (fig. 4.6b). It has been proposed that nuclear Tau plays a role in the nucleolar organization and/or heterochromatization of rRNA genes and in DNA integrity [260], [261], [262]. Furthermore, unpublished work by Dr. Irina Stefana suggests that nuclear pTau-E178 may play a role in β cell proliferation (Appendix A, fig. A.2). This is because hyperphosphorylated Tau levels increase in the EndoC-βH1 cell line during mitosis (Appendix A, fig. A.2a) and this phenomenon replicates in human pancreas tissue

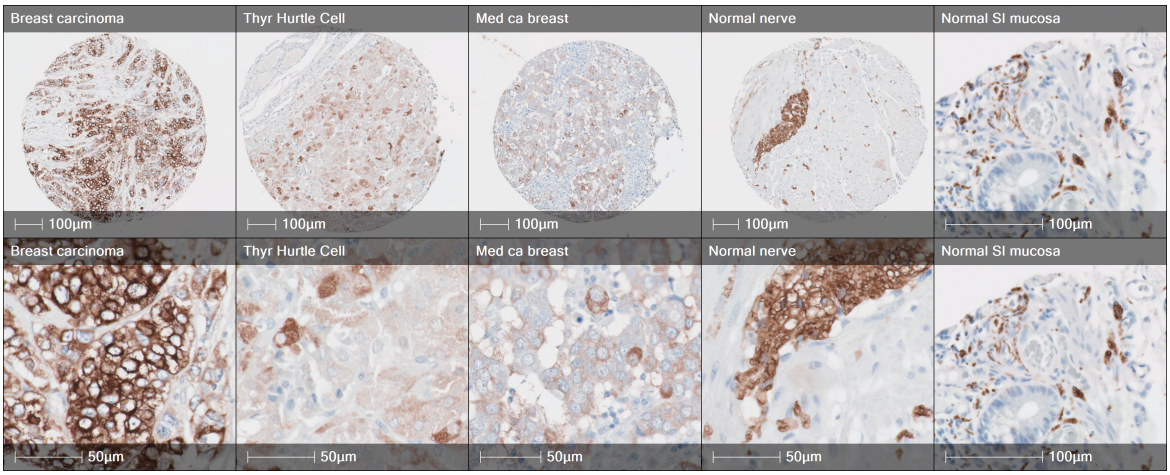

(a) pTau-E178 cytoplasmic staining

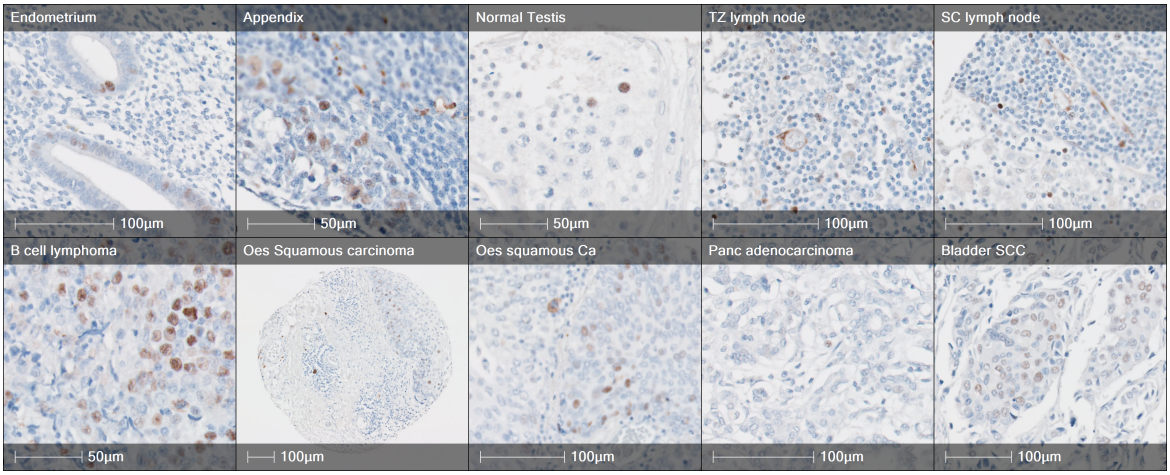

(b) pTau-E178 nuclear staining

Fig. 4.6 **Representative micrographs demonstrating the presence and localisation of pTau-E178 form in a tissue microarray of human cancer and control tissues. 4.6a** | Cytoplasmic staining in breast carcinoma, hurthle cell cancer (thyroid gland), breast cancer, normal nerve normal small intestine mucosa. **4.6b** | Nuclear staining in endometrium, appendix, normal testis, TZ lymph node, SC lumph node, B cell lymphoma, squamous carcinoma, pancreatic adenocarcinoma, Squamous cell carcinoma of the urinary bladder.

sections from a ND organ donor, where pTau-E178 and Ki67, a proliferation marker, co-localise in a proliferative cell (Appendix A, fig. A.2b). Interestingly, WB data also revealed that some phospho-specific Tau antibodies detected a HMW band of 90 kDa corresponding to the MW of HMW Tau (Chapter 3). In addition, the 'Big Tau' #HPA048895 antibody detecting the HMW Tau isoform also produced nuclear signal.

The 'Big Tau' #HPA048895 antibody is raised against exon 4a of Tau and exon 4a has almost no homology to known proteins [24] rendering it unlikely to cross-react with non-specific targets.

One potential explanation for any discrepancies is that the total and isoform-specific Tau antibodies cannot access nuclear Tau. This could be explained by two scenarios; (i) Nuclear Tau is hyperphosphorylated and total antibodies cannot bind Tau which is in agreement with previous observations that total Tau antibodies are inhibited by excess phosphorylation (Chapter 3). (ii) Tau has a number of binding partners (i.e. DNA, RNA-binding proteins) and acquires a conformation that inhibits the binding of total Tau antibodies. This is further supported by the fact that total Tau antibodies usually detect larger epitopes of Tau and as such would be more affected by conformational changes.

4.4 Tau in islet cells in the adult pancreas

So far, the expression of different Tau forms has been characterised in different cellular compartments of the adult human pancreas (islets, acinar, duct cells and nerves) utilising TLS-validated antibodies. The data confirm that Tau is expressed in the cytoplasm of a subset of islet cells and propose that hyperphosphorylated forms of Tau are expressed both in the nucleus and the cytoplasm of a subset of islet cells as well as in the nucleus of acinar and duct cells. To further characterise the cellular localisation of Tau within the islets focusing on the expression of Tau in the β cells, IF staining was performed (Chapter 2, section 2.4.2). Each Tau antibody was combined with (i) insulin (cyan), a marker of β cells, (ii) glucagon (green), a marker of α cells and, (iii) DAPI (blue), a marker of the nucleus. In order to explore Tau expression in health and disease at a preliminary phase, both ND and T1D tissue sections were stained.

4.4.1 Total Tau antibodies

Standard HRP staining revealed that all total Tau antibodies (with only exception being the SP70 antibody) labeled the cytoplasm of a subset of islet cells (fig. 4.3). Most total Tau antibodies (Tau-12, Tau-13, 43D 2G9.F10) were tested in IF in combination with insulin and glucagon to investigate which islet cell types express Tau and demonstrated the same immunostaining pattern, only two total Tau antibodies, Tau-13 and 2G9.F10, are presented here. Both total Tau antibodies stained the cytoplasm of β cells (fig. 4.7). In addition, Tau was also present in a few select α cells. It is worth noting, that the different immunostaining technique used did not affect the ability of total Tau antibodies to detect nuclear Tau in that total Tau antibodies still did not label nuclear forms.

Tau-2 and Tau-1 Both Tau-2 (total Tau) and Tau-1 (dephosphorylation-specific) antibodies labeled punctate structures in the cytoplasm of acinar cells. To investigate whether these antibodies recognise the same structures, IF staining was performed combining (i) Tau-1 antibody (green) , (ii) Tau-2 antibody (red), (iii) insulin (cyan) and, (iv) DAPI (blue). Both Tau-1 and Tau-2 antibodies are mouse antibodies and as such, Tau-1 was TSA'd (Chapter 2, section 2.4.2). Tau-1 and Tau-2 antibodies colocalise in the cytoplasm of acinar cells (fig. 4.8). Tau-2 antibody demonstrated no signal in the pancreatic nerves (fig. 4.4a) whereas Tau-1 did (fig. 4.4b) in agreement with HRP staining. The signal within the cytoplasm of the acinar cells produced by Tau-2 antibody was judged as non-specific and it was deduced that Tau-1 signal from the punctate structures in the cytoplasm of acinar cells is also non-specific.

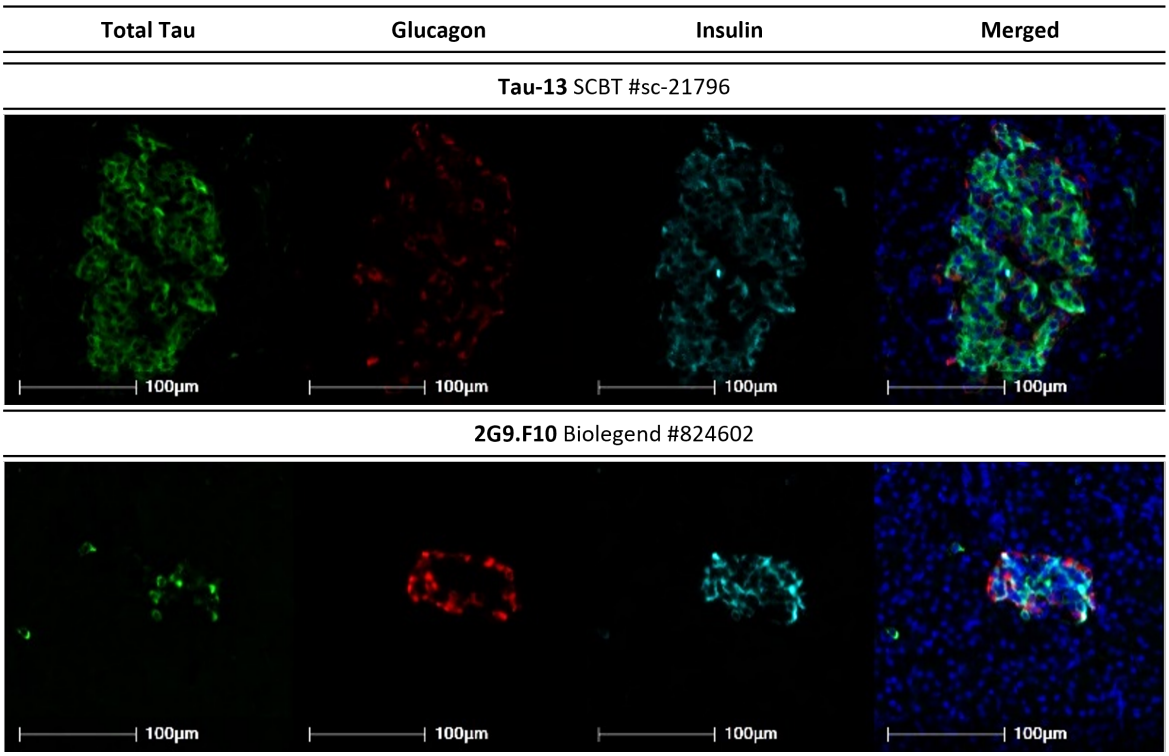

Fig. 4.7 **Total anti-Tau antibody profiles within the adult human islets.** Representative immunofluorescent micrographs demonstrating the presence and the cellular localisation of different total anti-Tau antibodies in islet cells. FFPE pancreas tissue of a non diabetic adult organ donor was stained for the total Tau antibody of interest (Tau-13, 2G9.F10; green), glucagon (red), insulin (cyan) and DAPI (blue). Whole slide scans were imaged at X20. Scale bars 100μm.

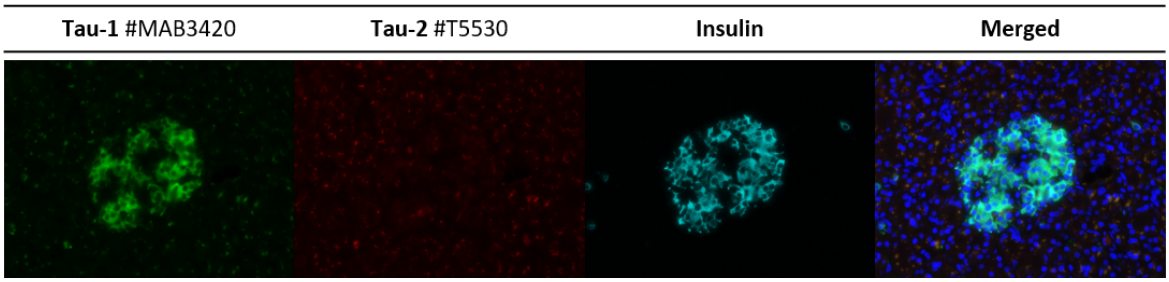

Fig. 4.8 **Dephosphorylation-specific and total anti-Tau antibody profiles within the adult human islets.** FFPE pancreas tissue sections of adult non diabetic organ donor were stained with Tau-1 (dephosphorylation-specific, green), Tau-2 (total, red), insulin (cyan) and DAPI (blue). Slides imaged using an upright microscope. Magnification x40.

4.4.2 Isoform-specific Tau antibodies

As with the total Tau antibodies, each isoform-specific Tau antibody was used to stain a single FFPE pancreas tissue section in combination with insulin and glucagon. Agreeing with the standard HRP staining findings, not all Tau isoforms are present in the human pancreas (fig. 4.9a). '1N and 2N' antibody labelled the cytoplasm of β cells whereas, 0N and 2N antibodies did not produce any signal within the islets. As such, our findings suggest that the 1N Tau isoform is strongly expressed in the adult human pancreas, whereas 0N and 2N Tau isoforms are not detectable in adult human islets.

Ser622 and 3R It is important to note that the following experiment was conducted prior to TLS validation. To investigate the pattern of Ser622 antibody (which was thought to be a 4R-Tau isoform-specific antibody) in relation to the RD3 Tau antibody, IF staining was performed combining (i) Ser622 antibody, (ii) RD3 antibody and (iii) insulin. In ND pancreas, RD3 and Ser622 antibodies labelled β cells (fig. 4.9b). Even though the antibodies colocalised in places, they also demonstrated some differential staining in islet cells. However, firm conclusions about the expression of 4R Tau isoforms cannot be made because the TLS-validation suggests that Ser622 (i) has a preference for 4R Tau isoforms but it can also bind 3R Tau isoforms under specific circumstances and, (ii) it also cross-reacts with MAP-2. As such, these data may suggest that Ser622 can label 3R Tau isoforms (due to the colocalisation with RD3 antibody), 4R Tau isoforms (for which it has a preference) or MAP2 (differential staining, non-specific signal). It is however interesting that the signal of Ser622 is drastically reduced in the ICI of a T1D organ donor compared to that of a ND organ donor. It would be interesting to explore whether Ser622 detects Tau and/or MAP2 in the human pancreas and further expand the analysis to explore whether there is a decreased signal in T1D.

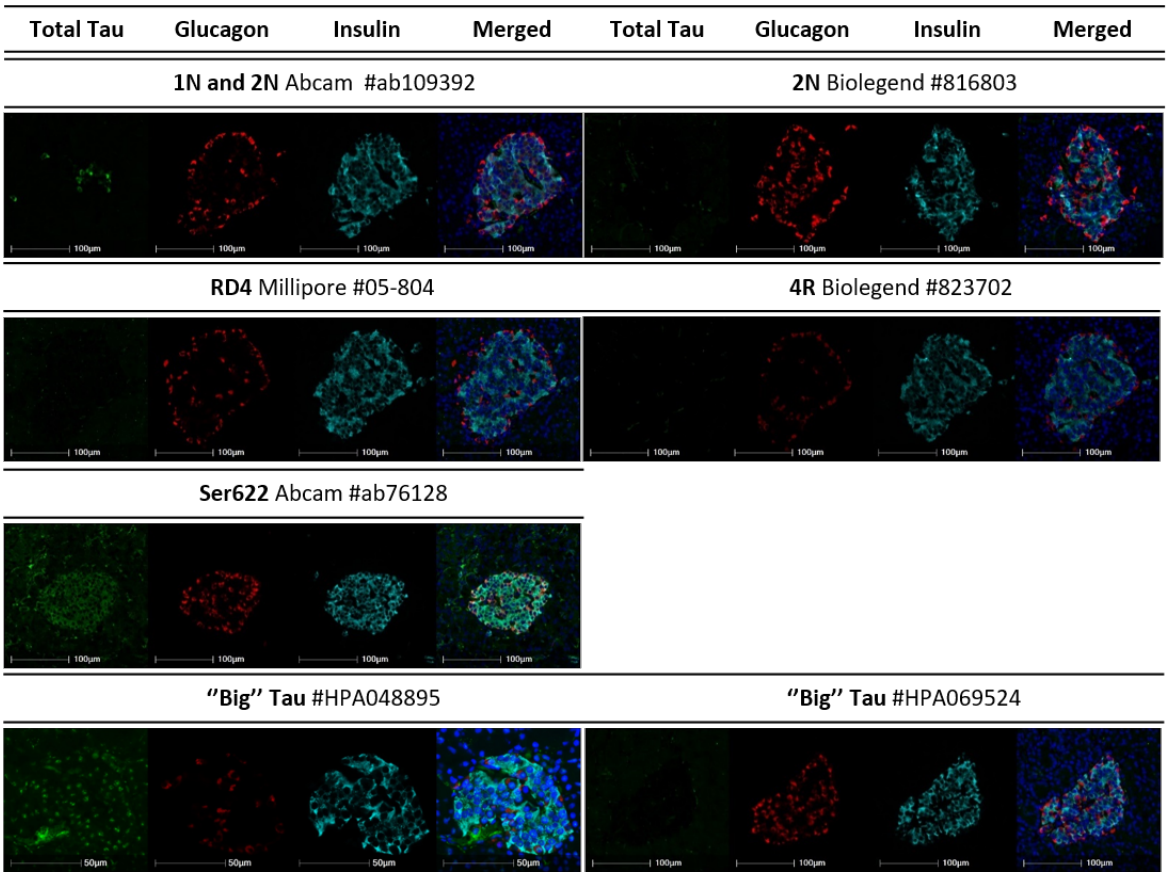

(a)

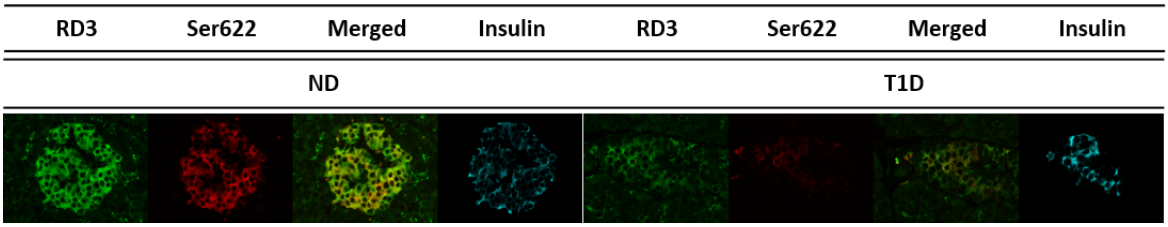

(b)

Fig. 4.9 **Isoform-specific anti-Tau antibody profiles within the adult human islets. 4.9a** | Representative immunofluorescent micrographs demonstrating the presence and the cellular localisation of seven different isoform-specific anti-Tau antibodies in islet cells. FFPE pancreas tissue of an adult organ donor was stained for the isoform-specific Tau antibody of interest ('1N and 2N', 2N, RD4, 4R, Ser622, "Big Tau #HPA048895, 'Big Tau' #HPA069524; green), glucagon (red), insulin (cyan) and DAPI (blue). Whole slide scans were imaged at X20. Scale bars 100μm. **4.9b** | FFPE pancreas tissue sections of adult ND and T1D ODs were stained for 3R-Tau isoforms (RD3, green), 4R-Tau isoforms (Ser622, red) and insulin (cyan). Slides imaged using an upright microscope. Magnification x40.

4.4.3 Phosphorylation-specific Tau antibodies

Standard HRP staining revealed that most peptide-raised phosphorylation-specific Tau antibodies (pSer198, pSer199, pSer202/pThr205, pThr217, pThr231, pSer262, pSer396, pTau-E178, pSer409) labeled the cytoplasm and/or the nucleus of a subset of islet cells (fig. 4.5). As such, five peptide-raised phosphorylation-specific Tau antibodies (pThr181, pSer198, pSer214, pSer238, pSer262) were selected to be tested in IF in combination with insulin and glucagon to investigate which Tau residues are phosphorylated in β cells. As expected, some of the peptide-raised phosphorylation-specific Tau antibodies stained the cytoplasm and the nucleus of β cells (pSer198, pSer262), whereas the signal was weaker in others (pThr181, pSer214, pSer238) (fig. 4.10).

pSer199 and pSer198 HRP staining suggested that the immunostaining pattern of the Ser198 antibody is similar to that of Ser199 antibody. As the two antibodies detect phosphorylated residues that are adjacent to each other, it is important to confirm the specificity of the antibodies and investigate whether they detect different epitopes. As such, IF staining was performed combining (i) pSer199 (TSA - green), (ii) pSer198 (red), (iii) insulin (cyan) and (iv) DAPI (blue). Both pSer198 and pSer199 antibodies are rabbit monoclonal antibodies. As such, in order to combine them, the TSA technique was used (Chapter 2, section 2.4.2) which allows the combination of antibodies of the same species. The pSer198 and pSer199 antibodies colocalised in the cytoplasm of β cells, but had differential staining patterns present as well (fig. 4.11a). This suggests that the Ser198 and Ser199 antibodies detect different phospho-epitopes and that both pTau forms are present in β cells.

pSer199 and pSer404 Phosphorylation of Tau at residue Ser404 has been reported both in the normal and AD brain whereas phosphorylation at Ser409 is AD specific.

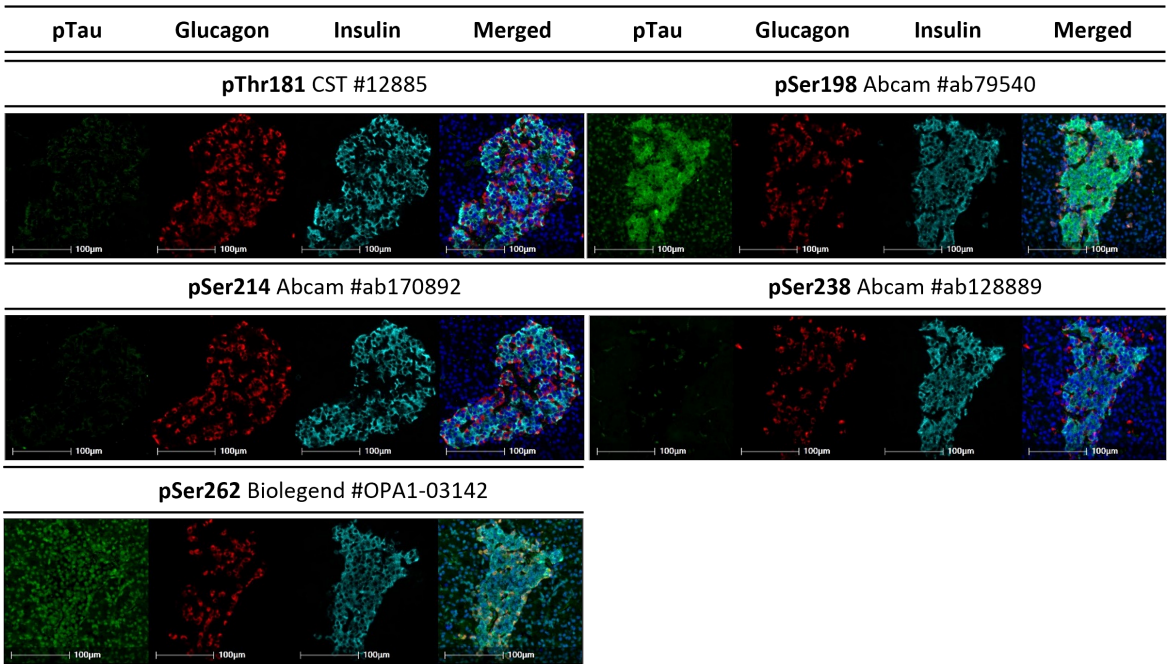

Fig. 4.10 **Phosphorylation-specific anti-Tau antibody profiles within the adult human islets.** Representative immunofluorescent micrographs demonstrating the presence and the cellular localisation of six different phosphorylation-specific anti-Tau antibodies in islet cells. FFPE pancreas tissue of an adult organ donor was stained for the phosphorylation-specific anti-Tau antibody of interest (pThr181, pSer198, pSer214, pSer238, pSer262; green), glucagon (red), insulin (cyan) and DAPI (blue). Whole slide scans were imaged at X20. Scale bars 100μm.

Standard HRP staining suggested that Ser404 may not be phosphorylated in the adult human pancreas (fig. 4.10). A pancreas tissue section from a T1D organ donor was stained for (i) Ser404 (TSA - green), (ii) Ser199 (red), (iii) insulin (cyan) and (iv) DAPI (blue). This revealed that Ser404 is only minimally present in the cytoplasm of β cells (fig. 4.11b). No firm conclusions can be drawn about its nuclear localisation.

pSer199 and pSer409 Tau is phosphorylated at Ser409 in AD brain. A pancreas tissue section from a T1D organ donor was stained for (i) Ser199 (green - TSA), (ii) Ser409 (red), (iii) insulin (cyan) and (iv) DAPI (blue). In T1D, the pSer409 antibody labeled both the nucleus and the cytoplasm of a subset of islet cells (fig. 4.11c). In

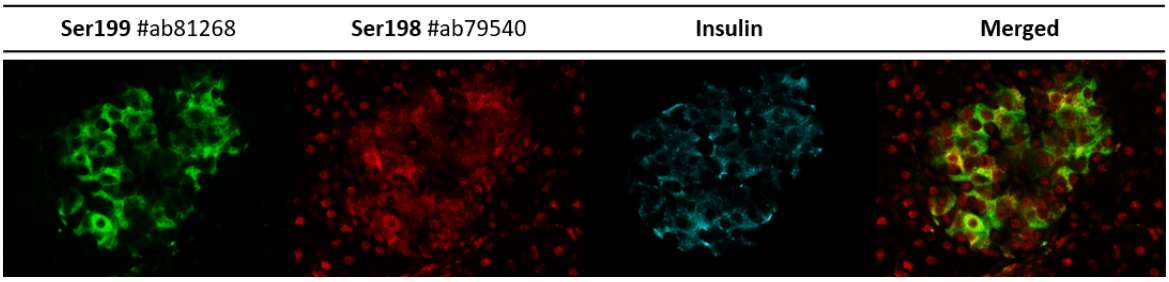

(a) pSer199 and pSer198

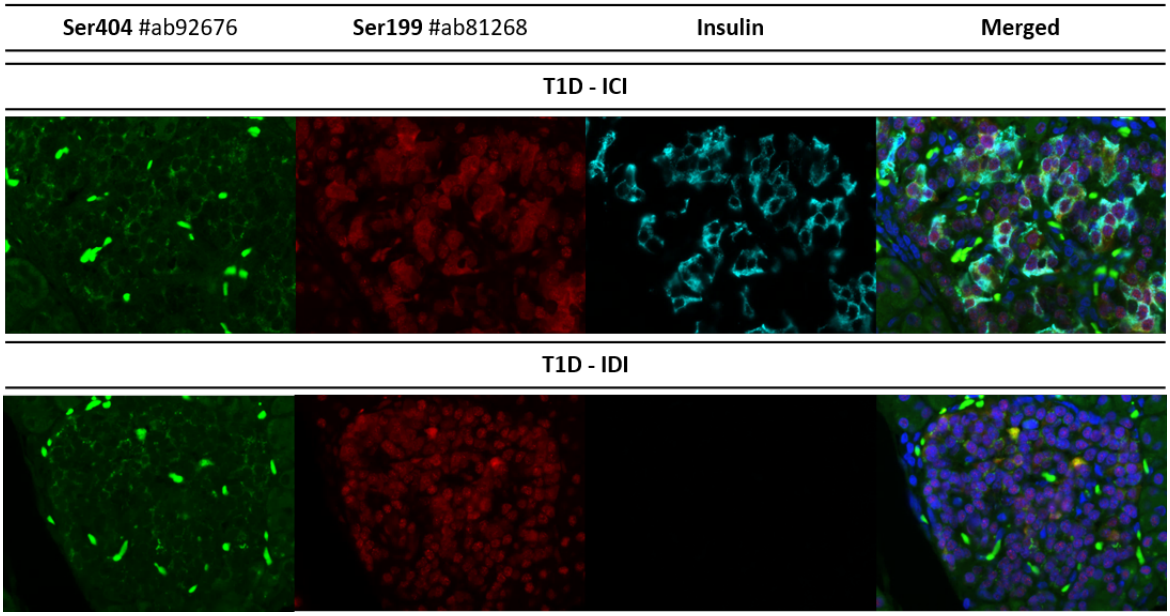

(b) pSer199 and pSer404

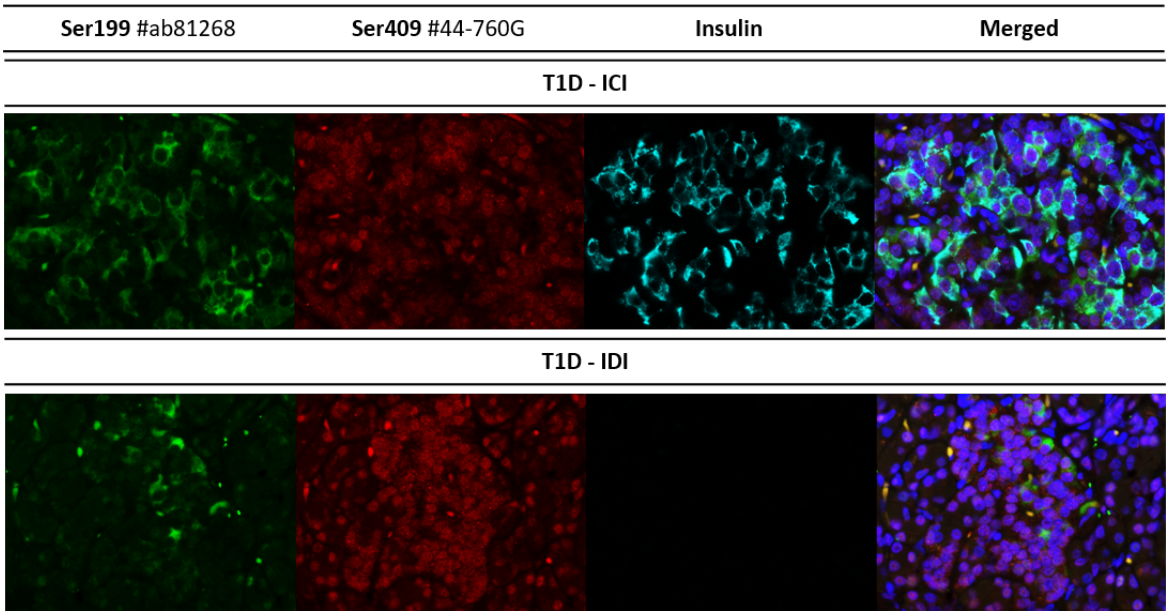

(c) pSer199 and pSer409

Fig. 4.11 **Phosphorylation-specific anti-Tau antibody profiles within the adult human islets.** Representative immunofluorescent micrographs demonstrating the presence and the cellular localisation of different phosphorylation-specific anti-Tau antibodies in islet cells. FFPE pancreas tissue of an adult organ donor was stained for pSer199 (green-TSA), pSer198 (red) and insulin (cyan) (**4.11a**), pSer404 (green-TSA), pSer199 (red), insulin (cyan) and DAPI (**4.11b**) and, pSer199 (green-TSA), pSer409 (red), insulin (cyan) and DAPI (**4.11b**). Slides imaged using an upright microscope. Magnification x40.

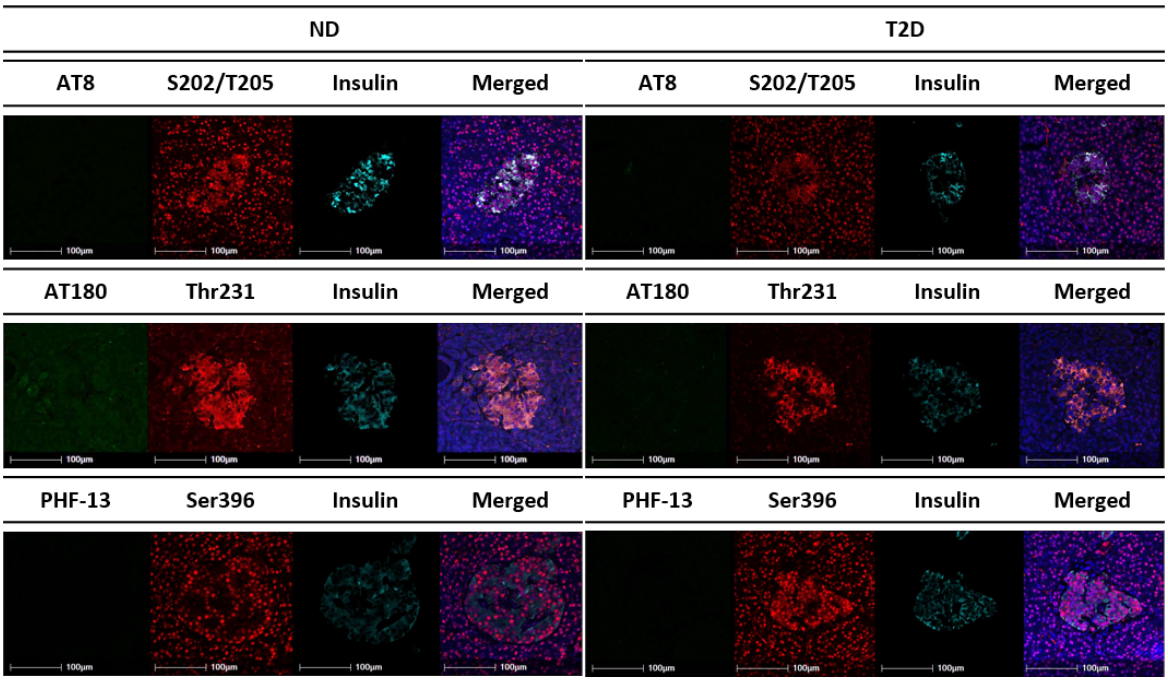

Fig. 4.12 **Peptide-raised and PHF-raised Tau antibodies in the human pancreas of those diagnosed with or without T2D.** Representative immunofluorescence images demonstrating the presence/absence and localisation of phosphorylation-specific Tau antibodies. FFPE pancreas tissue of twelve adult organ donors from the nPOD collection were stained for peptide-raised (red), PHF-raised (green) and insulin (cyan). Confocal microscopy was performed.

ICIs, these cells were identified as β cells whereas, in IDIs, these cells were not defined as a non-α and non-β cells.

4.4.4 PHF-raised and peptide-raised antibodies

As previously discussed, peptide-raised antibodies label both physiological and pathogenic Tau forms, while PHF-raised antibodies only detect alleged pathological Tau forms (Chapter 3). The peptide raised antibodies pSer202/pThr205, pThr231 and pSer396 label both physiological and pathogenic Tau forms whereas, the relevant AT8, AT180 and PHF-13 antibodies, detecting similar epitopes respectively, only label pathological Tau forms. According to the supplier's information, PHF-13 is mouse-reactive but not human reactive. However, TLS validation of this antibody demonstrates that it reacts

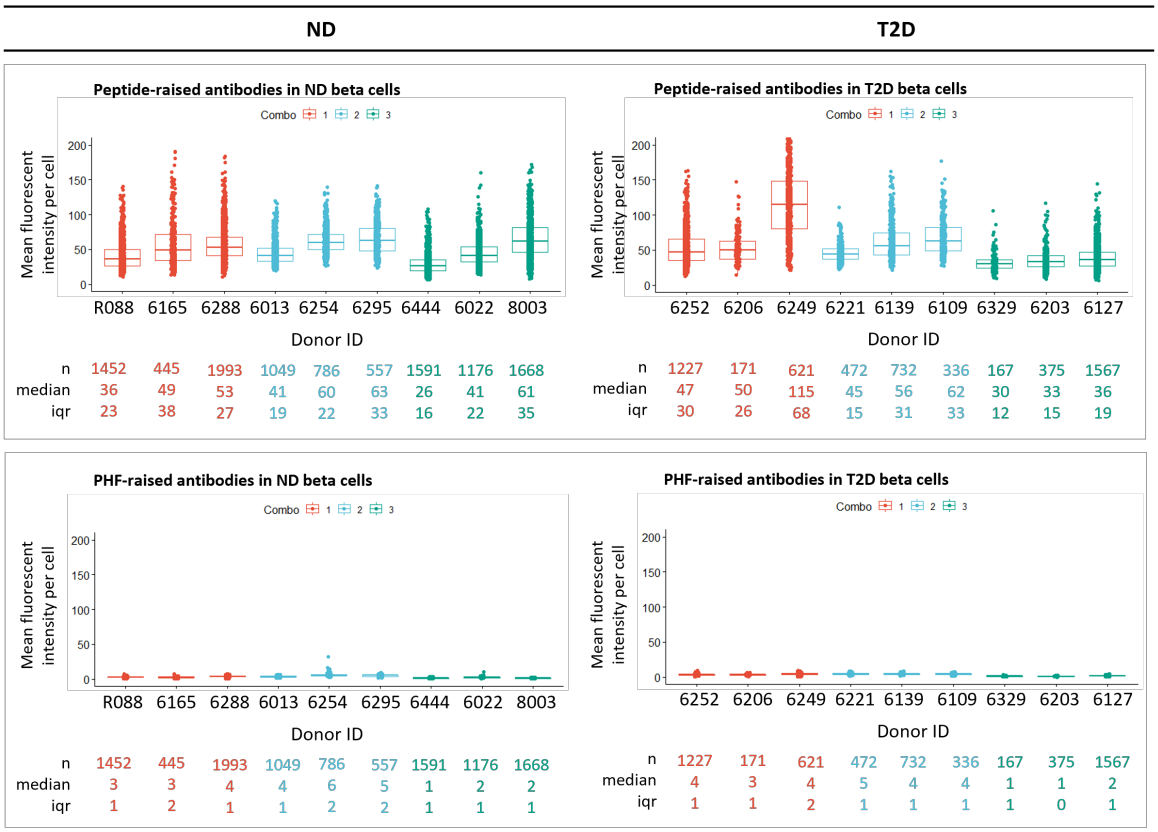

Fig. 4.13 **Quantification of peptide-raised and PHF-raised Tau antibodies mean fluorescent intensity in the human pancreas of those diagnosed with or without T2D.** Quantification of the mean fluorescence intensity of peptide- and PHF-raised Tau antibodies in the ND and T2D pancreas. The images were analysed using Halo software and the output was analysed using the R software. Each boxplot represents a donor and each data point represents a cell. The x axis shows the donor ID and the y axis shows the mean fluorescent intensity per cell. The statistical table below each plot has the n, median and iqr.

with human Tau in the rTg4510 mouse cortex (Chapter 3, section 3.11). It has already been reported here that pSer202/pThr205, pThr231 and pSer396 antibodies label Tau forms in human pancreas demonstrating that these residues are phosphorylated in the adult pancreas.

To further explore whether these residues are phosphorylated both in health and disease (T2D) and determine whether PHF-raised antibodies label Tau forms in the T2D pancreas, pancreas tissue sections were stained for insulin, DAPI and, one of the following combinations; (i) pSer202/pThr205 and AT8, (ii) pThr231 and AT180 or (iii)

pSer396 and PHF-13. Each combination was used to stain ND (n=3) and T2D (n=3) donor pancreas tissue sections. As expected, pSer202/pThr205, pThr231 and pSer396 antibodies labeled Tau forms both in ND and T2D pancreas (fig. **??**). However, AT8, AT180 and PHF-13 antibodies did not stain the islets of ND and interestingly, they did not stain the T2D islets either. (fig. **??**).

Three islets per donor were imaged and quantification analysis confirmed that the peptide-raised antibodies stained the relevant phosphorylated residues in β cells (fig. 4.13). By contrast, the median signal intensity of the PHF-raised antibodies in β cells was minimal showing that these PHF-raised antibodies failed to label Tau forms in ND and T2D islets (fig. 4.13). As both the peptide- and PHF-raised antibodies are TLS-validated, these data indicate that the PHF-raised antibodies are likely to detect pathogenic Tau having a specific conformation and that this conformation is not be a typical pancreatic Tau feature.

4.5 Unmasking nuclear Tau

As previously mentioned, it was unexpected that total and isoform-specific Tau antibodies immunostained only the cytoplasm of β cells whereas the phospho-specific antibodies immunostained both the cytoplasm and the nucleus of β cells. After careful consideration, we concluded that nuclear Tau is likely hyperphosphorylated Tau and the reason why total Tau antibodies fail to detect it is either because (i) most total Tau antibodies are inhibited by excess phosphorylation events or (ii) Tau is bound to a number of partners (eg. DNA, RNA-binding proteins) either blocking its epitopes or changing its conformation and, thus, inhibiting the binding of total Tau antibodies.

Previous work has demonstrated that select phospho-specific Tau antibodies (pSer199, pSer214, pThr231, pSer262, pSer396, PHF-13, pTau-E178, pSer409) labeled Tau forms in the rTg4510 mouse brain even after λPP treatment (Chapter 3, fig.

3.16). In addition, they co-localised with ThioS, a β-sheet dye that specifically detects protein aggregates. As such, these data demonstrate that these phospho-specific Tau antibodies can detect hyperphosphorylated and/or aggregated Tau forms. Therefore, the differential immunostaining pattern could be explained by several hypotheses; (i) the total and isoform-specific Tau antibodies cannot access the nuclei, (ii) the nuclear Tau could be the the HMW Tau isoform and due to conformation and/or phosphorylation events, it is not detectable by total and isoform-specific antibodies or, both. To investigate whether λPP would have an effect on the binding of total Tau antibodies in the human pancreas, we performed λPP treatment experiments and tried alternative antigen retrieval techniques.

4.5.1 λPP treatment

To investigate whether total Tau antibodies fail to detect nuclear Tau due to hyperphosphorylation, we performed λPP treatment. FFPE serial sections of pancreas were treated with and without λPP and were then stained with (i) total Tau (Tau-12; green), (ii) phosphorylation-specific Tau (pSer199; red), (iii) insulin (cyan) and, (iv) DAPI (blue). Tau-12 antibody was TLS-validated and was classified as a green antibody that did not demonstrate non-specific signal. Interestingly, WB data revealed that Tau-12 antibody detected a band of approximately 90 kDa, suggesting that Tau-12 could weakly detect a HMW-Tau isoform. As such, we would expect that after the λPP treatment, Tau-12 antibody may be able to bind nuclear Tau and, hence, produce nuclear signal. As expected, upon λPP treatment, binding of pSer199 antibody was abolished confirming its specificity for phosphorylated Tau forms in the human pancreas (fig. 4.14). Tau-12 signal remained unchanged and no labeling of the nuclear form was observed (fig. 4.14). These data suggest that treatment with λPP alone does not unmask the nuclear Tau epitopes. It is likely that the nuclear form, that could be

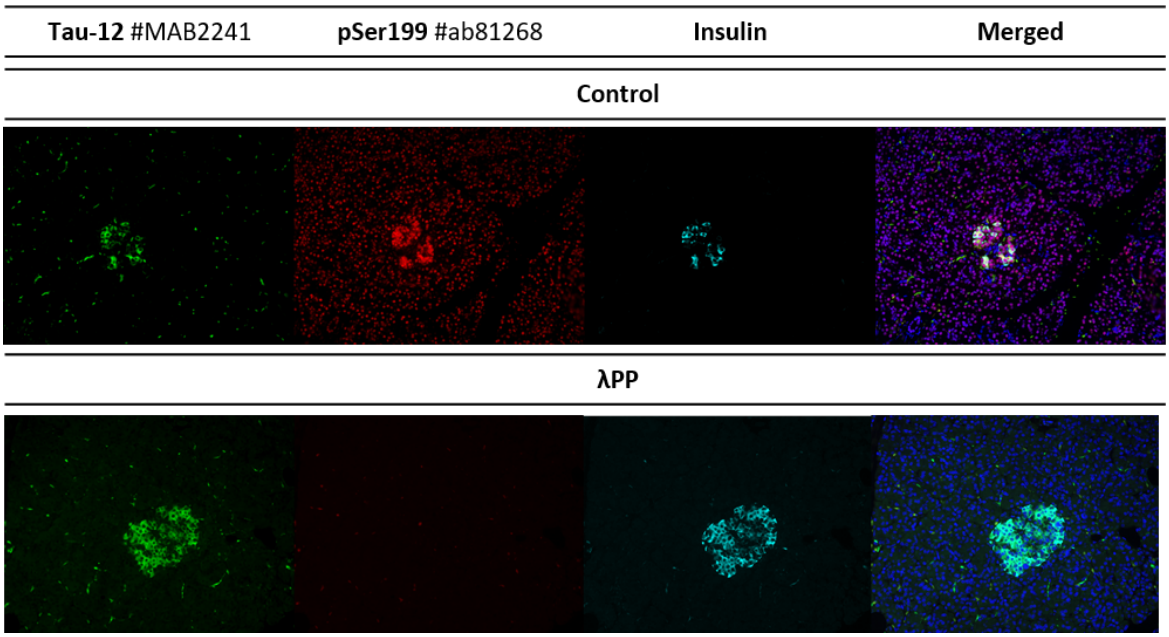

Fig. 4.14 **Total and phosphorylation-specific anti-Tau antibody profiles within the adult human islets in control and λPP-treated tissue.** FFPE pancreas tissue sections of adult non diabetic organ donor were pre-incubated with and without lambda phosphatase (λPP) treatment and were stained with Tau-12 (total anti-Tau antibody, green), pSer199 (phospho-specific anti-Tau antibody, red), insulin (cyan) and DAPI (blue). Slides imaged using an upright microscope. Magnification x40.

HMW Tau, either acquires a specific conformation that blocks the binding of total Tau antibodies or is bound to the DNA and RNA-binding proteins inhibiting access to the total Tau antibodies or, both. However, more evidence is required to support this.

4.5.2 Formic acid

Previous studies have used formic acid (FA) treatment to expose Tau epitopes in autopsy brain tissue [241]. To investigate whether FA treatment has an effect on Tau antibody binding, four serial pancreas sections were treated with and without λPP followed by treatment with and without FA. The slides were then stained for (i) 'Big Tau' (#HPA048895; green), (ii) total Tau (Tau-12, red), (iii) insulin (cyan) and (iv) DAPI (blue). #HPA048895 antibody labelling seemed to be improved after the

λPP treatment (fig. 4.15a) and it was not affected by the FA treatment (fig. 4.15b). Tau-12 antibody immunostaining remained unchanged before and after FA and/or λPP treatment (fig. 4.15b). It is concluded that FA may not have an impact on the binding of Tau-12 and #HPA048895. Furthermore, we propose that λPP treatment improves the binding of #HPA048895 to nuclear Tau forms suggesting that the nuclear HMW-Tau isoform is hyperphosphorylated.

4.5.3 Two distinct Tau forms are present in β cells

As the immunostaining pattern of total and phosphorylation-specific Tau antibodies is differential in that total Tau antibodies do not stain the nucleus of β cells. Further combinations of total and pTau forms were tested. FFPE pancreas tissue sections from ND (n=1) and T1D (n=1) organ donors were stained for (i) total Tau (Tau-5 (Abcam); green), (ii) phosphorylation-specific Tau (pTau-E178; red), (iii) insulin (cyan) and, (iv) DAPI (blue).

As expected Tau-5 labelled the cytoplasm of β cells. Tau-5 and pTau-E178 do not always co-localise in the cytoplasm of β cells (fig. 4.16). It was observed that β cells with low Tau-5 levels had strong pTau-E178 staining. Second, β cells that express high levels of insulin, express high levels of total Tau (as detected by the Tau-5 antibody) but low levels of pTau (as detected by the pTau-E178 antibody) (fig. 4.16). By contrast, β cells that express low levels of insulin and low levels of total Tau had high levels of pTau. Thirdly, as expected, T1D IDIs (that do not have insulin-containing β cells), also lacked total Tau staining. On the other hand, pTau-E178 antibody detected both nuclear and cytoplasmic Tau in select cells in T1D IDIs (fig. 4.16). These cells could be dedifferentiated β cells.

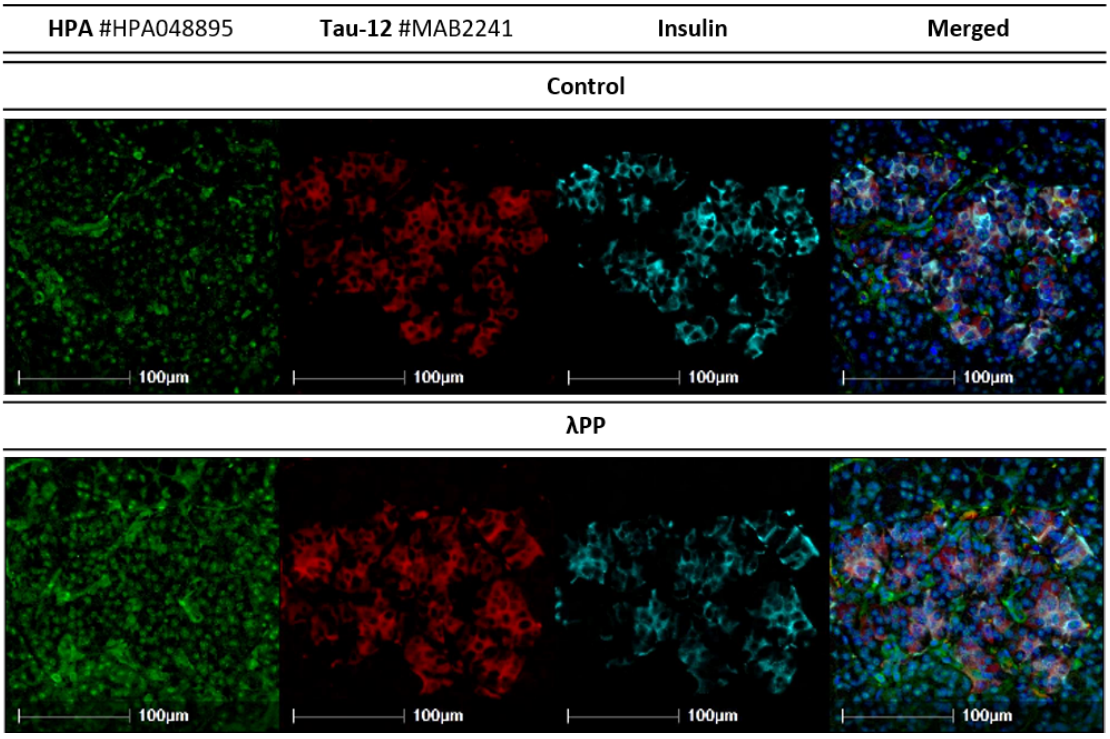

(a)

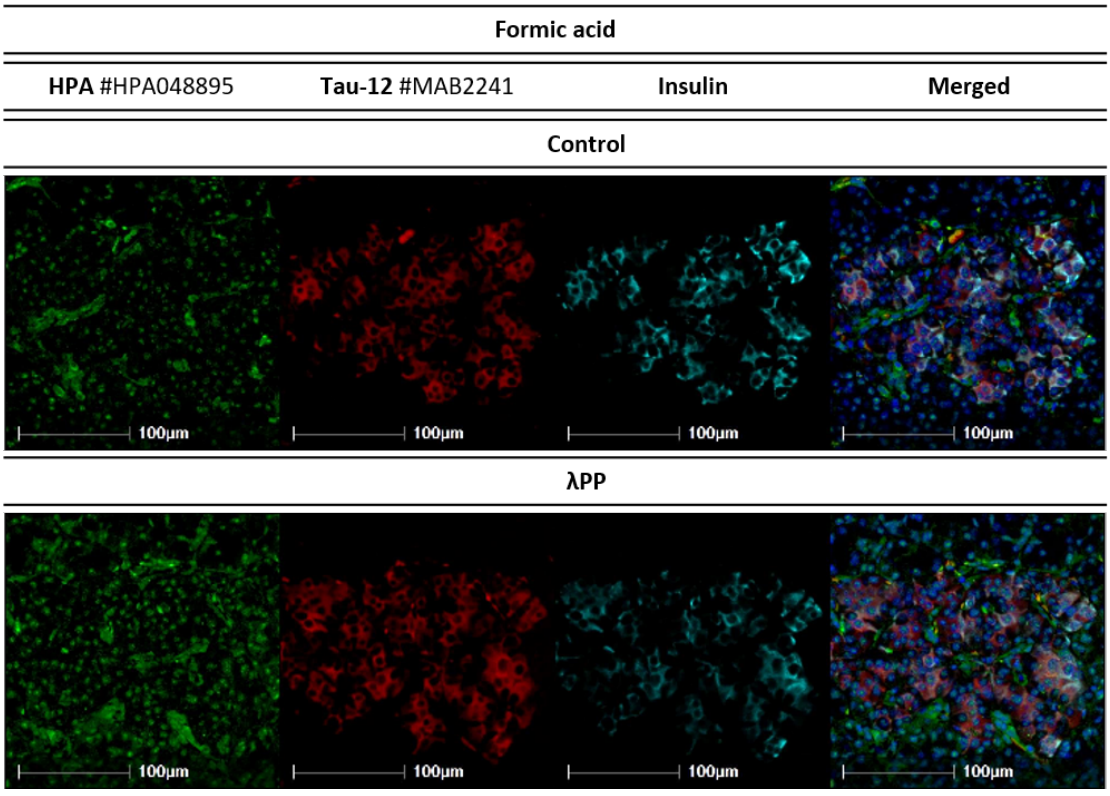

(b)

Fig. 4.15 **Isoform-specific and phosphorylation-specific Tau antibody profiles in the human pancreas before and after λPP and formic acid treatments.** Representative immunofluorescent micrographs demonstrating the presence and localisation of total, isoform-specific and phosphorylation-specific Tau in the islets in the pancreas of an organ donor. **4.15a-4.15b** | Four serial sections were treated with and without λPP treatment, were treated with (**4.15b**) or without (**4.15a**) formic acid (FA) and stained with #HPA048895 (green), Tau-12 (red), insulin (cyan) and, DAPI (blue). Magnification x40.

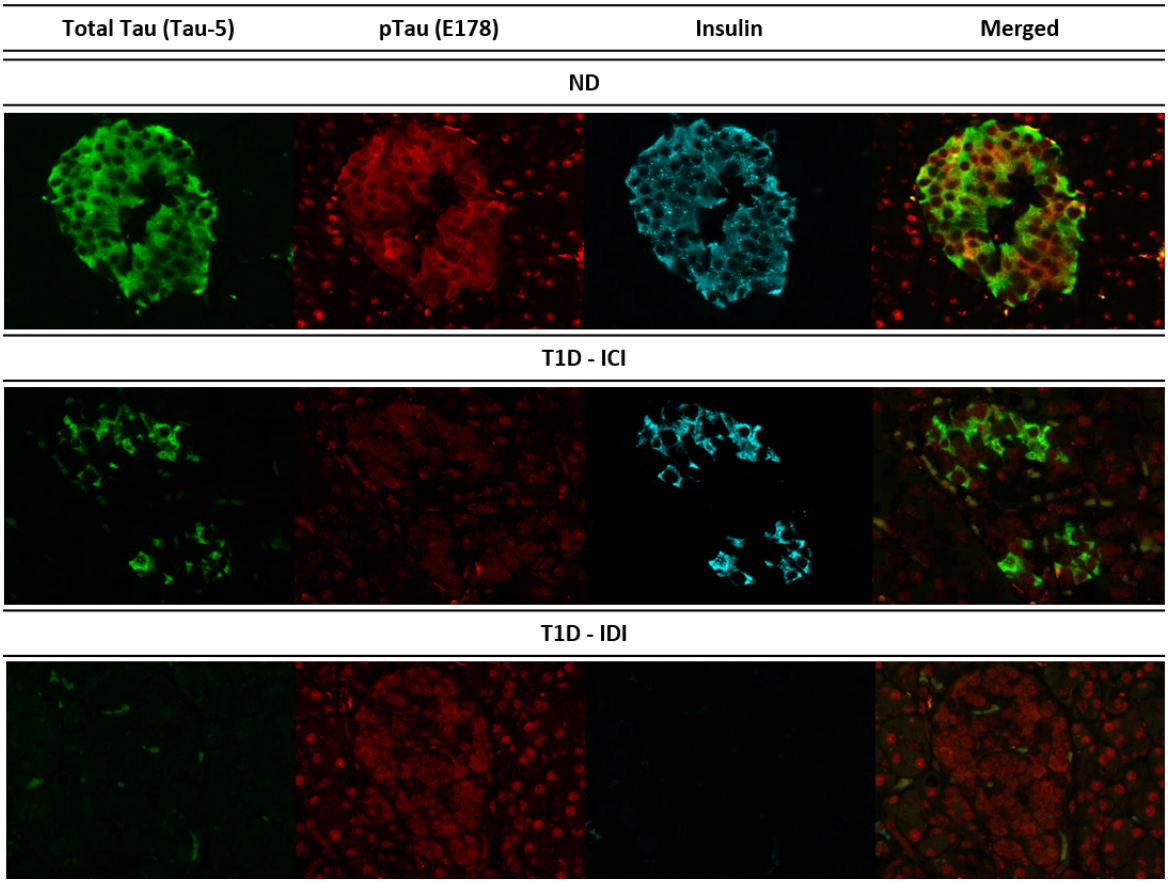

Fig. 4.16 **Total (Tau-5) and phosphorylation-specific (pTau-E178) antibody profiles within the adult human islets** Representative immunofluorescent micrographs demonstrating the presence and localisation of Tau-5 and pTau-E178 antibodies in the islets. FFPE pancreas tissue of a non diabetic and a type 2 diabetic adult organ donor from the EADB collection were stained for Tau-5 (total, green), pTau-E178 (phospho-specific, red) and, insulin (cyan). Slides imaged using an upright microscope. Magnification x40.

4.6 Anti-pTau-E178 epitope

The pTau-E178 antibody was initially defined as a total Tau antibody and its epitope is proprietary but located in the C-terminal region. It is proposed that pTau-E178 is a phosphorylation-specific Tau antibody that detects Tau phosphorylated at the Ser396 residue. In agreement with that, we have previously demonstrated that pTau-E178 is a phospho-specific Tau antibody (Chapter 3). Interestingly, pTau-E178, like pSer199, detects a form of pTau that moves from the nucleus to the cytoplasm with

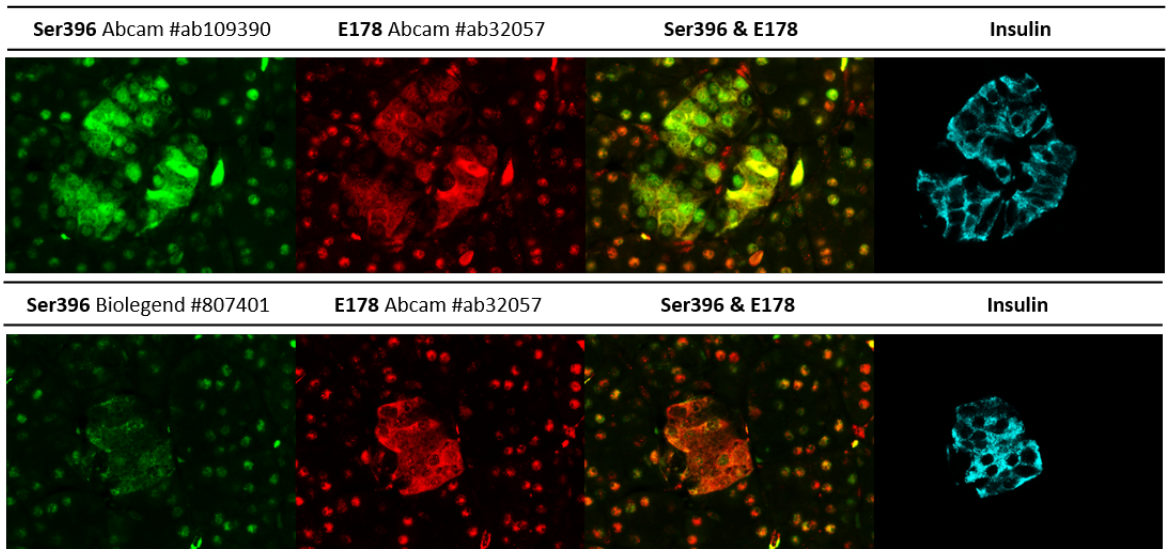

Fig. 4.17 **pTau-Ser396 and pTau-E178 antibody profiles within the adult human islets.** Representative immunofluorescent micrographs demonstrating the presence and localisation of pTau-Ser396 and pTau-E178 antibodies in the islets in the pancreas of an organ donor. FFPE pancreas tissue of an adult organ donor was stained for pTau-Ser396 (green), pTau-E178 (red) and insulin (cyan). Slides imaged using an upright microscope. Magnification x40.

age (discussed in detail in section 4.7 of this Chapter). To further investigate whether pTau-E178 specifically detects Tau phosphorylated at Ser396, a series of experiments followed.

4.6.1 pSer396 and pTau-E178

Two ND FFPE pancreas tissue sections were stained with (i) pSer396 (abcam or biolegend; green), (ii) pTau-E178 (red) and, (iii) insulin (cyan). The pSer396 and pTau-E178 antibodies colocalised in places, but differential staining was also identified (fig. 4.17). As such, pTau-E178 may detect pSer396 but it is not clear whether pTau-E178 is specific only for Ser396. Interestingly, we observed that β cells that express high levels of insulin, have low levels of pTau forms (as detected by Ser396 and pTau-E178) and vice versa, in agreement with data provided in section 4.5.3.

4.6.2 Blocking peptide experiments

To investigate whether pTau-E178 detects the same epitope as pSer396 Abcam antibody, blocking peptides experiments were performed (Chapter 2, section 2.4.2.1). Blocking peptides (BP) will bind specifically to the target antibody, preventing subsequent antibody binding to the target epitope. The control antibody can bind the target epitope in the tissue and the BP-bound antibody cannot. Four tissue sections were stained; (i) pSer396 and pTau-E178, (ii) BP-bound Ser396 and BP-bound pTau-E178, (iii) BP-bound Ser396 and pTau-E178 and, (iv) Ser396 and BP-bound pTau-E178. In all, BP-bound Ser396 and BP-bound pTau-E178 antibodies failed to label the pancreas, whereas control Ser396 and pTau-E178 stained the islets as expected (fig. 4.18). These data confirmed that pTau-E178 is capable of detecting pSer396. However, it is not clear if pTau-E178 detects only a single phosphorylation events at Ser396. It is possible that it also detects other nearby phosphorylated residues, such as pSer409, however, further analysis is required to study this.

4.7 pTau-E178 in islet cells

4.7.1 Preliminary work

Previous work by IBEx team has demonstrated that the cellular localisation of some pTau forms is altered with ageing. FFPE pancreas tissue from a young donor and an older donor were stained with pSer199 (red), pTau-E178 (green) and DAPI. It was observed that both phospho-specific Tau antibodies labelled the nucleus of β cells from the young donor, whereas they labelled both the nucleus and the cytoplasm of β cells from the older donor (fig. 4.19a).

To investigate whether the subcellular localisation of pTau forms changes with ageing, a panel of pancreas tissue sections from 130 organ donors were stained for

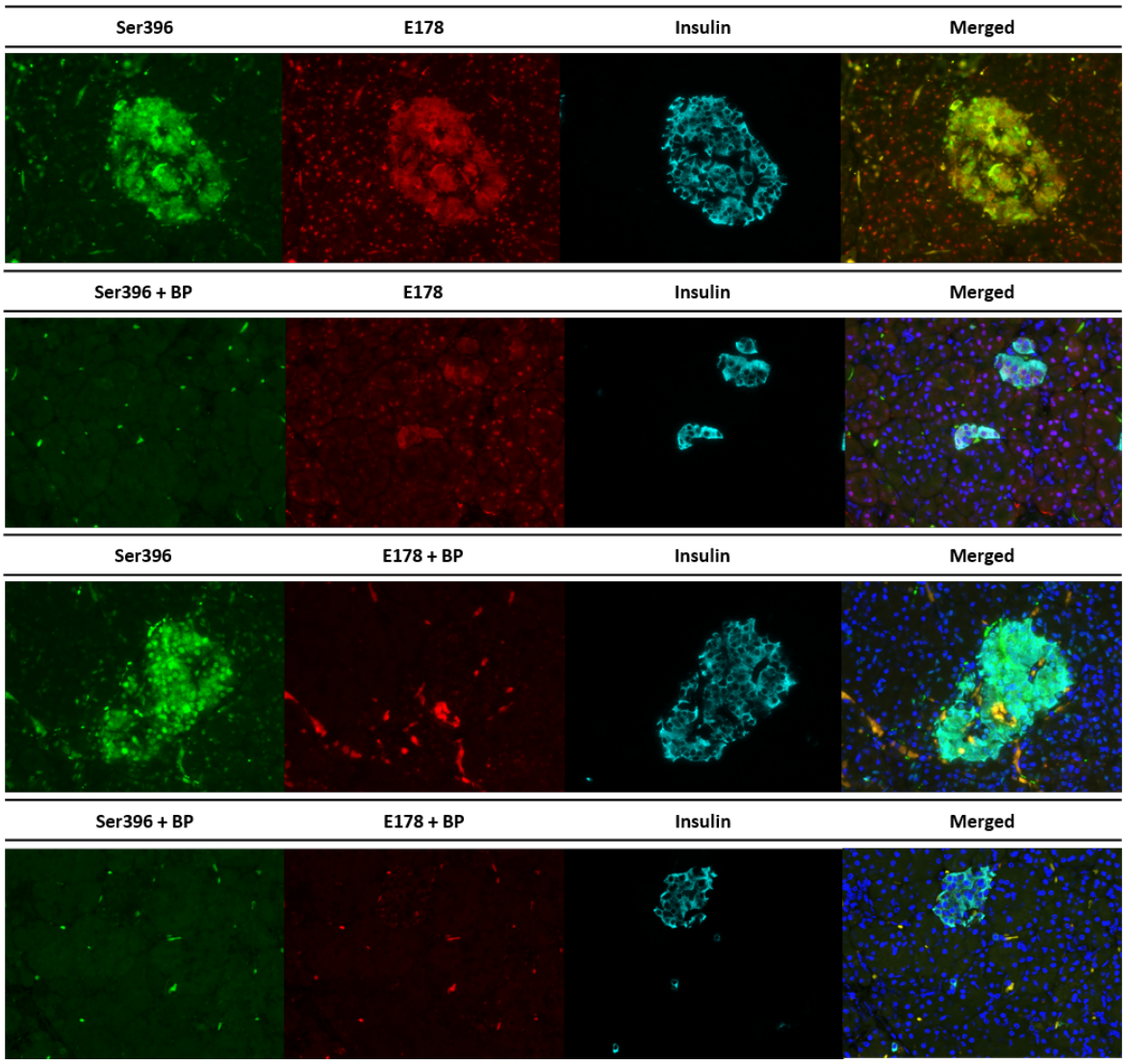

Fig. 4.18 **pTau-Ser396 and pTau-E178 antibody profiles within the adult human islets.** Serial sections of FFPE pancreas tissue of an adult organ donor were stained for pTau-Ser396 (green), pTau-E178 (red), insulin (cyan) and, DAPI (blue). Primary Tau antibodies, pSer396 (abcam) and Tau E178 were pre-incubated with or without a pSer396 blocking peptide (BP). Slides imaged using an upright microscope.

pTau-E178, insulin, a marker of β cells and glucagon, a marker of α cells. FFPE pancreas tissue sections were obtained from the nPOD biobank (Appendix A, fig. A.4) and the donor panel was constructed based on two main criteria; (i) representative ND donors from each decade of life were included, (ii) for each of the T1D and T2D (short- and long-duration of disease) organ donors, age-matched ND controls were

also selected. In total, FFPE nPOD pancreas tissue sections from 40 non-obese ND (BMI<26), 38 obese ND (BMI>26), 30 T1D and 24 T2D organ donors were stained for (i) pTau-E178, (ii) insulin, (iii) glucagon and, (iv) DAPI. Twenty islets per donor were imaged generating a pool of approximately 2,440 islets to be analysed. The construction of the panel, the staining of the tissue sections and the imaging was performed by Dr. M.L. Zeissler.

Islet analysis Image analysis was performed using MATLAB, a programming language and computing environment. The raw fluorescent images were inputted into MATLAB (fig. 4.19b). For each of the three channels detecting glucagon (green), insulin (cyan) and pTau-E178 (red), a threshold was set. This threshold determined whether a given cell was positive or negative for a particular marker. Based on that the raw images were converted into binary images; in the binary images, the white region corresponds to the immunostaining pattern of the relevant marker and the black region represents the background (e.g. exocrine tissue). The binary images were then merged and the white area was defined as the islet. The signal of pTau-E178 was defined as the overall pTau-E178 within the islet. DAPI was used to define the nucleus and as such, the pTau-E178 signal overlapping with DAPI was defined as the nuclear pTau-E178. Next, the cytoplasmic pTau was calculated as the overall pTau minus the nuclear pTau (fig. 4.19c). To assess whether there is an increase in the cytoplasmic pTau-E178 within the islet, the ratio of cytoplasmic pTau-E178 by the overall pTau-E178 within the islet was calculated; the higher the ratio, the more cytoplasmic pTau-E178 within the islet. This analysis revealed that there is an increase in the cytoplasmic pTau-E178 with ageing in non-diabetic donors (fig. 4.19d). This analysis was conducted by Dr. John Chilton.

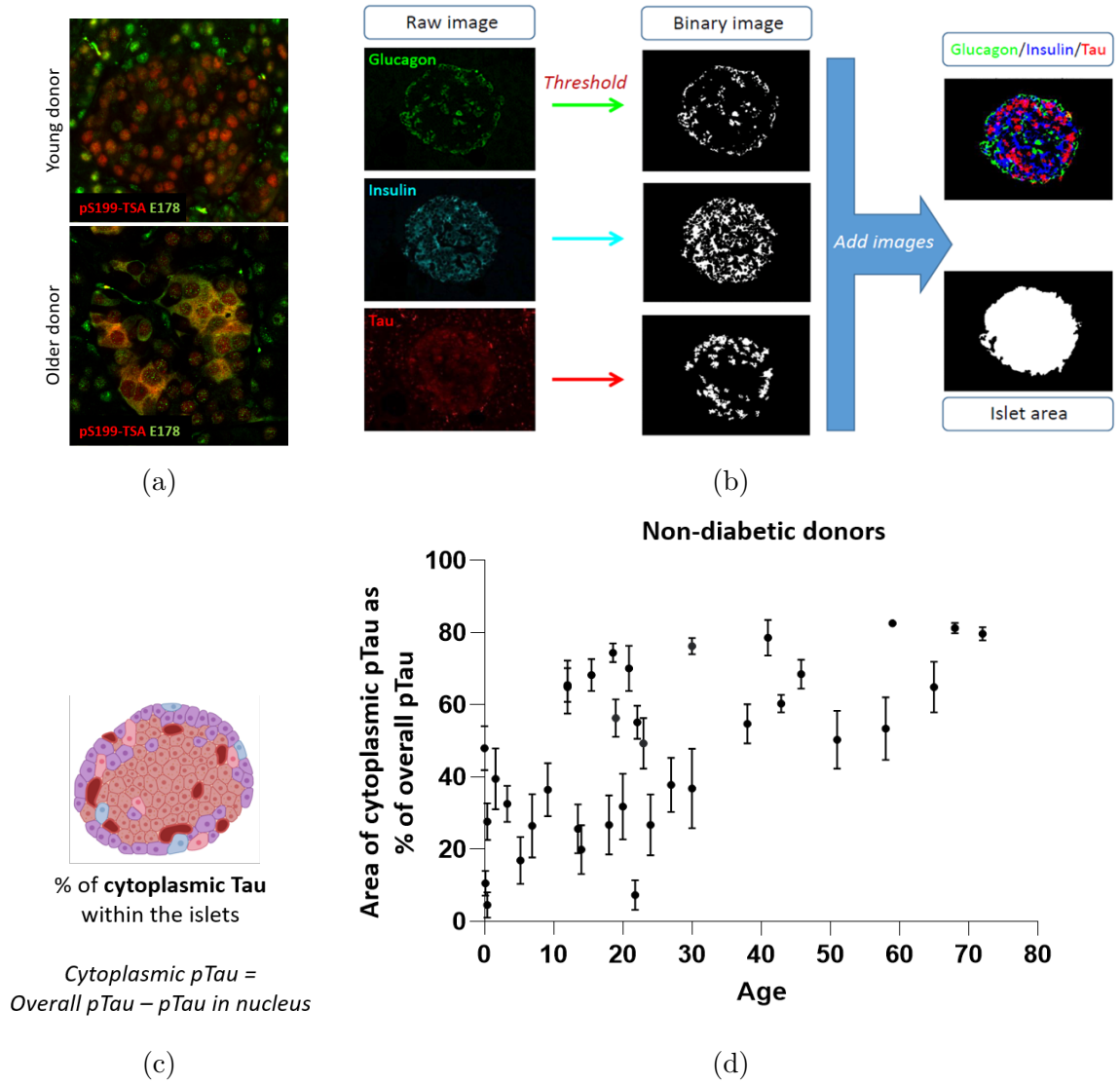

Fig. 4.19 **Image analysis on an islet basis reveals that some pTau forms translocate to the cytoplasm of β cells with ageing. 4.19a** | FFPE pancreas tissue from a young (0y) and an older (72y) donors were stained for pSer199 (TSA-red) and pTau-E178 (green). Microscopy was performed using a fluorescent microscope at magnification x40. **4.19b** | FFPE pancreas tissue from 130 organ donors were stained for pTau-E178, insulin and glucagon. Image analysis was performed on an islet basis using MATLAB. The raw images were imported into MATLAB and were converted into binary images, using a separate threshold for each of the three channels. The binary images were merged and the white region was defined as the islet area. The overall pTau-E178 was calculated. Using DAPI, the nuclear pTau-E178 was calculated. **4.19c** | The cytoplasmic pTau-E178 was calculated by extracting the nuclear pTau-E178 from the overall pTau-E178. **4.19d** | The cytoplasmic pTau-E178 was plotted as the area of cytoplasmic pTau-E178 as percentage of the overall pTau-E178 in the islet by age. Each data point represents a non-diabetic organ donor.

Limitations The methodology described above represents the absolute amount of pTau-E178 within an islet. However, it does not allow for quantification of pTau-E178 on a cell-by-cell basis and therefore, pTau-E178 within the β cells is not measurable. In addition, the pancreas is heavily vascularised and innervated. Therefore, it is likely that blood vessels (producing high autofluorescence) and nerves (containing high amount of Tau) cannot be excluded from the area of interest. As such, in order to investigate the expression of pTau-E178 on a cell-by-cell basis, focusing in β cells, the development of a new pipeline was necessary.

4.7.2 Development of a cell-by-cell analysis

To investigate the expression of pTau-E178 on a cell-by-cell basis, Halo software, which allows for quantification of multiple markers within single cells, was employed. The images were imported into Halo and the regions of interest were annotated as described previously (Chapter 2, section 2.4.3). In summary, the region of interest (islets) was manually annotated. Next, blood vessels and nerves were further annotated to be excluded from the region of interest. This is because signal from blood vessels (autofluorescence) and nerves (high expression of pTau-E178) may interfere with the signal from the islets. Following the annotation process, the islet cells were phenotyped. DAPI was used to define the nucleus, whereas the cytoplasm radius of β and α cells was set manually due to the lack of cell membrane markers. Appropriate thresholds were set to define the fluorescent signal for each of the three markers (pTau, insulin, glucagon) in the nucleus and the cytoplasm.

Manual autofluorescence removal Prior to data analysis, manual autofluorescence removal was performed. For each image, two regions were annotated; (i) The first region was the islet and (ii) the second region was a small part of the acinar tissue equal to approximately 15 cells - Tau is not expressed in the cytoplasm of acinar

cells and therefore any signal within that region is attributed to tissue AF. The mean cytoplasmic MFI of the acinar cells was calculated and was then subtracted from the cytoplasmic and nuclear MFI of the islets.

4.7.2.1 Data handling

The HALO data were outputted into an Excel file and provided information about the nuclear and cytoplasmic intensity for each of the markers in each cell. The intensity of the fluorescent signal for each cell is presented as the mean fluorescent intensity (MFI). In addition, it provides information about the cell area (μm2), cytoplasm area (μm2), nuclear area (μm2), nucleus perimeter (μm) and nucleus roundness. The data were analysed using R, a software environment for statistical computing.

4.7.2.2 Cell phenotyping

In total, 183,159 cells from ND and T2D pancreas were identified. Due to time limitations, T1D analysis was paused. Using insulin and glucagon as markers of β and α cells, respectively, the cells were phenotyped as β, α, non-insulin non-glucagon containing and bihormonal (insulin and glucagon containing) cells. β cells were defined as insulin-positive and glucagon-negative cells. It is possible that a cell that does not contain any insulin might still be a β cell (Chapter 1, section 1.7.1.2). However, to date, there is no marker to detect dedifferentiated cells. As such, the analysis inevitably included only insulin-containing β cells. α cells were defined as insulin-negative and glucagon-positive cells. Cells that were double negative for insulin and glucagon were defined as non-insulin non-glucagon containing cells. Such cells could represent a broad category of cells, e.g. insulin-deficient β cells, γ, δ, ϵ cells. Cells that were double positive for insulin and glucagon were defined as bihormonal cells. Bihormonal cells should be studied with caution. That is because the tissue sections were imaged using

an upright microscope. This means that some of the bihormonal cells could be false positive, e.g. two overlapping cells, one insulin-containing and one glucagon-containing cell. As the data presented so far demonstrates that Tau is predominately localised in β cells, this analysis focuses on β cells only.

pTau-E178 containing cell The cells were divided into four pTau cell groups based on the cellular localisation of pTau. A cell could either have (i) no pTau (pTau -ve), (ii) have pTau only in the cytoplasm (pTau cyto +ve), (iii) pTau only in the nucleus (pTau nuc +ve) or (iv) have pTau both in the cytoplasm and the nucleus (pTau +ve).

4.7.3 pTau-E178 in ageing, obesity and T2D

4.7.3.1 pTau-E178 in islet cells

To validate the quality of this pipeline, the initial analysis was performed using five islets from a young donor (0.17y) and five islets from an older donor (72y). The pipeline allowed the analysis of a large amount of islet cells containing pTau-E178 in the nucleus, the cytoplasm or both (fig. 4.19a). The cytoplasmic to nuclear ratio was used to assess whether the amount of pTau-E178 in the nucleus and the cytoplasm changes in β, α and non-insulin non-glucagon cells from both donors. Interestingly, the ratio was higher in the β cells of an older donor compared to a young donor (fig. 4.20). Furthermore, a moderate increase in the ratio is observed in α cells but no difference is observed in the non-insulin non-glucagon cells. The data agree with RNAseq data and IHC data proposing that Tau is predominately expressed in β cells compared to other islet cells and further implies that the subcellular expression of pTau-E178 in β cells is different between the two donors. As the β cells expressed the highest levels of pTau-E178 the remainder of the analyses focused solely on the β cells.

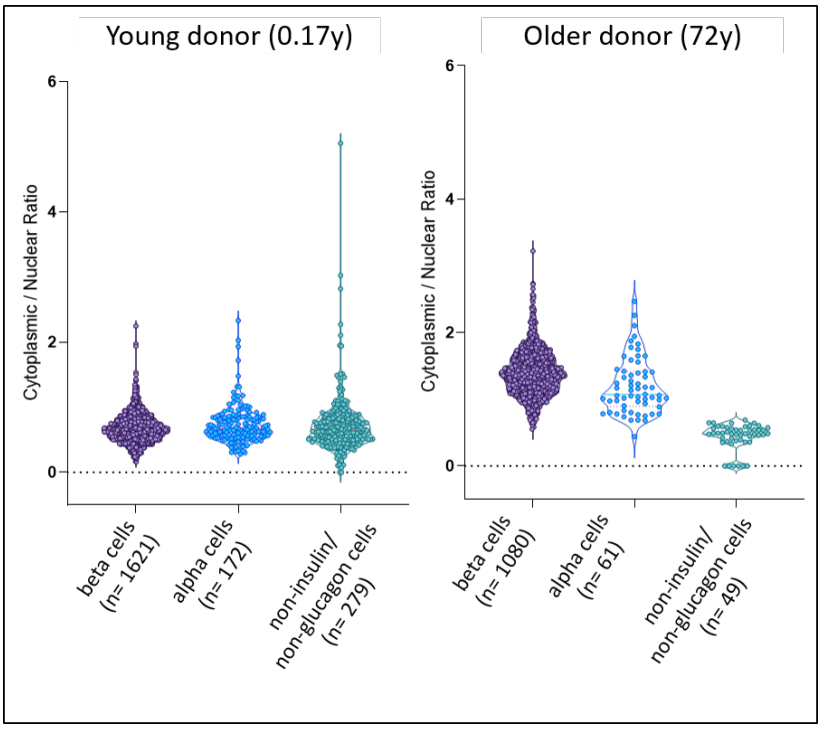

Fig. 4.20 **The subcellular localisation of pTau-E178 in β, α and non-insulin non-glucagon cells from young and older donors.** FFPE pancreas tissue from a young (0.17y) and an older (72y) were stained for pTau-E178, insulin, glucagon and DAPI. Five islets per donor were imaged and the fluorescent images were imported into the Halo software for quantitative analysis. The islets were defined as the region of interest and β, α and non-insulin non-glucagon cells were phenotyped.

4.7.3.2 pTau-E178 in ageing, obesity and T2D

This pipeline allowed the study of 40,682 β cells from non obese (BMI<26) non diabetic organ donors, 34,740 β cells from obese (BMI>26) ND organ donors and 20,397 β cells from T2D organ donors. For each cell, the overall pTau-E178 and the cytoplasmic to overall pTau-E178 ratio was calculated. The median ratio value for each donor was then determined and plotted against age (fig. 4.21a). The higher the ratio, the more cytoplasmic pTau-E178 within the β cells. Interestingly, the data suggest that there is a trend for increase in the ratio in the β cells from ND non-obese individuals (fig. 4.21a, Appendix A, table A.6). It is further observed that the ratio varies between 0.2-0.6 in ages below 35 years whereas it varies between 0.4-0.8 in ages above the age

of 35 years. No such trend is observed in the ND obese cohort in which the data are variable. Interestingly, no trend is observed in the T2D cohort. However, that is reasonable, as there are not many data for ages below 35 years. To further the analysis of pTau-E178 it would be interesting to explore whether there is an increase in the presence of cytoplasmic pTau-E178 with duration of disease.

Based on the observation described above, an age threshold at the age of 35 years was set. Statistical analysis revealed that the median cytoplasmic / overall pTau-E178 is significantly increased above the above of 35 years in ND non-obese individuals compared to the individuals below the age of 35 years (fig. 4.21b). Although a trend for increase was also observed in obese and T2D donors, statistical analysis revealed that there was no significant difference.

Limitations Due to time limitations, this work is still preliminary in nature. Further analysis would involve; (i) analysis of the proportion of pTau positive and negative β cells in ageing, obesity and disease status (T1D,T2D), (ii) the development of strategies to investigate the expression of Tau in ICIs and IDIs from individuals with T1D, (iii) analysis of the impact of diabetes duration on the presence of cytoplasmic pTau, (iv) exploration of the relationship between insulin and cytoplasmic pTau in β cells in ageing, obesity and disease status (T1D,T2D) and (v) expand the analysis of pTau-E178 expression in the remaining islet cells that were phenotyped.

4.8 Discussion

In this chapter we provide evidence at both RNA and protein level that Tau and pTau forms are expressed in control, T1D and T2D pancreas. Expression of Tau was assessed in ductal, acinar and islets cells, with a particular focus on β cells, and in pancreatic nerves (internal positive control). Tau is highly expressed in the β cells. In

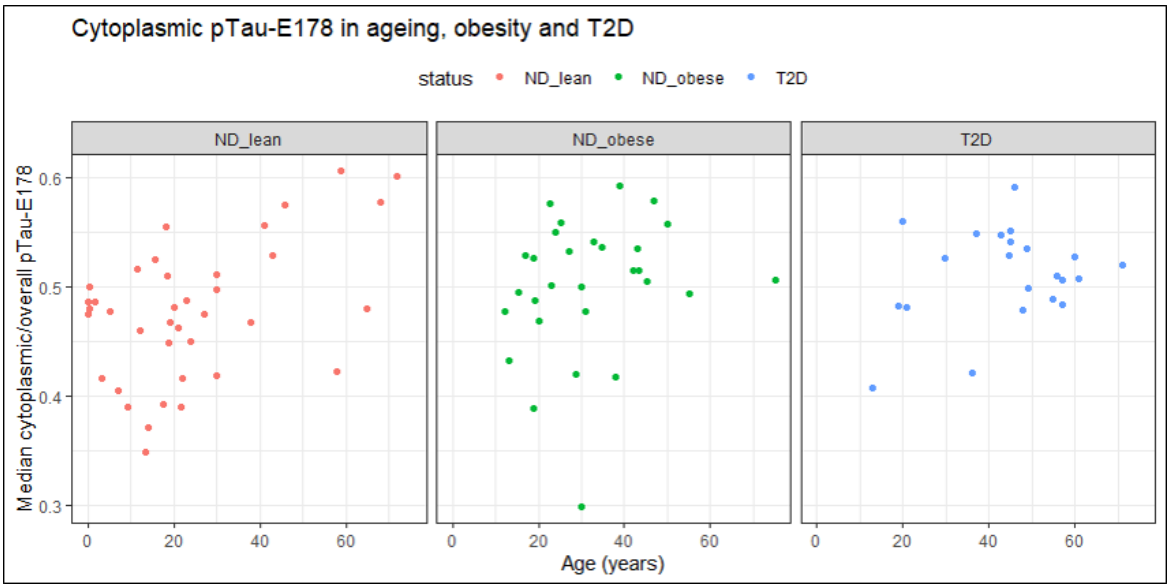

(a)

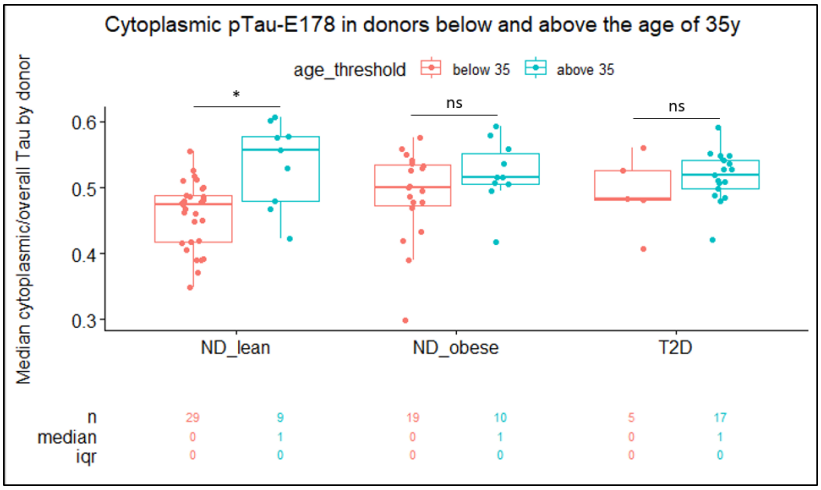

(b)

Fig. 4.21 **Cytoplasmic pTau-E178. 4.21a** | The cytoplasmic pTau-E178 in ageing, obesity and T2D plotted as the mean cytoplasmic/overall pTau ratio by donor by age (years). Each data point represents a donor. ND lean (BMI<26); orange, ND obese (BMI>26); green, T2D; blue. **4.21b** | Cytoplasmic pTau-E178 in donors below and above the age of 35 years plotted as the median cytoplasmic/overall Tau by donor. Donors below the age of 35 years; red, donors above the age of 53 years; blue.

addition, Tau is phosphorylated at multiple residues (pSer198, pSer199,pSer202/Thr205, pThr231, pSer396, pTau-E178, pSer409) and is present at high levels in the nucleus of

endocrine and acinar cells in the pancreas. Intriguingly, it is reported that total Tau antibodies do not recognise the nuclear form of pTau.

In the adult pancreas, the data suggests that two main Tau isoforms are present within β cells, a cytoplasmic Tau (1N3R) and a nuclear pTau (hyperphosphorylated) forms which could have distinct functional roles in β cells. It is most likely that nuclear pTau protects DNA during cell replication whereas cytoplasmic Tau plays an important role in insulin secretion by regulating the assembly of the microtubules. However, functional work is required to support these proposed functions of Tau in β cells.

Another interesting finding is that the phosphorylation signature of Tau differs in neurons and β cells both in health and disease. The phosphorylation signature of Tau in the adult human pancreas is described in Table 4.2. Notably, Tau is phosphorylated at Thr181 in the control and AD brain but not the pancreatic β cells. Residues Ser198, Ser199, Ser202, Thr205, Thr217, Thr231, Ser396 and Ser404 are phosphorylated both in the brain and in β cells. Residues Thr214, Thr238 and Ser422 are phosphorylated in the AD brain but not the β cells. Ser409 is phosphorylated in the AD brain and in the β cells. As such, the phosphorylation signature of Tau may be isoform- and cell-specific.

In contrast to previous studies suggesting that the PHF-raised Tau antibodies (AT8, AT100, AT180 and PHF-13) can detect Tau forms in β cells [177], these studies demonstrate that these antibodies do not detect Tau in β cells in control or in those with T2D (fig. 4.12). These antibodies have been validated carefully in Chapter 3 and only organ donor pancreas tissue was used for this study as post mortem alterations impacted staining (section 4.3). Together this supports our argument that PHF-raised anti-Tau antibodies do not stain the islets. However, this is does not mean that Tau is not hyperphosphorylated in human pancreas. Rather, we propose that the PHF-raised

Table 4.2 **Phosphorylation signature of Tau in the adult human pancreas.** Tau resides as detected by the relevant Tau antibodies and their phosphorylation status in the nucleus and the cytoplasm of β, acinar and ductal cells, as well as in pancreatic nerves. n; nucleus, c; cytoplasm

ND pancreas	T181	S198	S199	S202/T205	S214	T217	T231	S238	S262	S396	S404	S409	S422
β-cells (n)	×	✓	✓	✓	×	✓	×	×	✓	✓	×	✓	×
β-cells (c)	×	✓	✓	✓	×	✓	✓	×	✓	✓	✓	✓	×
Acinar (n)	×	✓	✓	✓	×	✓	✓	×	✓	✓	×	✓	×
Acinar (c)	×	×	×	×	×	×	×	×	×	×	×	×	×
Duct (n)	×	✓	✓	✓	×	✓	✓	×	✓	✓	×	✓	×
Duct (c)	×	×	×	×	×	×	×	×	✓	✓	×	×	×
Nerves	✓	✓	✓	✓	✓	✓	✓	×	✓	✓	✓	✓	✓

antibodies which detect a specific conformation of Tau that is present in the AD brain but may not be present in the β cells.

Interestingly, it is reported here that the localisation of pTau-E178 form in β cells is age-dependent. pTau-E178 is expressed predominately in the nucleus of β cells in young individuals and both in the nucleus and the cytoplasm of β cells in older individuals and the presence of cytoplasmic pTau-E178 in β cells is increased in the ND non-obese cohort above the age of 35 years compared to the cohort below the age of 35 years. Strikingly, it is also reported that T2D does not affect the localisation of the pTau-E178. However, even though, pTau-E178 may not be affected by T2D, it cannot be assumed that the localisation of other pTau forms are not affected by T2D. As such, further analysis is required.

To date, this is the first attempt to fully characterise the expression and localisation of Tau isoforms and pTau forms in the human pancreas and, strong emphasis was given on the expression of Tau in β cells. The analysis reveals an interesting expression pattern of Tau in the human pancreas and demonstrates that the phosphorylation signature of Tau differs from that observed in the CNS. The full characterisation and understanding of Tau expression would set a strong basis to further investigate the role of Tau in β cells potentially unravelling physiological mechanisms such as cell replication and insulin secretion.

4.8.1 Limitations

Due to time limitations, this study has focused on the expression and localisation of pTau forms but not other forms of Tau such as acetylated Tau. Recent studies suggest that phosphorylation alone does not lead to disease phenotypes and that acetylated Tau forms mimic the distribution of pTau forms in the AD brain. As such, it would also be interesting to investigate other forms of Tau, such as acetylated Tau. Moreover, it would be interesting to also characterise Tau expression in the pancreas from individuals with AD and, in the brain from individuals with T1D/T2D. However, we did not have access to such resources for the present study. An additional limitation is that there is no appropriate membrane marker for β cells in the control and the diabetes pancreas, this would have made cell identification more robust in cell based analyses.

4.8.2 Next steps

This analysis provides the basis for Tau characterisation in the human pancreas. All TLS-validated antibodies (apart from pTau-E178) were used to stain limited pancreas donor material and allowed for the initial description of Tau expression in the adult human pancreas. The findings from the pTau-E178 analysis revealed that the localisation of pTau forms may be influenced with age and by obesity and, as such, it is important to explore the expression and localisation of the different Tau isoforms and pTau forms in the human pancreas in ageing, obesity and disease. A pipeline that allows for multiplex staining analysis was initiated (Chapter 2, section 2.5). This would achieve co-staining with up to seven fluorescent markers on a single pancreas section. This analysis would allow us to expand on the characterisation of a variety of pTau forms and Tau isoforms utilising fewer tissue sections. In addition, it is important to confirm if the pancreatic nuclear Tau is a HMW Tau isoform as proposed here. It would also be beneficial to explore the function of Tau in the nucleus and in

the cytoplasm of β cells. The relationship between cytoplasmic Tau and insulin also requires further study.

Chapter 5

Tau Modifiers

5.1 Introduction

β cells and neurons share many common features in their electrophysiology, function and gene expression [263–265]. For example, both pancreatic β cells and hypothalamic neurons can sense blood glucose levels in similar ways [266]. In addition, insulin, which is being predominately produced and secreted by β cells, is also expressed in the brain during development and in adulthood [267]. β cells share more similarities in global mRNA expression to neurons than any other cell type, including pancreatic acinar cells [267]. During development, pancreatic-specific genes, such as *PDX1*, are also turned on in the human brain [268] whereas, genes being consistently expressed in β cells are enriched for neuron-like properties [269]. One of the genes that is turned on both in β cells and neurons is *MAPT* which codes for Tau protein. Tau protein was traditionally known as a neuron-specific protein but it has now been demonstrated that the Tau promoter is active in β cells and Tau RNA and protein is detected in β cells [172–175, 258, 259, 177]. The similarities in the transcriptome of β cells and neurons alongside the electrophysiology of the two cell types suggest that Tau could be dynamically and tightly regulated in both cellular systems using similar mechanisms.

Phosphorylation of Tau is considered to be the key PTM associated with disease phenotypes in the brain and therefore, is one of the most studied PTMs of Tau, enlightening mechanisms both in upstream (i.e. kinases and phosphatases) and downstream targets (i.e. microtubules) as well as the function of Tau. The interaction between Tau and microtubules relies highly on the phosphorylation of Tau and is very dynamic [270–272]. Phosphorylation of Tau decreases its affinity for the microtubules making the microtubules unstable. Then, minimally phosphorylated Tau associates again with the microtubules to stabilise them. A recent study proposes that the microtubule stability in β cells is heterogenous and that the hyper-stabilization and depolymerization of the microtubules dynamically regulates β cell capacity for glucose stimulated insulin secretion [182], with highly stable microtubules suppressing the glucose stimulated insulin secretion. Phosphorylation of Tau is considered to be the key PTM associated with disease phenotypes in the brain and the disruption of the kinase:phosphatase equilibrium has been in the spotlight for several decades.

However, more and more evidence suggests that excess phosphorylation alone is not adequate to lead to Tau aggregation [273]. It is proposed that competition between PTMs alongside Tau fragmentation and truncation events may also contribute to disease pathogenesis by differentially regulating Tau function and aggregation in neurons [273]. Supporting this observation, recent studies show that the distribution of acetylated Tau (acetylTau) forms resembles that of pTau forms in AD brains and, certain acetylTau forms have been associated with AD pathology in patient brains even at early Braak stages [274]. Adding to the complexity, it is now known that Tau has intrinsic acetyltransferase activity [120] which is coupled to auto-proteolytic Tau fragmentation [275]. However, whether the Tau pathogenesis is due to its intrinsic deregulation, the disruption of Tau modifier equilibrium or both, remains unknown.

The aim of the previous chapter was to characterise the PTM signature of Tau in the human pancreas and in more detail in β cells. In this chapter, the expression of Tau modifiers in the human pancreas and more specifically in the pancreatic β cells is explored. It has been proposed that Tau PTMs are region-dependent and disease-specific and therefore this chapter aims to begin to identify the major Tau modifiers that may play a role in β cells under different circumstances (e.g. age, disease state). This is achieved by characterising their RNA and protein expression levels and their physiological subcellular localisation within the islet cells.

Objectives

Tau modifiers have not been previously studied in the human pancreas in the context of diabetes and the fact that Tau is a heavily post-translationally modified protein, makes it time-consuming to try to characterise the expression of all brain-related Tau modifiers in the human pancreas. As such, we developed a workflow to help narrow down the physiological Tau modifiers and to identify which may play an important role in the human pancreas (fig. 5.1, Table 5.1). First, we identified the key Tau modifiers in the brain. Based on the published literature and the TauPTM webpage (https://abbvie1.outsystemsenterprise.com/tauptm/, [233]), a panel of Tau modifiers involved in phosphorylation, acetylation and proteolytic cleavage as discussed in the introduction was constructed (Chapter 1, pg. 1). Then, for each modifier, the relevant Tau residues being targeted was identified (Table 5.1).

To explore if the identified Tau modifiers are expressed in the human pancreas and potentially play a role in β cells, three RNAseq databases; (i) Next Generation RNASeq bulk β cell data from individuals diagnosed with (n=4) and without T1D (n=12) [239], (ii) Next Generation RNASeq data from adult (n=7) and foetal (n=6) β cells and adult (n=6) and foetal (n=5) α cells [240] and, (iii) Next Generation

Table 5.1 **Tau modifiers and relevant Tau residues.** This table is a list of Tau modifiers and contains information about the name of each protein (abbreviation and full name), the gene and the Tau residues that they modify based on the published literature. The proteins have been categorised based on the type of modification and are listed alphabetically.

Protein	Full name	Gene	Modification	Tau site
CBP	CREB-binding protein	CREBBP	acetylation	K280, K281
HDAC6	Histone deacetylase 6	HDAC6	deacetylation	K259, K280, K281, K290, K321, K353
p300	Histone acetyltransferase p300	EP300	acetylation	K174, K259, K290, K321, K353
SIRT1	Sirtuin 1	SIRT1	deacetylation	K174
Abl	Tyrosine-protein kinase ABL1	ABL1	phosphorylation	Y394
Arg	Tyrosine-protein kinase ABL2	ABL2	phosphorylation	Y394
CAMK	Calcium/calmodulin-dependent protein kinase	CAMK4	phosphorylation	T231
CDC2	cell division cycle protein 2	CDK1	phosphorylation	T153
CDK5	Cyclin dependent kinase 5	CDK5	phosphorylation	T181, S199, S202, T205, T212, T231, S235, S396, S404
CK1	Casein kinase 1	CSNK1	phosphorylation	T17, S46, S113, S184, S202, S205, S238, T263, S396, S404
CK2	Casein kinase 2	CSNK2	phosphorylation	T39, S199, S400
DYRK1A	Dual specificity tyrosine-phosphorylation-regulated kinase 1A	DYRK1A	phosphorylation	T181, T212, T231
Fyn	Tyrosine-protein kinase Fyn	FYN	phosphorylation	Y18
GSK3b	Glycogen Synthase Kinase 3 Beta	GSK3b	phosphorylation	S46, T69, T175, T181, S184, S198, S199, S202, T205, S208, S210, T212, S214, T217, T231, S235, S262, S356, S396, S400, S404, S409, S413
MARK	MAP/microtubule affinity-regulating kinase 4	MARK4	phosphorylation	S262, S356
p70S6K	Ribosomal protein S6 kinase beta-1	RPS6KB1	phosphorylation	S214
PhK	Phosphorylase kinase	PhK	phosphorylation	S237, S262
PIN1	Peptidylprolyl Cis/Trans Isomerase, NIMA-Interacting 1	PIN1	dephosphorylation	T231
PKA	Protein kinase A	PRKACA	phosphorylation	S198, S199, S202, T205, S210, T212, S214, T217, T231, S235, S262, S356, S396, S409, S412
PKC	Protein kinase C	PRKC	phosphorylation	S262
PP2A	Protein phosphatase 2	PPP2CA	dephosphorylation	S198, S199, S202, T217, S396, S404
PP5	Serine/threonine-protein phosphatase 5	PPP5C	phosphorylation	S198, S199, S202
PSK	Protein-bound polysaccharide-K	TAOK2	phosphorylation	S184, S185, S191, S198, T205, T212, S214, T231, S238, S258, S262, S289, S400, T403, S409, S412, T414, T427, S433
SAPK1	Stress-activated protein kinase 1	MAPK8	phosphorylation	S202
SAPK4	Stress-activated protein kinase 4	MAPK13	phosphorylation	T50
SGK1	Serine/threonine-protein kinase 1	SGK1	phosphorylation	S214
SIK	Serine/threonine-protein kinase	SIK1	phosphorylation	S262
Syk	Tyrosine-protein kinase	SYK	phosphorylation	Y18
TTBK1	Tau-tubulin kinase 1	TTBK1	phosphorylation	Y197, S199, S202, S422, T427
AEP	Asparagine endopeptidase	AEP	proteolytic cleavage	N255, N368
Caspase-1	Caspase-1	CASP1	proteolytic cleavage	D421
Caspase-2	Caspase-2	CASP2	proteolytic cleavage	D314
Caspase-3	Caspase-3	CASP3	proteolytic cleavage	D421
Caspase-6	Caspase-6	CASP6	proteolytic cleavage	D13, D421
Caspase-7	Caspase-7	CASP7	proteolytic cleavage	D421
Caspase-8	Caspase-8	CASP8	proteolytic cleavage	D421
SET	SET Nuclear Proto-Oncogene	SET	inhibitor of dephosphatase	N/A

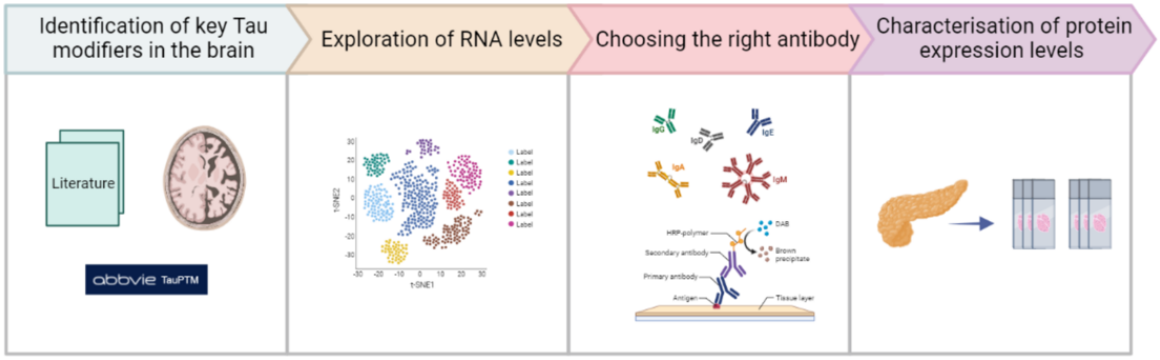

Fig. 5.1 **Pipeline schematic to illustrate the process of characterising Tau modifiers in the human pancreas.** This 4-step workflow summarises the methodology used to identify and characterise Tau modifiers that could potentially play a role in Tau regulation in β cells; (i) Identification of physiological Tau modifiers in the brain, both in health and disease, based on published literature and the TauPTM website (https://abbvie1.outsystemsenterprise.com/tauptm/). (ii) Exploration of the RNA levels of the modifiers identified utilising RNAseq databases; RNAseq bulk β cell data (12 ND and 4 T1D) [239], adult and foetal β and α cells [240] and, ND and T2D (https://sandberglab.se/tool/pancreas/, [175]). (iii) consideration of appropriate antibodies directed against Tau modifiers for immunostaining. (iv) Characterisation of protein expression levels in the human pancreas in health, disease and ageing. Created in Biorender (https://biorender.com/).

RNASeq data from individuals diagnosed with (n=4) and without T2D (n=6) (https://sandberglab.se/tool/pancreas/, [175]) were explored. Utilising these datasets, the RNA expression of the modifiers expressed in the pancreas are described in health and disease (T1D/T2D) and, in foetal and adult β and α cells. The RNASeq data used was normalised in different ways and therefore the gene expression levels between these datasets are not directly comparable but can give an indication of relative levels of expression.

Statistical analyses were performed to assess whether there were significant differences between two groups (e.g. cell type, disease status). t-tests were used followed by a Bonferroni correction to adjust probability (p) values because of the increased risk of a type I error (false positive). The corrected p values were used to determine if there was a significant difference. This is important because all RNAseq datasets described

above consist of a limited amount of cells and/or donors, and multiple different target transcripts were assessed. However, where appropriate, a description of trend for increase or decrease will be provided.

For the Tau modifiers identified utilising the above resources, relevant antibodies were acquired (Chapter 2, section 2.1.2, fig. 2.2). Standard HRP staining was performed to optimise the staining conditions (Chapter 2, section 2.4.1). The HRP immunostaining results were then compared to what was reported in the Human Protein Atlas (HPA; https://www.proteinatlas.org/). Following the antibody optimisation and the assessment of the staining results, IF staining was performed to determine the cellular localisation of each modifier within the pancreas (i.e. nerves, ductal cells) and more specifically within the islets (Chapter 2, section 2.4.2).

It is important to highlight that due to time limitations and COVID restrictions impacting on lab accessibility, we present preliminary work that sets the basis to expand the analysis to more donors. It is important to highlight that the observations made here are based on pancreas tissue sections of one non-obese adult ND and one adult T1D donor and the conclusions will require further verification in additional donors. As such, firm conclusions about the expression of Tau modifiers in the human pancreas cannot be made and further work in additional donors is required.

5.2 RNA expression of Tau modifiers

5.2.1 Tau kinases

According to the published literature and the TauPTM webpage (https://abbvie1.outsystemsenterprise.com/tauptm/, [233]), there are at least 38 Tau kinases in the human brain. To investigate which of these kinases are present in the human pancreas, their gene expression was studied in the β cells of those diagnosed with (n=4) or without

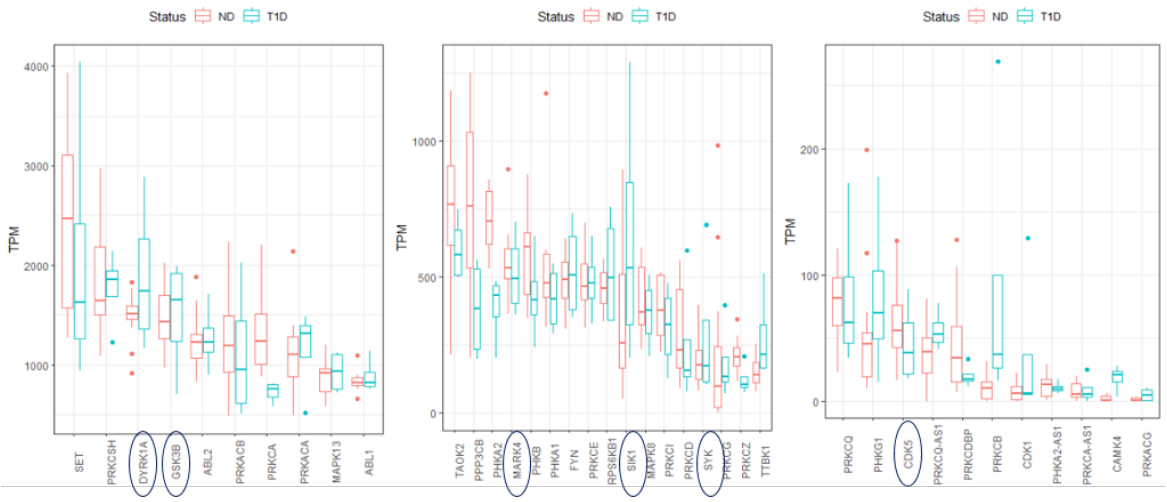

Fig. 5.2 **Gene expression levels of Tau kinases in the β cells of those diagnosed with and without type 1 diabetes.** Boxplots showing the gene expression of 38 Tau kinases in 12 ND and 4 T1D donors with x axis containing the gene name of the kinases and the y axis the transcript per million (TPMs). TPMs for every 1,000,000 RNA molecules in the RNA-seq samples. Kinases have been plotted in descending order based on TPM value. Three panels of box plots with three different y axis scales (high to low gene expression). Statistical analysis using the t-test showed no significant difference between ND and T1D (full stats table A.7, pg. 252). Modifiers marked with a dark blue oval have been selected for further analysis.

(n=12) T1D (fig. 5.2) [239]. The expression level varies between the 38 Tau kinases studied. The following genes were expressed in high levels (*SET*, *PRKCSH*, *DYRK1A*, *GSK3-β*, *ABL2*, *PRKACB*, *PRKCA*, *PRKACA*, *MAPK13*, *ABL1*), moderate levels (*TAOK2*, *PPP3CB*, *PHKA2*, *MARK4*, *PHKB*, *PHKA1*, *FYN*, *PRKCE*, *RPS6KB1*, *SIK1*, *MAPK8*, *PRKCI*, *PRKCD*, *SYK*, *PRKCG*, *PRKCZ*, *TTBK1*) and, low levels (*PRKCQ*, *PHKG1*, *CDK5*, *PRKCQ-AS1*, *PRKCDBP*, *PRKCB*, *CDK1*, *PHKA2-ASI1*, *PRKCA-AS1*, *CAMK4*, *PRKACG*) (fig. **??**). Statistical analysis (t-test) followed by Bonferroni correction demonstrated that there was no significant difference between ND and T1D pancreas (full stats table A.7, pg. 252). However, it is important to note that (i) RNA expression of particular proteins may vary between individuals and the limited number of donors (12 ND and 4 T1D) does not allow for firm conclusions and

that (ii) the RNA expression level does not necessarily reflect the protein activity but it is rather indicative of the transcription rhythm of the relevant gene.

Key Tau kinases associated to neurodegeneration and/or previous evidence of dysregulated expression in diabetes or aging in human β cells were selected for a more in depth analysis. The final Tau kinases panel was narrowed down to six; CDK5, GSK3-β, MARK4, DYRK1A, SIK1 and SYK (figs. 5.3, 5.4). SIK1 and CDK5 are involved in insulin secretion and CDK5 is activated by high glucose [276–278]. Inhibition of GSK3-β or DYRK1A induces human β cell proliferation [279]. Inactivation of MARK4 leads to insulin hypersensitivity and resistance to diet-induced obesity [280].

The expression level of these Tau kinases varied and statistical analysis (t-test) demonstrated that there was no significant difference between ND and T1D (full stats table in Appendix A, Table A.7). Therefore, careful consideration was given to the gene expression levels that showed a tendency to increase or decrease.

The expression of Tau kinases was examined in foetal and adult β cells as well as foetal and adult α cells. No significant difference was demonstrated between foetal and adult β cells and between foetal and adult α cells (Appendix A, stats Table A.8, A.9). However, DYRK1A demonstrated a tendency to increase in the adult compared to foetal β cells (fig. 5.3b), MARK4, SIK1 and SYK showed a tendency to decrease (fig. 5.4a, 5.4b, 5.4c), whereas the expression level of CDK5 and GSK3-β remained unaltered (figs. 5.3a, 5.3c). These observations demonstrated that select Tau kinases are present at higher levels in foetal islet cells, whereas others are present at higher RNA levels in adult islet cells, suggesting that the transcriptome of the islet cells is altered during development. Also, the data suggest that these genes behave differently in β and α cells during ageing implying that their expression may be cell-specific.

Interestingly, some key Tau kinases (CDK5, GSK3-β, MARK4), as well as SYK showed a tendency to decrease in the β cells in T1D compared to that of ND pancreas.

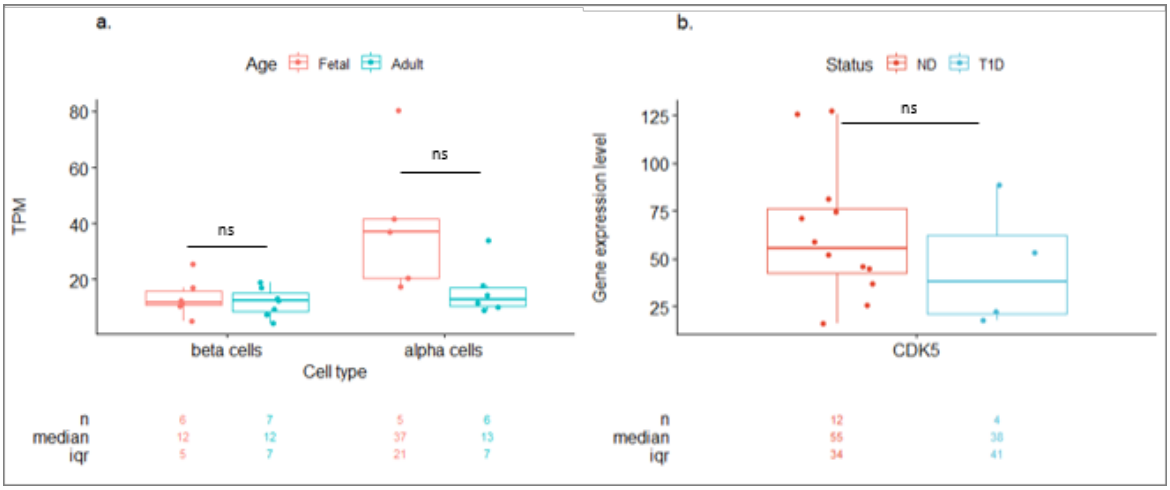

(a) CDK5

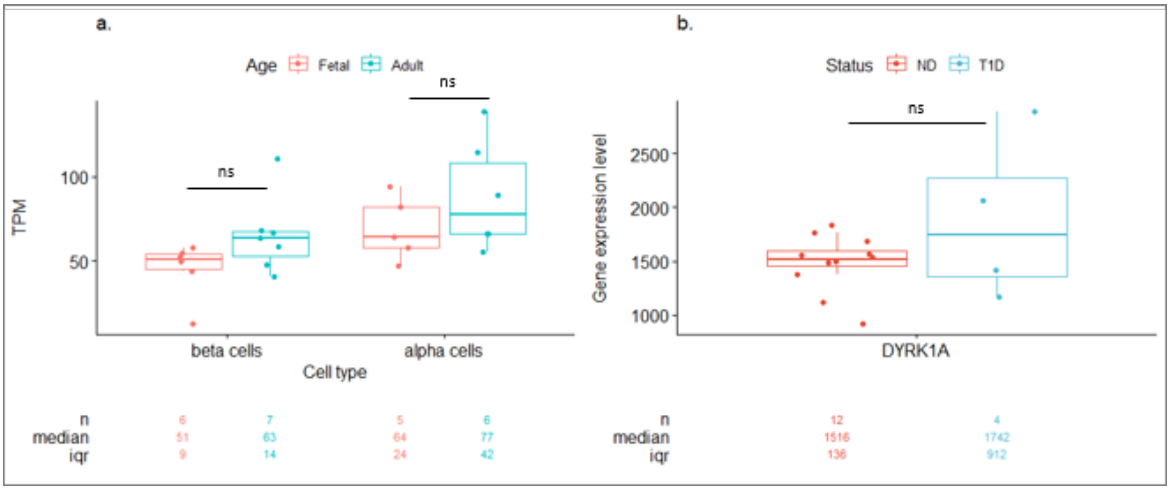

(b) DYRK1A

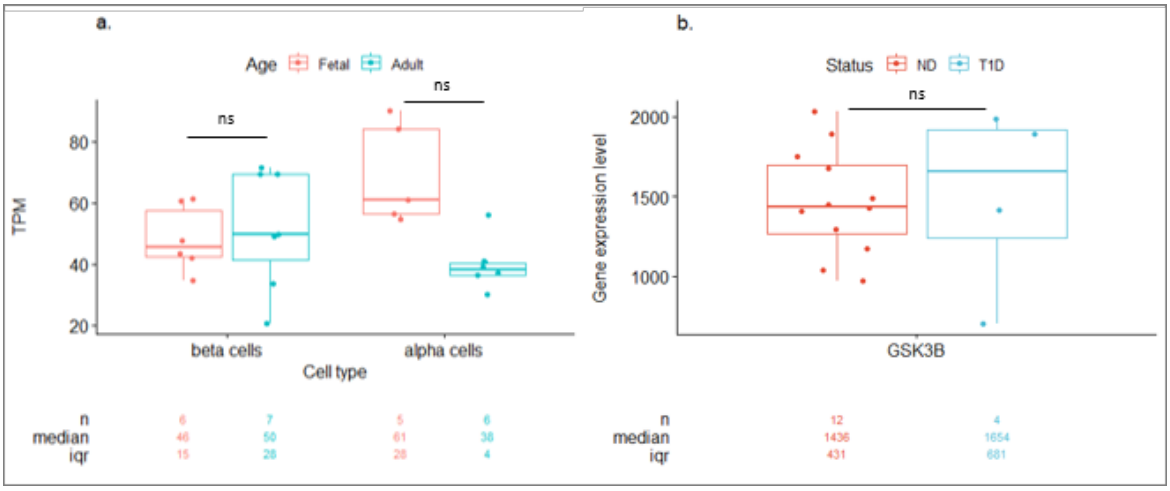

(c) GSK3-β

Fig. 5.3 **Gene expression levels of Tau kinases in foetal and adult β and α cells and in β cells of those diagnosed with and without type 1 diabetes.** Boxplots showing the gene expression of Tau kinases; 5.3a | CDK5, 5.3b | DYRK1A, 5.3c | GSK3-β. Tau kinases expression from foetal and adult β and α cells (RNAseq data from [240], left hand side plot) and in β cells of those diagnosed with and without T1D (RNAseq data from [239], right hand side plot). RNAseq data have been normalised in different ways and therefore, the gene expression levels between the two datasets are not directly comparable but give an indication of relative levels of expression. Statistical analysis using the t-test showed no significant difference in all cases (full stats tables A.7, A.9 pg. 252, 254).

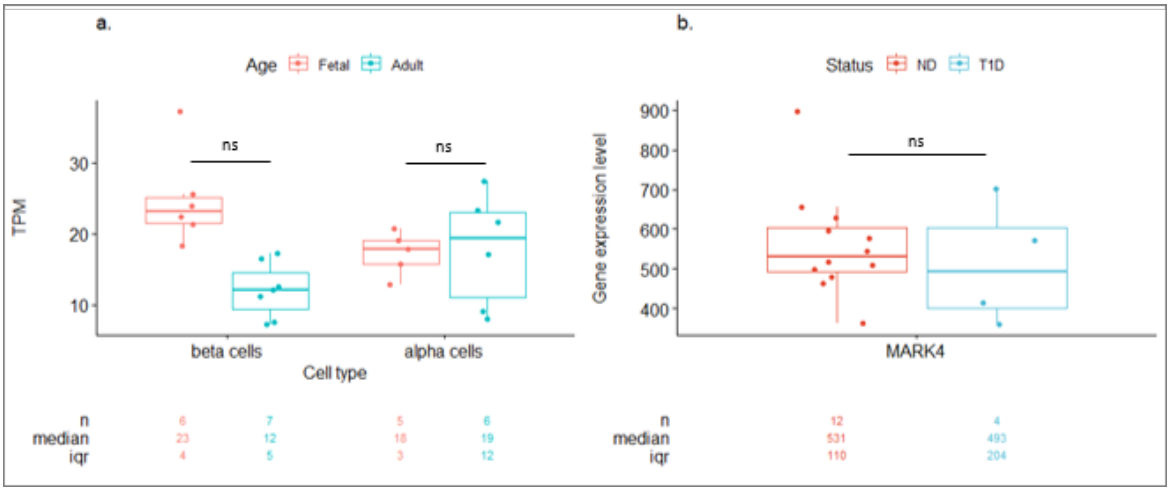

(a) MARK4

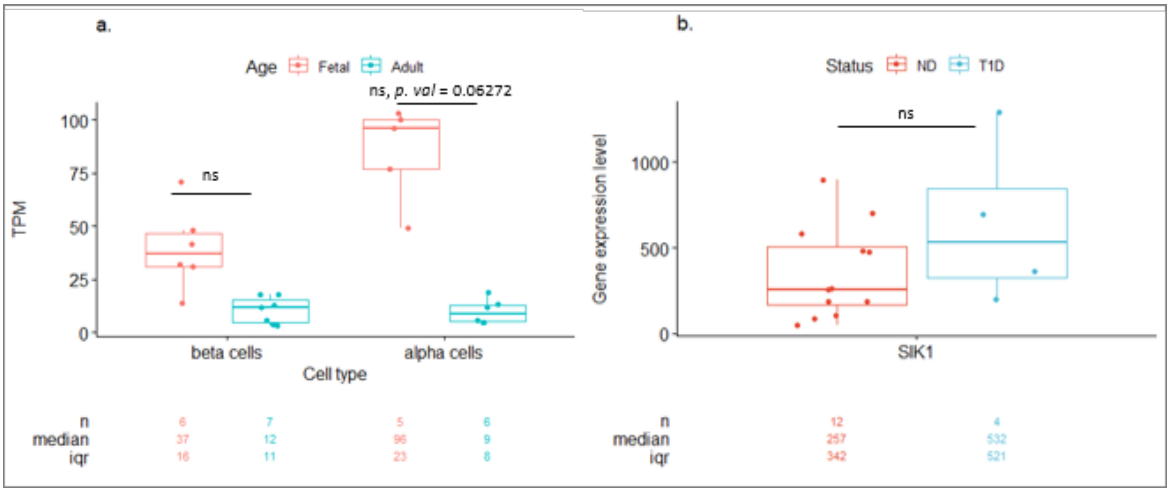

(b) SIK1

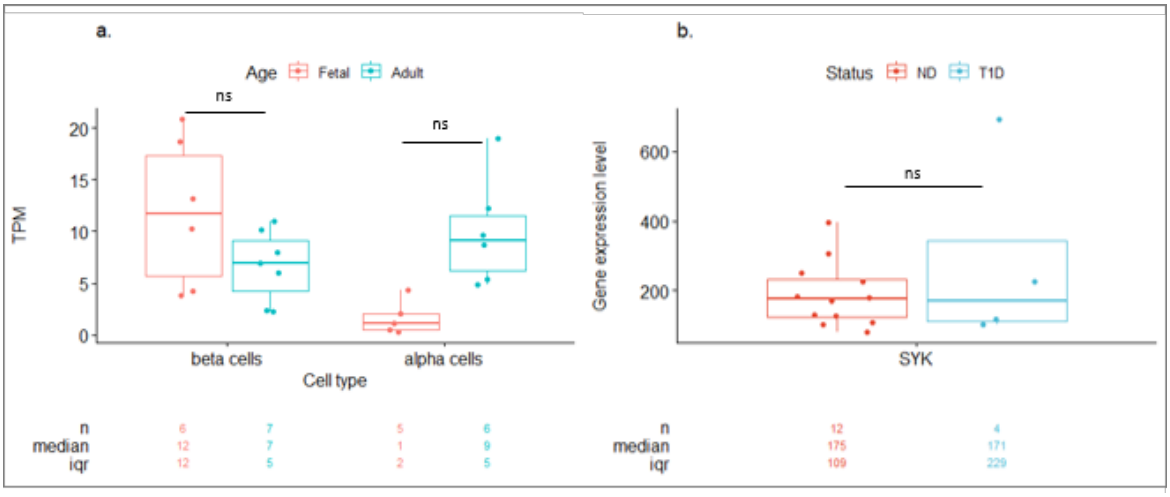

(c) SYK

Fig. 5.4 **Gene expression levels of Tau kinases in foetal and adult β and α cells and in β cells of those diagnosed with and without type 1 diabetes.** Boxplots showing the gene expression of Tau kinases; 5.4a | MARK4, 5.4b | SIK1 and 5.4c | SYK. Tau kinases expression from foetal and adult β and α cells (RNAseq data from [240], left hand side plot) and in β cells of those diagnosed with and without T1D (RNAseq data from [239], right hand side plot). RNAseq data have been normalised in different ways and therefore, the gene expression levels between the two datasets are not directly comparable but give an indication of relative levels of expression. Statistical analysis using the t-test showed no significant difference in all cases (full stats tables A.7, A.9 pg. 252, 254).

Only two kinases (DYRK1A, SIK1) demonstrated a tendency to increase in the β cells in T1D compared to that of ND pancreas.

Two of the Tau kinases (that were not included in the kinases panel), Protein Kinase C α (PKCα) and Protein Kinase C ϵ (PKCϵ) encoded by the PRKCA and PRKCE genes, respectively, showed no significant difference between ND and T1D (Table A.6). However, interestingly, PKCα and PKCϵ demonstrated a significant increase in gene expression level in adult β cells when compared to foetal β cells (fig. A.5, Table A.8, pg. 253). Due to time and COVID limitations, PKCα and PKCϵ were not included in the analysis and further analysis may be beneficial.

5.2.2 Tau phosphatases

In comparison to the Tau kinases, Tau phosphatases are fewer in number. Two Tau phosphatases (PP2A and PP5) expressed in the human brain were identified in pancreas (Table 5.1, fig. 5.5). PP2A is the major Tau phosphatase and therefore, SET, an inhibitor of PP2A, was also included in the panel (fig. 5.5c). Elevated expression or activity of SET would block PP2A resulting in elevated phosphorylation levels of Tau and a reduction in SET expression or activity would result in reduced phosphorylation of Tau. No significant difference was demonstrated in the gene expression levels of Tau phosphatases between foetal and adult islet cells or between ND and T1D β cells (Appendix A, Tables A.7-A.9). However, it is worth to mention that all Tau phosphatases (PP2A and PP5), showed a tendency to decrease in the β cells in T1D compared to ND pancreas (fig. 5.5a, 5.5b). SET also showed a tendency to decreased in T1D compared to ND pancreas (fig. 5.5c). Interestingly, the expression level of these phosphatases remained approximately the same between adult and foetal β cells and between adult and foetal α cells (fig. 5.5). These observations suggest that

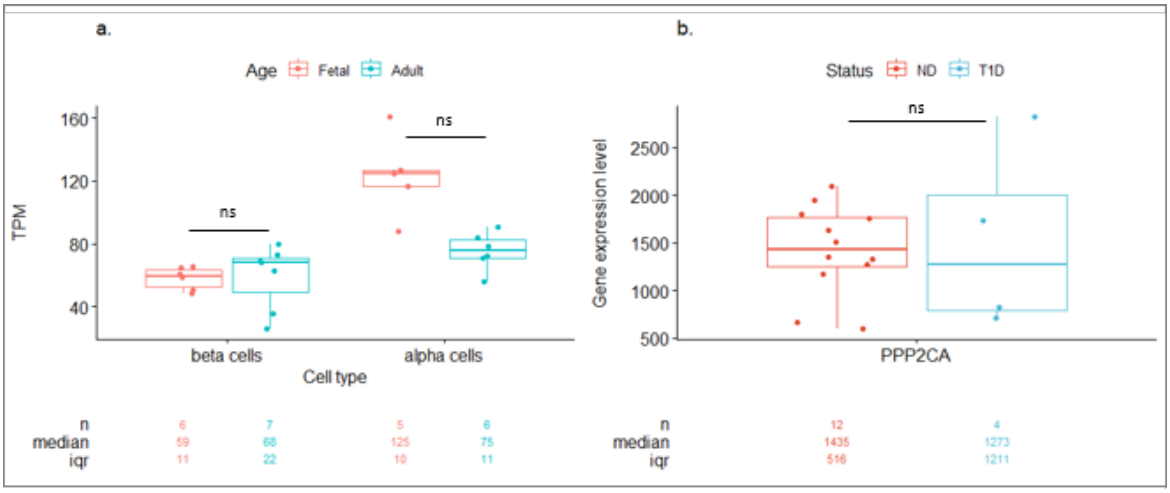

(a) PPP2CA

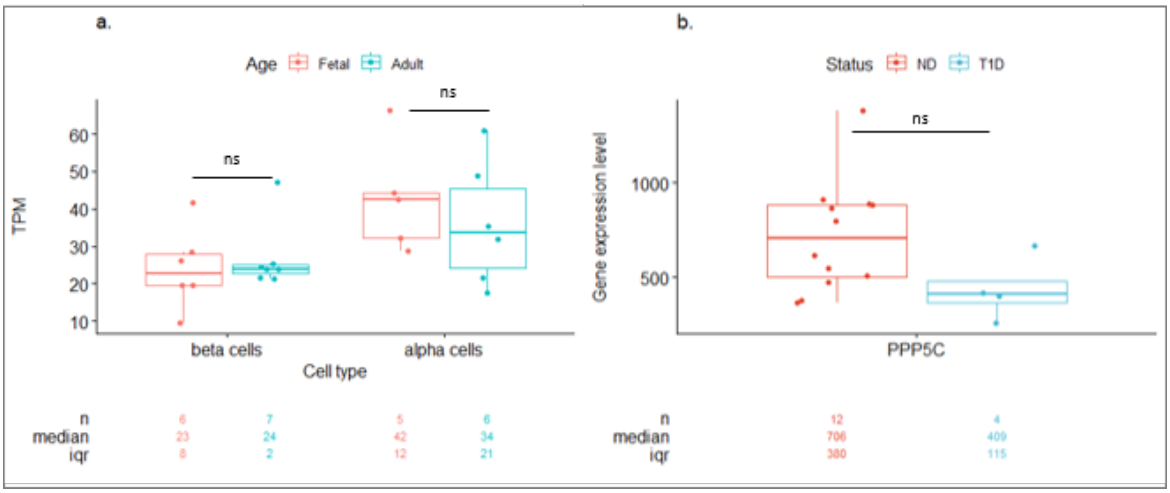

(b) PPP5C

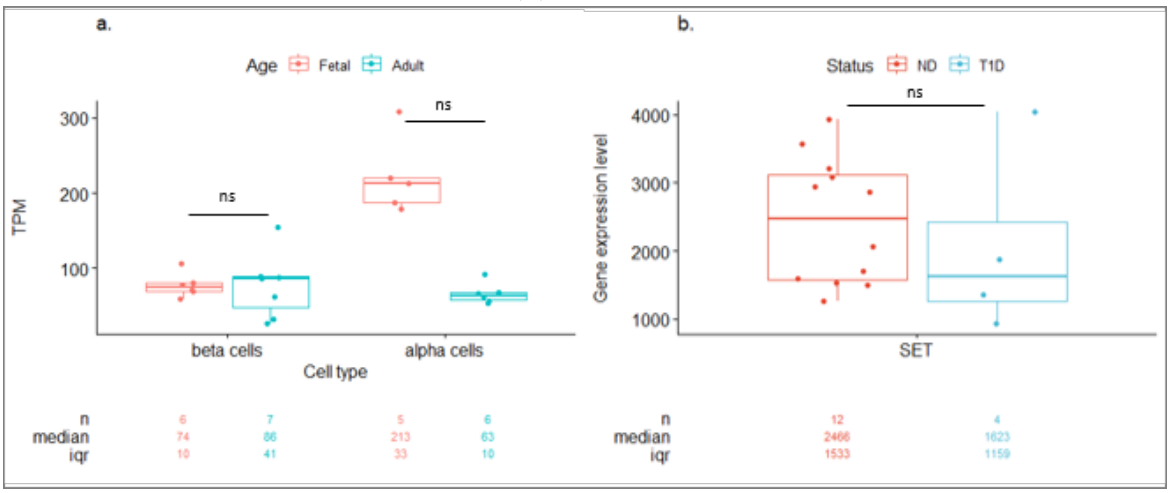

(c) SET*

Fig. 5.5 **Gene expression levels of Tau phosphatases in foetal and adult β and α cells and in β cells of those diagnosed with and without type 1 diabetes.** Boxplots showing the gene expression of Tau phosphatases; 5.5a | *PPP2CA* gene which codes for PP2A, 5.5b | *PPP5C* gene which codes for PP5 and 5.5c | SET - SET is not a Tau phosphatase but rather a PP2A phosphatase inhibitor. Tau phosphatases expression from foetal and adult β and α cells (RNAseq data from [240], left hand side plot) and in β cells of those diagnosed with and without T1D (RNAseq data from [239], right hand side plot). RNAseq data have been normalised in different ways and therefore, the gene expression levels between the two datasets are not directly comparable but give an indication of relative levels of expression.

Tau phosphatases may be important for β cells throughout development and may be impacted in disease states.

5.2.3 Tau deacetylases

Tau acetylation regulates normal Tau function and has also been linked with pathological conditions, such as AD [118, 274]. The Tau deacetylases SIRT1 and HDAC6 have been identified as important mediators of Tau acetylation (fig. 5.6a, 5.6b) [281, 282]. SIRT1 deacetylases Tau reducing pathogenic spread in a mouse model brain [281]. HDAC6 suppresses the accumulation of Tau, potentially protecting against the progression of AD [283]. No significant difference was demonstrated in the gene expression of SIRT1 and HDAC6 between foetal and adult islet cells or between ND and T1D β cells (Appendix A, Tables A.7-A.9). However, both HDAC6 and SIRT1 showed a tendency to decrease in the T1D β cells compared to ND β cells (figs 5.6a, 5.6b). Decreased level of deacetylases would result in elevated levels of Tau acetylation. Although some acetylation events are protection against hyperphosphorylation and self-aggregation, highly acetylated Tau forms have been associated with AD pathology [274, 284].

5.2.4 Tau caspases

The proteolytic cleavage of Tau has been linked with the physiological degradation of Tau while specific forms of truncated Tau forms, such as Tau truncated at Asp421, have been associated with AD (Table 5.1). Two caspases, Caspase-1 and -8, that cleave Tau at Asp421 were identified in the pancreas at low levels (fig. 5.7a, 5.7b). No significant difference was demonstrated in the gene expression levels of Tau caspases between foetal and adult β and α cells or ND and T1D β cells (Appendix A, Tables A.7-A.9). It is important to note that caspases have to be cleaved themselves prior to activation. Therefore, presence alone is not an indicator of activity.

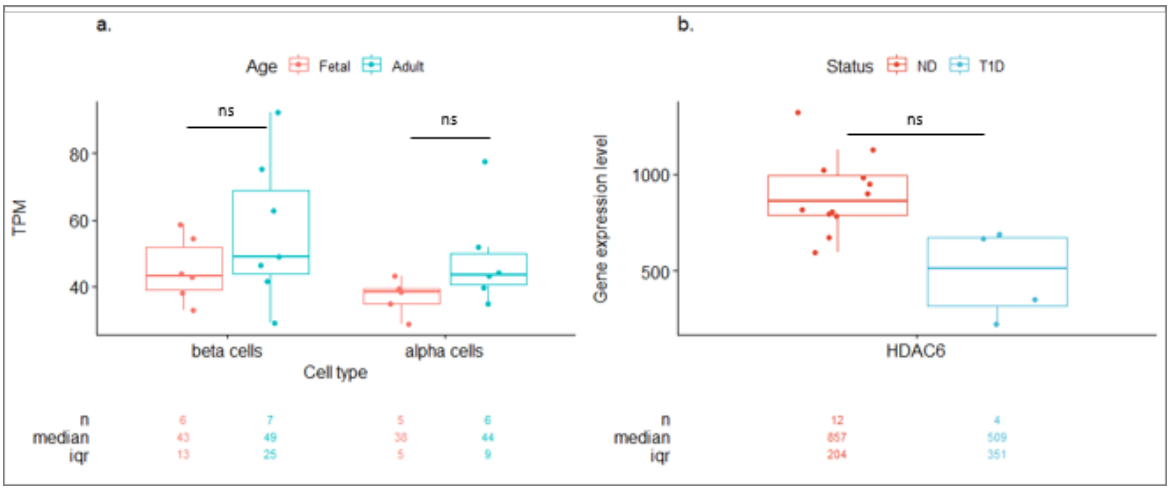

(a) HDAC6

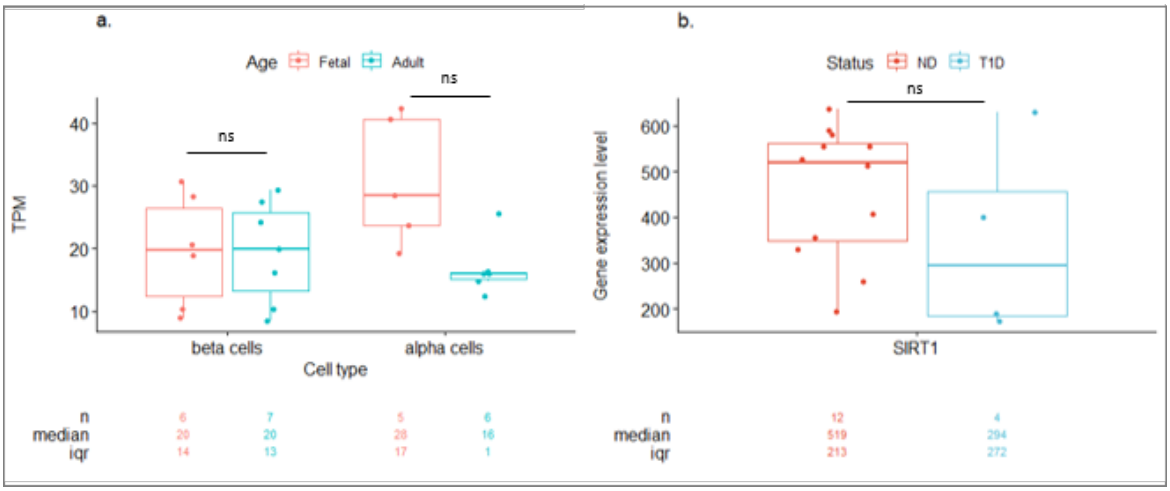

(b) SIRT1

Fig. 5.6 **Gene expression levels of Tau modifiers (acetylases, deacetylases, caspases) in foetal and adult β and α cells and in β cells of those diagnosed with and without type 1 diabetes.** Boxplots showing the gene expression of Tau deacetylases; **??** | HDAC6 and 5.5a | SIRT1. Tau modifiers expression from foetal and adult β and α cells (RNAseq data from [240], left hand side plot) and in β cells of those diagnosed with and without T1D (RNAseq data from [239], right hand side plot). RNAseq data have been normalised in different ways and therefore, the gene expression levels between the two datasets are not directly comparable but give an indication of relative levels of expression. Statistical analysis using the t-test showed no significant difference in all cases (full stats tables A.7, A.9 pg. 252, 254).

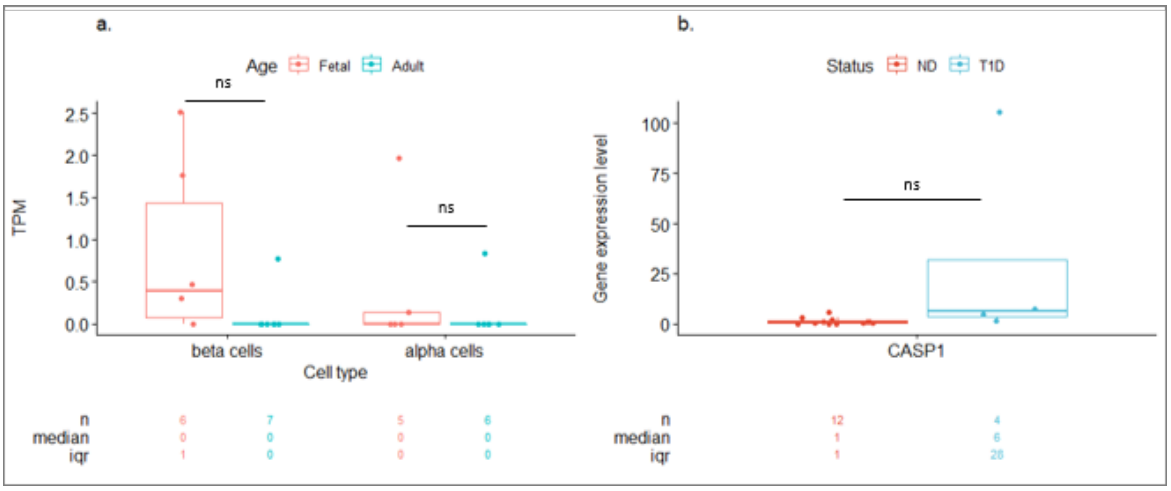

(a) Caspase-1

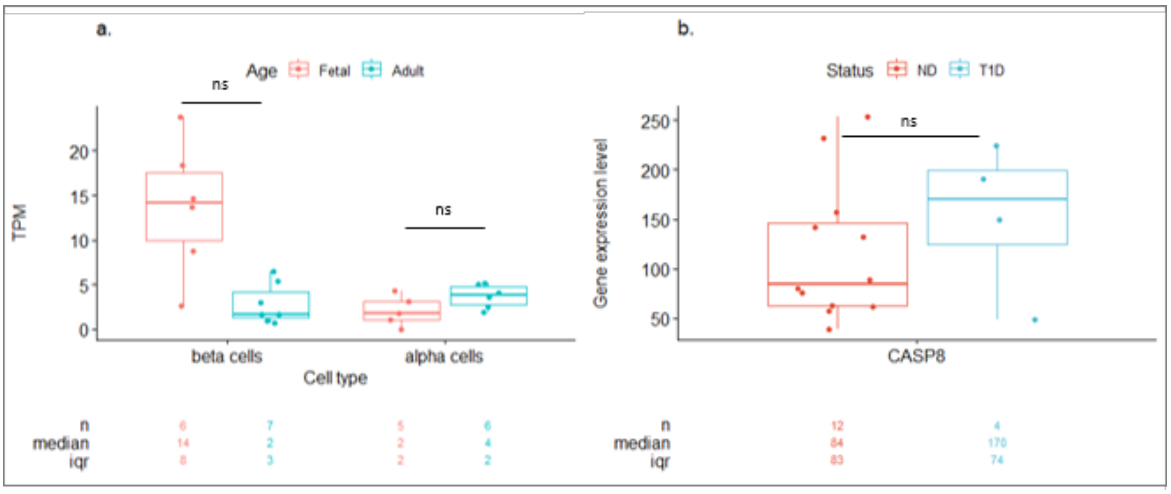

(b) Caspase-8

Fig. 5.7 **Gene expression levels of Tau modifiers (acetylases, deacetylases, caspases) in foetal and adult β and α cells and in β cells of those diagnosed with and without type 1 diabetes.** Boxplots showing the gene expression of Tau caspases; 5.5b | Caspase-1 and 5.5c | Caspase-8. Tau modifiers expression from foetal and adult β and α cells (RNAseq data from [240], left hand side plot) and in β cells of those diagnosed with and without T1D (RNAseq data from [239], right hand side plot). RNAseq data have been normalised in different ways and therefore, the gene expression levels between the two datasets are not directly comparable but give an indication of relative levels of expression. Statistical analysis using the t-test showed no significant difference in all cases (full stats tables A.7, A.9 pg. 252, 254).

5.3 Protein expression of Tau modifiers

The RNAseq data worked as a guide for further analysis of the following kinases (GSK3β, CDK5, DYRK1A), phosphatase (PP2A) and its inhibitor (SET) and deacetylase

(HDAC6). As such, the next step was to decide on appropriate antibodies against Tau modifiers for immunostaining to verify the protein expression of selected Tau modifiers in the human pancreas. The antibodies were selected using the criteria outlined in Chapter 2 (fig. 2.1.2) and optimised using standard HRP staining (Chapter 2, section 2.4.1). Due to time and COVID limitations impacting on lab accessibility, here we present preliminary data on the protein expression of Tau kinases, phosphatases and deacetylase in the human pancreas. Most antibodies have been used to stain a single ND (n=1) or T1D (n=1) pancreas and, as such, firm conclusions about the expression of these Tau modifiers cannot be made. In total, 11 antibodies in total were tested against Tau kinases (n=7), Tau phosphatases (n=3) and Tau deacetylases (n=1) (Table 2.2, pg. 44).

5.3.1 Tau kinases

In total, seven antibodies against Tau kinases, detecting GSK3-β (n=3), CDK5 (n=2), MARK4 (n=1) and DYRK1A (n=1) were tested in human pancreas (Chapter 2, Table 2.2). A brief summary of each Tau kinase expression profile as described in the HPA is provided and this is followed by a description of the immunostaining observed in the EADB human pancreas tissue.

5.3.1.1 GSK3-β

GSK3-β is a multikinase involved in many pathways and it would be expected to be detected in the cytoplasm of a range of different cell types. According to HPA, the protein expression of GSK3-β is low in the endocrine and exocrine pancreas tissue and is predominantly present in the cytoplasm of islet cells and within the intrapancreatic nerves. Three anti-GSK3-β antibodies were tested on serial sections of human pancreas; two antibodies detect the active (dephosphorylated) GSK3-β form

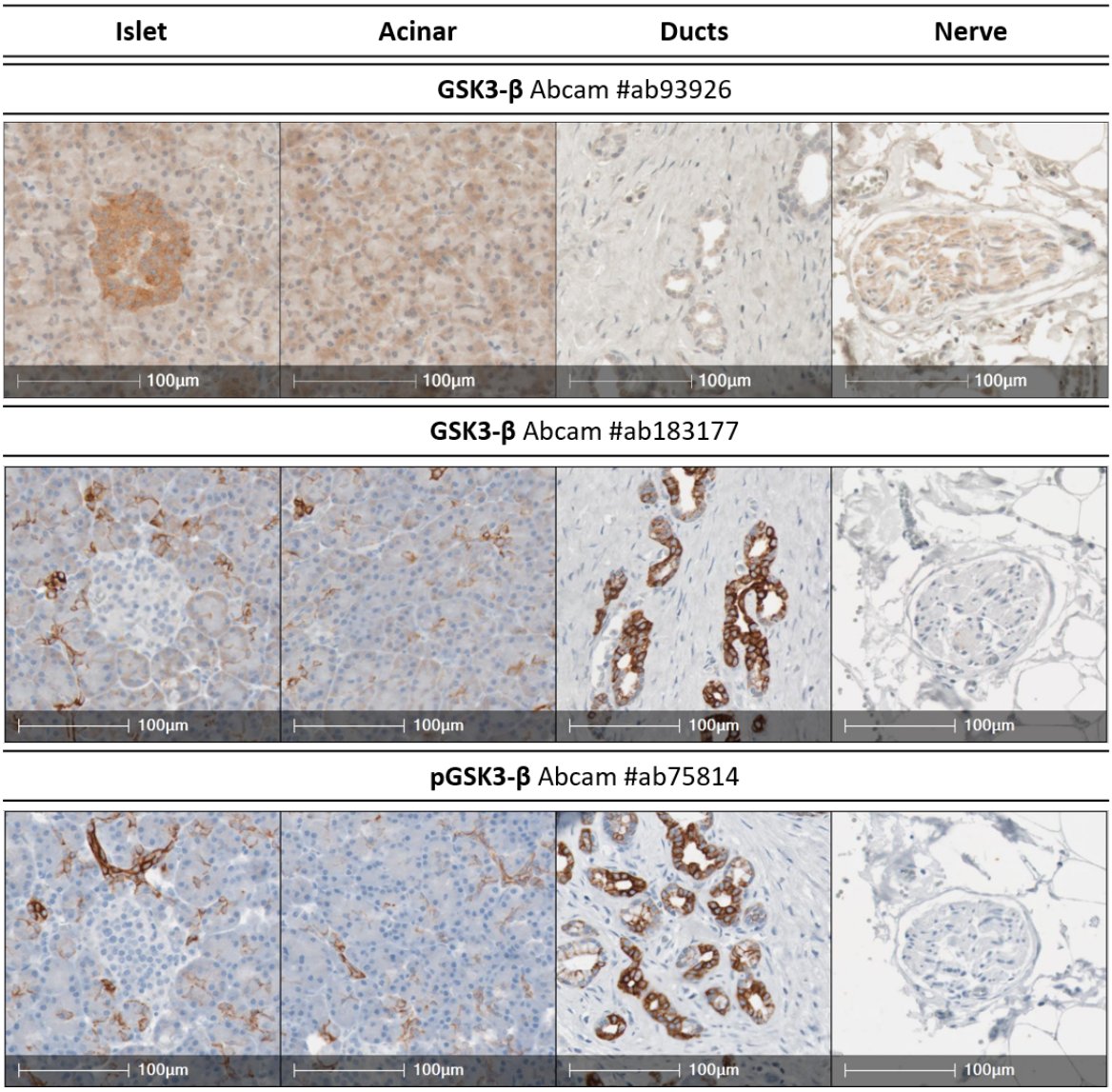

Fig. 5.8 **Anti-GSK3-β antibody profiles in the human pancreas.** Representative HRP micrographs demonstrating the presence and localisation of GSK3-β forms in the pancreas of an organ donor. Whole slide scans were imaged at X40. Scale bars 50μm or 100μm.

(#ab93926, #ab183177) and one detects the inactive (phosphorylated) pGSK3-β form (#ab75814) (fig. 5.8). Anti-GSK3-β #ab93926, detecting the active form, stained the cytoplasm of a subset of islets. However, unexpectedly, anti-GSK3-β #ab183177 and anti-pGSK3-β #ab75814 presented similar immunoreactive pattern to one another,

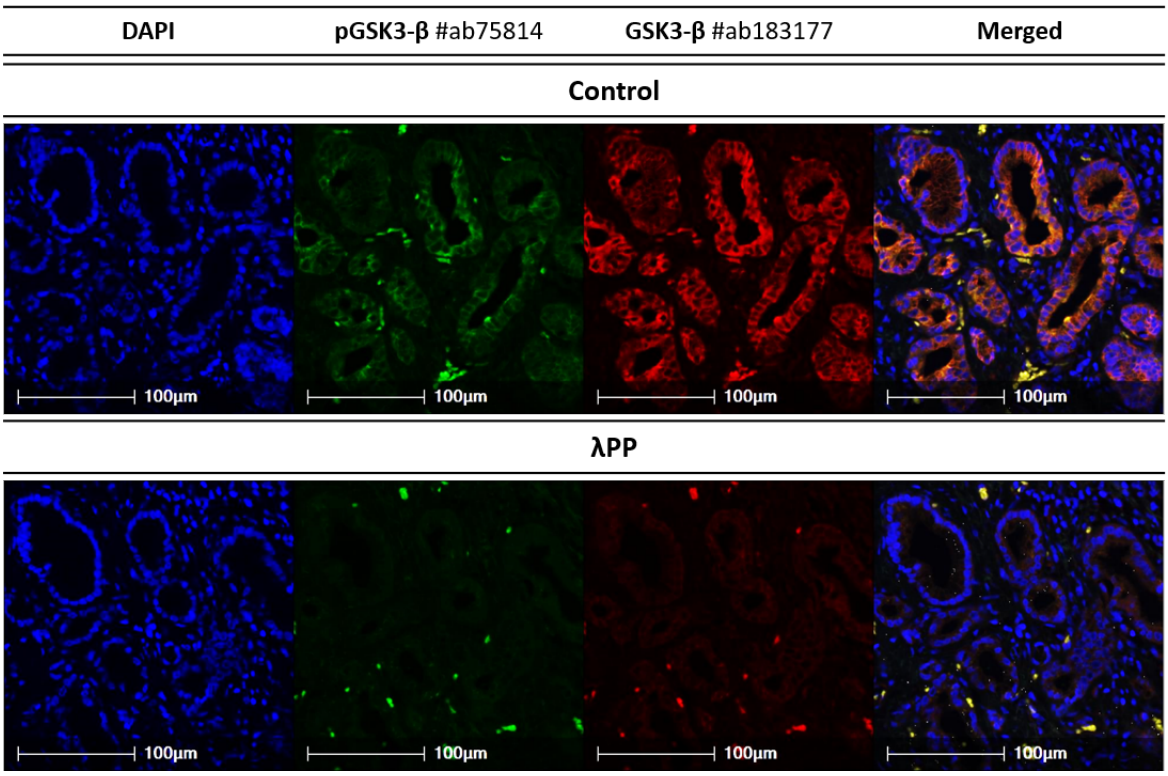

Fig. 5.9 **The effect of λPP treatment on the anti-GSK3-β antibody profiles in the human pancreas.** Representative immunofluorescence micrographs demonstrating the presence and localisation of GSK3-β forms in the ductal cells of an adult organ donor. Two serial FFPE pancreas sections/antibody were pre-incubated with or without lambda phosphatase (λPP), before incubation with each of the two antibodies. Microscopy was performed.

staining the pancreatic ducts but not the islets. This suggests that the latter two anti-GSK3-β antibodies may recognise the same form.

Anti-GSK3-β antibodies and λPP treatment To investigate whether anti-GSK3-β #ab183177 and anti-pGSK3-β #ab75814 antibodies detect the active (dephosphorylated) GSK3-β form or the inactive (phosphorylated) pGSK3-β form, serial sections of human pancreas tissue were treated with and without λPP, to remove phospho-residues. The untreated and λPP treated sections were then co-stained with (i) anti-pGSK3-β #ab75814, (ii) anti-GSK3-β #ab183177 and, (iii) DAPI. As seen previously, the anti-GSK3-β #ab183177 and anti-pGSK3-β #ab75814 co-localised in

the pancreatic ducts and did not stain the β cells (Fig. 5.9, top panel). Following the λPP treatment, the signal for each antibody was abolished (Fig. 5.9, bottom panel). These data suggest that both #ab75814 and #ab183177 antibodies recognise the inactive (phosphorylated) form of GSK3-β. As such, from the antibodies tested, only the #ab93926 is expected to detect the active form of GSK3-β and therefore this antibody will be further tested in this chapter. These findings highlight the benefit of using more than one antibody to detect the same target and further demonstrate the importance of appropriate antibody validation.

5.3.1.2 CDK5

CDK5 phosphorylates a range of Tau residues, including Thr181, Ser199, Ser202, Thr205, Thr212, Thr231, Ser235, Ser396 and Ser404. These residues play an important role both in control and AD brain [62–66] and as such, CDK5 is considered an important Tau kinase both in health and disease.

According to HPA, the protein expression of CDK5 is low in the exocrine and higher in the endocrine tissue where, interestingly, it demonstrates nuclear signal in islet cells. Nuclear expression of CDK5 has been previously described in neurons, where CDK5 plays a role in cell cycle regulation [285]. The subcellular localisation of CDK5 shifts (from the nucleus to the cytoplasm) when a cell re-enters the cell cycle [286]. Two antibodies against CDK5 were tested in IHC. Anti-CDK5 #2506 antibody stained weakly the cytoplasm of a subset of islet and ductal cells but not the acinar cells (fig. 5.10). Anti-CDK5 #ab40773 antibody stained the cytoplasm of a subset of islet cells and faint signal was also detectable in the nerves (fig. 5.10). In contrast to HPA protein expression data, no nuclear signal was detected with either of the antibodies. However, it is important to note that the EADB donors are autopsy which has been shown to impact on the localisation of nuclear protein [287]. Nevertheless,

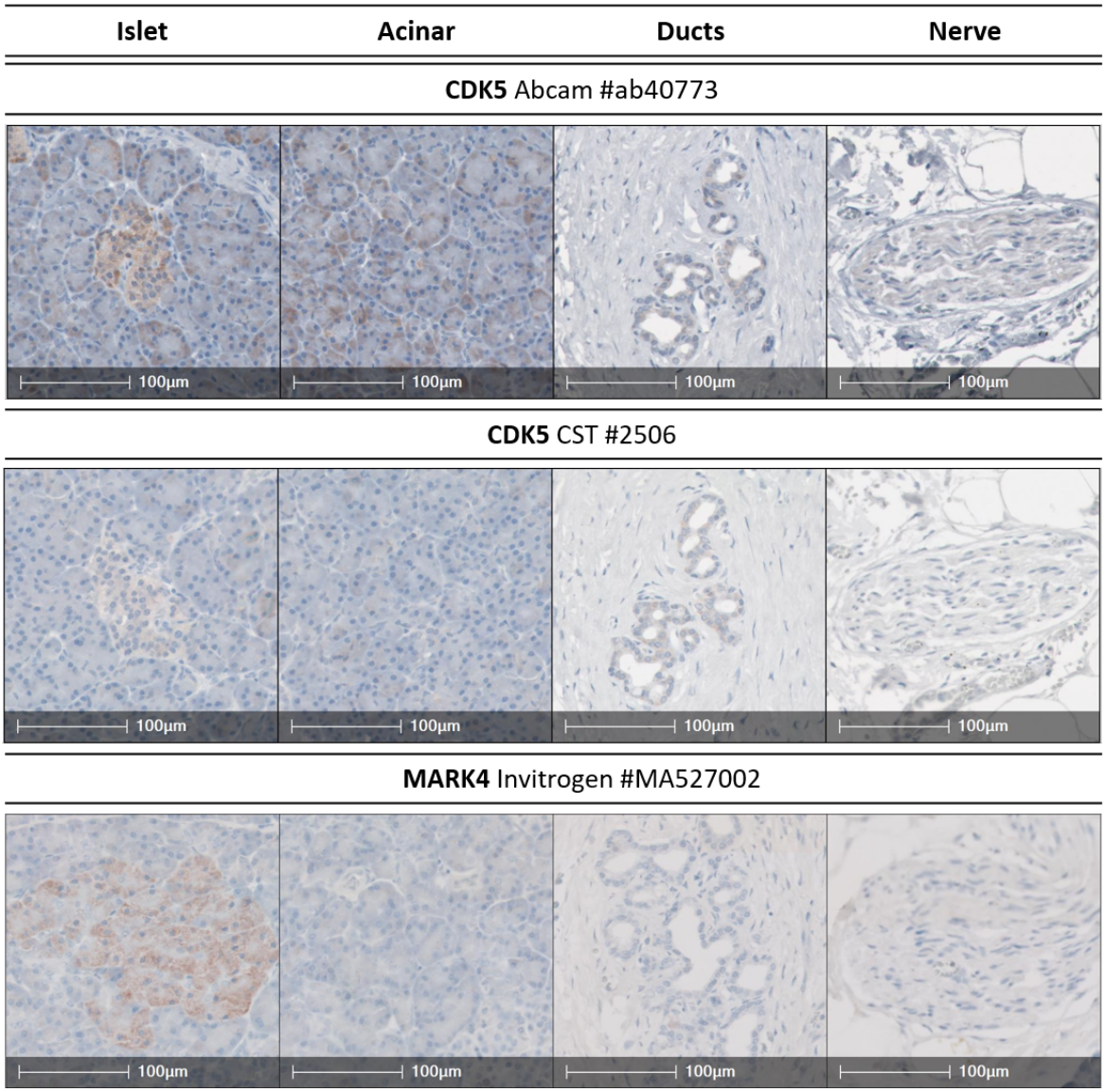

Fig. 5.10 **Tau kinase antibody profiles in the human pancreas.** Representative HRP micrographs demonstrating the presence and localisation of different Tau kinase antibodies (anti-CDK5 Abcam #ab40773, anti-CDK5 CST #2506, anti-MARK4 Invitrogen #MA527002) in the islet, acinar, ductal cells and in the nerves in the pancreas of an organ donor. Whole slide scans were imaged at X40. Scale bars 100μm.

our data agree with the HPA in regard to the cytoplasmic signal. These antibodies could benefit from further optimisation testing different antigen retrieval techniques to explore whether they would impact on the ability of the antibodies to detect nuclear epitopes.

5.3.1.3 MARK4

MARK4 has been associated with early phosphorylation events of Tau in AD [78] and is known to phosphorylate Tau at residues Ser262 and Ser356. Phosphorylation of Tau at Ser262 is a highly important event that drives the dissociation of Tau from the microtubules and protects Tau from self-aggregation [46]. Therefore MARK4 could be considered an important mediator of the Tau:microtubules interaction.

Unlike the HPA which implies that MARK4 is present in islet, acinar and some ductal cells, the anti-MARK4 #TA808507 antibody, recognising amino acids 390-467 of human MARK4, immunostained only a subset of islet cells whereas acinar, ductal and nerve cells were negative (fig. 5.10). This antibody may benefit from further validation steps and additional testing.

5.3.1.4 DYRK1A

DYRK1A is a kinase involved in gene transcription, mRNA splicing, synapse function, and neurodegeneration [80] having both a nuclear and a cytoplasmic localization signal [84, 81]. According to the HPA, DYRK1A is present in the cytoplasm of a subset of islet cells but not in the nucleus and/or ducts. In agreement with the HPA, the anti-DYRK1A antibody immunostained the cytoplasm of a subset of islet cells, but not the the acinar cells or the nerves, in either a ND and T1D donor (fig. 5.11). DYRK1A expression was detected in the nucleus of duct cells but not of other cell types.

5.3.2 Tau phosphatases

Antibodies against PIN1 (n=2), PP2A (n=1) and SET (n=3) were tested in control pancreas (Table 2.2, pg. 44). As for the Tau kinases, a brief summary of each Tau phosphatase expression profile as reported in the HPA is followed be a description of the immunostaining observed in the EADB human pancreas tissue.

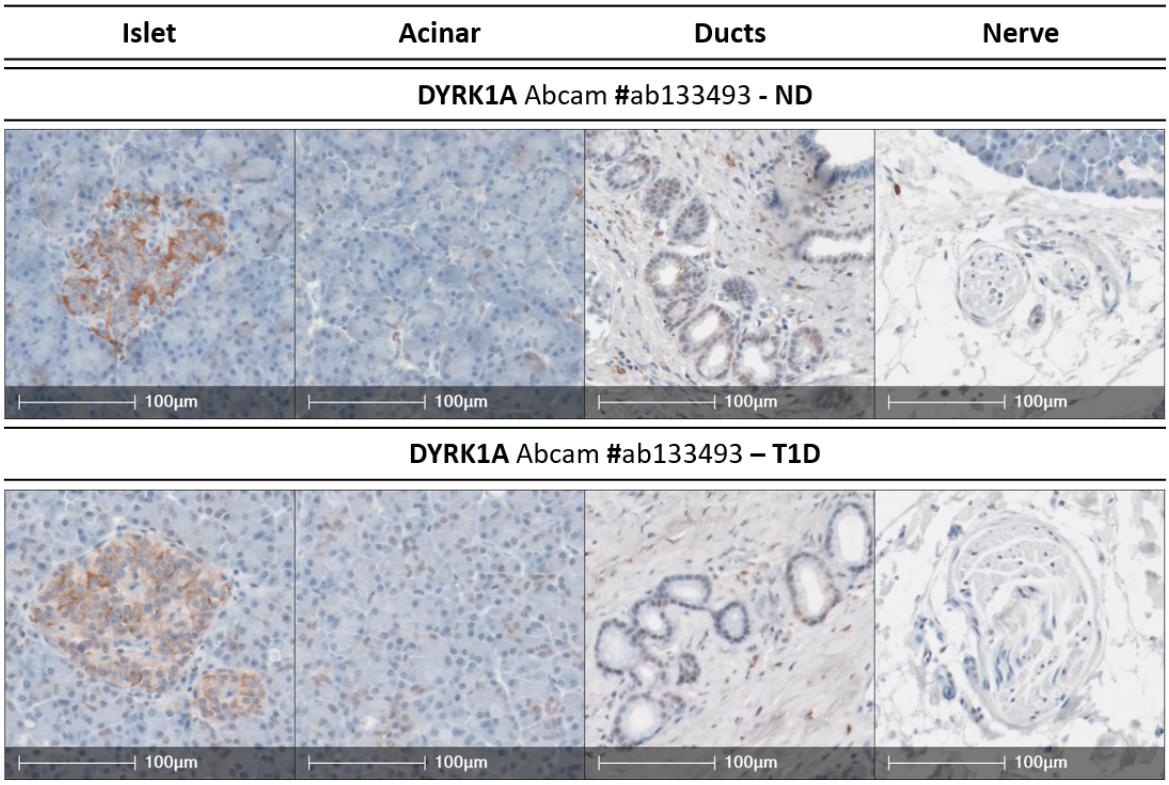

Fig. 5.11 **Tau kinase antibody, DYRK1A, profiles in the control and type I diabetes human pancreas.** Representative HRP micrographs demonstrating the presence and localisation of different Tau kinase DYRK1A in the islet, acinar, ductal cells and in the nerves in the pancreas of adult organ donors diagnosed with or without type I diabetes (T1D). Whole slide scans were imaged at X40. Scale bars 100μm.

5.3.2.1 PP2A

PP2A is the major Tau phosphatase dephosphorylating Tau at multiple sites, such as Ser198, Ser199, Ser202, Thr217, Ser396, Ser404 in the human brain [95] (Table 5.1) and, is also the most efficient phosphatase acting on abnormally hyperphosphorylated Tau protein [96, 105–109, 94].

According to the HPA, PP2A is expressed at a moderate level in the exocrine and endocrine tissue. The anti-PP2A antibody #2041 detected PP2A expression in the cytoplasm of the islets, but failed to immunostain the acinar and ductal cells. Faint signal from the nerves suggests that further optimisation may be required.

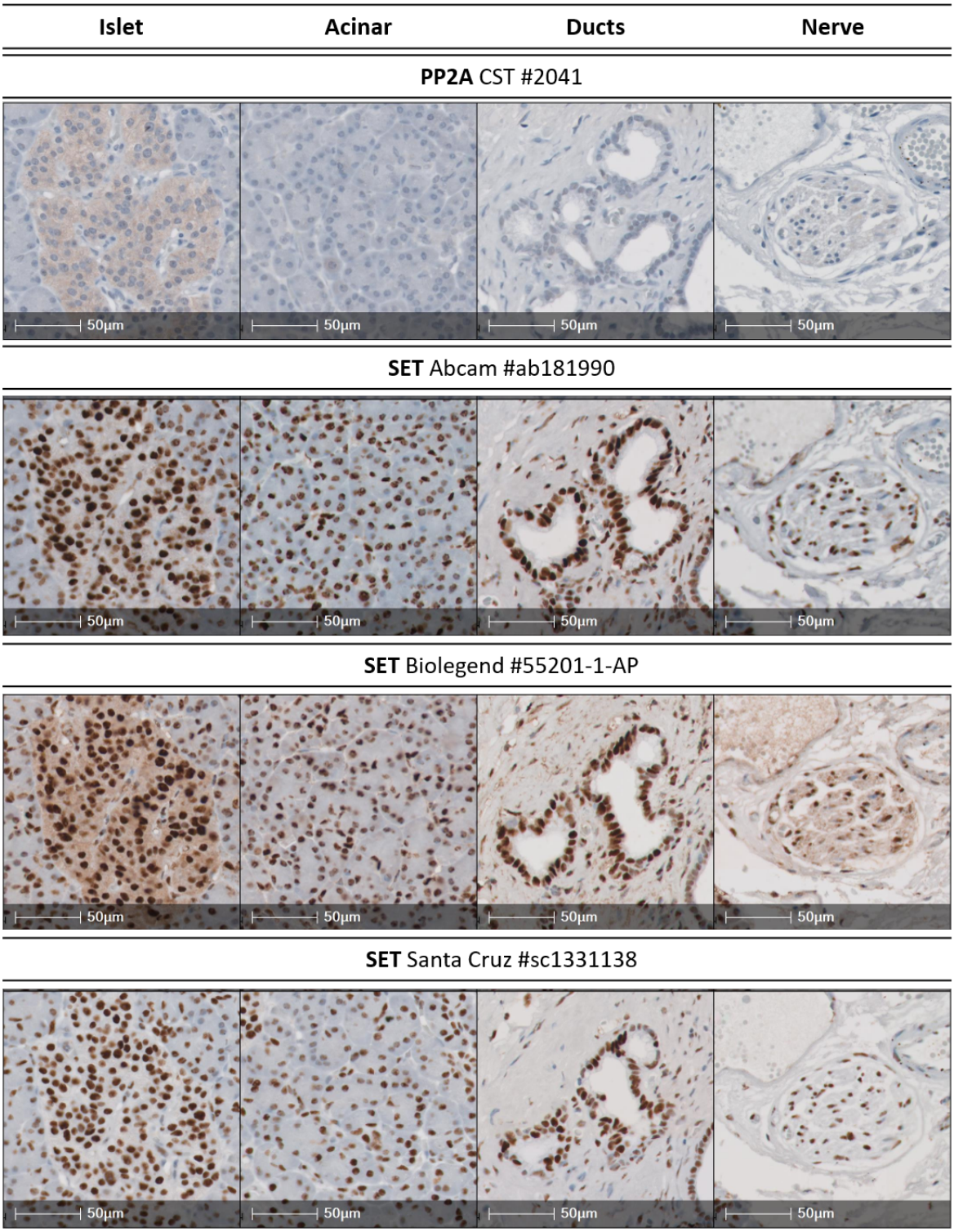

Fig. 5.12 **Tau phosphatase antibody profiles in the human pancreas.** Representative HRP micrographs demonstrating the presence and localisation of Tau phosphatase antibody anti-PP2A CS #2041 and of its inhibitor SET, as detected by three different anti-SET antibodies (anti-SET Abcam #ab181990, anti-SET Biolegend #55201-1-AP, anti-SET Santa Cruz #sc1331138) in the islet, acinar, ductal cells and in the nerves in the pancreas of an organ donor. Whole slide scans were imaged at X40. Scale bars 50μm.

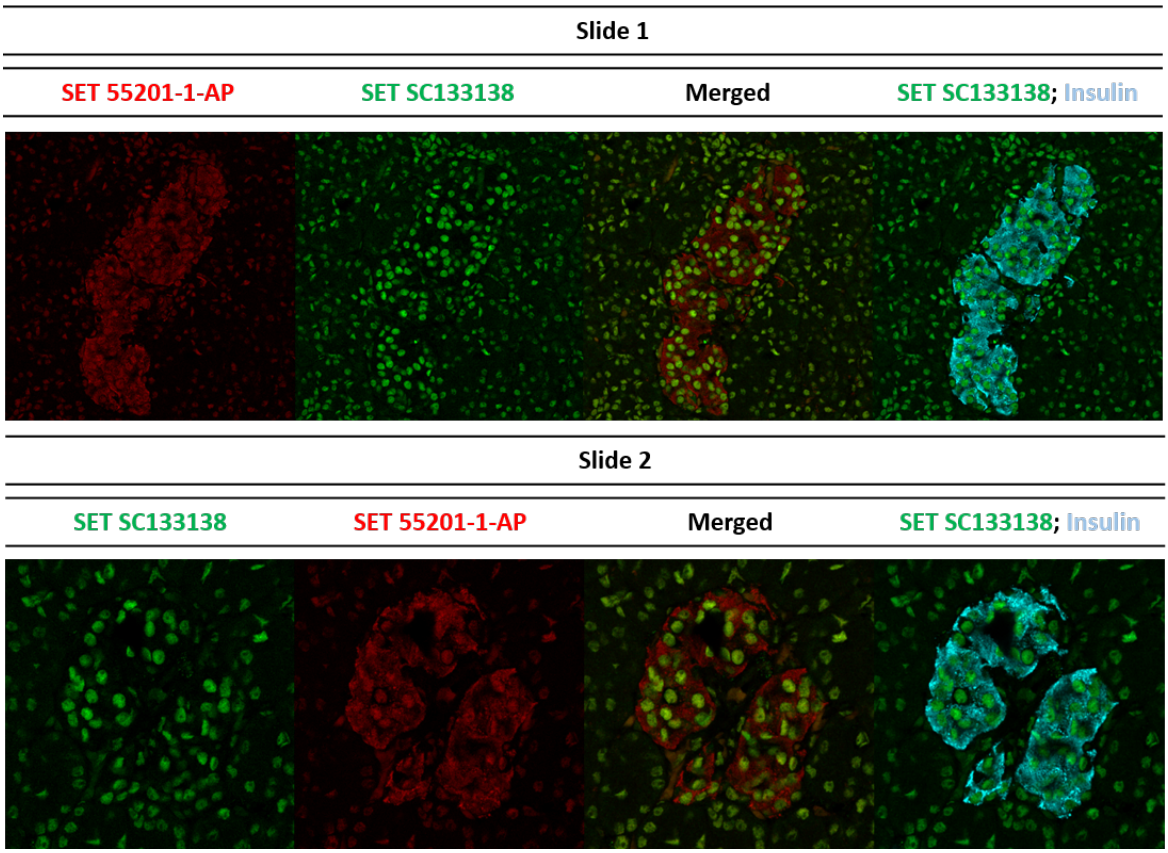

Fig. 5.13 **PP2A inhibitor, SET, antibody profiles in the human pancreas.** Representative immunofluorescence micrographs demonstrating the presence and localisation of two different SET antibodies in the islets in the pancreas of an adult organ donor. Two serial slides were stained with (i) SET #55201-1-AP (red), (ii) SET #sc1331138 (green) and (iii) insulin (cyan). The order of the two SET antibodies was altered; Slide 1 was stained first stained for SET #55201-1-AP (red) and then for SET #sc1331138 (green) and Slide 2 was first stained for SET #sc1331138 (green) and then for SET #55201-1-AP (red). Confocal microscopy was performed.

5.3.2.2 SET

The activity of PP2A is regulated by an inhibitor protein, SET, meaning that elevated expression of SET could lead to decreased PP2A activity and, subsequently, higher phosphorylation levels of Tau. According to the HPA, SET is highly expressed in the nucleus of islet, acinar and ductal cells. Three antibodies against SET protein supplied from different suppliers were tested (Table 2.2). Anti-SET #ab181990 and anti-SET #sc1331138 antibodies strongly detected SET forms in the nucleus of the islets, acinar

and ductal cells and the nerves (fig. 5.12). Interestingly, anti-SET #55201-1-AP antibody labeled all of the above and also stained the cytoplasm of the islets (fig. 5.12). The strong immunostaining signal of all three anti-SET antibodies agree with gene expression data that implied high gene expression in ND pancreas (fig. **??**, 5.5c).

Anti-SET antibodies may detect different SET isoforms IF staining combining the anti-SET #sc1331138 and anti-SET #55201-1-AP was performed to investigate whether the two anti-SET antibodies recognise different isoforms or the same epitope but with different specificity. Tissue sections were stained with; (i) SET #55201-1-AP as the first primary and SET #sc1331138 as the second primary antibody and, (ii) vice versa (fig. 5.13). In both cases, staining patterns were unaffected by the order of the antibody addition suggesting that they do not inhibit each others binding. Therefore, the two antibodies could recognise different SET epitopes. Co-staining in the nucleus helps confirm the antibodies specificity. The staining in the cytoplasm with anti-SET #55201AP could suggest a different isoform detected only by this antibody. Based on the literature, there are two different SET isoforms, isoform 1 and 2. SET isoform 1 is expressed in the nucleus and SET isoform 2 is expressed both in the nucleus and the cytosol of pancreatic cancer cell lines [288].

5.3.3 Tau deacetylases

Based on literature and the RNAseq data from the human pancreas, strong emphasis should be given to the study of Tau acetylation in β cells. However, due to time and COVID limitations impacting access to the lab, work on deacetylases was limited. One antibody against HDAC6 was tested in the human pancreas (Chapter 2, Table 2.2). The selection of HDAC6 was based on its importance for deacetylation of the α-tubulin of the microtubules, and of the Tau protein. As both the microtubule assembly and the Tau:microtubules association are dynamically regulated, HDAC6 equilibrium may

Table 5.2 **Acetylation residues and function.** This table is a list of select Tau lysine residues that can be acetylated and the relevant implications that each modification has to the regulation of Tau.

Tau residue	Modification	Function
Lys174	acetylation	prevents degradation
Lys259	acetylation	inhibits aggregation, prevents phosphorylation, promotes degradation
Lys274	acetylation	promotes synaptic dysfunction, tau mislocalization
Lys280	acetylation	increases aggregation, prevents clearance, modulates phosphorylation
Lys281	acetylation	promotes aggregation, synaptic dysfunction, tau mislocalization
Lys290	acetylation	inhibits aggregation, prevents phosphorylation, promotes degradation
Lys321	acetylation	inhibits aggregation, prevents phosphorylation, promotes degradation
Lys353	acetylation	inhibits aggregation, prevents phosphorylation, promotes degradation

be of great importance in β cells. RNAseq data suggested that HDAC6 gene had a tendency to be lower in T1D compared to ND (fig. 5.6a).

5.3.3.1 HDAC6

HDAC6 deacetylates Tau at a number of Lys residues some of which residues promote aggregation and prevent clearance while others inhibit aggregation and promote degradation (Table 5.2). This implies that HDAC6-mediated deacetylation has a dual effect on Tau and that the acetylase:deacetylase equilibrium could be critical for Tau function. According to the HPA, the protein expression of HDAC6 is modest in islet, acinar and ductal cells. Our data indicate that anti-HDAC6 #ab133493 immunostained the cytoplasm of a subset of islet and ductal cells of a ND organ donor and weak staining was observed in the acinar cells and the nerves (fig. 5.14).

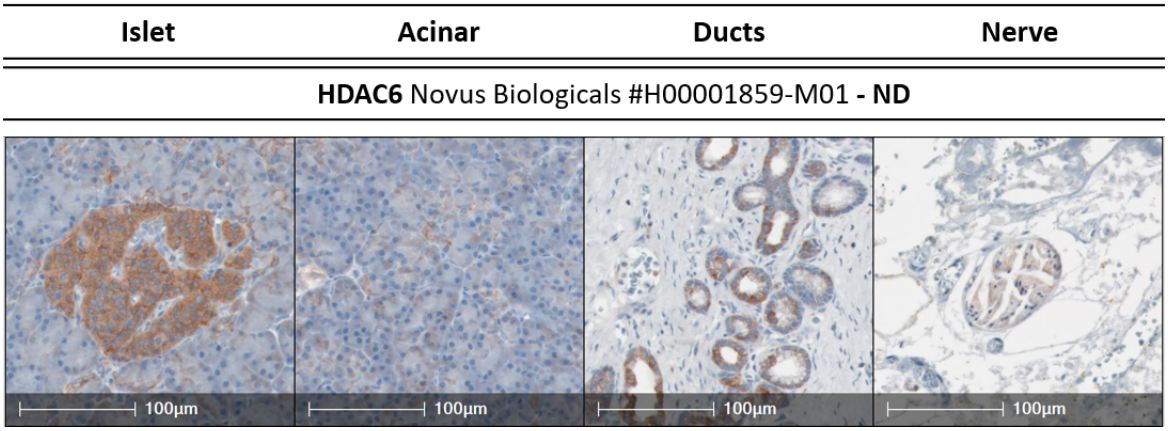

Fig. 5.14 **Tau deacetylase, HDAC6, antibody profile in the control and type I diabetes human pancreas.** Representative HRP micrographs demonstrating the presence and localisation of Tau deacetylase anti-HDAC6 antibody in the islet, acinar, ductal cells and in the nerves in the pancreas of organ donors. Whole slide scans were imaged at X40. Scale bars 50μm.

5.4 Subcellular localisation of Tau modifiers in human islets

5.4.1 Tau kinases and phosphatases

After the preliminary characterisation of a range of Tau modifiers in the human pancreas, the subcellular localisation of major Tau kinases (GSK3-β and CDK5) and the major phosphatase (PP2A) was assessed within human pancreatic islet cells by performing IF staining on pancreas tissue sections of donors diagnosed with and without T1D combining antibodies against the (i) modifier of interest (GSK3-β, CDK5 or PP2A), (ii) insulin, as a marker of β cells, (iii) glucagon, as a marker of α cells and (iv) DAPI to define the nuclei (Chapter 2, section 2.4.2).

GSK3-β in islet cells Our IF data agree with the RNAseq data suggesting that GSK3-β is expressed in pancreatic β cells (fig. 5.15a). Interestingly, RNAseq data suggests that GSK3-β may not not affected by age or disease state in β cells (figs. 5.3c,

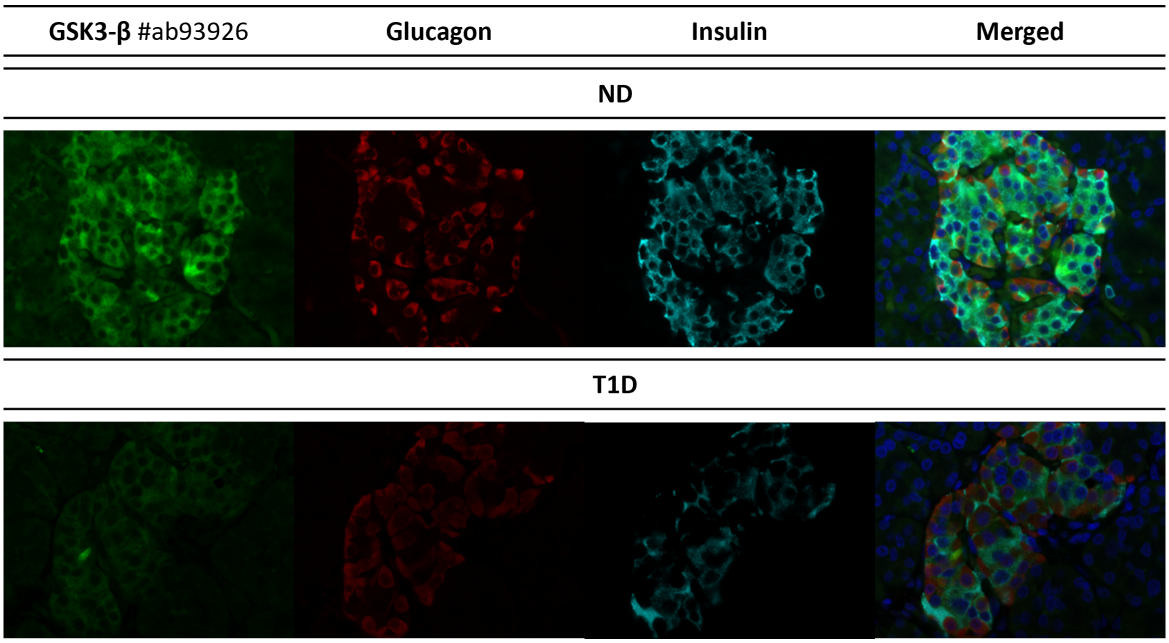

(a)

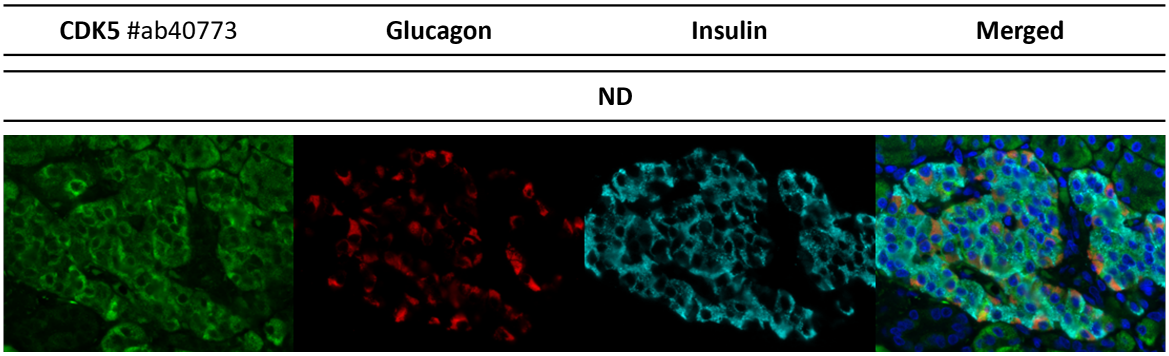

(b)

Fig. 5.15 **Tau kinase antibody profiles within the human pancreatic islets.** Representative immunofluorescence micrographs demonstrating the presence and localisation of 5.15a GSK3-β antibodies in the islets in the pancreas of a non-diabetic and a type 1 diabetic organ donor and, 5.15b CDK5 in the pancreas of a non-diabetic organ donor. FFPE pancreas tissue sections were stained for the Modifier of interest (GSK3-β, CDK5; green), glucagon (red), insulin (cyan) and, DAPI (blue). Microscopy was performed. Magnification X40.

A.6b). However, preliminary staining data reveal that the protein expression of active (dephosphorylated) GSK3-β as detected by the GSK3-β #ab93926 antibody, may be reduced in islet cells in T1D when compared to ND (fig. 5.15a). This observation raises further questions about whether the active form of GSK3-β or total GSK3-β

may be reduced in T1D and, also, highlights the importance of expanding the analysis to include more pancreas tissue sections.

CDK5 in islet cells HRP staining suggested that CDK5 is expressed at low levels in islet cells which is in agreement with HPA immunostaining data. Next step would be to perform IF staining to co-stain for CDK5 and insulin to explore whether CDK5 is expressed in β cells. However, an important difference between HRP and IF staining is that the HRP technique boosts the signal of the relevant antibody whereas IF may dampen it. As such, normal IF staining with CDK5 would result in significantly lower levels of anti-CDK5. Therefore, the signal of anti-CDK5 was boosted by performing the TSA technique. Unfortunately, by doing so, any nuclear signal of CDK5 would be abolished. The preliminary IF data confirms the RNAseq data suggesting that CDK5 is expressed in pancreatic β cells (fig. 5.15b). Furthermore, CDK5 was present in the cytoplasm of both islet and acinar cells (fig. 5.15b) which is in agreement with immunostaining observed with HPA.

PP2A in islet cells Although the RNAseq data implied that the PP2A gene is transcribed both in β and α cells (figs. 5.5a, A.7b), the anti-PP2A antibody detected low level protein expression predominately in β cells (fig. 5.16). RNAseq data suggests that PP2A showed a tendency to decrease in β cells in T1D compared to ND (figs. 5.5a, 5.5c) and preliminary immunostaining data further confirmed that the protein expression level of PP2A may also be reduced in islet cells in T1D when compared to ND (fig. 5.16). Reduction of PP2A expression levels would result in elevated levels of Tau phosphorylation, and therefore more work is required to reach firm conclusions about PP2A expression in control and T1D pancreas.

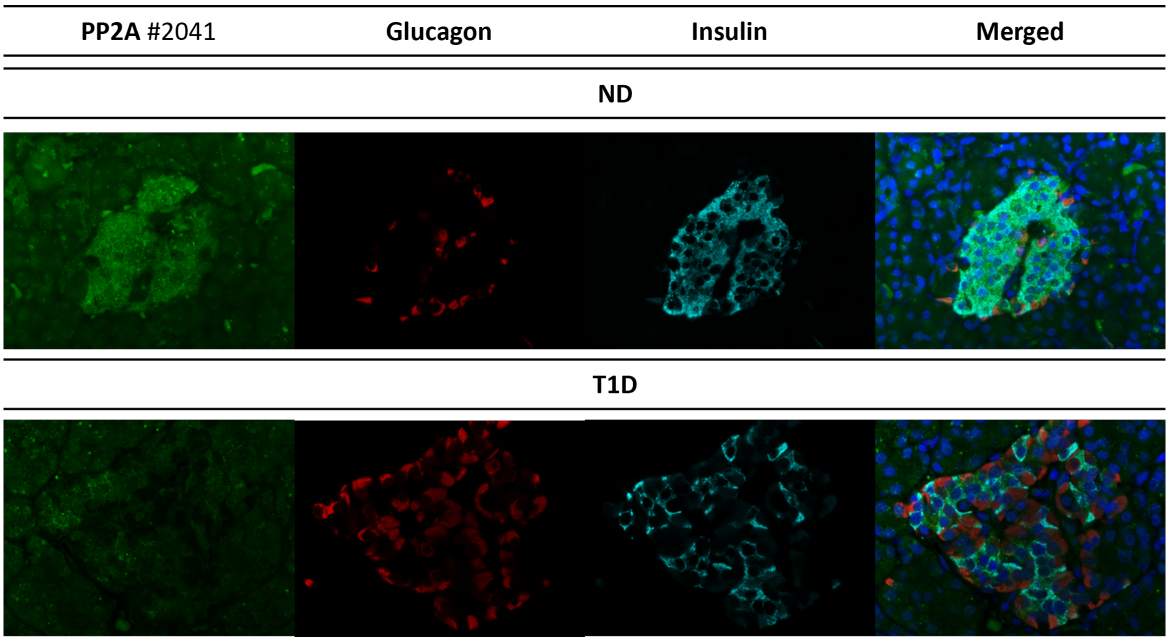

Fig. 5.16 **Tau phosphatase antibody profiles within the human pancreatic islets.** Representative immunofluorescence micrographs demonstrating the presence and localisation of PP2A antibody in the islets in the pancreas of a non-diabetic and a type 1 diabetic organ donor. FFPE pancreas tissue sections were stained for the PP2A (green), glucagon (red), insulin (cyan) and, DAPI (blue). Microscopy was performed. Magnification X40.

5.4.2 Tau modifiers and pTau-E178

Previous work suggests that the pancreatic Tau form phosphorylated at the epitope recognised by the anti-E178 antibody (pTau-E178) may play an important role in age and potentially obesity and in disease states (Chapter 4). Therefore to investigate whether Tau modifiers may be associated with presumed pathogenic forms of pTau within β cells, IF staining was performed on pancreas tissue sections of donors diagnosed with and without T1D combining antibodies against the (i) modifier of interest, (ii) anti-pTau-E178, as a marker of an allegedly pathogenic form of Tau, (iii) insulin, as a marker of β cells and (iv) DAPI to mark the nuclei (Chapter 2, section 2.4.2). Due to time and COVID limitations, only two antibodies against Tau modifiers were combined with anti-E178.

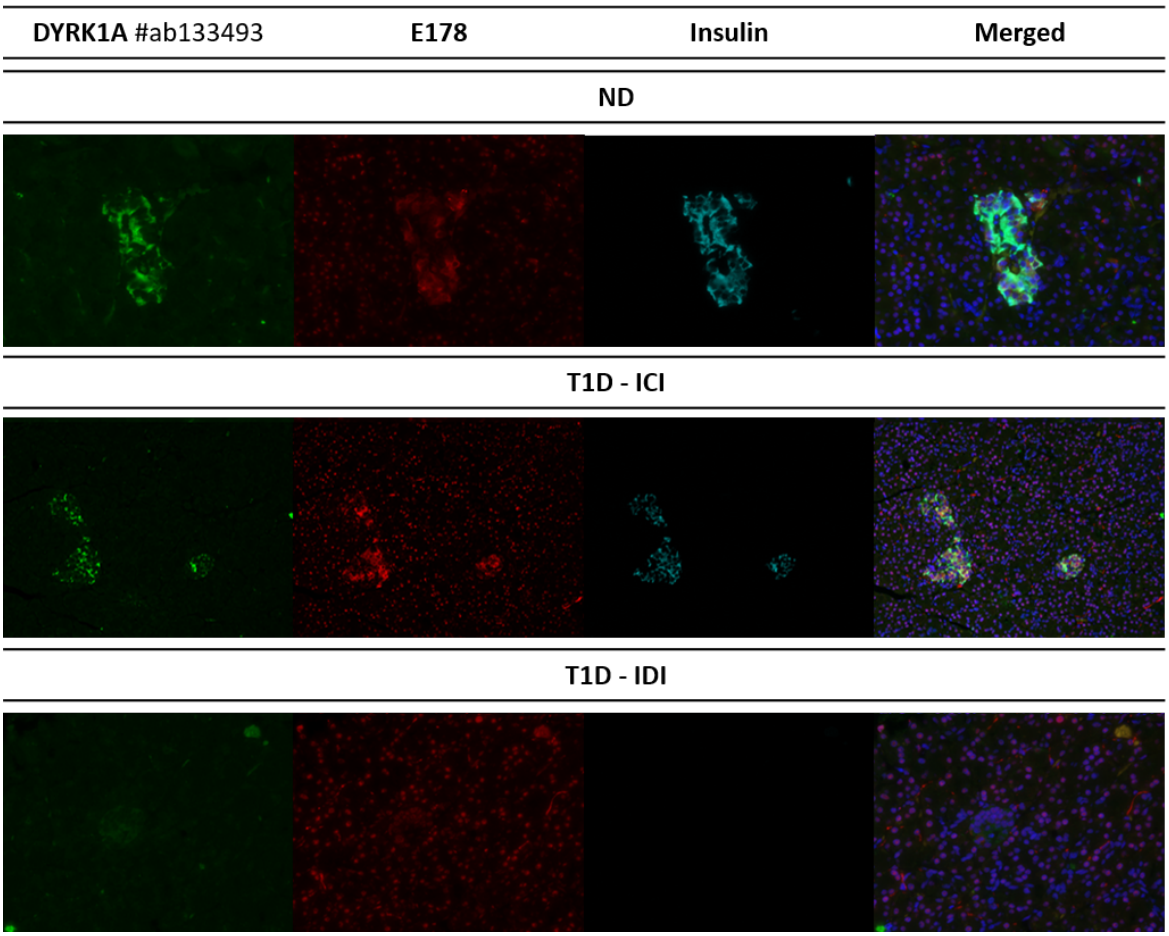

Fig. 5.17 **DYRK1A and pTau-E178 antibody profiles within the human pancreatic islets.** Representative immunofluorescence micrographs demonstrating the presence and localisation of pTau-E178 in relation to DYRK1A in the islets in the pancreas of a non-diabetic (ND) and a type 1 diabetic (T1D) organ donor. ICI; insulin-containing islet, IDI; insulin-deficient islet. DYRK1A; green, E178; red, insulin; cyan, DAPI; blue. Microscopy was performed. Magnification X40.

DYRK1A and pTau-E178 in β cells In the ND pancreas, anti-DYRK1A labeled proteins present in β cells (fig. 5.17). The strong immunostaining using the anti-DYRK1A antibody is in agreement with the high gene expression level of DYRK1A (fig. 5.3b). Interestingly, β cells expressing high levels of insulin, also had high levels of anti-DYRK1A staining, yet expressed lower levels of pTau-E178 (fig. 5.17). In T1D ICIs, anti-DYRK1A stained mostly the β cells. Again, cells that stained strongly positive for both DYRK1A and insulin can be identified. In T1D IDIs, anti-DYRK1A

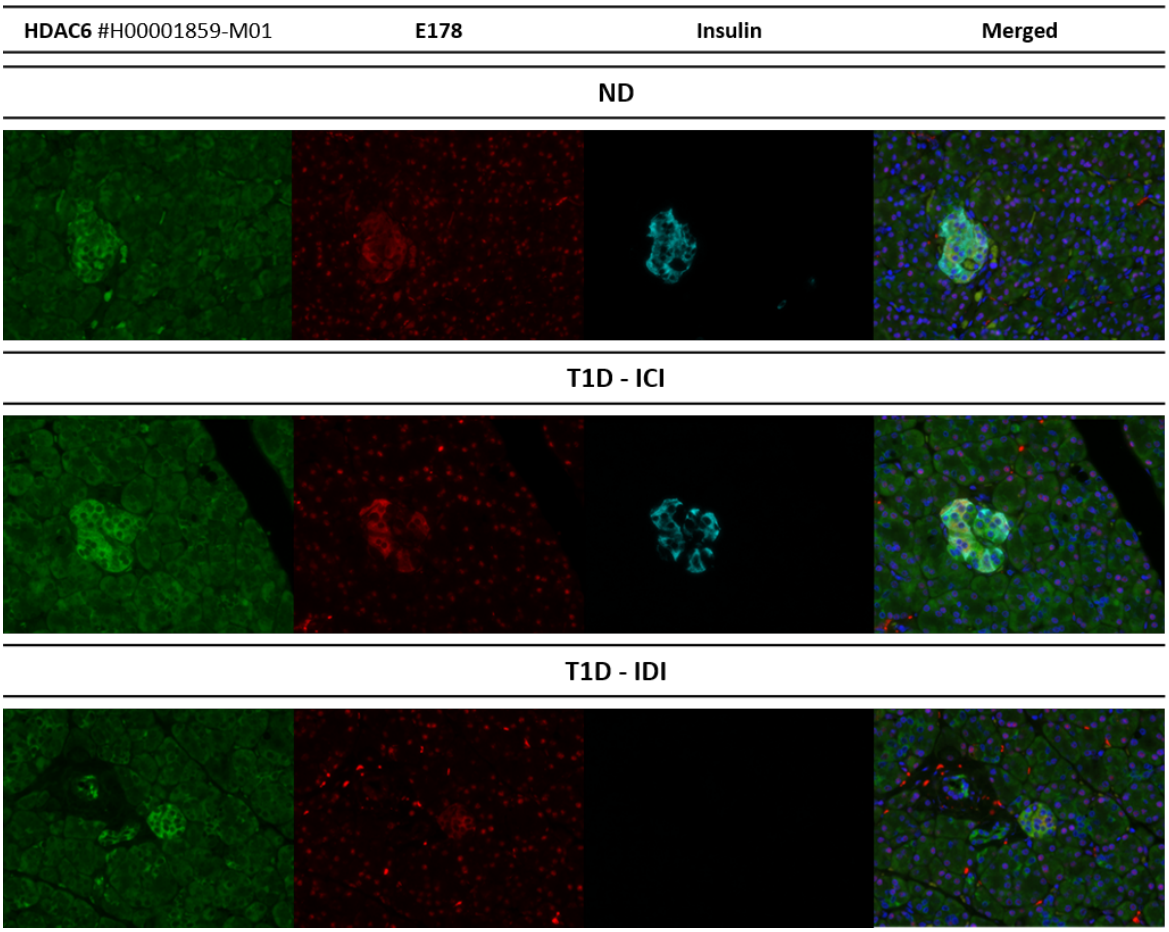

Fig. 5.18 **HDAC6 and pTau-E178 antibody profiles within the human pancreatic islets.** Representative immunofluorescence micrographs demonstrating the presence and localisation of pTau-E178 in relation to HDAC6 in the islets in the pancreas of a non-diabetic (ND) and a type 1 diabetic (T1D) organ donor. ICI; insulin-containing islet, IDI; insulin-deficient islet. HDAC6; green, E178; red, insulin; cyan, DAPI; blue. Microscopy was performed. Magnification X40.

signal is almost abolished (fig. 5.17) presumably due to the DYRK1A expression being predominately in insulin-containing β cells. These preliminary observations alongside the RNAseq data confirm that DYRK1A is expressed in β cells (fig. 5.3b). Further analysis in more donors and further quantification analysis are required to determine if there are differences between donors and disease states.

HDAC6 and pTau-E178 in β cells In ND pancreas, the anti-HDAC6 antibody labels β cells (fig. 5.18). Interestingly, β cells expressing low levels of insulin appear to contain high levels of both HDAC6 and pTau-E178 and, vice versa. Intriguingly, while in ND islets, the immunostaining of anti-HDAC6 and anti-pTau-E178 are similar, in T1D IDIs, cells with higher pTau-E178 levels have less HDAC6 and cells with low pTau-E178 levels have higher HDAC6. The RNAseq data suggested a reduction in the gene expression levels of HDAC6 in the β cells of T1D pancreas compared to ND (fig. 5.6a) although immunostaining data suggested that HDAC6 protein expression may be increased or that HDAC6 is uniformally expressed within the T1D islet cells. However, further analysis is required.

5.5 Discussion

Tau was traditional thought to be a neuronal protein and it is now known to be expressed in the pancreatic β cells. As β cells and neurons share many common features, it was hypothesised that the regulation of Tau in the human pancreas could be compared to that in neurons. Therefore, this chapter provides an overview of the key Tau modifiers in the pancreas. Publicly available RNAseq datasets [240, 175, 239] and HPA immunostaining data (HPA, https://www.proteinatlas.org/) confirmed the expression of a selection of key Tau modifiers in the human pancreas and more importantly in the endocrine region (Table 6.1). Based on this, antibodies against a range of key Tau modifiers were tested in the human pancreas and the protein expression level of these Tau modifiers was explored in a preliminary phase (Table 6.1). Although further studies are required to make firm conclusions, the data hints that some of these modifiers may be affected in an age- and/or disease-dependent way which would have the potential to influence the PTM signature of Tau. This preliminary work serves as a guide to expand the analysis to more donors of different age and disease states.

Table 5.3 **Expression of Tau modifiers in β cells based on RNAseq and immunostaining data.** The expression of Tau modifiers in β cells was assessed in RNA and protein level. The modifiers have been categorised based on relevant PTMs. RNAseq summary is based on the RNAseq data from [240, 175, 239]. Protein levels were assessed based on the Human Protein Atlas (HPA, https://www.proteinatlas.org/) and in-house staining. Tau residues modified by these modifiers are also described. ✓indicates the presence of each modifier in the endocrine region of the human pancreas (✓; low expression, ✓✓; moderate expression, ✓✓✓; high expression). nt; not tested.

Modifiers	RNA	Protein (HPA)	Protein	Tau residues
Kinases				
CDK5	✓	✓	✓	Ser199, Ser396, Ser404
DYRK1A	✓✓✓	✓	✓✓	Thr181, Ser212, Thr231
GSK3-β	✓✓✓	✓	✓	Ser198, Ser199, Ser262, Ser396, Ser404, Ser409
MARK4	✓✓	✓	✓	Ser262, Ser356
PKC	✓	✓✓	nt	Ser262
SIK1	✓	✓✓	nt	Ser262
SYK	✓	✓	nt	Thr18
Phosphatases				
PIN1	✓	✓✓	very low	Th231
PP2A	✓✓	✓✓	✓	Ser198, Ser199, Ser262, Ser396, Ser404
PP5	✓✓	✓✓	nt	Ser198, Ser199
SET	✓✓✓	✓✓✓	✓✓✓	
Deacetylases				
HDAC6	✓✓	✓✓	✓✓✓	Lys259, Lys280, Lys281, Lys290, Lys321, Lys353
SIRT1	✓	✓✓	nt	Lys174
Caspases				
Caspase-1	very low	✓	nt	Asp421
Caspase-8	✓	✓✓	nt	Asp421

The expression level of the Tau kinases appear to vary both in an RNA and protein level (Table 6.1). RNAseq suggests that the most highly expressed Tau kinases are DYRK1A and GSK3-β followed by MARK4 and then CDK5, PKC, SIK1 and SYK. Due to time limitations, PKC, SIK1 and SYK were not further tested. Preliminary in-house immunostaining data showed that DYRK1A is expressed at a high level whereas, CDK5, GSK3-β and MARK4 are moderately expressed. DYRK1A, which is highly expressed in the islets, is known to phosphorylate Tau at Thr181, Ser212 and Thr231. Previous data suggest that Thr231 is moderately phosphorylated in β cells and that Thr181 may not be phosphorylated in the human adult pancreas (Chapter 4, pg. 4), however, more donors should be tested to confirms this. Unfortunately, no antibody against Ser212 has been tested.

GSK3-β and MARK4 phosphorylate Tau at Ser262 (Table 6.1). Phosphorylation of Tau at Ser262 detaches Tau from the microtubules and prevents its aggregation [46]. Data presented in Chapter 4 suggests that this residue is phosphorylated in the β cells (Chapter 4). MARK4 also phosphorylates Tau at Ser356 which has been shown to promote the further phosphorylation of Tau at Ser412 and Thr361, suggesting that phosphorylation of Tau by MARK4 could stimulate a cascade of further phosphorylation events [71, 289, 290]. Although GSK3-β and MARK4 may play a protective role for Tau in the β cells in terms of self-aggregation, elevated expression or hyperactivation of these kinases could still potentially lead to Tau hyperphosphorylation and its detachment from the microtubules.

CDK5 and GSK3-β phosphorylate Tau at Ser199, Ser396 and Ser404 and, these residues have been associated with pathogenic phenotypes [65]. Although the exact epitope of anti-E178 remains unknown, it is proprietary to the C-tail of Tau and, more specifically around Ser396. Preliminary data by Dr. Irina Stefana has shown that pTau-E178 may play an important role in cell cycle (Chapter 4, pg. 4). Interestingly, it has been shown that the subcellular localisation of CDK5 shifts (from the nucleus to the cytoplasm) when a cell re-enters the cell cycle in neurons [286]. Unfortunately, in-house immunostaining has not detected nuclear CDK5 in β cells, but HPA immunostaining data suggest that CDK5 is nuclear in islet cells. Considering that pTau-E178 altered subcellular localisation during ageing and that CDK5 has also been reported to migrate between the nucleus and the cytoplasm, this is an area warranting further investigation.

Elevated expression or hyperactivation of CDK5 would result in Tau hyperphosphorylation inhibiting its interaction with the microtubules. This has been previously been observed in diabetes-associated neurodegeneration where exposure of high glucose leads to p25 generation, CDK5 hyperactivation and, Tau hyperphosphorylation in neurons [291] resulting in unstable microtubules. Even though CDK5 has not been extensively

studied within the diabetes context, recent studies demonstrate that CDK5 signaling pathways are downregulated in T1D [292], complementing our preliminary IF data that CDK5 may be reduced in T1D. It is expected that decreased expression of CDK5 would result in decreased Tau phosphorylation and highly stable microtubules suppressing the glucose stimulated insulin secretion [182]. However, this argues with studies that show that decreased function of the CDK5/p35 complex results in enhanced insulin secretion in response to elevated glucose concentration both *in vitro* and *in vivo* [276]. As this is a highly dynamic system, a possible explanation could be that the amount of Tau molecules or of Tau phosphorylation have a direct effect on how stable the microtubules are and that the % of microtubule stability has a different effect on insulin secretion.

Tau hyperphosphorylation has been mostly attributed to the hyperactivation of GSK3-β and/or the inhibition of PP2A in the AD brain. GSK3-β is a ubiquitously expressed protein involved in many key signalling pathways and is considered to be a potential therapeutic target for the development of treatments for both AD and T2D [293]. However, recent studies have dampened enthusiasm for GSK3-β as a therapeutic target in β cells for T2D [294], as the group proposes that specific inhibition of GSK3-β in β cells worsens the health of mice, reduces the expression of *PDX1* and *MAFA* genes, decreases β cell mass and has no effect on insulin secretion. Moreover, it is important to highlight that GSK3-β phosphorylates proteins that have been prior phosphorylated by other kinases. As such, GSK3-β may 'boost' Tau hyperphosphorylation, but it is highly unlikely that GSK3-β is the major cause of Tau hyperphosphorylation, it could rather be a consequence. In addition, preliminary RNAseq data analysis suggests that GSK3-β expression levels in β cells may not be affected by age and disease status, implying that it does not drive Tau expression.

Preliminary data suggest that the overall RNA and protein expression of Tau phosphatases is higher compared to that of Tau kinases in β cells (Table 6.1). This could suggest that even though Tau kinases outnumber Tau phosphatases, Tau phosphatases may be more specific and effective in regulating the phosphorylation status of Tau. PP2A and PP5 dephosphorylate Tau at Ser198 and Ser199 and PP2A can also dephosphorylate Tau at Ser396 and Ser404 and, all these residues have been associated with pathogenic phenotypes. Reduced levels or activity of these phosphatases would have a direct a effect on the phosphorylation status of Tau by increasing its phosphorylation. Preliminary work propose that PP2A expression may be decreased in T1D, suggesting that Tau could be hyperphosphorylated in the β cells of those diagnosed with T1D, however, further work is required to investigate this. Furthermore, the high expression of SET, a PP2A inhibitor, in the nucleus of β cells would imply that SET suppresses Tau phosphatases potentially resulting in elevated levels of phosphorylated Tau forms in the nucleus. This agrees with the observations in Chapter 3 that suggests that nuclear Tau is hyperphosphorylated in β cells (Chapter 4, pg. 115).

HDAC6 regulates insulin signaling in pancreatic β cells [295] and inhibition of HDAC6 overcomes leptin resistance in obesity [296]. It has also been shown that lysine deacetylases are produced in pancreatic β cells and are differentially regulated by proinflammatory cytokines [297]. Intriguingly, HDAC6 demonstrated a differential immunostaining pattern in ICIs and IDIs. In ND islets, the immunostaining of anti-HDAC6 and anti-pTau-E178 are similar, in T1D IDIs, cells expressing higher pTau-E178 levels have less HDAC6 and cells expressing low pTau-E178 levels have higher HDAC6. This is an area worth exploring further.

This chapter provides an overview of the expression of a selection of Tau modifiers in β cells and explores their expression in ageing and disease states at a very preliminary phase. Even though Tau modifiers have not been studied in the context of diabetes,

studies on this dynamic system could enrich our understanding of a range of mechanisms, such as cell cycle regulation and insulin secretion.

5.5.1 Limitations

Due to time limitations, emphasis was given to Tau kinases and phosphatases and unfortunately, the protein expression of most Tau deacetylases and caspases was not explored. Moreover, RNAseq data were extracted from a limited amount of donors and/or cells and firm conclusions about the gene expression of Tau modifiers cannot be made. Due to COVID limitations impacting on lab accessibility, antibodies against Tau modifiers were only tested in a small number of pancreas tissue sections (and have not been tested in positive control tissue) which does not allow for full characterisation of their protein expression in the human pancreas. Moreover, careful selection of antibodies using the pipeline in should help

5.5.2 Next steps

Next steps would involve (i) further validation of promising modifiers and (ii) the full characterisation of Tau modifiers in the human pancreas in an increased number of donors. Pancreatic Tau is phosphorylated at a variety of residues that are modified by several kinases. As such, it would be interesting to correlate pTau residues and kinases/phosphatases in the β cells and further explore whether their expression is altered in age, obesity and disease (T1D, T2D) and determine how these changes may affect other vital signalling pathways in β cells, especially those impacting on insulin secretion.

Chapter 6

Discussion

6.1 Introduction

Diabetes mellitus describes a set of chronic metabolic disorders; the predominant forms are T1D and T2D. T1D is an autoimmune disorder characterised by absolute insulin deficiency which is caused due to pancreatic β cell destruction, whereas T2D is a progressive disease caused by either β cell dysfunction or insulin resistance. Insulin resistance is a condition of insufficient or defective insulin signalling [184, 185]. Epidemiological studies have strongly linked T2D and AD [189, 188]. AD is the most common neurodegenerative disorder characterised by the irreversible loss of neurons and one of its major hallmarks is the presence of intracellular aggregates of hyperphosphorylated Tau protein in NFTs in the brain [191]. Recent studies demonstrate that a T1D protective SNP was identified within the MAPT gene, suggesting that Tau protein may play a role in T1D and others propose that hyperphosphorylated Tau is also present in the pancreas of individuals with T2D [177].

Even though the first evidence that specific Tau exons are expressed in normal and tumoral pancreatic acinar cells dates back to 1998 [258, 259], little is still known about the expression of Tau in the human pancreas under basal and diseased conditions.

Recent studies have shown that the MAPT promoter is active in human islets [172, 173] and that Tau RNA and Tau protein are present in human islets [174, 175, 177]. A role in insulin secretion has been proposed as a putative function of Tau in β cells [183]. In addition, Tau has been shown to be upregulated in insulinomas (3x higher compared to control islets) with a characteristic isoform imbalance of 3R:4R $>$ 1 [176, 178]. Contrary to these, a recent study argues that the expression of Tau is restricted to autonomic nerve fibres [181]. Together these examples and inconsistencies emphasise the importance of studying Tau in the pancreas.

Aims Tau is a very complex and heavily post-translationally modified protein whose expression is age-, cell- and region-dependent. The work presented in this thesis describes the generation of a comprehensive toolbox of validated antisera that detect a wide range of relevant Tau forms (isoforms, phosphorylated, and cleavage products; Chapter 3) and relevant Tau modifiers (Chapter 5). It further describes the profile of Tau expression within the pancreas, with a particular focus on the pancreatic β cell (Chapter 4) and links this to the presence of relevant Tau modifiers (Chapter 5). Based on these findings, preliminary work to optimise the combination of relevant Tau antibodies using a 7-colour multiplex staining technique which will allow the simultaneous analysis of multiple markers in disease-relevant and control pancreas, is also described (Methods, fig. 2.8).

6.2 Antibody validation

The complexity of Tau expression and of its PTM signature has led to the generation of many Tau antibodies that detect various forms of Tau. Antibodies are widely used in research and yet it is alarming that some of the most commonly used antibodies can be unreliable [247]. There are a multitude of Tau antibodies available commercially and

several studies validating specific Tau antibodies have been published in the last decade [232–234]. However, there is still a long way to go. In collaboration with Dr Irina Stefana (University of Oxford), we have validated 53 Tau antibodies for WB (Oxford) and a subset of 35 antibodies for IHC (Exeter) applications. Using relevant recombinant proteins, cell lines, mouse models (transgenic overexpression and, importantly, models where Tau is expressed at endogenous levels) and phosphatase treatments, we have carefully validated a series of commonly used Tau reagents (Chapter 3).

6.2.1 Traffic light system (TLS)

Here, for the first time, we develop and describe a TLS to visualise the suitability and specificity of antibodies for use in WB and IHC. The TLS allows visualisation of the specificity of immunostaining with each Tau antibody by combining our observations into a simple: Red – STOP; Amber – proceed with caution; and Green – GO label. The antibody validation strategies and the TLS visualisation method have greatly enriched the existing Tau antibody validation data and have identified a range of important observations that will impact the study of Tau in the future.

6.2.2 Total Tau antibodies do not detect all forms of Tau

One of the most important observations is that many widely used total Tau antibodies (Tau N-term, 5A6, SP70, Tau-12, Tau-5, HT7, 77E9, K9JA) do not detect all forms of Tau. Crucially, the phosphorylation status of Tau impacts these antibodies' ability to recognise their epitope. This is clearly demonstrated by the finding that pre-treatment of either the tissue, or protein lysate, with a phosphatase enzyme dramatically increases the antibody recognition. This observation is alarming and urges careful re-evaluation of previously published data. Many papers use the signal from total Tau antibodies to quantify the absolute amount of Tau in cells and to normalise changes

in phosphorylated forms. According to the data presented here, this would lead to a dramatic underestimation of Tau protein levels within the system and over-inflate the change in phosphorylation status. In total, four out of six Tau antisera with epitopes directed against the N-terminal domain, four out of four at PRD and one out of two at the C-terminal domain were impacted by the phosphorylation status of Tau. The antisera least affected have epitopes in N-terminal domain (43D, Tau-12 and Tau-13) or in the C-terminal domain (Tau-46, although this one is impacted by cross reaction if Tau is present at low levels). As such, antibodies with epitopes in the N-terminal domain, which is the least prone to phosphorylation, and the end of the C-terminal, are likely to be more appropriate for studies examining total Tau expression and localisation compared to antibodies with epitopes in the PRD.

Another important observation relates to the ability of different total Tau antibodies to recognise Tau from different species. For example, K9JA efficiently recognises murine Tau, and is less likely to recognise human Tau when expressed at endogenous low levels. In contrast, Tau-12 and Tau-13 recognise human Tau more efficiently than mouse Tau. Tau-5 (Abcam) and HT7 Tau antibodies could not detect Tau at endogenous levels in the WT or hTau mice. This would preclude their use in studies where Tau is expressed at low levels. The differences in reactivity are likely explained by sequence differences in the epitope regions and the original species of Tau used as the immunogen and the sensitivity of different Total Tau antibodies to recognise endogenous levels of Tau. Based on these findings, the following recommendations are made.

1. If the goal is to quantify Total Tau expression in human FFPE brain studies, Tau-13 is the most suitable antibody. Alternatively, tissues or lysates could be pre-treated with phosphatase before assessment. However, this does not rule out other Tau modifications impacting on recognition.

2. Ensure that the choice of Total Tau antisera reflects the species in which the studies are being performed.

3. Ensure that when examining endogenous Tau levels the total Tau antisera selected are capable of recognising low levels of expression without cross reactivity.

6.3 Characterisation of Tau in human pancreas

Using the carefully validated antisera described in Chapter 3, it is confirmed that Tau forms are present in the pancreas. In agreement with previous studies, both RNA and protein expression of Tau and pTau forms are observed in control, T1D and T2D pancreas. Expression was assessed in ductal, acinar and islets cells, with a particular focus on β cells, and in pancreatic nerves (internal positive control). Key observations are summarised below:

1. Tau is highly expressed in the cytoplasm of β cells. Immunostaining with isoform-specific Tau antibodies suggests that the predominant form is the 1N3R form. Unfortunately, firm conclusions about the presence of 4R-Tau isoforms cannot be made, due to the lack of a reliable 4R-Tau isoform-specific antibody.

2. Tau is phosphorylated at multiple residues (pSer198, pSer199,pSer202/Thr205, pThr231, pSer396, pTau-E178, pSer409) at high levels and located in the nucleus in endocrine and acinar cells in the pancreas. The observation that multiple specific pTau antisera are immunopositive in the nucleus argues that Tau is present. The localisation of Tau in the nucleus has been previously discussed both in neuronal and non-neuronal cells and it may play a role in the nucleolar organization and/or heterochromatization of rRNA genes and in DNA integrity [260], [261], [262]. The study of nuclear Tau is challenging because the nuclear Tau epitopes are not easily detectable. As such, most studies have used formic

acid (FA) to reveal the nuclear epitopes of Tau. FA, however, removes phosphate groups from proteins and therefore, the phosphorylation state of nuclear Tau remains unexplored.

3. Total Tau antisera, do not recognise the nuclear form of pTau, even in situations where the tissue has been pre-treated with λPP and/or FA. This suggests that other modifications and/or conformational changes have impacted on binding.

6.3.1 Tau has at least two functional roles in the β cells

The work presented here suggests that there are at least two forms of Tau in the β cells; a cytoplasmic Tau form and a nuclear Tau form and therefore, it is likely that the cytoplasmic Tau and the nuclear Tau forms also have two distinct functional roles in the β cells (fig. 6.1). A recent study has demonstrated that glucose regulates microtubule disassembly and the degree of insulin secretion via an impact on Tau phosphorylation and therefore cytosolic Tau may play an important role in insulin secretion [183]. Furthermore, our preliminary data suggest that nuclear Tau plays a role in cell replication (fig A.2) but more evidence is required to support this fully.

6.3.2 The phosphorylation status of Tau differs in β cells and neurons

The phosphorylation signature of Tau differs in neurons and β cells both in health and disease (Table 6.1). Tau is phosphorylated at Thr181 in the control and AD brain but not in pancreatic β cells. Residues Ser198, Ser199, Ser202, Thr205, Thr217, Thr231, Ser396 and Ser404 are phosphorylated both in the brain (control and AD) and in β cells (control, T1D). Residues Thr214, Thr238 and Ser422 are phosphorylated in the AD brain but not in β cells. Ser409 is phosphorylated in the AD brain and in the β

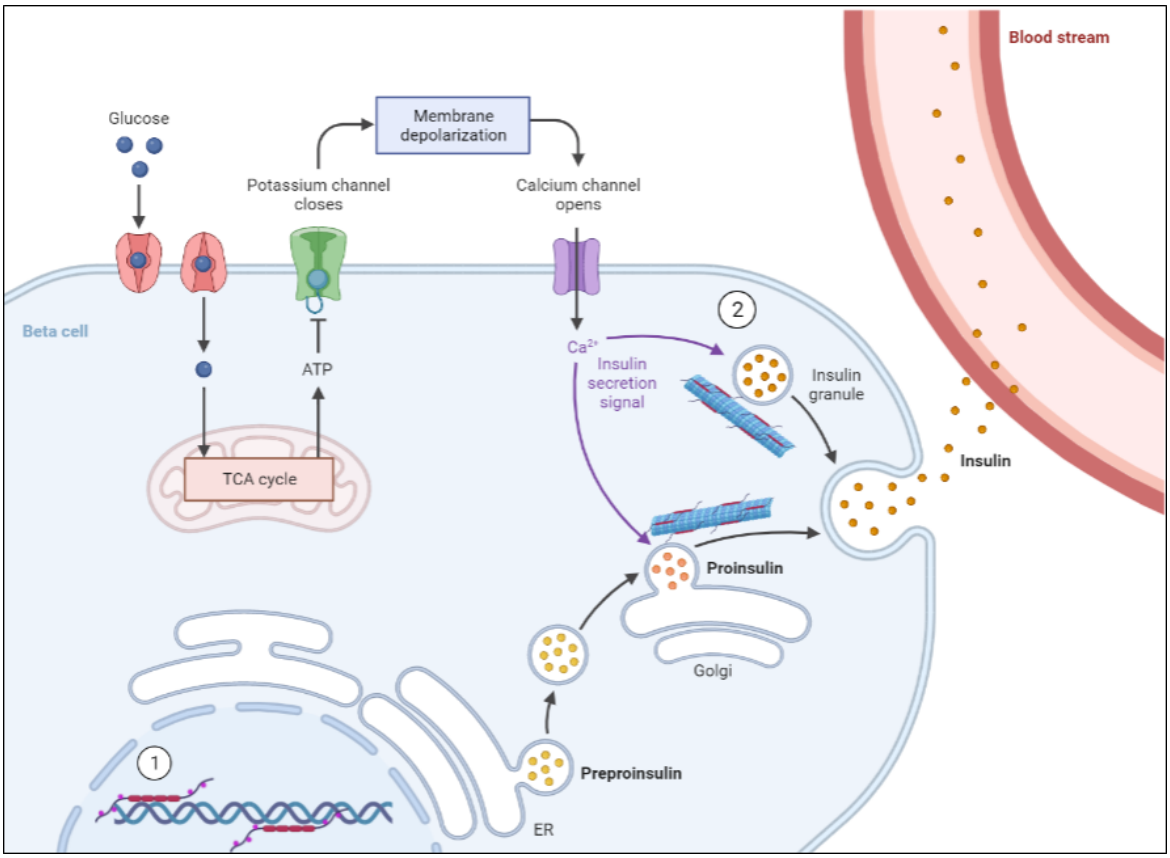

Fig. 6.1 **Putative function of Tau in β cells.** 1. Under basal conditions, nuclear pTau binds to the DNA and 2. cytoplasmic Tau attaches to the microtubules promoting microtubule assembly and stability. Apapted from Biorender (https://biorender.com/).

cells (control and T1D). These observations suggest that the phosphorylation signature of Tau may be cell- and disease-specific. It would be interesting to further investigate whether the phosphorylation status of other Tau forms are affected by age and also to explore whether the phosphorylation pattern of nuclear and cytoplasmic forms of Tau differs.

6.3.3 PHFs may not be a typical feature of pancreatic Tau

It has previously been reported that elevated Tau expression and hyperphosphorylated Tau forms are present in the pancreatic islets of subjects diagnosed with T2D [179, 177, 180]. Contrary to these studies implying that the PHF-raised Tau antibodies

Table 6.1 **Pancreatic Tau is phosphorylated at multiple residues.** This table contains information about which Tau residues can be modified by which kinases and phosphatases and describes there expression in the β cells (control and T1D) and in the brain (control and AD).

Tau residue	Kinases	Phosphatases	Pancreas (β cells)	Brain
pT181	GSK3-β, CDK5		x	control, AD
pS198	GSK3-β	PP2A	control, T1D	control, AD
pS199	GSK3-β, CDK5	PP2A	control, T1D	control, AD
pS202/Thr205	GSK3-β, CDK5	PP2A	control, T1D	control, AD
pT214	GSK3-β, CDK5		x	AD
pT217	GSK3-β, CDK5	PP2A	control, T1D	control, AD
pT231	GSK3-β, CDK5	PIN1	control, T1D	control, AD
pT238	CK1, PSK2		x	AD
pS262	MARK, GSK3-β	PP2A	?	AD
pS396	CDK5, GSK3-β	PP2A	control, T1D	control, AD
pS404	GSK3-β, CDK5	PP2A	very low (T1D)	control, AD
pS409	GSK3-β		control, T1D	AD
pS422	TTBK1		x	AD

detect Tau forms in the β cells [177], the work presented here suggest that these antibodies do not detect Tau forms in the β cells of those diagnosed with or without T2D. The TLS-validation demonstrates their specificity for Tau in FFPE brain tissue but no signal was detected with these antibodies in the FFPE pancreas tissues from organ donors. This does not necessarily argue that Tau is not hyperphosphorylated in human pancreas. Rather, the work presented here agrees that pancreatic Tau can be phosphorylated at multiple residues and suggests that the PHF-raised antibodies detect a specific conformation of Tau that is present in the AD brain but may not be present in the β cells and further imply that the regulation and function of Tau may also be cell-dependent.

6.3.4 pTau translocation

Based on the observation that Tau may be highly phosphorylated in the nucleus, the pTau-E178 antisera was selected to study the impact of ageing and disease status on the

localisation of this form of Tau. The studies presented here demonstrate that in young individuals, pTau (as detected with the pTau-E178) is present primarily within the nucleus, with limited pTau present in the cytoplasm. Interestingly, preliminary work suggests that proliferation induces the translocation of pTau to the cytoplasm. This provides further support for the association of pTau forms, perhaps influencing DNA stability or structure. During proliferation though, when the DNA is replicating, the pTau is transported to the cytoplasm. As individuals age or under disease conditions, an accumulation of pTau forms in the cytoplasm is observed. It is well known that the accumulation of pTau forms in the cytoplasm of neuronal cells impacts on normal function, potentially through interference with non-phosphorylated forms. It is tempting to speculate that under certain circumstances (ageing, obesity, pathological or stress conditions), nuclear Tau translocates to the cytoplasm of the β cells, where it impacts on microtubule dynamics and, subsequently, insulin secretion, potentially by trapping the insulin granules and blocking insulin secretion (fig. 6.2). This is supported by immunostaining data suggesting that β cells with cytoplasmic pTau either have low levels of insulin and high levels of cytoplasmic pTau or high levels of insulin and low levels of cytoplasmic pTau.

An interesting aspect for future studies would be to explore the nucleocytoplasmic transport (NCT) mechanism in the β cells. NCT is the mechanism to control the import and export of molecules in the nucleus and is mainly regulated by the nuclear pore complex (NPC), which further consists of nucleoporins (Nups) [298]. While the number of Nups depends on the cell cycle phase, there are a few classes of Nups that are quite fragile in non-dividing cells. NCT defects, such as the mislocalisation of Nups (either to the cytoplasm or the nucleus), have been associated with neurodegeneration and progeria. Interestingly, pTau interacts directly with Nup98 [299, 300]. Upon interaction, the Nup98:pTau complex accumulates in the cytoplasm. Such mislocalisation events

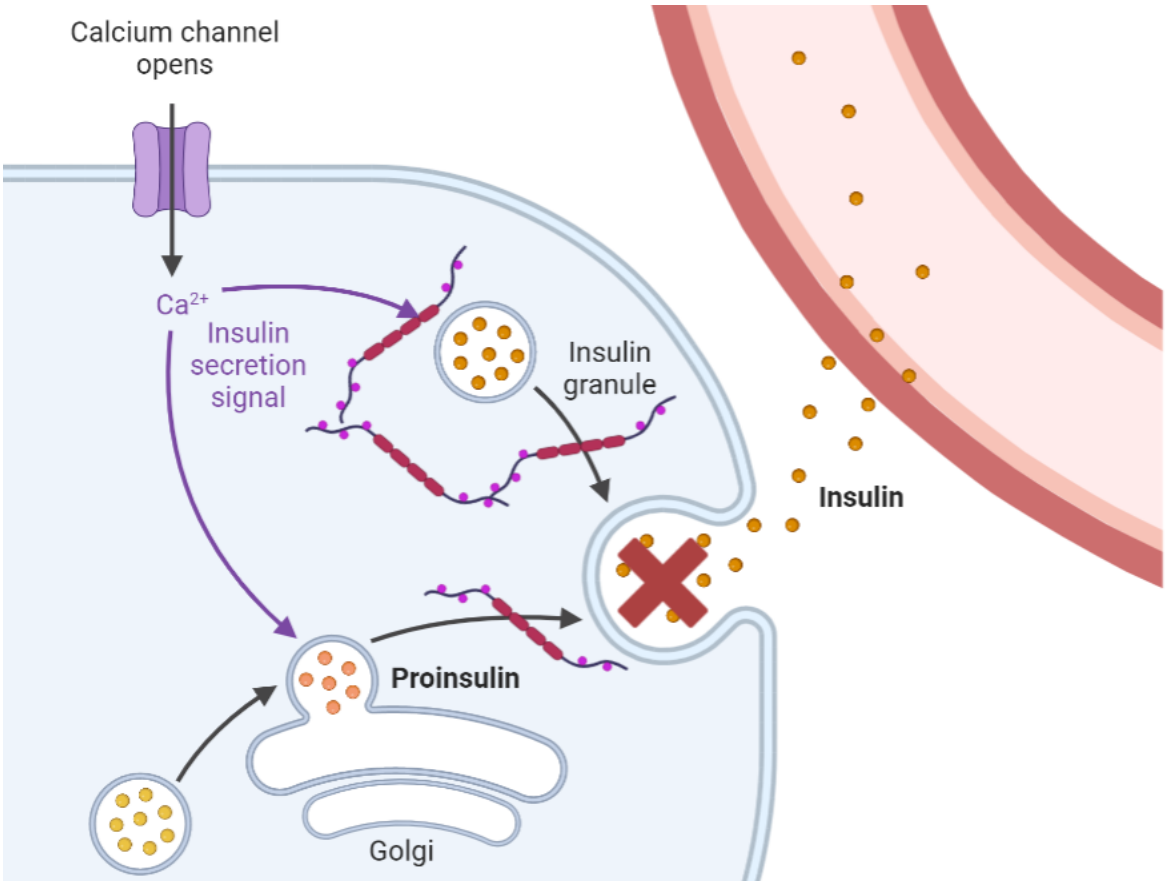

Fig. 6.2 **Insulin secretion and microtubules in disease.** Upon glucose uptake, the membrane is depolarised and the calcium channel open. Elevated intracellular calcium stimulates insulin secretion by promoting the exocytosis of insulin granules. The presence of pTau in the cytoplasm of β cells may trap insulin and inhibit its secretion. Created in Biorender (https://biorender.com/).

cause the nucleus:cytoplasm barrier to become leaky potentially permitting more pTau molecules to travel to the cytoplasm and promoting the mislocalisation of other molecules as well.

6.3.5 Detection of nuclear Tau epitopes using total Tau antisera

It remains unknown whether total Tau antibodies can recognise pTau in the cytoplasm. We speculate that total Tau antibodies do not bind nuclear pTau, because the latter is

bound to DNA. If pTau is no longer associated with DNA, it is expected that these antibodies may now access such forms. The observation that total and phospho-specific Tau antibodies do co-localise in the cytoplasm of β cells supports this hypothesis, however, further studies are required to confirm this. For example, it would be interesting to test total (Tau-12, Tau-13) and phospho-specific Tau antibodies (pTau-E178) using proximity ligation assays (PLA) to assess if pTau forms in the cytoplasm are recognised by total Tau antibodies. A positive PLA signal in this scenario would suggest that the total Tau antibody and the pTau antibody are located in close proximity, i.e. on the same Tau molecule. Further studies could identify ways to artificially modulate pTau forms and assess impacts on insulin secretion. This will likely be challenging though as the pTau form present appears to be modified at multiple residues which are modulated by a range of different Tau modifiers. Studies focused on altering just one of the modifiers may not recapitulate the observations *in vivo*.

6.4 Tau modifiers

Tau phosphorylation is one of the key PTMs associated with brain pathologies, and the disruption of the kinase:phosphatase equilibrium has been in the spotlight for several decades. Tau modifiers have not been studied extensively in the human pancreas, and certainly not in relation to Tau modifications. The work presented here provides a comprehensive overview of the key Tau modifiers that are expressed in β cells (Table 6.1). RNA and protein data support the presence of DYRK1A, SET and HDAC6 at high levels in beta cells, whereas CDK5, GSK3-β and MARK4 are present at more modest levels. Although the RNAseq data suggest that these modifiers may be age- and/or disease-dependent and could influence the PTM signature of Tau, the data is limited and requires more extensive studies. The protein expression level of these Tau

modifiers was explored in a preliminary phase that yielded promising observations that require further follow-up. Taken together, this work demonstrates that pancreatic Tau is phosphorylated at multiple residues (Chapter 4) and that kinases which are highly expressed in β cells (Chapter 5) may phosphorylate Tau at the corresponding residues (Table 6.1).

6.5 Multiplex staining

OPAL™ is a staining method for multiplex fluorescent IHC in FFPE tissue. This technique allows the analysis of whole slide scans stained for up to seven markers ensuring that there is limited possibility of antibody cross reactivity, fluorophore crosstalk and interference from tissue AF signal within the tissue. Although the Tau antibody panel for multiplex staining has been finalised, due to time and COVID limitations impacting on accessibility to the lab, the staining was not performed and as such the analysis remains ongoing. This analysis will allow for quantification of total tau in the β cells in ageing and in diabetes, thorough investigation of whether there is an isoform imbalance associated with age, BMI and/or disease, further confirmation of which residues are phosphorylated and examination of whether there is a change in the cellular localisation of multiple pTau forms. Taking this to a next step, multiplex would allow for the further association between relevant Tau residues and relevant Tau modifiers.

6.6 Conclusions

Tau is a very complex protein that was traditionally known as a neuron-specific protein. Recently, more and more data suggest that Tau may play an important role in the pancreatic β cells. The complexity of Tau renders the full characterisation of its

expression and phosphorylation signature prior to any functional experiments a vital step and it would be beneficial to take into account what is already known in the brain prior to applying it to the pancreas. This work highlights the importance of appropriate validation of Tau antibodies and sets the basis for the careful characterisation of Tau protein in the β cells. In summary this project;

- Highlights the importance of appropriate antibody validation. Validation of Tau antibodies and the development of the TLS system provides crucial information about the specificity and efficacy of widely used antibodies and not only sets a strong basis for the further characterisation of Tau in the human pancreas but also urges for careful re-evaluation of published data.

- Provides the base for the full characterisation of Tau and pTau forms in the human pancreas proposing that the phosphorylation signature of Tau in human pancreas and brain is different. This work provides evidence that there are at least two different functional roles of Tau in the nucleus and the cytoplasm of β cells further proposing that the nuclear pTau form may translocate to the cytoplasm with age impacting on insulin secretion.

- Provides an overview of some of the key Tau modifiers expression in the human pancreas in RNA and protein level.

References

[1] Alois Alzheimer. Über eine eigenartige erkrankung der hirnrinde [article in german]. *Allg Z Psych Psych-gerich Med*, 64:146–148, 1907.

[2] Hanns Hippius and Gabriele Neundörfer. The discovery of alzheimer's disease. *Dialogues in clinical neuroscience*, 2022.

[3] MB Graeber, S Kösel, R Egensperger, RB Banati, U Müller, K Bise, P Hoff, HJ Möller, K Fujisawa, and P Mehraein. Rediscovery of the case described by alois alzheimer in 1911: historical, histological and molecular genetic analysis. *Neurogenetics*, 1(1):73–80, 1997.

[4] Murray D Weingarten, Arthur H Lockwood, Shu-Ying Hwo, and Marc W Kirschner. A protein factor essential for microtubule assembly. *Proceedings of the National Academy of Sciences*, 72(5):1858–1862, 1975.

[5] Jean Pierre Brion, AM Couck, E Passareiro, and Jacqueline Flament-Durand. Neurofibrillary tangles of alzheimer's disease: an immunohistochemical study. *Journal of submicroscopic cytology*, 17(1):89–96, 1985.

[6] Inge Grundke-Iqbal, Khalid Iqbal, Yunn-Chyn Tung, Maureen Quinlan, Henryk M Wisniewski, and Lester I Binder. Abnormal phosphorylation of the microtubule-associated protein tau (tau) in alzheimer cytoskeletal pathology. *Proceedings of the National Academy of Sciences*, 83(13):4913–4917, 1986.

[7] Yasuo IHARA, Nobuyuki NUKINA, Reiko MIURA, and Midori OGAWARA. Phosphorylated tau protein is integrated into paired helical filaments in alzheimer's disease. *The Journal of Biochemistry*, 99(6):1807–1810, 1986.

[8] Stéphane Flament, André Delacourte, Brigitte Hémon, and André Défossez. Characterization of two pathological tau protein variants in alzheimer brain cortices. *Journal of the neurological sciences*, 92(2-3):133–141, 1989.

[9] SG Greenberg, P Davies, JD Schein, and LI Binder. Hydrofluoric acid-treated tau phf proteins display the same biochemical properties as normal tau. *Journal of Biological Chemistry*, 267(1):564–569, 1992.

[10] Jocelyne Léger, Martina Kempf, Gloria Lee, and Roland Brandt. Conversion of serine to aspartate imitates phosphorylation-induced changes in the structure and function of microtubule-associated protein tau. *Journal of Biological Chemistry*, 272(13):8441–8446, 1997.

[11] Susanne Illenberger, Qingyi Zheng-Fischhofer, Ute Preuss, Karsten Stamer, Karlheinz Baumann, Bernhard Trinczek, Jacek Biernat, Robert Godemann, Eva-Maria Mandelkow, and Eckhard Mandelkow. The endogenous and cell cycle-dependent phosphorylation of tau protein in living cells: implications for alzheimer's disease. *Molecular biology of the cell*, 9(6):1495–1512, 1998.

[12] Virginia MY Lee, Michel Goedert, and John Q Trojanowski. Neurodegenarative tauopathies. *Annual review of neuroscience*, 24:1121, 2001.

[13] Felix Hernández and Jesús Avila. Tauopathies. *Cellular and Molecular Life Sciences*, 64(17):2219–2233, 2007.

[14] Gabor G Kovacs. Tauopathies. *Handbook of clinical neurology*, 145:355–368, 2018.

[15] Dah-eun Chloe Chung, Shanu Roemer, Leonard Petrucelli, and Dennis W Dickson. Cellular and pathological heterogeneity of primary tauopathies. *Molecular neurodegeneration*, 16(1):1–20, 2021.

[16] Heiko Braak and Eva Braak. Neuropathological stageing of alzheimer-related changes. *Acta neuropathologica*, 82(4):239–259, 1991.

[17] Heiko Braak and EVA Braak. Staging of alzheimer's disease-related neurofibrillary changes. *Neurobiology of aging*, 16(3):271–278, 1995.

[18] Heiko Braak, Kelly Del Tredici, Udo Rüb, Rob AI De Vos, Ernst NH Jansen Steur, and Eva Braak. Staging of brain pathology related to sporadic parkinson's disease. *Neurobiology of aging*, 24(2):197–211, 2003.

[19] Davina Biel, Matthias Brendel, Anna Rubinski, Katharina Buerger, Daniel Janowitz, Martin Dichgans, Nicolai Franzmeier, Alzheimer's Disease Neuroimaging Initiative (ADNI, et al. Tau-pet and in vivo braak-staging as a prognostic marker in alzheimer's disease. *medRxiv*, 2021.

[20] Marie Jouanne, Sylvain Rault, and Anne-Sophie Voisin-Chiret. Tau protein aggregation in alzheimer's disease: an attractive target for the development of novel therapeutic agents. *European Journal of Medicinal Chemistry*, 139:153–167, 2017.

[21] Christopher Edward James Lovejoy. *iPSC derived cerebral organoids as a model of tauopathy*. PhD thesis, UCL (University College London), 2021.

[22] Athena Andreadis. Tau gene alternative splicing: expression patterns, regulation and modulation of function in normal brain and neurodegenerative diseases. *Biochimica Et Biophysica Acta (BBA)-Molecular Basis Of Disease*, 1739(2-3):91–103, 2005.

[23] Irene S Georgieff, RK Liem, Dominique Couchie, Carmelo Mavilia, Jacques Nunez, and Michael L Shelanski. Expression of high molecular weight tau in the central and peripheral nervous systems. *Journal of cell science*, 105(3):729–737, 1993.

[24] Itzhak Fischer and Peter W Baas. Resurrecting the mysteries of big tau. *Trends in neurosciences*, 43(7):493–504, 2020.

[25] M Goedert, CM Wischik, RA Crowther, JE Walker, and A Klug. Cloning and sequencing of the cdna encoding a core protein of the paired helical filament of alzheimer disease: identification as the microtubule-associated protein tau. *Proceedings of the National Academy of Sciences*, 85(11):4051–4055, 1988.

[26] Kenneth S Kosik, Lisa D Orecchio, Shelley Bakalis, and Rachael L Neve. Developmentally regulated expression of specific tau sequences. *Neuron*, 2(4):1389–1397, 1989.

[27] Daniah Trabzuni, Selina Wray, Jana Vandrovcova, Adaikalavan Ramasamy, Robert Walker, Colin Smith, Connie Luk, J Raphael Gibbs, Allissa Dillman, Dena G Hernandez, et al. Mapt expression and splicing is differentially regulated by brain region: relation to genotype and implication for tauopathies. *Human molecular genetics*, 21(18):4094–4103, 2012.

[28] Bruce L Goode and Stuart C Feinstein. Identification of a novel microtubule binding and assembly domain in the developmentally regulated inter-repeat region of tau. *The Journal of cell biology*, 124(5):769–782, 1994.

[29] Gloria Lee, Rachael L Neve, and Kenneth S Kosik. The microtubule binding domain of tau protein. *Neuron*, 2(6):1615–1624, 1989.

[30] Sadasivam Jeganathan, Martin von Bergen, Henrik Brutlach, Heinz-Jürgen Steinhoff, and Eckhard Mandelkow. Global hairpin folding of tau in solution. *Biochemistry*, 45(7):2283–2293, 2006.

[31] F Braak, Heiko Braak, and E M Mandelkow. A sequence of cytoskeleton changes related to the formation of neurofibrillary tangles and neuropil threads. *Acta neuropathologica*, 87:554–567, 1994.

[32] Gilles Carmel, Edward M Mager, Lester I Binder, and Jeff Kuret. The structural basis of monoclonal antibody alz50's selectivity for alzheimer's disease pathology. *Journal of Biological Chemistry*, 271(51):32789–32795, 1996.

[33] B Trinczek, A Ebneth, EM Mandelkow, and E Mandelkow. Tau regulates the attachment/detachment but not the speed of motors in microtubule-dependent transport of single vesicles and organelles. *Journal of cell science*, 112(14):2355–2367, 1999.

[34] A Ebneth, R Godemann, K Stamer, S Illenberger, B Trinczek, E-M Mandelkow, and E Mandelkow. Overexpression of tau protein inhibits kinesin-dependent trafficking of vesicles, mitochondria, and endoplasmic reticulum: implications for alzheimer's disease. *The Journal of cell biology*, 143(3):777–794, 1998.

[35] Amy M Pooler and Diane P Hanger. Functional implications of the association of tau with the plasma membrane. *Biochemical Society Transactions*, 38(4):1012–1015, 2010.

[36] J Chen, Y Kanai, NJ Cowan, and N Hirokawa. Projection domains of map2 and tau determine spacings between microtubules in dendrites and axons. *Nature*, 360(6405):674–677, 1992.

[37] Tamta Arakhamia, Christina E Lee, Yari Carlomagno, Mukesh Kumar, Duc M Duong, Hendrik Wesseling, Sean R Kundinger, Kevin Wang, Dewight Williams, Michael DeTure, et al. Posttranslational modifications mediate the structural diversity of tauopathy strains. *Cell*, 180(4):633–644, 2020.

[38] Carolina Alquezar, Shruti Arya, and Aimee W Kao. Tau post-translational modifications: dynamic transformers of tau function, degradation, and aggregation. *Frontiers in Neurology*, 11:595532, 2021.

[39] Philip Cohen. The origins of protein phosphorylation. *Nature cell biology*, 4(5):E127–E130, 2002.

[40] Waltraud Mair, Jan Muntel, Katharina Tepper, Shaojun Tang, Jacek Biernat, William W Seeley, Kenneth S Kosik, Eckhard Mandelkow, Hanno Steen, and Judith A Steen. Flexitau: quantifying post-translational modifications of tau protein in vitro and in human disease. *Analytical chemistry*, 88(7):3704–3714, 2016.

[41] Friedel Drepper, Jacek Biernat, Senthilvelrajan Kaniyappan, Helmut E Meyer, Eva Maria Mandelkow, Bettina Warscheid, and Eckhard Mandelkow. A combinatorial native ms and lc-ms/ms approach reveals high intrinsic phosphorylation of human tau but minimal levels of other key modifications. *Journal of Biological Chemistry*, 295(52):18213–18225, 2020.

[42] Hanna Ksiezak-Reding, Wan-Kyng Liu, and Shu-Hui Yen. Phosphate analysis and dephosphorylation of modified tau associated with paired helical filaments. *Brain research*, 597(2):209–219, 1992.

[43] A Watanabe, M Hasegawa, M Suzuki, K Takio, M Morishima-Kawashima, K Titani, T Arai, KS Kosik, and Y Ihara. In vivo phosphorylation sites in fetal and adult rat tau. *Journal of Biological Chemistry*, 268(34):25712–25717, 1993.

[44] Carmen Feijoo, David G Campbell, Ross Jakes, Michel Goedert, and Ana Cuenda. Evidence that phosphorylation of the microtubule-associated protein tau by sapk4/p38δ at thr50 promotes microtubule assembly. *Journal of cell science*, 118(2):397–408, 2005.

[45] J Biernat, N Gustke, G Drewes, E Mandelkow, et al. Phosphorylation of ser262 strongly reduces binding of tau to microtubules: distinction between phf-like immunoreactivity and microtubule binding. *Neuron*, 11(1):153–163, 1993.

[46] A Schneider, J Biernat, M Von Bergen, E Mandelkow, and E-M Mandelkow. Phosphorylation that detaches tau protein from microtubules (ser262, ser214) also protects it against aggregation into alzheimer paired helical filaments. *Biochemistry*, 38(12):3549–3558, 1999.

[47] Hirotaka Yoshida and Yasuo Ihara. τ in paired helical filaments is functionally distinct from fetal τ: Assembly incompetence of paired helical filament-τ. *Journal of neurochemistry*, 61(3):1183–1186, 1993.

[48] Eriko S Matsuo, Ryong-Woon Shin, Melvin L Billingsley, Andre Van deVoorde, Michael O'Connor, John Q Trojanowski, and Virginia MY Lee. Biopsy-derived adult human brain tau is phosphorylated at many of the same sites as alzheimer's disease paired helical filament tau. *Neuron*, 13(4):989–1002, 1994.

[49] M Hasegawa, R Jakes, RA Crowther, VM-Y Lee, Y Ihara, and M Goedert. Characterization of mab ap422, a novel phosphorylation-dependent monoclonal antibody against tau protein. *FEBS letters*, 384(1):25–30, 1996.

[50] Yuxing Xia, Stefan Prokop, Kimberly-Marie M Gorion, Justin D Kim, Zachary A Sorrentino, Brach M Bell, Alyssa N Manaois, Paramita Chakrabarty, Peter Davies, and Benoit I Giasson. Tau ser208 phosphorylation promotes aggregation and reveals neuropathologic diversity in alzheimer's disease and other tauopathies. *Acta Neuropathologica Communications*, 8(1):1–17, 2020.

[51] Valeriy Duka, Jae-Hoon Lee, Joel Credle, Jonathan Wills, Adam Oaks, Ciaran Smolinsky, Ketul Shah, Deborah C Mash, Eliezer Masliah, and Anita Sidhu. Identification of the sites of tau hyperphosphorylation and activation of tau kinases in synucleinopathies and alzheimer's diseases. *PloS one*, 8(9):e75025, 2013.

[52] Amitabha Sengupta, Juraj Kabat, Michal Novak, Qiongli Wu, Inge Grundke-Iqbal, and Khalid Iqbal. Phosphorylation of tau at both thr 231 and ser 262 is required for maximal inhibition of its binding to microtubules. *Archives of biochemistry and biophysics*, 357(2):299–309, 1998.

[53] Gerard Manning, David B Whyte, Ricardo Martinez, Tony Hunter, and Sucha Sudarsanam. The protein kinase complement of the human genome. *Science*, 298(5600):1912–1934, 2002.

[54] Ludovic Martin, Xenia Latypova, Cornelia M Wilson, Amandine Magnaudeix, Marie-Laure Perrin, Catherine Yardin, and Faraj Terro. Tau protein kinases: involvement in alzheimer's disease. *Ageing research reviews*, 12(1):289–309, 2013.

[55] Taeko Kimura, Govinda Sharma, Koichi Ishiguro, and Shin-ichi Hisanaga. Phospho-tau bar code: Analysis of phosphoisotypes of tau and its application to tauopathy. *Frontiers in Neuroscience*, 12:44, 2018.

[56] Sheelagh Frame and Philip Cohen. Gsk3 takes centre stage more than 20 years after its discovery. *Biochemical Journal*, 359(1):1–16, 2001.

[57] Adrian J Harwood. Regulation of gsk-3: a cellular multiprocessor. *Cell*, 105(7):821–824, 2001.

[58] Bradley W Doble and James R Woodgett. Gsk-3: tricks of the trade for a multi-tasking kinase. *Journal of cell science*, 116(7):1175–1186, 2003.

[59] Karelle Leroy, Zehra Yilmaz, and J-P Brion. Increased level of active gsk-3β in alzheimer's disease and accumulation in argyrophilic grains and in neurones at different stages of neurofibrillary degeneration. *Neuropathology and applied neurobiology*, 33(1):43–55, 2007.

[60] Haruyasu Yamaguchi, Koichi Ishiguro, Tsuneko Uchida, Akihiko Takashima, Cynthia A Lemere, and Kazutomo Imahori. Preferential labeling of alzheimer neurofibrillary tangles with antisera for tau protein kinase (tpk) i/glycogen synthase kinase-3β and cyclin-dependent kinase 5, a component of tpk ii. *Acta neuropathologica*, 92(3):232–241, 1996.

[61] Jin-Jing Pei, Toshihisa Tanaka, Yunn-Chyn Tung, EVA Braak, Khalid Iqbal, and Inge Grundke-Iqbal. Distribution, levels, and activity of glycogen synthase kinase-3 in the alzheimer disease brain. *Journal of Neuropathology & Experimental Neurology*, 56(1):70–78, 1997.

[62] Kazutomo Imahori and Tsuneko Uchida. Physiology and pathology of tau protein kinases in relation to alzheimer's disease. *The Journal of Biochemistry*, 121(2):179–188, 1997.

[63] Wendy Noble, Vicki Olm, Kazuyuki Takata, Evelyn Casey, O Mary, Jordana Meyerson, Kate Gaynor, John LaFrancois, Lili Wang, Takayuki Kondo, et al. Cdk5 is a key factor in tau aggregation and tangle formation in vivo. *Neuron*, 38(4):555–565, 2003.

[64] Jonathan C Cruz and Li-Huei Tsai. Cdk5 deregulation in the pathogenesis of alzheimer's disease. *Trends in molecular medicine*, 10(9):452–458, 2004.

[65] Olivia Engmann and Karl P Giese. Crosstalk between cdk5 and gsk3β: Implications for alzheimer's disease. *Frontiers in molecular neuroscience*, page 2, 2009.

[66] Taeko Kimura, Koichi Ishiguro, and Shin-ichi Hisanaga. Physiological and pathological phosphorylation of tau by cdk5. *Frontiers in molecular neuroscience*, 7:65, 2014.

[67] Gentry N Patrick, Lawrence Zukerberg, Margareta Nikolic, Suzanne de La Monte, Pieter Dikkes, and Li-Huei Tsai. Conversion of p35 to p25 deregulates cdk5 activity and promotes neurodegeneration. *Nature*, 402(6762):615–622, 1999.

[68] Malika Hamdane, Anne-Véronique Sambo, Patrice Delobel, Séverine Bégard, Anne Violleau, André Delacourte, Philippe Bertrand, Jesus Benavides, and Luc Buée. Mitotic-like tau phosphorylation by p25-cdk5 kinase complex. *Journal of Biological Chemistry*, 278(36):34026–34034, 2003.

[69] Neelima B Chauhan, George J Siegel, and Douglas L Feinstein. Propentofylline attenuates tau hyperphosphorylation in alzheimer's swedish mutant model tg2576. *Neuropharmacology*, 48(1):93–104, 2005.

[70] Diane P Hanger, Brian H Anderton, and Wendy Noble. Tau phosphorylation: the therapeutic challenge for neurodegenerative disease. *Trends in molecular medicine*, 15(3):112–119, 2009.

[71] Taro Saito, Toshiya Oba, Sawako Shimizu, Akiko Asada, Koichi M Iijima, and Kanae Ando. Cdk5 increases mark4 activity and augments pathological tau accumulation and toxicity through tau phosphorylation at ser262. *Human molecular genetics*, 28(18):3062–3071, 2019.

[72] Kaori Sato and Seiichi Kawashima. Calpain function in the modulation of signal transduction molecules. *Biological chemistry*, 382(5):743–752, 2001.

[73] Ming-sum Lee, Young T Kwon, Mingwei Li, Junmin Peng, Robert M Friedlander, and Li-Huei Tsai. Neurotoxicity induces cleavage of p35 to p25 by calpain. *Nature*, 405(6784):360–364, 2000.

[74] Michael K Ahlijanian, Nestor X Barrezueta, Robert D Williams, Amy Jakowski, Kim P Kowsz, Sheryl McCarthy, Timothy Coskran, Anthony Carlo, Patricia A Seymour, John E Burkhardt, et al. Hyperphosphorylated tau and neurofilament and cytoskeletal disruptions in mice overexpressing human p25, an activator of cdk5. *Proceedings of the National Academy of Sciences*, 97(6):2910–2915, 2000.

[75] Bernhard Trinczek, Miro Brajenovic, Andreas Ebneth, and Gerard Drewes. Mark4 is a novel microtubule-associated proteins/microtubule affinity-regulating kinase that binds to the cellular microtubule network and to centrosomes. *Journal of Biological Chemistry*, 279(7):5915–5923, 2004.

[76] Armin Schneider, Rico Laage, Oliver Von Ahsen, Achim Fischer, Moritz Rossner, Sigrid Scheek, Sylvia Grünewald, Rohini Kuner, Daniela Weber, Carola Krüger, et al. Identification of regulated genes during permanent focal cerebral ischaemia: characterization of the protein kinase 9b5/markl1/mark4. *Journal of neurochemistry*, 88(5):1114–1126, 2004.

[77] Davide Rovina, Laura Fontana, Laura Monti, Chiara Novielli, Nicolò Panini, Silvia Maria Sirchia, Eugenio Erba, Ivana Magnani, and Lidia Larizza. Microtubule-associated protein/microtubule affinity-regulating kinase 4 (mark4) plays a role in cell cycle progression and cytoskeletal dynamics. *European Journal of Cell Biology*, 93(8-9):355–365, 2014.

[78] Harald Lund, Elin Gustafsson, Anne Svensson, Maria Nilsson, Margareta Berg, Dan Sunnemark, and Gabriel von Euler. Mark4 and mark3 associate with early tau phosphorylation in alzheimer's disease granulovacuolar degeneration bodies. *Acta neuropathologica communications*, 2(1):1–15, 2014.

[79] Gucci Jijuan Gu, Harald Lund, Di Wu, Andries Blokzijl, Christina Classon, Gabriel von Euler, Ulf Landegren, Dan Sunnemark, and Masood Kamali-Moghaddam. Role of individual mark isoforms in phosphorylation of tau at ser262 in alzheimer's disease. *Neuromolecular medicine*, 15(3):458–469, 2013.

[80] Joongkyu Park, Woo-Joo Song, and Kwang Chul Chung. Function and regulation of dyrk1a: towards understanding down syndrome. *Cellular and molecular life sciences*, 66(20):3235–3240, 2009.

[81] Mónica Álvarez, Xavier Estivill, and Susana de la Luna. Dyrk1a accumulates in splicing speckles through a novel targeting signal and induces speckle disassembly. *Journal of cell science*, 116(15):3099–3107, 2003.

[82] Ariadna Laguna, Sergi Aranda, María José Barallobre, Rima Barhoum, Eduardo Fernández, Vassiliki Fotaki, Jean Maurice Delabar, Susana de la Luna, Pedro de la Villa, and Maria L Arbonés. The protein kinase dyrk1a regulates caspase-9-mediated apoptosis during retina development. *Developmental cell*, 15(6):841–853, 2008.

[83] Javier Fernandez-Martinez, Eva M Vela, Mireille Tora-Ponsioen, Oscar H Ocaña, M Angela Nieto, and Juan Galceran. Attenuation of notch signalling by the down-syndrome-associated kinase dyrk1a. *Journal of cell science*, 122(10):1574–1583, 2009.

[84] Heiner Kentrup, Walter Becker, Jörg Heukelbach, Anja Wilmes, Annette Schürmann, Christine Huppertz, Heikki Kainulainen, and Hans-Georg Joost. Dyrk, a dual specificity protein kinase with unique structural features whose activity is dependent on tyrosine residues between subdomains vii and viii. *Journal of Biological Chemistry*, 271(7):3488–3495, 1996.

[85] Barbara Hämmerle, Carina Elizalde, and Francisco J Tejedor. The spatio-temporal and subcellular expression of the candidate down syndrome gene mnb/dyrk1a in the developing mouse brain suggests distinct sequential roles in neuronal development. *European Journal of Neuroscience*, 27(5):1061–1074, 2008.

[86] Wei Qian, Nana Jin, Jianhua Shi, Xiaomin Yin, Xiaoxia Jin, Shibao Wang, Maohong Cao, Khalid Iqbal, Cheng-Xin Gong, and Fei Liu. Dual-specificity tyrosine phosphorylation-regulated kinase 1a (dyrk1a) enhances tau expression. *Journal of Alzheimer's Disease*, 37(3):529–538, 2013.

[87] Yvonne L Woods, Philip Cohen, Walter Becker, Ross Jakes, Michel Goedert, Xuemin Wang, and Christopher G Proud. The kinase dyrk phosphorylates protein-synthesis initiation factor eif2b at ser539 and the microtubule-associated protein tau at thr212: potential role for dyrk as a glycogen synthase kinase 3-priming kinase. *Biochemical Journal*, 355(3):609–615, 2001.

[88] Fei Liu, Zhihou Liang, Jerzy Wegiel, Yu-Wen Hwang, Khalid Iqbal, Inge Grundke-Iqbal, Narayan Ramakrishna, and Cheng-Xin Gong. Overexpression of dyrk1a contributes to neurofibrillary degeneration in down syndrome. *The FASEB Journal*, 22(9):3224, 2008.

[89] Soo-Ryoon Ryoo, Hey Kyeong Jeong, Chinzorig Radnaabazar, Jin-Ju Yoo, Hyun-Jeong Cho, Hye-Won Lee, In-Sook Kim, Young-Hee Cheon, Young Soo Ahn, Sul-Hee Chung, et al. Dyrk1a-mediated hyperphosphorylation of tau. *Journal of Biological Chemistry*, 282(48):34850–34857, 2007.

[90] Clément Despres, Cillian Byrne, Haoling Qi, François-Xavier Cantrelle, Isabelle Huvent, Béatrice Chambraud, Etienne-Emile Baulieu, Yves Jacquot, Isabelle Landrieu, Guy Lippens, et al. Identification of the tau phosphorylation pattern that drives its aggregation. *Proceedings of the National Academy of Sciences*, 114(34):9080–9085, 2017.

[91] Jianhua Shi, Tianyi Zhang, Chunlei Zhou, Muhammad Omar Chohan, Xiaosong Gu, Jerzy Wegiel, Jianhua Zhou, Yu-Wen Hwang, Khalid Iqbal, Inge Grundke-Iqbal, et al. Increased dosage of dyrk1a alters alternative splicing factor (asf)-regulated alternative splicing of tau in down syndrome*. *Journal of Biological Chemistry*, 283(42):28660–28669, 2008.

[92] Xiaomin Yin, Nana Jin, Jianhua Shi, Yanchong Zhang, Yue Wu, Cheng-Xin Gong, Khalid Iqbal, and Fei Liu. Dyrk1a overexpression leads to increase of 3r-tau expression and cognitive deficits in ts65dn down syndrome mice. *Scientific reports*, 7(1):1–12, 2017.

[93] Stanislaw Zolnierowicz. Type 2a protein phosphatase, the complex regulator of numerous signaling pathways. *Biochemical pharmacology*, 60(8):1225–1235, 2000.

[94] Ludovic Martin, Xenia Latypova, Cornelia M Wilson, Amandine Magnaudeix, Marie-Laure Perrin, and Faraj Terro. Tau protein phosphatases in alzheimer's disease: the leading role of pp2a. *Ageing research reviews*, 12(1):39–49, 2013.

[95] Fei Liu, Inge Grundke-Iqbal, Khalid Iqbal, and Cheng-Xin Gong. Contributions of protein phosphatases pp1, pp2a, pp2b and pp5 to the regulation of tau phosphorylation. *European Journal of Neuroscience*, 22(8):1942–1950, 2005.

[96] Cheng-Xin Gong, Toolsee J Singh, Inge Grundke-Iqbal, and Khalid Iqbal. Phosphoprotein phosphatase activities in alzheimer disease brain. *Journal of neurochemistry*, 61(3):921–927, 1993.

[97] Cheng-Xin Gong, Sadia Shaikh, Jian-Zhi Wang, Tanweer Zaidi, Inge Grundke-Iqbal, and Khalid Iqbal. Phosphatase activity toward abnormally phosphorylated τ: decrease in alzheimer disease brain. *Journal of neurochemistry*, 65(2):732–738, 1995.

[98] Fei Liu, Khalid Iqbal, Inge Grundke-Iqbal, Sandra Rossie, and Cheng-Xin Gong. Dephosphorylation of tau by protein phosphatase 5: impairment in alzheimer's disease. *Journal of Biological Chemistry*, 280(3):1790–1796, 2005.

[99] Abdur Rahman, Inge Grundke-Iqbal, and Khalid Iqbal. Phosphothreonine-212 of alzheimer abnormally hyperphosphorylated tau is a preferred substrate of protein phosphatase-1. *Neurochemical research*, 30(2):277–287, 2005.

[100] Parthasarathy Seshacharyulu, Poomy Pandey, Kaustubh Datta, and Surinder K Batra. Phosphatase: Pp2a structural importance, regulation and its aberrant expression in cancer. *Cancer letters*, 335(1):9–18, 2013.

[101] Marc C Mumby and Gernot Walter. Protein serine/threonine phosphatases: structure, regulation, and functions in cell growth. *Physiological reviews*, 73(4):673–699, 1993.

[102] Craig Kamibayashi, Robert Estes, Ronald L Lickteig, Sung-Il Yang, Cheryl Craft, and Marc C Mumby. Comparison of heterotrimeric protein phosphatase 2a containing different b subunits. *Journal of Biological Chemistry*, 269(31):20139–20148, 1994.

[103] Estelle Sontag, Viyada Nunbhakdi-Craig, George S Bloom, and Marc C Mumby. A novel pool of protein phosphatase 2a is associated with microtubules and is regulated during the cell cycle. *The Journal of cell biology*, 128(6):1131–1144, 1995.

[104] Michel Goedert, E Suzanne Cohen, Ross Jakes, and Philip Cohen. p42 map kinase phosphorylation sites in microtubule-associated protein tau are dephosphorylated by protein phosphatase 2a1 implications for alzheimer's disease. *FEBS letters*, 312(1):95–99, 1992.

[105] Jian-Zhi Wang, Cheng-Xin Gong, Tanweer Zaidi, Inge Grundke-Iqbal, and Khalid Iqbal. Dephosphorylation of alzheimer paired helical filaments by protein phosphatase-2a and- 2b. *Journal of Biological Chemistry*, 270(9):4854–4860, 1995.

[106] Jian-Zhi Wang, Inge Grundke-Iqbal, and Khalid Iqbal. Restoration of biological activity of alzheimer abnormally phosphorylated τ by dephosphorylation with protein phosphatase-2a,- 2b and- 1. *Molecular brain research*, 38(2):200–208, 1996.

[107] Malika Bennecib, Cheng-Xin Gong, Inge Grundke-Iqbal, and Khalid Iqbal. Role of protein phosphatase-2a and-1 in the regulation of gsk-3, cdk5 and cdc2 and the phosphorylation of tau in rat forebrain. *FEBS letters*, 485(1):87–93, 2000.

[108] Magdalena Kuszczyk, Wanda Gordon-Krajcer, and Jerzy W Lazarewicz. Homocysteine-induced acute excitotoxicity in cerebellar granule cells in vitro is accompanied by pp2a-mediated dephosphorylation of tau. *Neurochemistry international*, 55(1-3):174–180, 2009.

[109] Ludovic Martin, Amandine Magnaudeix, Françoise Esclaire, Catherine Yardin, and Faraj Terro. Inhibition of glycogen synthase kinase-3β downregulates total tau proteins in cultured neurons and its reversal by the blockade of protein phosphatase-2a. *Brain research*, 1252:66–75, 2009.

[110] Wei Qian, Jianhua Shi, Xiaomin Yin, Khalid Iqbal, Inge Grundke-Iqbal, Cheng-Xin Gong, and Fei Liu. Pp2a regulates tau phosphorylation directly and also indirectly via activating gsk-3β. *Journal of Alzheimer's Disease*, 19(4):1221–1229, 2010.

[111] Jason C Mills, VM Lee, and Randall N Pittman. Activation of a pp2a-like phosphatase and dephosphorylation of tau protein characterize onset of the execution phase of apoptosis. *Journal of Cell Science*, 111(5):625–636, 1998.

[112] Wang Min, Yan Lin, Shibo Tang, Luyang Yu, Haifeng Zhang, Ting Wan, Tricia Luhn, Haian Fu, and Hong Chen. Aip1 recruits phosphatase pp2a to ask1 in tumor necrosis factor–induced ask1-jnk activation. *Circulation research*, 102(7):840–848, 2008.

[113] Chi-Wu Chiang, Ling Yan, and Elizabeth Yang. Phosphatases and regulation of cell death. *Methods in enzymology*, 446:237–257, 2008.

[114] Maud Gratuze, Jacinthe Julien, Franck R Petry, Françoise Morin, and Emmanuel Planel. Insulin deprivation induces pp2a inhibition and tau hyperphosphorylation in htau mice, a model of alzheimer's disease-like tau pathology. *Scientific Reports*, 7(1):1–13, 2017.

[115] Lisette Arnaud, She Chen, Fei Liu, Bin Li, Sabiha Khatoon, Inge Grundke-Iqbal, and Khalid Iqbal. Mechanism of inhibition of pp2a activity and abnormal hyperphosphorylation of tau by i2 pp2a/set. *FEBS letters*, 585(17):2653–2659, 2011.

[116] Takeo Narita, Brian T Weinert, and Chunaram Choudhary. Functions and mechanisms of non-histone protein acetylation. *Nature reviews Molecular cell biology*, 20(3):156–174, 2019.

[117] Casey Cook, Yari Carlomagno, Tania F Gendron, Judy Dunmore, Kristyn Scheffel, Caroline Stetler, Mary Davis, Dennis Dickson, Matthew Jarpe, Michael DeTure, et al. Acetylation of the kxgs motifs in tau is a critical determinant in modulation of tau aggregation and clearance. *Human molecular genetics*, 23(1):104–116, 2014.

[118] Todd J Cohen, Jing L Guo, David E Hurtado, Linda K Kwong, Ian P Mills, John Q Trojanowski, and Virginia MY Lee. The acetylation of tau inhibits its function and promotes pathological tau aggregation. *Nature communications*, 2(1):1–9, 2011.

[119] Sang-Won Min, Xu Chen, Tara E Tracy, Yaqiao Li, Yungui Zhou, Chao Wang, Kotaro Shirakawa, S Sakura Minami, Erwin Defensor, Sue Ann Mok, et al. Critical role of acetylation in tau-mediated neurodegeneration and cognitive deficits. *Nature medicine*, 21(10):1154–1162, 2015.

[120] Todd J Cohen, Dave Friedmann, Andrew W Hwang, Ronen Marmorstein, and Virginia MY Lee. The microtubule-associated tau protein has intrinsic acetyltransferase activity. *Nature structural & molecular biology*, 20(6):756–762, 2013.

[121] Vincent G Allfrey, R Faulkner, and AE300163 Mirsky. Acetylation and methylation of histones and their possible role in the regulation of rna synthesis. *Proceedings of the National Academy of Sciences*, 51(5):786–794, 1964.

[122] James E Brownell, Jianxin Zhou, Tamara Ranalli, Ryuji Kobayashi, Diane G Edmondson, Sharon Y Roth, and C David Allis. Tetrahymena histone acetyltransferase a: a homolog to yeast gcn5p linking histone acetylation to gene activation. *Cell*, 84(6):843–851, 1996.

[123] Jack Taunton, Christian A Hassig, and Stuart L Schreiber. A mammalian histone deacetylase related to the yeast transcriptional regulator rpd3p. *Science*, 272(5260):408–411, 1996.

[124] Michael Grunstein. Histone acetylation in chromatin structure and transcription. *Nature*, 389(6649):349–352, 1997.

[125] Charlotte Hubbert, Amaris Guardiola, Rong Shao, Yoshiharu Kawaguchi, Akihiro Ito, Andrew Nixon, Minoru Yoshida, Xiao-Fan Wang, and Tso-Pang Yao. Hdac6 is a microtubule-associated deacetylase. *Nature*, 417(6887):455–458, 2002.

[126] Huiping Ding, Philip J Dolan, and Gail VW Johnson. Histone deacetylase 6 interacts with the microtubule-associated protein tau. *Journal of neurochemistry*, 106(5):2119–2130, 2008.

[127] Stephen J Haggarty, Kathryn M Koeller, Jason C Wong, Christina M Grozinger, and Stuart L Schreiber. Domain-selective small-molecule inhibitor of histone deacetylase 6 (hdac6)-mediated tubulin deacetylation. *Proceedings of the National Academy of Sciences*, 100(8):4389–4394, 2003.

[128] Didier Portran, Laura Schaedel, Zhenjie Xu, Manuel Théry, and Maxence V Nachury. Tubulin acetylation protects long-lived microtubules against mechanical ageing. *Nature cell biology*, 19(4):391–398, 2017.

[129] Zhenjie Xu, Laura Schaedel, Didier Portran, Andrea Aguilar, Jérémie Gaillard, M Peter Marinkovich, Manuel Théry, and Maxence V Nachury. Microtubules acquire resistance from mechanical breakage through intralumenal acetylation. *Science*, 356(6335):328–332, 2017.

[130] Lisa Eshun-Wilson, Rui Zhang, Didier Portran, Maxence V Nachury, Daniel B Toso, Thomas Löhr, Michele Vendruscolo, Massimiliano Bonomi, James S Fraser, and Eva Nogales. Effects of α-tubulin acetylation on microtubule structure and stability. *Proceedings of the National Academy of Sciences*, 116(21):10366–10371, 2019.

[131] Carsten Janke and Maria M Magiera. The tubulin code and its role in controlling microtubule properties and functions. *Nature Reviews Molecular Cell Biology*, 21(6):307–326, 2020.

[132] MD Weingarten, AH Lockwood, SY Hwo, and MW Kirschner. Separation of tubulin from microtubule-associated proteins on phosphocellulose. accompanying alterations in concentrations of buffer components. *Proc. Natl. Acad. Sci. USA*, 72:1858–1862, 1975.

[133] GLORIA Lee and SUSAN L Rook. Expression of tau protein in non-neuronal cells: microtubule binding and stabilization. *Journal of Cell Science*, 102(2):227–237, 1992.

[134] Audrey Sultan, Fabrice Nesslany, Marie Violet, Séverine Bégard, Anne Loyens, Smail Talahari, Zeyni Mansuroglu, Daniel Marzin, Nicolas Sergeant, Sandrine Humez, et al. Nuclear tau, a key player in neuronal dna protection. *Journal of Biological Chemistry*, 286(6):4566–4575, 2011.

[135] Fabrizio Biundo, Dolores Del Prete, Hong Zhang, Ottavio Arancio, and Luciano D'Adamio. A role for tau in learning, memory and synaptic plasticity. *Scientific reports*, 8(1):1–13, 2018.

[136] Moxin Wu, Manqing Zhang, Xiaoping Yin, Kai Chen, Zhijian Hu, Qin Zhou, Xianming Cao, Zhiying Chen, and Dan Liu. The role of pathological tau in synaptic dysfunction in alzheimer's diseases. *Translational Neurodegeneration*, 10(1):1–11, 2021.

[137] Jakub Sinsky, Karoline Pichlerova, and Jozef Hanes. Tau protein interaction partners and their roles in alzheimer's disease and other tauopathies. *International Journal of Molecular Sciences*, 22(17):9207, 2021.

[138] Qi Wang, Marcos VAS Navarro, Gary Peng, Evan Molinelli, Shih Lin Goh, Bret L Judson, Kanagalaghatta R Rajashankar, and Holger Sondermann. Molecular mechanism of membrane constriction and tubulation mediated by the f-bar protein pacsin/syndapin. *Proceedings of the National Academy of Sciences*, 106(31):12700–12705, 2009.

[139] Elavarasi Dharmalingam, Akvile Haeckel, Roser Pinyol, Lukas Schwintzer, Dennis Koch, Michael Manfred Kessels, and Britta Qualmann. F-bar proteins of the syndapin family shape the plasma membrane and are crucial for neuromorphogenesis. *Journal of Neuroscience*, 29(42):13315–13327, 2009.

[140] Christopher A Ross and Michelle A Poirier. Protein aggregation and neurodegenerative disease. *Nature medicine*, 10(Suppl 7):S10–S17, 2004.

[141] Alix De Calignon, Leora M Fox, Rose Pitstick, George A Carlson, Brian J Bacskai, Tara L Spires-Jones, and Bradley T Hyman. Caspase activation precedes and leads to tangles. *Nature*, 464(7292):1201–1204, 2010.

[142] Catherine M Cowan and Amrit Mudher. Are tau aggregates toxic or protective in tauopathies? *Frontiers in neurology*, 4:114, 2013.

[143] Khalid Iqbal, Tanweer Zaidi, GuangY Wen, Inge Grundke-Iqbal, PatriciaA Merz, SadiaS Shaikh, HenrykM Wisniewski, Irina Alafuzoff, and Bengt Winblad. Defective brain microtubule assembly in alzheimer's disease. *The Lancet*, 328(8504):421–426, 1986.

[144] Khalid Iqbal, Inge Grundke-Iqbal, Alan J Smith, Lalu George, Yunn-Chyn Tung, and Tanweer Zaidi. Identification and localization of a tau peptide to paired helical filaments of alzheimer disease. *Proceedings of the National Academy of Sciences*, 86(14):5646–5650, 1989.

[145] Sabiha Khatoon, Inge Grundke-Iqbal, and Khalid Iqbal. Levels of normal and abnormally phosphorylated tau in different cellular and regional compartments of alzheimer disease and control brains. *FEBS letters*, 351(1):80–84, 1994.

[146] Nadeeja Wijesekara, Rafaella Araujo Gonçalves, Rosemary Ahrens, Fernanda G De Felice, and Paul E Fraser. Tau ablation in mice leads to pancreatic β cell dysfunction and glucose intolerance. *The FASEB Journal*, 32(6):3166–3173, 2018.

[147] Pamela McMillan, Elena Korvatska, Parvoneh Poorkaj, Zana Evstafjeva, Linda Robinson, Lynne Greenup, James Leverenz, Gerard D Schellenberg, and Ian D'Souza. Tau isoform regulation is region-and cell-specific in mouse brain. *Journal of Comparative Neurology*, 511(6):788–803, 2008.

[148] Marco M Hefti, Kurt Farrell, SoongHo Kim, Kathryn R Bowles, Mary E Fowkes, Towfique Raj, and John F Crary. High-resolution temporal and regional mapping of mapt expression and splicing in human brain development. *PloS one*, 13(4):e0195771, 2018.

[149] PA Loomis, TH Howard, RP Castleberry, and LI Binder. Identification of nuclear tau isoforms in human neuroblastoma cells. *Proceedings of the National Academy of Sciences*, 87(21):8422–8426, 1990.

[150] Yan Wang, Patricia A Loomis, Raymond P Zinkowski, and Lester I Binder. A novel tau transcript in cultured human neuroblastoma cells expressing nuclear tau. *The Journal of cell biology*, 121(2):257–267, 1993.

[151] Virginia C Thurston, Raymond P Zinkowski, and Lester I Binder. Tau as a nucleolar protein in human nonneural cells in vitro and in vivo. *Chromosoma*, 105(1):20–30, 1996.

[152] Daniel C Cross, Juan P Muñoz, Paula Hernández, and Ricardo B Maccioni. Nuclear and cytoplasmic tau proteins from human nonneuronal cells share common structural and functional features with brain tau. *Journal of cellular biochemistry*, 78(2):305–317, 2000.

[153] Roseann M Rady, Raymond P Zinkowski, and Lester I Binder. Presence of tau in isolated nuclei from human brain. *Neurobiology of aging*, 16(3):479–486, 1995.

[154] Marcela K Sjöberg, Elena Shestakova, Zeyni Mansuroglu, Ricardo B Maccioni, and Eliette Bonnefoy. Tau protein binds to pericentromeric dna: a putative role for nuclear tau in nucleolar organization. *Journal of cell science*, 119(10):2025–2034, 2006.

[155] Marie Violet, Lucie Delattre, Meryem Tardivel, Audrey Sultan, Alban Chauderlier, Raphaelle Caillierez, Smail Talahari, Fabrice Nesslany, Bruno Lefebvre, Eliette Bonnefoy, et al. A major role for tau in neuronal dna and rna protection in vivo under physiological and hyperthermic conditions. *Frontiers in cellular neuroscience*, 8:84, 2014.

[156] Tomas Kavanagh, Aditi Halder, and Eleanor Drummond. Tau interactome and rna binding proteins in neurodegenerative diseases. *Molecular Neurodegeneration*, 17(1):66, 2022.

[157] Thomas Geuens, Delphine Bouhy, and Vincent Timmerman. The hnrnp family: insights into their role in health and disease. *Human genetics*, 135:851–867, 2016.

[158] Michael H Glickman and Aaron Ciechanover. The ubiquitin-proteasome proteolytic pathway: destruction for the sake of construction. *Physiological reviews*, 2002.

[159] Hwan-Ching Tai, Alberto Serrano-Pozo, Tadafumi Hashimoto, Matthew P Frosch, Tara L Spires-Jones, and Bradley T Hyman. The synaptic accumulation of hyperphosphorylated tau oligomers in alzheimer disease is associated with dysfunction of the ubiquitin-proteasome system. *The American journal of pathology*, 181(4):1426–1435, 2012.

[160] Fang-lin Weng and Ling He. Disrupted ubiquitin proteasome system underlying tau accumulation in alzheimer's disease. *Neurobiology of aging*, 99:79–85, 2021.

[161] Shanya Jiang and Kiran Bhaskar. Degradation and transmission of tau by autophagic-endolysosomal networks and potential therapeutic targets for tauopathy. *Frontiers in Molecular Neuroscience*, 13:586731, 2020.

[162] Yipeng Wang, Marta Martinez-Vicente, Ulrike Krüger, Susmita Kaushik, Esther Wong, Eva-Maria Mandelkow, Ana Maria Cuervo, and Eckhard Mandelkow. Tau fragmentation, aggregation and clearance: the dual role of lysosomal processing. *Human molecular genetics*, 18(21):4153–4170, 2009.

[163] Ranjit Sahu, Susmita Kaushik, Cristina C Clement, Elvira S Cannizzo, Brian Scharf, Antonia Follenzi, Ilaria Potolicchio, Edward Nieves, Ana Maria Cuervo, and Laura Santambrogio. Microautophagy of cytosolic proteins by late endosomes. *Developmental cell*, 20(1):131–139, 2011.

[164] Valerie Uytterhoeven, Liesbeth Deaulmerie, and Patrik Verstreken. Increased endosomal microautophagy reduces tau driven synaptic dysfunction. *Front. Neurosci*, 12(10.3389), 2018.

[165] Tadanori Hamano, Tania F Gendron, Ena Causevic, Shu-Hui Yen, Wen-Lang Lin, Ciro Isidoro, Michael DeTure, and Li-wen Ko. Autophagic-lysosomal perturbation enhances tau aggregation in transfectants with induced wild-type tau expression. *European Journal of Neuroscience*, 27(5):1119–1130, 2008.

[166] Jose A Rodríguez-Navarro, Laura Rodríguez, María J Casarejos, Rosa M Solano, Ana Gómez, Juan Perucho, Ana María Cuervo, Justo García de Yébenes, and María A Mena. Trehalose ameliorates dopaminergic and tau pathology in parkin deleted/tau overexpressing mice through autophagy activation. *Neurobiology of disease*, 39(3):423–438, 2010.

[167] Antonio Piras, Ludovic Collin, Fiona Grüninger, Caroline Graff, and Annica Rönnbäck. Autophagic and lysosomal defects in human tauopathies: analysis of post-mortem brain from patients with familial alzheimer disease, corticobasal degeneration and progressive supranuclear palsy. *Acta neuropathologica communications*, 4(1):1–13, 2016.

[168] Ulrike Krüger, Yipeng Wang, Satish Kumar, and Eva-Maria Mandelkow. Autophagic degradation of tau in primary neurons and its enhancement by trehalose. *Neurobiology of aging*, 33(10):2291–2305, 2012.

[169] João Vaz-Silva, Patrícia Gomes, Qi Jin, Mei Zhu, Viktoriya Zhuravleva, Sebastian Quintremil, Torcato Meira, Joana Silva, Chrysoula Dioli, Carina Soares-Cunha, et al. Endolysosomal degradation of tau and its role in glucocorticoid-driven hippocampal malfunction. *The EMBO journal*, 37(20):e99084, 2018.

[170] Fiona M Menzies, Angeleen Fleming, Andrea Caricasole, Carla F Bento, Stephen P Andrews, Avraham Ashkenazi, Jens Füllgrabe, Anne Jackson, Maria Jimenez Sanchez, Cansu Karabiyik, et al. Autophagy and neurodegeneration: pathogenic mechanisms and therapeutic opportunities. *Neuron*, 93(5):1015–1034, 2017.

[171] Min Jae Lee, Jung Hoon Lee, and David C Rubinsztein. Tau degradation: The ubiquitin–proteasome system versus the autophagy-lysosome system. *Progress in neurobiology*, 105:49–59, 2013.

[172] Lorenzo Pasquali, Kyle J Gaulton, Santiago A Rodríguez-Seguí, Loris Mularoni, Irene Miguel-Escalada, Ildem Akerman, Juan J Tena, Ignasi Morán, Carlos Gómez-Marín, Martijn Van De Bunt, et al. Pancreatic islet enhancer clusters enriched in type 2 diabetes risk-associated variants. *Nature genetics*, 46(2):136–143, 2014.

[173] Loris Mularoni, Mireia Ramos-Rodríguez, and Lorenzo Pasquali. The pancreatic islet regulome browser. *Frontiers in Genetics*, 8:13, 2017.

[174] Mauro J Muraro, Gitanjali Dharmadhikari, Dominic Grün, Nathalie Groen, Tim Dielen, Erik Jansen, Leon Van Gurp, Marten A Engelse, Francoise Carlotti, Eelco Jp De Koning, et al. A single-cell transcriptome atlas of the human pancreas. *Cell systems*, 3(4):385–394, 2016.

[175] Åsa Segerstolpe, Athanasia Palasantza, Pernilla Eliasson, Eva-Marie Andersson, Anne-Christine Andréasson, Xiaoyan Sun, Simone Picelli, Alan Sabirsh, Maryam Clausen, Magnus K Bjursell, et al. Single-cell transcriptome profiling of human pancreatic islets in health and type 2 diabetes. *Cell metabolism*, 24(4):593–607, 2016.

[176] Magdalena Maj, Wolfgang Gartner, Aysegul Ilhan, Dashurie Neziri, Johannes Attems, and Ludwig Wagner. Expression of tau in insulin-secreting cells and its interaction with the calcium-binding protein secretagogin. *Journal of Endocrinology*, 205:25–36, 2010.

[177] Judith Miklossy, Hong Qing, Aleksandra Radenovic, Andras Kis, Bertrand Vileno, Forró Làszló, Lisa Miller, Ralph N Martins, Gerard Waeber, Vincent Mooser, et al. Beta amyloid and hyperphosphorylated tau deposits in the pancreas in type 2 diabetes. *Neurobiology of aging*, 31(9):1503–1515, 2010.

[178] Magdalena Maj, Gregor Hoermann, Sazan Rasul, Wolfgang Base, Ludwig Wagner, and Johannes Attems. The microtubule-associated protein tau and its relevance for pancreatic beta cells. *Journal of diabetes research*, 2016, 2016.

[179] Juliette Janson, Thomas Laedtke, Joseph E Parisi, Peter O'Brien, Ronald C Petersen, and Peter C Butler. Increased risk of type 2 diabetes in alzheimer disease. *Diabetes*, 53(2):474–481, 2004.

[180] Prashant Bharadwaj, Nadeeja Wijesekara, Milindu Liyanapathirana, Philip Newsholme, Lars Ittner, Paul Fraser, and Giuseppe Verdile. The link between type 2 diabetes and neurodegeneration: roles for amyloid-β, amylin, and tau proteins. *Journal of Alzheimer's Disease*, 59(2):421–432, 2017.

[181] Ranran Zhou, Wen Hu, Chun-Ling Dai, Cheng-Xin Gong, Khalid Iqbal, Dalong Zhu, and Fei Liu. Expression of microtubule associated protein tau in mouse pancreatic islets is restricted to autonomic nerve fibers. *Journal of Alzheimer's Disease*, 75(4):1339–1349, 2020.

[182] Kathryn P Trogden, Justin Lee, Kai M Bracey, Kung-Hsien Ho, Hudson McKinney, Xiaodong Zhu, Goker Arpag, Thomas G Folland, Anna B Osipovich, Mark A Magnuson, et al. Microtubules regulate pancreatic β-cell heterogeneity via spatiotemporal control of insulin secretion hot spots. *Elife*, 10:e59912, 2021.

[183] Kung-Hsien Ho, Xiaodun Yang, Anna B Osipovich, Over Cabrera, Mansuo L Hayashi, Mark A Magnuson, Guoqiang Gu, and Irina Kaverina. Glucose regulates microtubule disassembly and the dose of insulin secretion via tau phosphorylation. *Diabetes*, 69(9):1936–1947, 2020.

[184] Mark A Atkinson, George S Eisenbarth, and Aaron W Michels. Type 1 diabetes. *The Lancet*, 383(9911):69–82, 2014.

[185] Adrian Liston, John A Todd, and Vasiliki Lagou. Beta-cell fragility as a common underlying risk factor in type 1 and type 2 diabetes. *Trends in molecular medicine*, 23(2):181–194, 2017.

[186] Alewijn Ott, RP Stolk, F Van Harskamp, HAP Pols, A Hofman, and MMB Breteler. Diabetes mellitus and the risk of dementia: The rotterdam study. *Neurology*, 53(9):1937–1937, 1999.

[187] Michael Ristow. Neurodegenerative disorders associated with diabetes mellitus. *Journal of molecular medicine*, 82(8):510–529, 2004.

[188] Bhumsoo Kim, Carey Backus, SangSu Oh, and Eva L Feldman. Hyperglycemia-induced tau cleavage in vitro and in vivo: a possible link between diabetes and alzheimer's disease. *Journal of Alzheimer's Disease*, 34(3):727–739, 2013.

[189] Xiaohua Li, Dalin Song, and Sean X Leng. Link between type 2 diabetes and alzheimer's disease: from epidemiology to mechanism and treatment. *Clinical interventions in aging*, 10:549, 2015.

[190] Zina Kroner. The relationship between alzheimer's disease and diabetes: Type 3 diabetes. *Alternative Medicine Review*, 14(4), 2009.

[191] Jada Lewis and Dennis W Dickson. Propagation of tau pathology: hypotheses, discoveries, and yet unresolved questions from experimental and human brain studies. *Acta neuropathologica*, 131(1):27–48, 2016.

[192] Saıd El Messari, Ali Aıt-Ikhlef, Djennet-Hantaz Ambroise, Luc Penicaud, and Michel Arluison. Expression of insulin-responsive glucose transporter glut4 mrna in the rat brain and spinal cord: an in situ hybridization study. *Journal of chemical neuroanatomy*, 24(4):225–242, 2002.

[193] Jana Havrankova, Jesse Roth, and MICHAEL BROWNSTEIN. Insulin receptors are widely distributed in the central nervous system of the rat. *Nature*, 272(5656):827, 1978.

[194] JM Hill, MA Lesniak, CB Pert, and J Roth. Autoradiographic localization of insulin receptors in rat brain: prominence in olfactory and limbic areas. *Neuroscience*, 17(4):1127–1138, 1986.

[195] Raman Sankar, Shanthie Thamotharan, Don Shin, Kelle H Moley, and Sherin U Devaskar. Insulin-responsive glucose transporters—glut8 and glut4 are expressed in the developing mammalian brain. *Molecular brain research*, 107(2):157–165, 2002.

[196] Martin Heni, Stephanie Kullmann, Hubert Preissl, Andreas Fritsche, and Hans-Ulrich Häring. Impaired insulin action in the human brain: causes and metabolic consequences. *Nature Reviews Endocrinology*, 11(12):701, 2015.

[197] M Suzanne. Insulin resistance and neurodegeneration: progress towards the development of new therapeutics for alzheimer's disease. *Drugs*, 77(1):47–65, 2017.

[198] Konrad Talbot, Hoau-Yan Wang, Hala Kazi, Li-Ying Han, Kalindi P Bakshi, Andres Stucky, Robert L Fuino, Krista R Kawaguchi, Andrew J Samoyedny, Robert S Wilson, et al. Demonstrated brain insulin resistance in alzheimer's disease patients is associated with igf-1 resistance, irs-1 dysregulation, and cognitive decline. *The Journal of clinical investigation*, 122(4):1316–1338, 2012.

[199] Shuko Takeda, Naoyuki Sato, Kozue Uchio-Yamada, Kyoko Sawada, Takanori Kunieda, Daisuke Takeuchi, Hitomi Kurinami, Mitsuru Shinohara, Hiromi Rakugi, and Ryuichi Morishita. Diabetes-accelerated memory dysfunction via cerebrovascular inflammation and aβ deposition in an alzheimer mouse model with diabetes. *Proceedings of the National Academy of Sciences*, 107(15):7036–7041, 2010.

[200] Jose Morales-Corraliza, Harrison Wong, Matthew J Mazzella, Shaoli Che, Sang Han Lee, Eva Petkova, Janice D Wagner, Scott E Hemby, Stephen D Ginsberg, and Paul M Mathews. Brain-wide insulin resistance, tau phosphorylation changes, and hippocampal neprilysin and amyloid-β alterations in a monkey model of type 1 diabetes. *Journal of Neuroscience*, 36(15):4248–4258, 2016.

[201] Mini Sajan, Barbara Hansen, Robert Ivey, Joshua Sajan, Csilla Ari, Shijie Song, Ursula Braun, Michael Leitges, Margaret Farese-Higgs, and Robert V Farese. Brain insulin signaling is increased in insulin-resistant states and decreases in foxos and pgc-1α and increases in aβ1–40/42 and phospho-tau may abet alzheimer development. *Diabetes*, 65(7):1892–1903, 2016.

[202] David E Moller and Keith D Kaufman. Metabolic syndrome: a clinical and molecular perspective. *Annu. Rev. Med.*, 56:45–62, 2005.

[203] Waqar Ahmad, Bushra Ijaz, Khadija Shabbiri, Fayyaz Ahmed, and Sidra Rehman. Oxidative toxicity in diabetes and alzheimer's disease: mechanisms behind ros/rns generation. *Journal of biomedical science*, 24:1–10, 2017.

[204] Erik J Henriksen, Maggie K Diamond-Stanic, and Elizabeth M Marchionne. Oxidative stress and the etiology of insulin resistance and type 2 diabetes. *Free Radical Biology and Medicine*, 51(5):993–999, 2011.

[205] Kanwal Rehman and Muhammad Sajid Hamid Akash. Mechanism of generation of oxidative stress and pathophysiology of type 2 diabetes mellitus: how are they interlinked? *Journal of cellular biochemistry*, 118(11):3577–3585, 2017.

[206] Ana Lloret, Mari-Carmen Badia, Esther Giraldo, Gennady Ermak, Maria-Dolores Alonso, Federico V Pallardó, Kelvin JA Davies, and Jose Viña. Amyloid-β toxicity and tau hyperphosphorylation are linked via rcan1 in alzheimer's disease. *Journal of Alzheimer's Disease*, 27(4):701–709, 2011.

[207] Hiroaki Misonou, Maho Morishima-Kawashima, and Yasuo Ihara. Oxidative stress induces intracellular accumulation of amyloid β-protein (aβ) in human neuroblastoma cells. *Biochemistry*, 39(23):6951–6959, 2000.

[208] E Giraldo, A Lloret, T Fuchsberger, and J Viña. Aβ and tau toxicities in alzheimer's are linked via oxidative stress-induced p38 activation: protective role of vitamin e. *Redox biology*, 2:873–877, 2014.

[209] Hesham M Ismail, Leonardo Scapozza, Urs T Ruegg, and Olivier M Dorchies. Diapocynin, a dimer of the nadph oxidase inhibitor apocynin, reduces ros production and prevents force loss in eccentrically contracting dystrophic muscle. *PloS one*, 9(10):e110708, 2014.

[210] Frederick Grant Banting, Charles Herbert Best, James Bertram Collip, Walter Ruggles Campbell, Andrew Almon Fletcher, John James Rickard Macleod, and Edward Clark Noble. The effect produced on diabetes by extracts of pancreas. *Trans Assoc Am Physicians*, 37:337–47, 1922.

[211] Stuart J Brink. Insulin past, present, and future: 100 years from leonard thompson. *Diabetology*, 3(1):117–158, 2022.

[212] GS Eisenbarth. Autoimmune beta cell insufficiency—diabetes mellitus type 1. *Triangle*, 23(1):l, 1984.

[213] Paul Zimmet, KGMM Alberti, and Jonathan Shaw. Global and societal implications of the diabetes epidemic. *Nature*, 414(6865):782–787, 2001.

[214] Frank B Hu, JoAnn E Manson, Meir J Stampfer, Graham Colditz, Simin Liu, Caren G Solomon, and Walter C Willett. Diet, lifestyle, and the risk of type 2 diabetes mellitus in women. *New England journal of medicine*, 345(11):790–797, 2001.

[215] JoAnn E Manson, Umed A Ajani, Simin Liu, David M Nathan, and Charles H Hennekens. A prospective study of cigarette smoking and the incidence of diabetes mellitus among us male physicians. *The American journal of medicine*, 109(7):538–542, 2000.

[216] M Cullmann, A Hilding, and C-G Östenson. Alcohol consumption and risk of pre-diabetes and type 2 diabetes development in a swedish population. *Diabetic Medicine*, 29(4):441–452, 2012.

[217] Anna C Belkina and Gerald V Denis. Obesity genes and insulin resistance. *Current opinion in endocrinology, diabetes, and obesity*, 17(5):472, 2010.

[218] John A Williams. Regulation of acinar cell function in the pancreas. *Current opinion in gastroenterology*, 26(5):478, 2010.

[219] Anne Grapin-Botton. Ductal cells of the pancreas. *The international journal of biochemistry & cell biology*, 37(3):504–510, 2005.

[220] Dale E Bockman. Nerves in the pancreas: what are they for? *The American journal of surgery*, 194(4):S61–S64, 2007.

[221] Jean-Claude Henquin. Triggering and amplifying pathways of regulation of insulin secretion by glucose. *Diabetes*, 49(11):1751–1760, 2000.

[222] Daniel L Cook and Nicholas Hales. Intracellular atp directly blocks k+ channels in pancreatic b-cells. *Nature*, 311(5983):271–273, 1984.

[223] Martin Köhler, Svante Norgren, Per-Olof Berggren, Bertil B Fredholm, Olof Larsson, Christopher J Rhodes, Terence P Herbert, and Holger Luthman. Changes in cytoplasmic atp concentration parallels changes in atp-regulated k+-channel activity in insulin-secreting cells. *FEBS letters*, 441(1):97–102, 1998.

[224] David Mears. Regulation of insulin secretion in islets of langerhans by ca 2+ channels. *The Journal of membrane biology*, 200:57–66, 2004.

[225] Noel G Morgan and Sarah J Richardson. Fifty years of pancreatic islet pathology in human type 1 diabetes: insights gained and progress made. *Diabetologia*, 61(12):2499–2506, 2018.

[226] Sarah J Richardson and Alberto Pugliese. 100 years of insulin: Pancreas pathology in type 1 diabetes: an evolving story. *Journal of Endocrinology*, 252(2):R41–R57, 2022.

[227] Linda A DiMeglio, Carmella Evans-Molina, and Richard A Oram. Type 1 diabetes. *The Lancet*, 391(10138):2449–2462, 2018.

[228] Carmella Evans-Molina, Emily K Sims, Linda A DiMeglio, Heba M Ismail, Andrea K Steck, Jerry P Palmer, Jeffrey P Krischer, Susan Geyer, Ping Xu, Jay M Sosenko, et al. β cell dysfunction exists more than 5 years before type 1 diabetes diagnosis. *JCI insight*, 3(15), 2018.

[229] Pia Leete, Richard A Oram, Timothy J McDonald, Beverley M Shields, Clemens Ziller, Andrew T Hattersley, Sarah J Richardson, and Noel G Morgan. Studies of insulin and proinsulin in pancreas and serum support the existence of aetiopathological endotypes of type 1 diabetes associated with age at diagnosis. *Diabetologia*, 63(6):1258–1267, 2020.

[230] Alice LJ Carr, Jamie RJ Inshaw, Christine S Flaxman, Pia Leete, Rebecca C Wyatt, Lydia A Russell, Matthew Palmer, Dmytro Prasolov, Thomas Worthington, Bethany Hull, et al. Circulating c-peptide levels in living children and young people and pancreatic β-cell loss in pancreas donors across type 1 diabetes disease duration. *Diabetes*, 71(7):1591–1596, 2022.

[231] Ivan Martinez-Valbuena, Rafael Valenti-Azcarate, Irene Amat-Villegas, Mario Riverol, Irene Marcilla, Carlos E de Andrea, Juan Antonio Sánchez-Arias, Maria del Mar Carmona-Abellan, Gloria Marti, Maria-Elena Erro, et al. Amylin as a

potential link between type 2 diabetes and alzheimer disease. *Annals of neurology*, 86(4):539–551, 2019.

[232] Franck R Petry, Jérôme Pelletier, Alexis Bretteville, Françoise Morin, Frédéric Calon, Sébastien S Hébert, Robert A Whittington, and Emmanuel Planel. Specificity of anti-tau antibodies when analyzing mice models of alzheimer's disease: problems and solutions. *PloS one*, 9(5), 2014.

[233] Ebru Ercan, Sameh Eid, Christian Weber, Alexandra Kowalski, Maria Bichmann, Annika Behrendt, Frank Matthes, Sybille Krauss, Peter Reinhardt, Simone Fulle, et al. A validated antibody panel for the characterization of tau post-translational modifications. *Molecular neurodegeneration*, 12(1):87, 2017.

[234] Dan Li and Yong Ku Cho. High specificity of widely used phospho-tau antibodies validated using a quantitative whole-cell based assay. *Journal of neurochemistry*, 2019.

[235] Martin Ramsden, Linda Kotilinek, Colleen Forster, Jennifer Paulson, Eileen McGowan, Karen SantaCruz, Aaron Guimaraes, Mei Yue, Jada Lewis, George Carlson, et al. Age-dependent neurofibrillary tangle formation, neuron loss, and memory impairment in a mouse model of human tauopathy (p301l). *Journal of Neuroscience*, 25(46):10637–10647, 2005.

[236] K Santacruz, J Lewis, T Spires, J Paulson, L Kotilinek, M Ingelsson, A Guimaraes, M DeTure, M Ramsden, E McGowan, et al. Tau suppression in a neurodegenerative mouse model improves memory function. *Science*, 309(5733):476–481, 2005.

[237] Hana N Dawson, Adriana Ferreira, Michele V Eyster, Nupur Ghoshal, Lester I Binder, and Michael P Vitek. Inhibition of neuronal maturation in primary hippocampal neurons from τ deficient mice. *Journal of cell science*, 114(6):1179–1187, 2001.

[238] Mariana Vargas-Caballero, Franziska Denk, Heike J Wobst, Emily Arch, Chrysia-Maria Pegasiou, Peter L Oliver, Olivia A Shipton, Ole Paulsen, and Richard Wade-Martins. Wild-type, but not mutant n296h, human tau restores aβ-mediated inhibition of ltp in tau-/- mice. *Frontiers in neuroscience*, 11:201, 2017.

[239] Mark A Russell, Sambra D Redick, David M Blodgett, Sarah J Richardson, Pia Leete, Lars Krogvold, Knut Dahl-Jørgensen, Rita Bottino, Marcela Brissova, Jason M Spaeth, et al. Hla class ii antigen processing and presentation pathway components demonstrated by transcriptome and protein analyses of islet β-cells from donors with type 1 diabetes. *Diabetes*, 68(5):988–1001, 2019.

[240] David M Blodgett, Anetta Nowosielska, Shaked Afik, Susanne Pechhold, Anthony J Cura, Norman J Kennedy, Soyoung Kim, Alper Kucukural, Roger J Davis, Sally C Kent, et al. Novel observations from next-generation rna sequencing of highly purified human adult and fetal islet cell subsets. *Diabetes*, 64(9):3172–3181, 2015.

[241] K Ishizawa, H Ksiezak-Reding, P Davies, A Delacourte, P Tiseo, S-H Yen, and DW Dickson. A double-labeling immunohistochemical study of tau exon 10 in alzheimer's disease, progressive supranuclear palsy and pick's disease. *Acta neuropathologica*, 100(3):235–244, 2000.

[242] Benjamin L Wolozin, Alex Pruchnicki, Dennis W Dickson, and Peter Davies. A neuronal antigen in the brains of alzheimer patients. *Science*, 232(4750):648–650, 1986.

[243] Gregory A Jicha, Eric Lane, Inez Vincent, Laszlo Otvos Jr, Ralf Hoffmann, and Peter Davies. A conformation-and phosphorylation-dependent antibody recognizing the paired helical filaments of alzheimer's disease. *Journal of neurochemistry*, 69(5):2087–2095, 1997.

[244] Michel Goedert, MG Spillantini, NJ Cairns, and RA Crowther. Tau proteins of alzheimer paired helical filaments: abnormal phosphorylation of all six brain isoforms. *Neuron*, 8(1):159–168, 1992.

[245] Thomas A Waldmann. Monoclonal antibodies in diagnosis and therapy. *Science*, 252(5013):1657–1662, 1991.

[246] Nicolas Sergeant, André Delacourte, and Luc Buée. Tau protein as a differential biomarker of tauopathies. *Biochimica et Biophysica Acta (BBA)-Molecular Basis of Disease*, 1739(2-3):179–197, 2005.

[247] Monya Baker. Antibody anarchy: a call to order. *Nature*, 527(7579):545–551, 2015.

[248] Monya Baker. Blame it on the antibodies. *Nature*, 521(7552):274, 2015.

[249] Félix Hernández, Jesús Merchán-Rubira, Laura Vallés-Saiz, Alberto Rodríguez-Matellán, and Jesús Avila. Differences between human and murine tau at the n-terminal end. *Frontiers in aging neuroscience*, 12:11, 2020.

[250] Monica M Oblinger, Alexandra Argasinski, J Wong, and Kenneth S Kosik. Tau gene expression in rat sensory neurons during development and regeneration. *Journal of Neuroscience*, 11(8):2453–2459, 1991.

[251] David Drubin, Sumire Kobayashi, Doug Kellogg, and Marc Kirschner. Regulation of microtubule protein levels during cellular morphogenesis in nerve growth factor-treated pc12 cells. *The Journal of cell biology*, 106(5):1583–1591, 1988.

[252] T Chris Gamblin, Feng Chen, Angara Zambrano, Aida Abraha, Sarita Lagalwar, Angela L Guillozet, Meiling Lu, Yifan Fu, Francisco Garcia-Sierra, Nichole LaPointe, et al. Caspase cleavage of tau: linking amyloid and neurofibrillary tangles in alzheimer's disease. *Proceedings of the national academy of sciences*, 100(17):10032–10037, 2003.

[253] Robert A Rissman, Wayne W Poon, Mathew Blurton-Jones, Salvatore Oddo, Reidun Torp, Michael P Vitek, Frank M LaFerla, Troy T Rohn, Carl W Cotman, et al. Caspase-cleavage of tau is an early event in alzheimer disease tangle pathology. *The Journal of clinical investigation*, 114(1):121–130, 2004.

[254] Kate Lakoski Loveland, Daniella Herszfeld, Brendan Chu, Emily Rames, Elizabeth Christy, Lyndall J Briggs, Rushdi Shakri, David M de Kretser, and David A Jans. Novel low molecular weight microtubule-associated protein-2 isoforms contain a functional nuclear localization sequence. *Journal of Biological Chemistry*, 274(27):19261–19268, 1999.

[255] Michael R D'Andrea, Sergey Ilyin, and Carlos R Plata-Salaman. Abnormal patterns of microtubule-associated protein-2 (map-2) immunolabeling in neuronal nuclei and lewy bodies in parkinson's disease substantia nigra brain tissues. *Neuroscience letters*, 306(3):137–140, 2001.

[256] Thierry F Vandamme. Use of rodents as models of human diseases. *Journal of pharmacy & bioallied sciences*, 6(1):2, 2014.

[257] L Michalik, P Neuville, MT Vanier, and JF Launay. Pancreatic tau related maps: biochemical and immunofluorescence analysis in a tumoral cell line. *Molecular and cellular biochemistry*, 143(2):107–112, 1995.

[258] Marie-Thérèse Vanier, Pascal Neuville, Liliane Michalik, and Jean-François Launay. Expression of specific tau exons in normal and tumoral pancreatic acinar cells. *Journal of Cell Science*, 111(10):1419–1432, 1998.

[259] J Miklossy, Kevin Taddei, Ralph Martins, G Escher, R Kraftsik, O Pillevuit, D Lepori, and M Campiche. Alzheimer disease: curly fibers and tangles in organs other than brain. *Journal of neuropathology and experimental neurology*, 58(8):803–814, 1999.

[260] Qian Hua and Rong-qiao He. Tau could protect dna double helix structure. *Biochimica et Biophysica Acta (BBA)-Proteins and Proteomics*, 1645(2):205–211, 2003.

[261] Vasudevaraju Padmaraju, Shantinath Satappa Indi, and Kosagi Sharaf Jagannatha Rao. New evidences on tau–dna interactions and relevance to neurodegeneration. *Neurochemistry international*, 57(1):51–57, 2010.

[262] Yan Wei, Mei-Hua Qu, Xing-Sheng Wang, Lan Chen, Dong-Liang Wang, Ying Liu, Qian Hua, and Rong-Qiao He. Binding to the minor groove of the double-strand, tau protein prevents dna from damage by peroxidation. *PloS one*, 3(7):e2600, 2008.

[263] Fouad Atouf, Paul Czernichow, and Raphael Scharfmann. Expression of neuronal traits in pancreatic beta cells implication of neuron-restrictive silencing factor/repressor element silencing transcription factor, a neuron-restrictive silencer. *Journal of Biological Chemistry*, 272(3):1929–1934, 1997.

[264] Margot E Arntfield and Derek van der Kooy. β-cell evolution: How the pancreas borrowed from the brain: The shared toolbox of genes expressed by neural and pancreatic endocrine cells may reflect their evolutionary relationship. *Bioessays*, 33(8):582–587, 2011.

[265] Daniel Eberhard. Neuron and beta-cell evolution: Learning about neurons is learning about beta-cells. *Bioessays*, 35(7):584–584, 2013.

[266] XJ Yang, Lee-Ming Kow, Toshiya Funabashi, and Charles V Mobbs. Hypothalamic glucose sensor: similarities to and differences from pancreatic beta-cell mechanisms. *Diabetes*, 48(9):1763–1772, 1999.

[267] Sherin U Devaskar, Stephen J Giddings, Premeela A Rajakumar, Lynn R Carnaghi, Ram K Menon, and D Scott Zahm. Insulin gene expression and insulin synthesis in mammalian neuronal cells. *Journal of Biological Chemistry*, 269(11):8445–8454, 1994.

[268] Junghun Song, Yuanzhong Xu, Xiaoxia Hu, Brian Choi, and Qingchun Tong. Brain expression of cre recombinase driven by pancreas-specific promoters. *genesis*, 48(11):628–634, 2010.

[269] Alexandra C Nica, Halit Ongen, Jean-Claude Irminger, Domenico Bosco, Thierry Berney, Stylianos E Antonarakis, Philippe A Halban, and Emmanouil T Dermitzakis. Cell-type, allelic, and genetic signatures in the human pancreatic beta cell transcriptome. *Genome research*, 23(9):1554–1562, 2013.

[270] E-M Mandelkow, J Biernat, G Drewes, N Gustke, B Trinczek, and E Mandelkow. Tau domains, phosphorylation, and interactions with microtubules. *Neurobiology of aging*, 16(3):355–362, 1995.

[271] Andrey Samsonov, Jiang-Zhou Yu, Mark Rasenick, and Sergey V Popov. Tau interaction with microtubules in vivo. *Journal of cell science*, 117(25):6129–6141, 2004.

[272] Elea Prezel, Auréliane Elie, Julie Delaroche, Virginie Stoppin-Mellet, Christophe Bosc, Laurence Serre, Anne Fourest-Lieuvin, Annie Andrieux, Marylin Vantard, and Isabelle Arnal. Tau can switch microtubule network organizations: from random networks to dynamic and stable bundles. *Molecular biology of the cell*, 29(2):154–165, 2018.

[273] Susanne Wegmann, Jacek Biernat, and Eckhard Mandelkow. A current view on tau protein phosphorylation in alzheimer's disease. *Current opinion in neurobiology*, 69:131–138, 2021.

[274] David J Irwin, Todd J Cohen, Murray Grossman, Steven E Arnold, Sharon X Xie, Virginia M-Y Lee, and John Q Trojanowski. Acetylated tau, a novel pathological signature in alzheimer's disease and other tauopathies. *Brain*, 135(3):807–818, 2012.

[275] Todd J Cohen, Brian H Constance, Andrew W Hwang, Michael James, and Chao-Xing Yuan. Intrinsic tau acetylation is coupled to auto-proteolytic tau fragmentation. *PloS one*, 11(7):e0158470, 2016.

[276] Fan-Yan Wei, Kazuaki Nagashima, Toshio Ohshima, Yasunori Saheki, Yun-Fei Lu, Masayuki Matsushita, Yuichiro Yamada, Katsuhiko Mikoshiba, Yutaka Seino, Hideki Matsui, et al. Cdk5-dependent regulation of glucose-stimulated insulin secretion. *Nature medicine*, 11(10):1104–1108, 2005.

[277] Ya-Li Zheng, Congyu Li, Ya-Fang Hu, Li Cao, Hui Wang, Bo Li, Xiao-Hua Lu, Li Bao, Hong-Yan Luo, Varsha Shukla, et al. Cdk5 inhibitory peptide (cip) inhibits cdk5/p25 activity induced by high glucose in pancreatic beta cells and recovers insulin secretion from p25 damage. *PLoS One*, 8(9):e63332, 2013.

[278] Min-Jung Kim, Su-Kyung Park, Ji-Hyun Lee, Chang-Yun Jung, Dong Jun Sung, Jae-Hyung Park, Young-Sil Yoon, Jinyoung Park, Keun-Gyu Park, Dae-Kyu Song, et al. Salt-inducible kinase 1 terminates camp signaling by an evolutionarily conserved negative-feedback loop in β-cells. *Diabetes*, 64(9):3189–3202, 2015.

[279] Weijun Shen, Brandon Taylor, Qihui Jin, Van Nguyen-Tran, Shelly Meeusen, You-Qing Zhang, Anwesh Kamireddy, Austin Swafford, Andrew F Powers, John Walker, et al. Inhibition of dyrk1a and gsk3b induces human β-cell proliferation. *Nature communications*, 6(1):1–11, 2015.

[280] Chao Sun, Liang Tian, Jia Nie, Hai Zhang, Xiao Han, and Yuguang Shi. Inactivation of mark4, an amp-activated protein kinase (ampk)-related kinase, leads to insulin hypersensitivity and resistance to diet-induced obesity. *Journal of Biological Chemistry*, 287(45):38305–38315, 2012.

[281] Sang-Won Min, Peter Dongmin Sohn, Yaqiao Li, Nino Devidze, Jeffrey R Johnson, Nevan J Krogan, Eliezer Masliah, Sue-Ann Mok, Jason E Gestwicki, and Li Gan. Sirt1 deacetylates tau and reduces pathogenic tau spread in a mouse model of tauopathy. *Journal of Neuroscience*, 38(15):3680–3688, 2018.

[282] Jui-Heng Tseng, Ling Xie, Sheng Song, Youmei Xie, Lauren Allen, Deepa Ajit, Jau-Shyong Hong, Xian Chen, Rick B Meeker, and Todd J Cohen. The deacetylase hdac6 mediates endogenous neuritic tau pathology. *Cell reports*, 20(9):2169–2183, 2017.

[283] Hanna Trzeciakiewicz, Deepa Ajit, Jui-Heng Tseng, Youjun Chen, Aditi Ajit, Zarin Tabassum, Rebecca Lobrovich, Claire Peterson, Natallia V Riddick, Michelle S Itano, et al. An hdac6-dependent surveillance mechanism suppresses tau-mediated neurodegeneration and cognitive decline. *Nature communications*, 11(1):5522, 2020.

[284] Tara E Tracy and Li Gan. Acetylated tau in alzheimer's disease: An instigator of synaptic dysfunction underlying memory loss: Increased levels of acetylated tau blocks the postsynaptic signaling required for plasticity and promotes memory deficits associated with tauopathy. *Bioessays*, 39(4):1600224, 2017.

[285] Jie Zhang, Samantha A Cicero, Li Wang, Rita R Romito-DiGiacomo, Yan Yang, and Karl Herrup. Nuclear localization of cdk5 is a key determinant in the postmitotic state of neurons. *Proceedings of the National Academy of Sciences*, 105(25):8772–8777, 2008.

[286] Jie Zhang and Karl Herrup. Cdk5 and the non-catalytic arrest of the neuronal cell cycle. *Cell Cycle*, 7(22):3487–3490, 2008.

[287] Kazuto Taniguchi, Mark A Russell, Sarah J Richardson, and Noel G Morgan. The subcellular distribution of cyclin-d1 and cyclin-d3 within human islet cells varies according to the status of the pancreas donor. *Diabetologia*, 58:2056–2063, 2015.

[288] Hardik R Mody, Sau Wai Hung, Kineta Naidu, Haesung Lee, Caitlin A Gilbert, Toan Thanh Hoang, Rakesh K Pathak, Radhika Manoharan, Shanmugam Muruganandan, and Rajgopal Govindarajan. Set contributes to the epithelial-mesenchymal transition of pancreatic cancer. *Oncotarget*, 8(40):67966, 2017.

[289] Toshiya Oba, Taro Saito, Akiko Asada, Sawako Shimizu, Koichi M Iijima, and Kanae Ando. Microtubule affinity–regulating kinase 4 with an alzheimer's disease-related mutation promotes tau accumulation and exacerbates neurodegeneration. *Journal of Biological Chemistry*, 295(50):17138–17147, 2020.

[290] Toshiya Oba, Taro Saito, Akiko Asada, Sawako Shimizu, Koichi M Iijima, and Kanae Ando. Mark4 with an alzheimer's disease-related mutation promotes tau hyperphosphorylation directly and indirectly and exacerbates neurodegeneration. *bioRxiv*, pages 2020–05, 2020.

[291] Binukumar BK, Ya-Li Zheng, Varsha Shukla, Niranjana D Amin, Philip Grant, and Harish C Pant. Tfp5, a peptide derived from p35, a cdk5 neuronal activator, rescues cortical neurons from glucose toxicity. *Journal of Alzheimer's Disease*, 39(4):899–909, 2014.

[292] Teresa L Mastracci, Jean-Valery Turatsinze, Benita K Book, Ivan A Restrepo, Michael J Pugia, Eric A Wiebke, Mark D Pescovitz, Decio L Eizirik, and Raghavendra G Mirmira. Distinct gene expression pathways in islets from individuals with short-and long-duration type 1 diabetes. *Diabetes, obesity and metabolism*, 20(8):1859–1867, 2018.

[293] Chong Gao, Christian Hölscher, Yueze Liu, and Lin Li. Gsk3: a key target for the development of novel treatments for type 2 diabetes mellitus and alzheimer disease. 2012.

[294] Sue Murray, Jiangwei Zhang, Annie Ferng, Thazha Prakash, Richard Lee, EVA ANDERSSON, David Janzen, Laurent Knerr, Carina Ammala, and Shuling Guo. 2092-p: Invalidation of gsk3b in pancreatic beta cell as a therapeutic target for t2d. *Diabetes*, 69(Supplement_1), 2020.

[295] Hiroyuki Inoue, Shun-ichiro Asahara, Yumiko Sugiura, Yukina Kawada, Asuka Imai, Chisako Hara, Ayumi Kanno, Maki Kimura-Koyanagi, and Yoshiaki Kido. Histone deacetylase 6 regulates insulin signaling in pancreatic β cells. *Biochemical and Biophysical Research Communications*, 534:896–901, 2021.

[296] Rexford S Ahima. Hdac6 inhibition overcomes leptin resistance in obesity. *Nature Metabolism*, 4(1):11–12, 2022.

[297] M Lundh, DP Christensen, DN Rasmussen, P Mascagni, CA Dinarello, N Billestrup, LG Grunnet, and T Mandrup-Poulsen. Lysine deacetylases are produced in pancreatic beta cells and are differentially regulated by proinflammatory cytokines. *Diabetologia*, 53(12):2569–2578, 2010.

[298] Damien Devos, Svetlana Dokudovskaya, Rosemary Williams, Frank Alber, Narayanan Eswar, Brian T Chait, Michael P Rout, and Andrej Sali. Simple fold composition and modular architecture of the nuclear pore complex. *Proceedings of the National Academy of Sciences*, 103(7):2172–2177, 2006.

[299] Lisa Diez, Larisa E Kapinos, Janine Hochmair, Sabrina Huebschmann, Alvaro Dominguez-Baquero, Amelie Vogt, Marija Rankovic, Markus Zweckstetter, Roderick YH Lim, and Susanne Wegmann. Phosphorylation but not oligomerization drives the accumulation of tau with nucleoporin nup98. *International Journal of Molecular Sciences*, 23(7):3495, 2022.

[300] Timir Tripathi, Jay Prakash, and Yaron Shav-Tal. Phospho-tau impairs nuclear-cytoplasmic transport. *ACS chemical neuroscience*, 10(1):36–38, 2018.

Appendix A

Supplementary data

Table A.1 **Antigen retrieval buffers.** This table has detailed information about the recipes of antigen retrieval buffers; A.1a Citrate pH6

Citrate buffer pH6, 0.01M	**1X**	**10X**
Citric acid (Sigma C0759)	1.92g	19.2g
ddH2O	1L	1L
Add 2N NaOH to pH6 (approximately 12-15mls)		

(a) Citrate pH6

Table A.2 **General buffers.** This table has detailed information about the recipes of general buffers; A.2a Tris-buffered saline (TBS), A.2b 0.5% Copper sulphate and 0.9% saline solution, A.2c Scott's Tap Water Substitute (STWS).

Tris-buffered saline (TBS)	**1X**	**10X**
Tris Base (Sigma T1378)	6.1g (0.5M)	61g (50mM)
NaCl (Sigma S7653)	9g (9%)	90g (0.9%)
ddH2O	1L	1L
pH to 7.6		

(a) Tris-buffered saline (TBS)

0.5% Copper sulphate and 0.9% saline solution	
Copper sulphate	5g
NaCl (Sigma S7653)	9g
ddH2O	1L
Do NOT pH	

(b) 0.5% Copper sulphate and 0.9% saline solution

Scott's Tap Water Substitute (STWS)	
Sodium bicarbonate (Sigma S5761)	3.5g
Magnesium sulphate (Sigma M7506)	20g
ddH2O	up to 1L
Sodium azide	0.05%

(c) STWS

Table A.3 **Statistical analysis of the signal intensity of total Tau antibodies in untreated and λPP-treated rTg4510 mouse cortex.** t-test was performed to investigate whether there is a significant difference between the untreated and λPP-treated rTg4510 mouse cortex. *t-value* and *p-value* are displayed. Multiple comparisons were performed and the p value was corrected (p.adj). ns; not significant.

Antibody	group1	group2	n1	n2	statistic	df	p	p.adj	p.adj.signif
Nterm	control	λPP	200	245	-4.02402	433.8702	6.75E-05	0.000405	***
5A6	control	λPP	141	158	-2.75347	276.2523	0.00629	0.02516	*
SP70	control	λPP	263	256	6.865252	445.5572	2.24E-11	2.02E-10	****
43D	control	λPP	230	182	2.022723	397.8786	0.0438	0.1314	ns
Tau12	control	λPP	300	342	-2.8575	586.3501	0.00442	0.0221	*
Tau13	control	λPP	240	197	1.383633	424.0669	0.167	0.334	ns
Tau5	control	λPP	227	296	-28.1816	479.0119	9.6E-104	1.1E-102	****
HT7	control	λPP	219	223	-5.4999	386.0459	6.93E-08	5.54E-07	****
Dako	control	λPP	273	278	-13.388	539.2243	1.71E-35	1.71E-34	****
Tau46	control	λPP	218	207	-0.457	413.7416	0.648	0.648	ns
D421	control	λPP	197	246	-5.02591	424.553	7.4E-07	5.18E-06	****

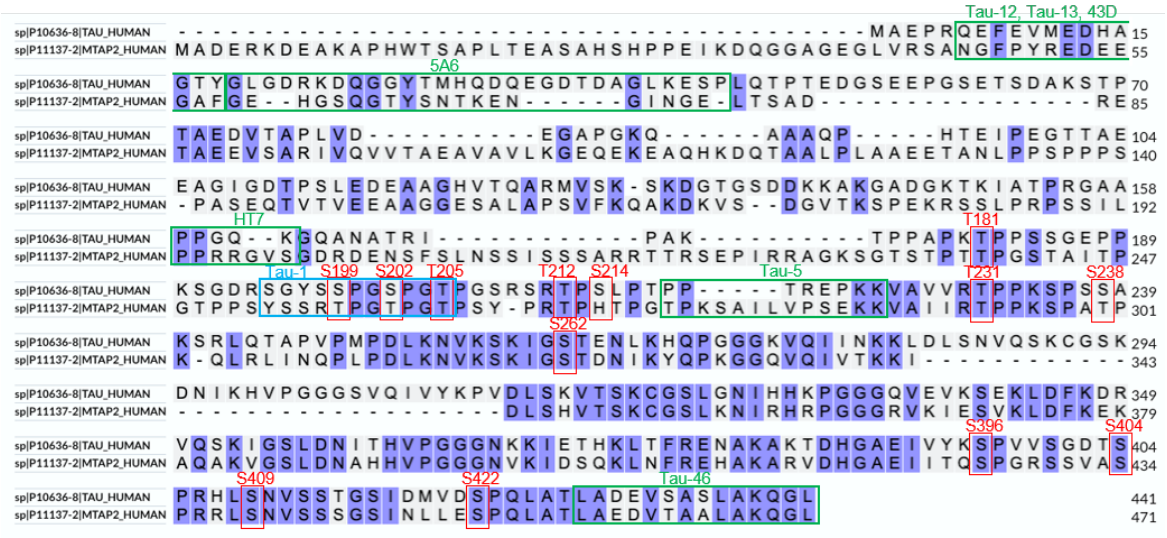

Fig. A.1 **Sequence alignments of Tau and MAP-2 protein.** CLUSTAL Omega alignment of the 2N4R human Tau protein sequence (441 amino acids, Uniprot ID P10636-8) with the human MAP2c protein isoform sequence (471 amino acids, Uniprot ID P11137-2). Epitopes recognised by total Tau antibodies (green), by phospho-specific antibodies (red) and dephospho-specific antibody (blue) are indicated.

Table A.4 **Statistical analysis of the expression level of Tau in foetal and adult β and α cells.** t-test was performed to investigate whether there is a significant difference in the gene expression of Tau between adult and fetal β cells using the Next Generation RNA-Sequencing bulkβ cell data from adult (n=7) and fetal (n=6) β cells and from adult (n=6) and fetal (n=5) α cells [240]. *t-value* and *p-value* are displayed. Multiple comparisons were performed and the p value was corrected (p.adj). ns; not significant.

gene	.y.	group1	group2	n1	n2	t.value	df	p	p.adj	p.adj.signif
MAPT	TPM	adult alpha	adult beta	6	7	-3.92217	6.253678	0.007	0.036	*
MAPT	TPM	adult alpha	fetal alpha	6	5	0.620447	8.274213	0.552	0.552	ns
MAPT	TPM	adult alpha	fetal beta	6	6	-1.2726	9.652485	0.233	0.466	ns
MAPT	TPM	adult beta	fetal alpha	7	5	4.043262	6.365126	0.006	0.036	*
MAPT	TPM	adult beta	fetal beta	7	6	3.616581	6.371887	0.01	0.04	*
MAPT	TPM	fetal alpha	fetal beta	5	6	-1.73911	8.901842	0.116	0.348	ns

Table A.5 **Statistical analysis of the expression level of Tau modifiers in ND and T1D.** t-test was perform to investigate whether there is a significant difference in the gene expression of Tau modifiers between ND and T1D using the Next Generation RNA-Sequencing bulk β cell data from ND donors (group1, n1=12) and T1D (group2, n2=4) [239]. Multiple comparisons were performed and the p value was corrected (p.adj). *t-value* and *p-value* are displayed. ns; not significant.

gene	.y.	group1	group2	n1	n2	t.value	df	p	p.adj	p.adj.signif
MAPT	TPM	ND	T1D	12	4	3.098817	13.508	0.00814	0.00814	**

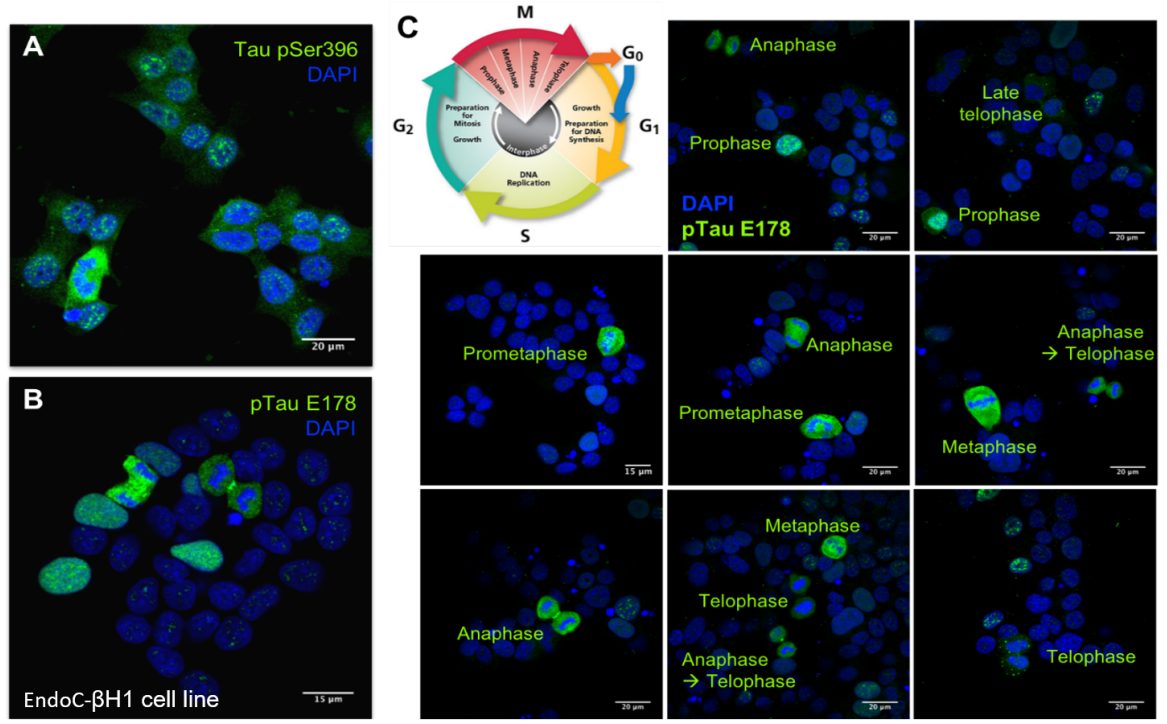

(a)

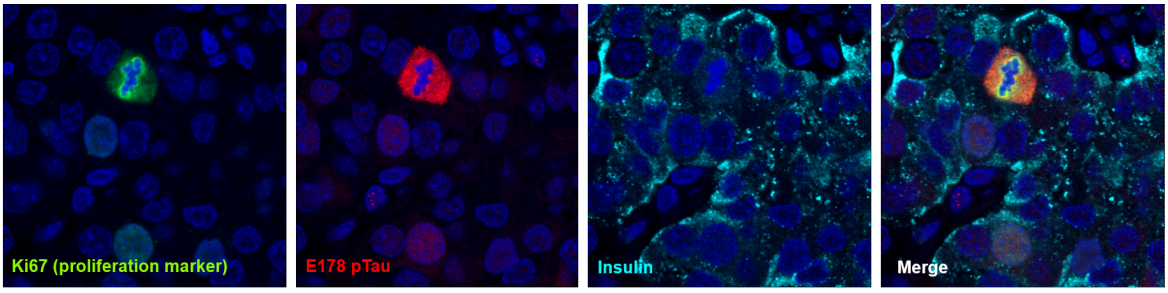

(b)

Fig. A.2 **pTau immunostaining profile in EndoC-βH1 cell line and FFPE pancreas tissue during proliferation. A.2a** | The EndoC-βH1 cell line was used for (A) pSer396 (green) and DAPI (blue) or for (B) pTau-E178 (green) and DAPI (blue). (C) Representative immunofluorescent micrographs demonstrating the presence of pTau in different stages of the cell cycle. **A.2b** | FFPE pancreas tissue was stained for Ki67 proliferation marker (green), pTau-E178 phospho-specific Tau antibody (red), insulin (cyan) and DAPI (blue).

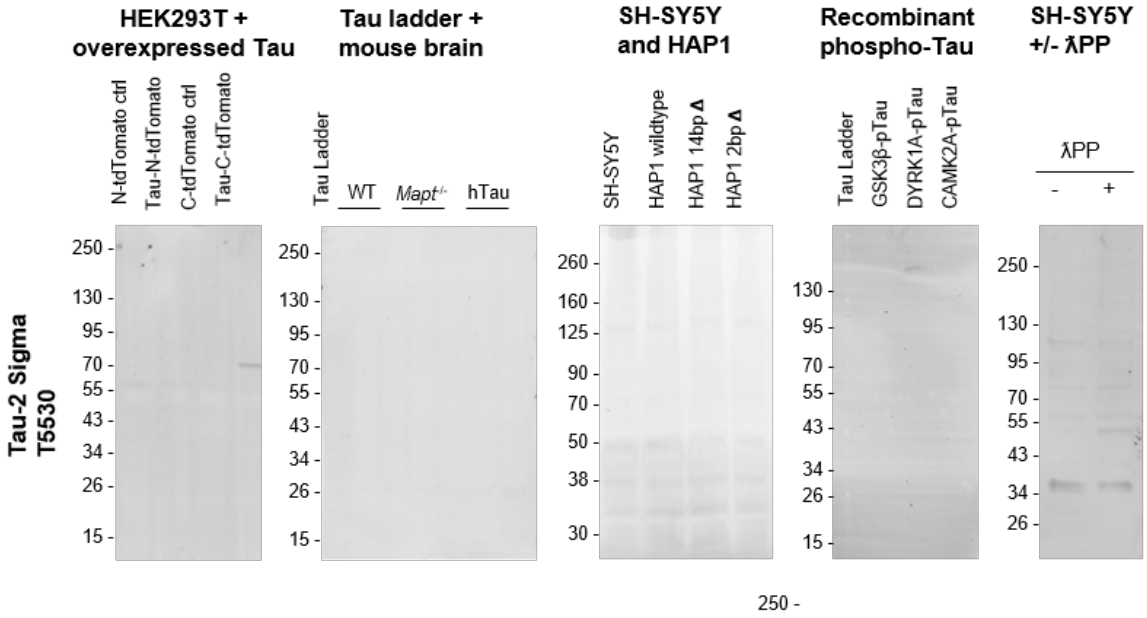

Fig. A.3 **Immunoblotting using a range of lysates to confirm the specificity of Tau-2 antibody.** Immunoblots demonstrating in the specificity of Tau-2 antibody and its reactivity for human and mouse Tau. WBs of lysates from HEK293T cells overexpressing 0N3R human Tau and corresponding control cells (first column); recombinant human Tau ladder (5 ng/isoform/lane), plus adult mouse brain lysates from wildtype, Mapt-/- and hTau mice (second column); lysates from SH-SY5Y neuroblastoma cells, plus HAP1 cells, parental (wildtype) and two cell lines carrying either a 14 bp deletion (14 bp Δ) or a 2-bp deletion (2 bp Δ) in MAPT exon 4 (third column); recombinant human Tau ladder (50 ng/isoform/lane) plus recombinant 2N4R Tau that has been phosphorylated by one of three known Tau kinases: GSK3β, DYRK1A or CAMKIIA (fourth column); lysates from SH-SY5Y neuroblastoma cells that have been either untreated (-) or treated (+) with λPP (fifth column).

Table A.6 **Statistical analysis of the signal intensity of pTau-E178 in ND non-obese, ND obese and T2D individuals above and below the age of 35 years.** t-test was performed to investigate whether there is a significant difference in cytoplasmic pTau-E178 expression in ND non-obese, ND obese and T2D individuals above and below the age of 35 years. *t-value* and *p-value* are displayed. Multiple comparisons were performed and the p value was corrected (p.adj). ns; not significant.

gene	.y.	group1	group2	n1	n2	t.value	df	p	p.adj	p.adj.signif
ND lean	median ratios by donor	below 35	above 35	29	9	-3.24	11.2	0.00763	0.0229	*
ND obese	median ratios by donor	below 35	above 35	19	10	1.48	23.7	0.153	0.459	ns
T2D	median ratios by donor	below 35	above 35	5	17	-0.928	5.06	0.396	1	ns

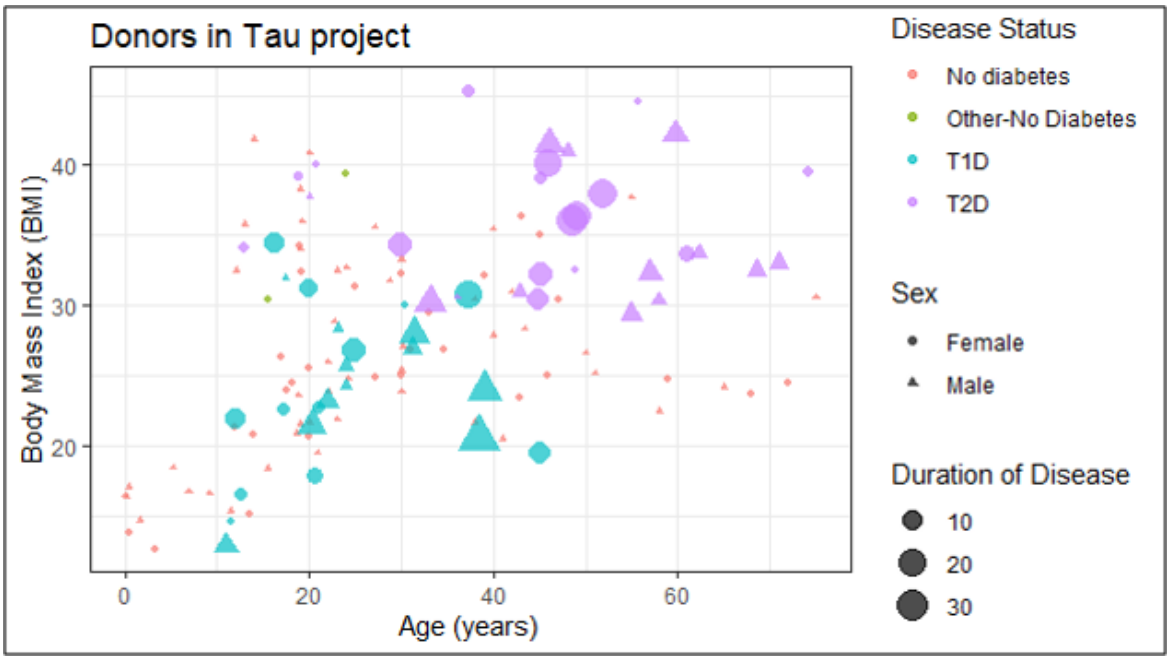

(a)

Donor Group	N	Median Age (Range)	Median BMI (Range)	Sex M/F (%M)	Disease duration (Range)
ND (Initial study)*	37	27y (0-75y)	23.6 (12.7-30.6)	23/14 (62.2%)	N/A
ND* (BMI>30)	21	27.1y (12-75y)	34.0 (30.1-41.9)	14/7 (66.7%)	N/A
T2D	27	46.2y (13-74.2y)	34.4 (30.4-45.5)	12/15 (44.4%)	7.5y (0.25-26y)
T1D	23	22y (11-45y)	6.5y (0-32.5y)		

(b)

Fig. A.4 **Donors in the Tau project.** Pancreas tissue sections were obtained from the network of Pancreatic Organ Donors (nPOD) biobank. Tissue sections from T1D and T2D organ donors (short- and long-duration of disease) and age matched controls were included in this analysis. y axis shows the Body Mass Index (BMI) and the x axis the age (in years) of the donors. The color represents the disease status; ND (orange), other-ND (green), T1D (blue), T2D (purple). The shape of the data points represents the sex of the donors; circle for female and triangle for male. The size of the data points represents the duration of the disease (where applicable); the bigger the size, the longer the duration.

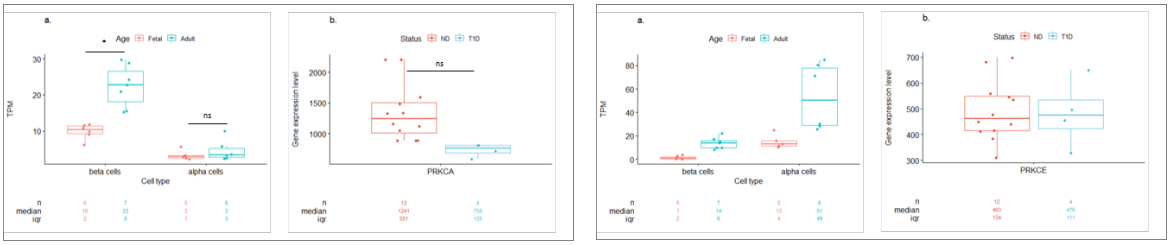

(a) PRKCA (b) PRKCE

Fig. A.5 **Gene expression levels of Tau kinases (PKC, PKE) in fetal and adult β and α cells and in β cells of those diagnosed with and without type 1 diabetes.** Boxplots showing the gene expression of Tau kinases; A.5a | *PRKCA* which codes for protein kinase C α (PKCα) and A.5b | *PRKCE* which codes for protein kinase C ϵ (PKCϵ). Tau kinases expression from fetal and adult β and α cells (RNAseq data from [240], left hand side plot) and in β cells of those diagnosed with and without T1D (RNAseq data from [239], right hand side plot). RNAseq data have been normalised in different ways and therefore, the gene expression levels between the two datasets are not directly comparable but give an indication of relative levels of expression. Statistical analysis using the t-test showed no significant difference in all cases (full stats tables A.7, A.9 pg. 252, 254).

Table A.7 **Statistical analysis of the expression level of Tau modifiers in ND and T1D.** t-test was performed to investigate whether there is a significant difference in the gene expression of Tau modifiers between ND and T1D using the Next Generation RNA-Sequencing bulk β cell data from ND donors (group1, n1=12) and T1D (group2, n2=4) [239]. *t-value* and *p-value* are displayed. ns; not significant.

Modifiers	.y.	group1	group2	n1	n2	t.value	df	p.value	p.adj	p.adj.signif
ABL1	TPM	ND	T1D	12	4	-0.51658	3.767194	0.634	1	ns
ABL2	TPM	ND	T1D	12	4	-0.10077	4.614566	0.924	1	ns
CAMK4	TPM	ND	T1D	12	4	-3.0204	3.11043	0.0542	1	ns
CASP1	TPM	ND	T1D	12	4	-1.12927	3.002227	0.341	1	ns
CASP2	TPM	ND	T1D	12	4	-1.11064	4.675162	0.321	1	ns
CASP3	TPM	ND	T1D	12	4	-0.21628	3.793669	0.84	1	ns
CASP6	TPM	ND	T1D	12	4	0.281897	6.000576	0.787	1	ns
CASP7	TPM	ND	T1D	12	4	-1.30553	3.942155	0.263	1	ns
CASP8	TPM	ND	T1D	12	4	-0.88348	4.803414	0.419	1	ns
CDK1	TPM	ND	T1D	12	4	-0.91923	3.032763	0.425	1	ns
CDK5	TPM	ND	T1D	12	4	0.921023	5.511816	0.396	1	ns
CREBBP	TPM	ND	T1D	12	4	-0.76528	3.783934	0.489	1	ns
CSNK1D	TPM	ND	T1D	12	4	-2.05037	13.93577	0.0596	1	ns
CSNK1E	TPM	ND	T1D	12	4	-0.20088	4.153213	0.85	1	ns
DYRK1A	TPM	ND	T1D	12	4	-1.02203	3.225302	0.377	1	ns
EP300	TPM	ND	T1D	12	4	-1.60519	3.386028	0.196	1	ns
FYN	TPM	ND	T1D	12	4	-0.36016	3.55931	0.739	1	ns
GSK3B	TPM	ND	T1D	12	4	-0.1111	3.638998	0.917	1	ns
HDAC6	TPM	ND	T1D	12	4	3.215254	4.614026	0.0264	1	ns
MAPK13	TPM	ND	T1D	12	4	-0.36951	4.589405	0.728	1	ns
MAPK8	TPM	ND	T1D	12	4	0.626049	5.165723	0.558	1	ns
MAPT	TPM	ND	T1D	12	4	3.098817	13.508	0.00814	0.49654	ns
MARK4	TPM	ND	T1D	12	4	0.558504	4.544393	0.603	1	ns
PHKA1	TPM	ND	T1D	12	4	1.211997	9.917827	0.254	1	ns
PHKA2	TPM	ND	T1D	12	4	4.415361	4.730657	0.00788	0.48856	ns
PHKA2-AS1	TPM	ND	T1D	12	4	0.48376	11.14146	0.638	1	ns
PHKB	TPM	ND	T1D	12	4	1.562879	4.825178	0.181	1	ns
PHKG1	TPM	ND	T1D	12	4	-0.74886	4.348343	0.492	1	ns
PHKG2	TPM	ND	T1D	12	4	-0.31392	7.810733	0.762	1	ns
PIN1	TPM	ND	T1D	12	4	0.111334	3.459084	0.918	1	ns
PPP1CA	TPM	ND	T1D	12	4	-0.30526	3.248475	0.779	1	ns
PPP1CB	TPM	ND	T1D	12	4	0.580325	5.335028	0.585	1	ns
PPP1CC	TPM	ND	T1D	12	4	0.381656	5.035052	0.718	1	ns
PPP2CA	TPM	ND	T1D	12	4	-0.17594	3.459931	0.87	1	ns
PPP3CA	TPM	ND	T1D	12	4	-0.61225	5.161701	0.566	1	ns
PPP3CB	TPM	ND	T1D	12	4	2.908727	10.03563	0.0155	0.93	ns
PPP3CC	TPM	ND	T1D	12	4	-0.48901	3.492044	0.654	1	ns
PPP5C	TPM	ND	T1D	12	4	2.360113	9.409451	0.0414	1	ns
PRKACA	TPM	ND	T1D	12	4	-0.14355	5.007247	0.891	1	ns
PRKACB	TPM	ND	T1D	12	4	0.34527	4.269152	0.746	1	ns
PRKACG	TPM	ND	T1D	12	4	-1.32854	3.152424	0.272	1	ns
PRKCA	TPM	ND	T1D	12	4	4.278999	13.532	0.000822	0.051786	ns
PRKCA-AS1	TPM	ND	T1D	12	4	-0.20943	3.706899	0.845	1	ns
PRKCB	TPM	ND	T1D	12	4	-1.30083	3.016072	0.284	1	ns
PRKCD	TPM	ND	T1D	12	4	0.358357	4.191271	0.737	1	ns
PRKCDBP	TPM	ND	T1D	12	4	1.998726	13.6462	0.066	1	ns
PRKCE	TPM	ND	T1D	12	4	0.135979	4.663953	0.898	1	ns
PRKCSH	TPM	ND	T1D	12	4	0.191803	7.058342	0.853	1	ns
PRKCZ	TPM	ND	T1D	12	4	2.535294	5.553249	0.0475	1	ns
PTPRA	TPM	ND	T1D	12	4	0.60105	6.655373	0.568	1	ns
RPS6KB1	TPM	ND	T1D	12	4	-0.66024	3.240668	0.553	1	ns
SET	TPM	ND	T1D	12	4	0.518894	3.946132	0.632	1	ns
SGK1	TPM	ND	T1D	12	4	-1.2542	3.025709	0.298	1	ns
SIK1	TPM	ND	T1D	12	4	-1.12236	3.649232	0.33	1	ns
SIRT1	TPM	ND	T1D	12	4	0.955995	3.944219	0.394	1	ns
SYK	TPM	ND	T1D	12	4	-0.67712	3.226577	0.544	1	ns
TAOK2	TPM	ND	T1D	12	4	1.68074	12.5145	0.118	1	ns
TTBK1	TPM	ND	T1D	12	4	-1.53031	3.225016	0.217	1	ns

Table A.8 **Statistical analysis of the expression level of Tau modifiers in fetal and adult β cells.** t-test was performed to investigate whether there is a significant difference in the gene expression of Tau modifiers between adult and fetal β cells using the Next Generation RNA-Sequencing bulkβ cell data from adult (group1, n1=7) and fetal (group2, n2=6) β cells [240]. *t-value* and *p-value* are displayed. ns; not significant.

Modifiers	.y.	group1	group2	n1	n2	statistic	df	p.value	p.adj	p.adj.signif
ABL1	TPM	adult beta	fetal beta	7	6	-1.57394	5.733525	0.169	1	ns
ABL2	TPM	adult beta	fetal beta	7	6	1.917189	7.481118	0.094	1	ns
CAMK4	TPM	adult beta	fetal beta	7	6	-1.78141	5.012239	0.135	1	ns
CASP1	TPM	adult beta	fetal beta	7	6	-1.65482	5.664244	0.152	1	ns
CASP2	TPM	adult beta	fetal beta	7	6	-3.78264	9.85873	0.00368	0.16928	ns
CASP3	TPM	adult beta	fetal beta	7	6	0.84285	9.204473	0.421	1	ns
CASP6	TPM	adult beta	fetal beta	7	6	-0.58765	9.64953	0.57	1	ns
CASP8	TPM	adult beta	fetal beta	7	6	-3.46981	5.804575	0.014	0.574	ns
CDK1	TPM	adult beta	fetal beta	7	6	-2.00661	7.782109	0.0807	1	ns
CDK5	TPM	adult beta	fetal beta	7	6	-0.52722	9.033731	0.611	1	ns
CREBBP	TPM	adult beta	fetal beta	7	6	-2.17779	9.22918	0.0567	1	ns
CSNK1D	TPM	adult beta	fetal beta	7	6	2.396357	10.95248	0.0356	1	ns
CSNK1E	TPM	adult beta	fetal beta	7	6	-1.4562	6.940108	0.189	1	ns
DYRK1A	TPM	adult beta	fetal beta	7	6	1.849571	10.78736	0.0919	1	ns
EP300	TPM	adult beta	fetal beta	7	6	-2.25002	9.501522	0.0495	1	ns
FYN	TPM	adult beta	fetal beta	7	6	1.615526	10.63932	0.135	1	ns
GSK3B	TPM	adult beta	fetal beta	7	6	0.42599	9.477374	0.68	1	ns
HDAC6	TPM	adult beta	fetal beta	7	6	1.262014	8.573999	0.24	1	ns
MAPK8	TPM	adult beta	fetal beta	7	6	0.510604	6.739359	0.626	1	ns
MAPT	TPM	adult beta	fetal beta	7	6	3.616581	6.371887	0.01	0.43	ns
MARK4	TPM	adult beta	fetal beta	7	6	-4.15344	7.866804	0.00331	0.15557	ns
PHKA1	TPM	adult beta	fetal beta	7	6	4.820156	6.551839	0.00231	0.11088	ns
PHKA2	TPM	adult beta	fetal beta	7	6	-2.5334	5.660905	0.0468	1	ns
PHKB	TPM	adult beta	fetal beta	7	6	0.350624	10.44348	0.733	1	ns
PHKG2	TPM	adult beta	fetal beta	7	6	-3.19468	6.002409	0.0187	0.748	ns
PIN1	TPM	adult beta	fetal beta	7	6	0.978067	9.158201	0.353	1	ns
PPP2CA	TPM	adult beta	fetal beta	7	6	0.127478	7.651502	0.902	1	ns
PPP5C	TPM	adult beta	fetal beta	7	6	0.469459	9.90725	0.649	1	ns
PRKACA	TPM	adult beta	fetal beta	7	6	-0.51421	8.697127	0.62	1	ns
PRKACB	TPM	adult beta	fetal beta	7	6	2.623112	10.12174	0.0252	0.9828	ns
PRKACG	TPM	adult beta	fetal beta	7	6	-1.58114	5	0.175	1	ns
PRKCA	TPM	adult beta	fetal beta	7	6	5.332013	7.783439	0.000767	0.037583	*
PRKCB	TPM	adult beta	fetal beta	7	6	-2.64441	5.000711	0.0457	1	ns
PRKCD	TPM	adult beta	fetal beta	7	6	-1.76961	10.31802	0.106	1	ns
PRKCDBP	TPM	adult beta	fetal beta	7	6	-1.85072	5.210759	0.121	1	ns
PRKCE	TPM	adult beta	fetal beta	7	6	6.344928	7.169928	0.000351	0.01755	*
PRKCG	TPM	adult beta	fetal beta	7	6	-3.52309	7.189235	0.00928	0.40832	ns
PRKCH	TPM	adult beta	fetal beta	7	6	3.529587	7.274713	0.00902	0.4059	ns
PRKCI	TPM	adult beta	fetal beta	7	6	-1.68653	10.67903	0.121	1	ns
PRKCQ	TPM	adult beta	fetal beta	7	6	-1.43206	7.366225	0.193	1	ns
PRKCSH	TPM	adult beta	fetal beta	7	6	1.517871	8.86109	0.164	1	ns
PRKCZ	TPM	adult beta	fetal beta	7	6	-0.59212	9.327139	0.568	1	ns
RPS6KB1	TPM	adult beta	fetal beta	7	6	-0.26829	10.76814	0.794	1	ns
SET	TPM	adult beta	fetal beta	7	6	-0.00959	7.852063	0.993	1	ns
SGK1	TPM	adult beta	fetal beta	7	6	0.70687	9.080153	0.497	1	ns
SIK1	TPM	adult beta	fetal beta	7	6	-3.55725	5.919495	0.0122	0.5124	ns
SIRT1	TPM	adult beta	fetal beta	7	6	-0.04886	10.29164	0.962	1	ns
SYK	TPM	adult beta	fetal beta	7	6	-1.61952	6.959457	0.15	1	ns
TAOK2	TPM	adult beta	fetal beta	7	6	-0.18483	10.53504	0.857	1	ns
TTBK1	TPM	adult beta	fetal beta	7	6	-0.64924	7.102972	0.537	1	ns

Table A.9 **Statistical analysis of the expression level of Tau modifiers in fetal and adult α cells.** t-test was perform to investigate whether there is a significant difference in the gene expression of Tau modifiers between adult and fetal α cells using the Next Generation RNA-Sequencing bulk cell data from adult (group1, n1=6) and fetal (group2, n2=5) α cells [240]. *t-value* and *p-value* are displayed. ns; not significant.

Modifiers	.y.	group1	group2	n1	n2	statistic	df	p.value	p.adj	p.adj.signif
ABL1	TPM	adult alpha	fetal alpha	6	5	-0.83161	5.429065	0.441	1	ns
ABL2	TPM	adult alpha	fetal alpha	6	5	-0.55512	7.222766	0.596	1	ns
CAMK4	TPM	adult alpha	fetal alpha	6	5	-2.52802	4.124573	0.0629	1	ns
CASP1	TPM	adult alpha	fetal alpha	6	5	-0.68374	5.041273	0.524	1	ns
CASP2	TPM	adult alpha	fetal alpha	6	5	-2.83556	6.820787	0.0259	0.9842	ns
CASP3	TPM	adult alpha	fetal alpha	6	5	0.103843	5.800299	0.921	1	ns
CASP6	TPM	adult alpha	fetal alpha	6	5	-1.21909	4.656346	0.281	1	ns
CASP8	TPM	adult alpha	fetal alpha	6	5	1.797105	7.530823	0.112	1	ns
CDK1	TPM	adult alpha	fetal alpha	6	5	-1.2855	4.419392	0.262	1	ns
CDK5	TPM	adult alpha	fetal alpha	6	5	-1.96454	4.900659	0.108	1	ns
CREBBP	TPM	adult alpha	fetal alpha	6	5	0.610795	7.906981	0.558	1	ns
CSNK1D	TPM	adult alpha	fetal alpha	6	5	3.122478	5.654558	0.0222	0.8658	ns
CSNK1E	TPM	adult alpha	fetal alpha	6	5	1.24965	8.922637	0.243	1	ns
DYRK1A	TPM	adult alpha	fetal alpha	6	5	1.212344	8.197135	0.259	1	ns
EP300	TPM	adult alpha	fetal alpha	6	5	0.060147	6.416818	0.954	1	ns
FYN	TPM	adult alpha	fetal alpha	6	5	-3.3075	8.20691	0.0104	0.4472	ns
GSK3B	TPM	adult alpha	fetal alpha	6	5	-3.56524	5.785323	0.0126	0.5166	ns
HDAC6	TPM	adult alpha	fetal alpha	6	5	1.726303	6.452689	0.132	1	ns
MAPK8	TPM	adult alpha	fetal alpha	6	5	-1.33379	8.009882	0.219	1	ns
MAPT	TPM	adult alpha	fetal alpha	6	5	0.620447	8.274213	0.552	1	ns
MARK4	TPM	adult alpha	fetal alpha	6	5	0.138703	6.700927	0.894	1	ns
PHKA1	TPM	adult alpha	fetal alpha	6	5	1.988067	6.687221	0.0891	1	ns
PHKA2	TPM	adult alpha	fetal alpha	6	5	0.357082	5.564984	0.734	1	ns
PHKB	TPM	adult alpha	fetal alpha	6	5	-2.64242	6.908386	0.0337	1	ns
PHKG2	TPM	adult alpha	fetal alpha	6	5	-0.69451	6.710877	0.511	1	ns
PIN1	TPM	adult alpha	fetal alpha	6	5	-1.11851	8.764888	0.293	1	ns
PPP2CA	TPM	adult alpha	fetal alpha	6	5	-3.80171	5.423941	0.0108	0.4536	ns
PPP5C	TPM	adult alpha	fetal alpha	6	5	-0.7186	8.925184	0.491	1	ns
PRKACA	TPM	adult alpha	fetal alpha	6	5	0.506129	5.943704	0.631	1	ns
PRKACB	TPM	adult alpha	fetal alpha	6	5	-4.4283	5.555004	0.00533	0.23985	ns
PRKCA	TPM	adult alpha	fetal alpha	6	5	0.920517	7.291444	0.387	1	ns
PRKCB	TPM	adult alpha	fetal alpha	6	5	-2.63572	4.044528	0.0572	1	ns
PRKCD	TPM	adult alpha	fetal alpha	6	5	-0.46676	8.80196	0.652	1	ns
PRKCDBP	TPM	adult alpha	fetal alpha	6	5	-2.37446	4.042259	0.0758	1	ns
PRKCE	TPM	adult alpha	fetal alpha	6	5	3.245193	5.51192	0.0198	0.792	ns
PRKCG	TPM	adult alpha	fetal alpha	6	5	-0.65877	5.497752	0.537	1	ns
PRKCH	TPM	adult alpha	fetal alpha	6	5	2.430647	7.753682	0.0421	1	ns
PRKCI	TPM	adult alpha	fetal alpha	6	5	-3.85235	8.998958	0.00389	0.17894	ns
PRKCQ	TPM	adult alpha	fetal alpha	6	5	-0.4331	6.83117	0.678	1	ns
PRKCSH	TPM	adult alpha	fetal alpha	6	5	2.407784	5.288074	0.0583	1	ns
PRKCZ	TPM	adult alpha	fetal alpha	6	5	-1.4699	6.416672	0.189	1	ns
RPS6KB1	TPM	adult alpha	fetal alpha	6	5	-4.31212	8.292522	0.00237	0.11139	ns
SET	TPM	adult alpha	fetal alpha	6	5	-6.55838	4.483299	0.00186	0.08928	ns
SGK1	TPM	adult alpha	fetal alpha	6	5	-1.63162	5.975356	0.154	1	ns
SIK1	TPM	adult alpha	fetal alpha	6	5	-7.26614	4.42847	0.00128	0.06272	ns
SIRT1	TPM	adult alpha	fetal alpha	6	5	-2.84649	5.294903	0.0337	1	ns
SYK	TPM	adult alpha	fetal alpha	6	5	3.679729	6.140158	0.00992	0.43648	ns
TAOK2	TPM	adult alpha	fetal alpha	6	5	0.147846	6.630602	0.887	1	ns
TTBK1	TPM	adult alpha	fetal alpha	6	5	0.928336	5.60826	0.391	1	ns

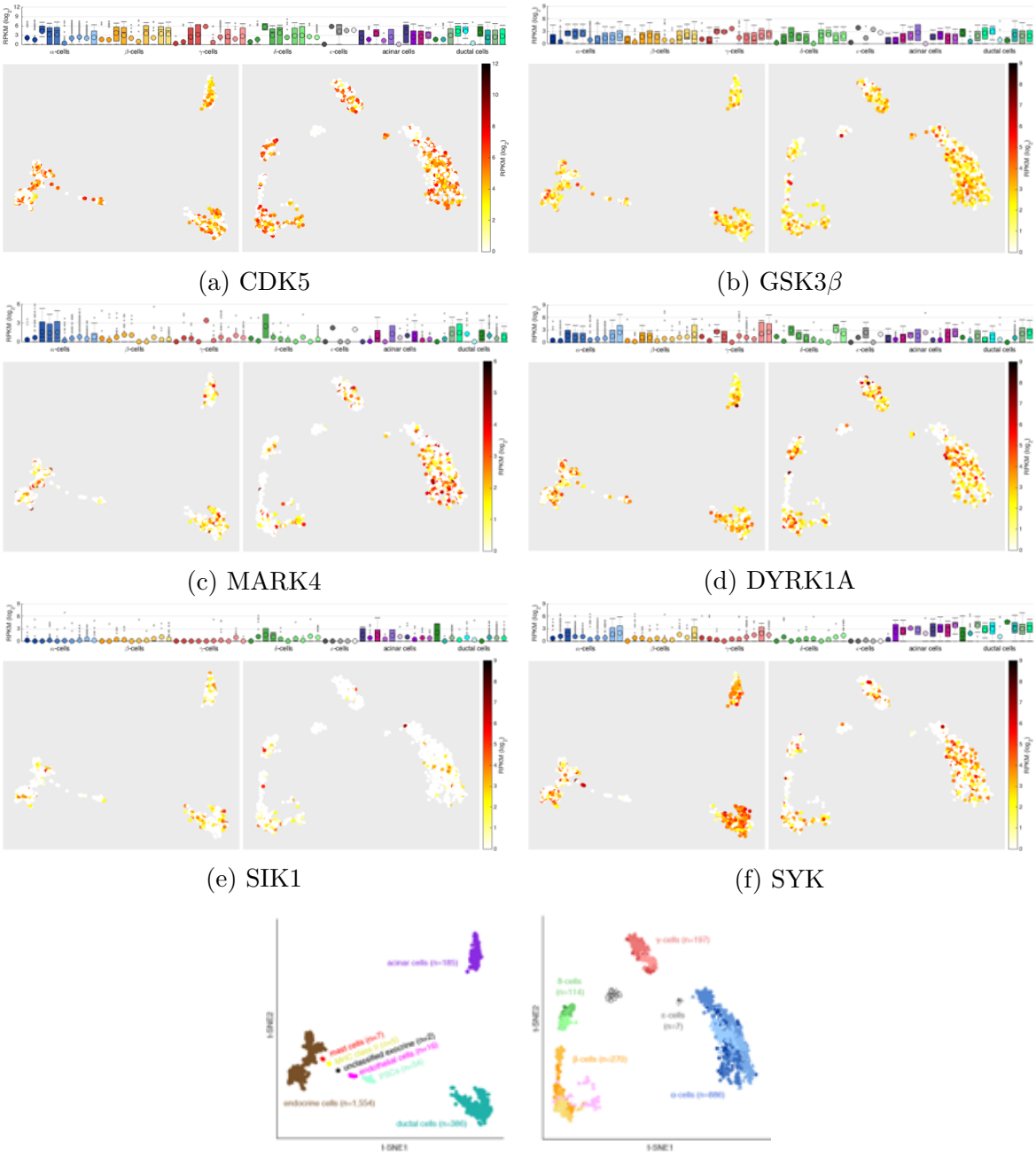

(a) CDK5

(b) GSK3β

(c) MARK4

(d) DYRK1A

(e) SIK1

(f) SYK

(g)

Fig. A.6 **RNA expression levels of Tau kinases in the human pancreas of those diagnosed with or without type 2 diabetes.** Boxplots summarising GCG expression levels of A.6a | CDK5, A.6b | GSK3-β, A.6c | MARK4, A.6d | DYRK1A, A.6e | SIK1 and A.6f | SYK, across the 7 major cell types (shown in different colors) for every donor (shown in different shades of each color). The first 6 boxes correspond to healthy individuals (H1 to H6) and the last 4 to T2D individuals (T2D1 to T2D4). ϵ-cells were captured only in 5 donors (H2, H3, H6, T2D1, T2D4). (https://sandberglab.se/tool/pancreas/, [175]).

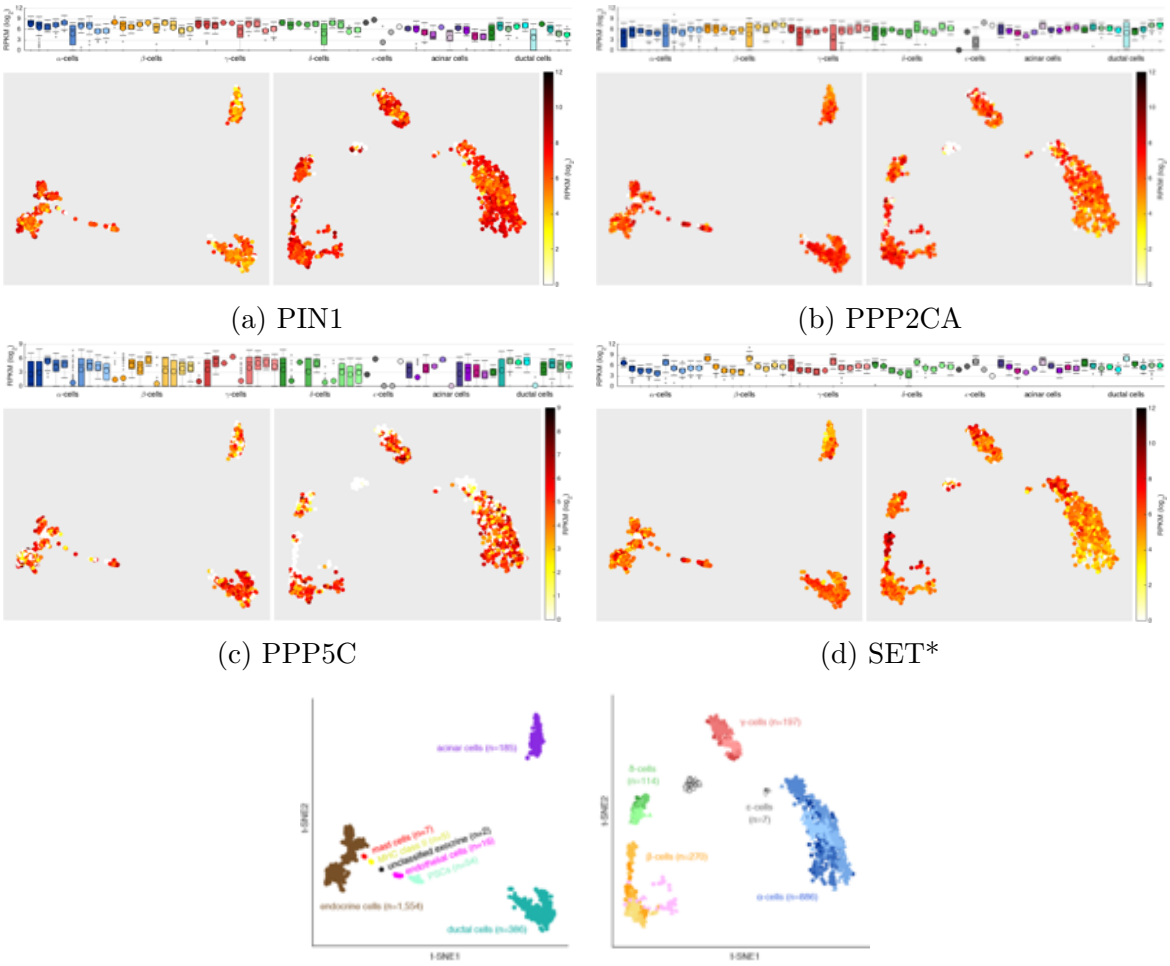

(a) PIN1 (b) PPP2CA

(c) PPP5C (d) SET*

(e)

Fig. A.7 **RNA expression levels of Tau phosphatases in the human pancreas of those diagnosed with or without type 2 diabetes.** Boxplots summarising GCG expression levels of A.7a | PIN1, A.7b | *PPP2CA* which codes for protein phosphatase 2A (PP2A), A.7c | *PPP5C* which codes for protein phosphatase 5 (PP5) and A.7d | SET (SET is not a Tau phosphatase but rather an inhibitor of PP2A), across the 7 major cell types (shown in different colors) for every donor (shown in different shades of each color). The first 6 boxes correspond to healthy individuals (H1 to H6) and the last 4 to T2D individuals (T2D1 to T2D4). ϵ-cells were captured only in 5 donors (H2, H3, H6, T2D1, T2D4). (https://sandberglab.se/tool/pancreas/, [175]).

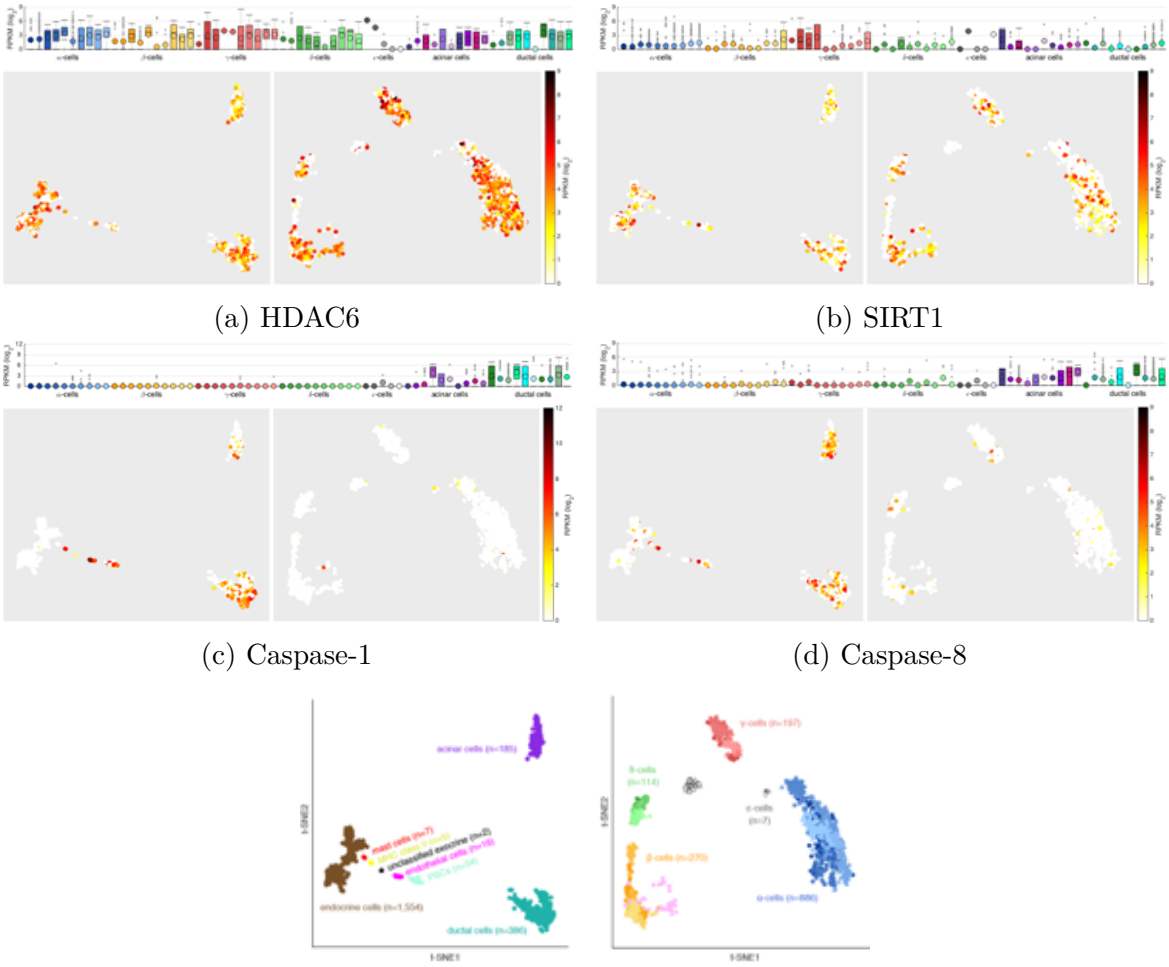

(a) HDAC6

(b) SIRT1

(c) Caspase-1

(d) Caspase-8

(e)

Fig. A.8 **RNA expression levels of Tau modifiers (acetylases, caspases) in the human pancreas of those diagnosed with or without type 2 diabetes.** Boxplots summarising GCG expression levels of deacetylase; A.8a | HDAC6, acetylase; A.8b | SIRT1 and caspases; A.8c | Caspase-1 and A.8d | Caspase-8, across the 7 major cell types (shown in different colors) for every donor (shown in different shades of each color). The first 6 boxes correspond to healthy individuals (H1 to H6) and the last 4 to T2D individuals (T2D1 to T2D4). ϵ-cells were captured only in 5 donors (H2, H3, H6, T2D1, T2D4). (https://sandberglab.se/tool/pancreas/, [175]).